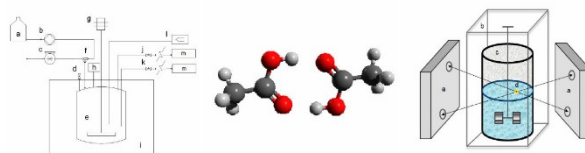
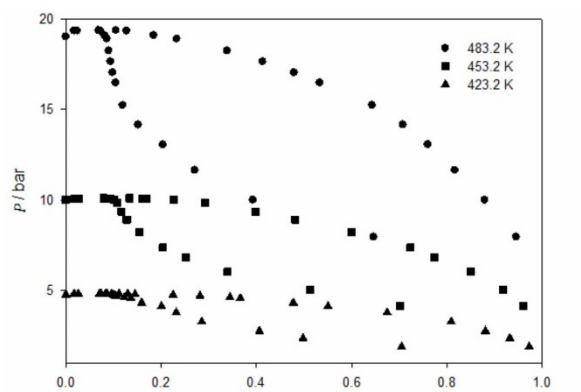


VAPOUR – LIQUID EQUILIBRIA OF ACETIC ACID + WATER AND PROPANOIC ACID + WATER: EXPERIMENTAL MEASUREMENT AND THERMODYNAMIC MODELLING

By

Luis Antonio Román-Ramírez

A thesis submitted to the University
of Birmingham for the degree of
DOCTOR OF PHILOSOPHY



School of Chemical Engineering
The University of Birmingham, UK
January 2015

UNIVERSITY OF
BIRMINGHAM

University of Birmingham Research Archive

e-theses repository

This unpublished thesis/dissertation is copyright of the author and/or third parties. The intellectual property rights of the author or third parties in respect of this work are as defined by The Copyright Designs and Patents Act 1988 or as modified by any successor legislation.

Any use made of information contained in this thesis/dissertation must be in accordance with that legislation and must be properly acknowledged. Further distribution or reproduction in any format is prohibited without the permission of the copyright holder.

Abstract

Vapour – liquid equilibria were measured for the acetic acid + water and the propanoic acid + water systems, in the temperature range of 412.6 to 483.2 K and pressures of 1.87 to 19.38 bar, over the entire range of concentrations. An experimental apparatus based on the static-analytical method with sampling of both phases was used with quantitative analysis by GC. A new experimental technique comprising positron emission particle tracking (PEPT) was developed and applied for the determination phase compositions and molar volumes for the acetic acid + water system at 412.6 K.

The Peng-Robinson (PR), the Cubic Plus Association (CPA), the Perturbed Chain Statistical Associating Fluid Theory (PC-SAFT) and the PC-polar-SAFT (PCP-SAFT) equations modelled the data. The 1A and 2B association schemes for propanoic acid and the 2B, 3B and 4C for water, were evaluated. In CPA, the ECR and CR1 combining rules were also tested. A single binary interaction parameter was used in all models. PCP-SAFT presented higher predictive and correlative capabilities when the organic acid was modelled as 1A and water as 2B. The best association combination among CPA and PC-SAFT was 2B and 4C for the acid and water, respectively. CR1 accounted for lower errors in predictive mode while ECR in correlative mode. CPA performance was intermediate between the PC-SAFT and PCP-SAFT models and the PR equation. PR predictions were rather poor but correlations were better than those of CPA, at the expense of a larger binary interaction parameter.

To
My Wife
and
My Family

No estudio para saber más, sino para ignorar menos.”
«I don't study to know more, but to ignore less.»

Sor Juana Inés de la Cruz
Mexican Writer, Women's Rights Activist, Nun
(1651–1695)

Acknowledgements

Foremost, I would like to thank my supervisor Prof Gary Leeke for his continuous encouragement, support and enthusiasm during the studies. Thank you for pushing me to my boundaries and for the helpful meetings at the coffee shop. I could have not imagined a better supervisor for my PhD.

A special thanks goes to my financial sponsor CONACyT, without which this work would have not been possible.

To Dr Regina Santos for her support especially at the beginning of the studies.

To Dr Teijun Lu for helping me with the initial laboratory work.

To Dr Tom Leadbeater for his help in the PEPT studies.

To Prof Fernando Sánchez for all his kind help, support and patience during the long distance phone calls.

To the Chemical Engineering workshop staff for their kind help. A very special thanks goes to Bob Sharpe for helping me through many situations and when I most needed, thank you for the coffee mornings and insightful discussions.

A big thanks also goes to the staff of the Chemical Engineering administrative office, especially to Lynn, Chris and Liz. Thank you for your kind help.

I would like to thank all my lab colleagues and friends, especially Ricardo, Luke, Fabio, Steven, Boris, Fabricio, Arielle, Raitis, Ifi and Salis.

Thanks to my dear friends in Mexico and to the new friends I have made in the UK during all this time.

Last but not least, to my parents and my sister, for believe in me and encouraging me to pursue my dreams. To all my family and my new family for your moral support. My very special thanks to my lovely wife Cecilia, to be at my side the whole time, for her endless patience, love and support.

Above all, thank you God for guiding me in this journey.

Table of contents

List of Figures	xi
List of Tables	xv
Nomenclature	xvii
Introduction	1
1. Carboxylic acids	5
1.1 <i>Acetic acid</i>	5
1.1.1 Uses	6
1.1.2 Production	7
1.1.2.1 Enzymatic oxidation of ethanol (aerobic oxidation)	7
1.1.2.2 Anaerobic oxidation	8
1.1.2.3 Acetaldehyde process	8
1.1.2.4 Oxidation of hydrocarbons	9
1.1.2.5 Carbonylation of methanol	10
1.1.2.6 BP Saabre™ Technology	13
1.1.3 Economic aspects	13
1.2 <i>Propanoic acid</i>	15
1.2.1 Uses	15
1.2.2 Production	16
1.2.2.1 Ethylene carbonylation	17
1.2.2.2 Oxidation of propanal	18
1.2.2.3 Oxidation of hydrocarbons	18
1.2.3 Economic aspects	18
1.3 <i>Biofuel context</i>	19
1.4 <i>Thermal decomposition</i>	24
1.5 <i>Association</i>	24
1.6 <i>Concluding remarks</i>	25
2. Phase Equilibrium Measurements	27
2.1 <i>Experimental methods</i>	28
2.1.1 Analytical method	31
2.1.2 Synthetic method	31
2.2 <i>Literature review</i>	32
2.2.1 Acetic acid + water	32
2.2.2 Propanoic acid + water	38
2.3 <i>Static – Analytical Measurements</i>	40
2.3.1 Chemical compounds	40
2.3.2 Apparatus description	41
2.3.2.1 Equilibrium cell and fittings	41
2.3.2.2 Peripherals	46
2.3.2.3 Thermocouples calibration	47
2.3.2.4 TCD calibration	49
2.3.3 Experimental procedure	55
2.3.4 Uncertainties determination	56



2.3.4.1	Temperature	57
2.3.4.2	Pressure	58
2.3.4.3	Mole fraction	59
2.3.5	Results and Discussion	60
2.3.5.1	Uncertainties	60
2.3.5.2	Water vapour pressures	61
2.3.5.3	Corrosion	62
2.3.5.4	Acetic acid + water	63
2.3.5.5	Propanoic acid + water	68
2.4	<i>Synthetic Measurements</i>	70
2.4.1	Overview	71
2.4.2	Literature review	73
2.4.3	Mass balance equations	75
2.4.4	PEPT technology	78
2.4.5	Chemical compounds	81
2.4.6	Apparatus description	81
2.4.6.1	Radioactive tracer	84
2.4.6.2	Thermocouples and pressure gauge calibration	85
2.4.6.3	Total volume Equilibrium cell	85
2.4.6.4	Phase volume – height calibration	87
2.4.7	Experimental procedure	90
2.4.8	Uncertainties determination	92
2.4.8.1	Temperature	92
2.4.8.2	Pressure	93
2.4.8.3	Molar density and mole fraction	94
2.4.9	Results	96
2.5	<i>Concluding remarks</i>	99
3.	Phase Equilibria Modelling	101
3.1	<i>Preliminary background</i>	103
3.1.1	Intermolecular forces	103
3.1.2	Intermolecular potential functions	107
3.1.3	Thermodynamic treatment of VLE	108
3.1.4	Equations of state	113
3.2	<i>The Peng-Robinson equation of state</i>	121
3.3	<i>The PC-SAFT equation of state</i>	123
3.3.1	Hard Chain Fluid reference term	124
3.3.2	Dispersion term	126
3.3.3	Association contribution	127
3.3.4	Dipolar contribution	131
3.4	<i>The CPA equation of state</i>	136
3.5	<i>Organic acids and water within CPA and PC-SAFT</i>	139
3.6	<i>Parameters estimation</i>	150
3.7	<i>Results and Discussion</i>	153
3.7.1	Pure component parameters	153
3.7.2	Mixtures	157
3.7.2.1	Predictive mode	158
3.7.2.2	Correlative mode	170
3.7.2.3	Synthetic measurements	180
3.7.2.4	Non-association scenario	183
3.8	<i>Concluding remarks</i>	185



Conclusions and Suggestions for future work	187
References	191
Appendix A. Brief databank of the compounds	225
Appendix B. Pressure gauge calibration certificate	227
Appendix C. Gas-Chromatograph methods	229
C.1 Acetic acid + water	229
C.2 Propanoic acid + water.	231
Appendix D. Table of results of the static – analytical measurements	233
D.1 Acetic acid + water	233
D.2 Propanoic acid + water	234
Appendix E. Spectrophotometric method of iron determination	235
Appendix F. Polypropylene technical data sheet	237
Appendix G. Data sets used in the synthetic measurements	239
Appendix H. Validation plots	241
H.1 CPA	241
H.2 PC-SAFT / PCP-SAFT	244
Appendix I. Average deviations	247
I.1 Predictive mode	247
I.1.1 Acetic acid + water	247
I.1.2 Propanoic acid + water	250
I.2 Correlative mode	252
I.2.1 Acetic acid + water	252
I.2.2 Propanoic acid + water	255
Appendix J. Binary interaction parameters	259
J.1 k_{ij}	259
J.1.1 Acetic acid + water	259
J.1.2 Propanoic acid + water	262
J.2 $k_{ij} = k_{ij}^0 + k_{ij}^1 T$	264
J.2.1 Acetic acid + water	264
J.2.2 Propanoic acid + water	265
Appendix K. Communications	267
K.1 Publications	267
K.2 Conferences	267

List of Figures

Figure 1.1. Acetic acid market volume share, by application, for 2013. Adapted from Grand View Research (2014).....	7
Figure 1.2. Acetic acid Chemische Werke Hüls process. (a) Reactor, (b) Air cooler, (c) Collector, (d) Separation vessel, (e) Pressure column, (f) Distillation column. Adapted from Cheung et al. (2011).....	9
Figure 1.3. Acetic acid BP Chemicals process. (a) Reactor, (b) Gas – liquid separator, (c) Liquid – liquid separator, (d) Distillation column, (e) Extraction, (f) Separation of extraction agent, (g) Formic acid distillation, (h) Acetic acid distillation, (i) Propanoic acid distillation. Adapted from Samel et al. (2011).	10
Figure 1.4. Acetic acid BASF process. (a) Preheater, (b) Reactor, (c) Cooler, (d) High-pressure separator, (e) Intermediate pressure separator, (f) Expansion chamber, (g) Degasser column, (h) Catalyst separation column, (i) Wash column, (j) Scrubbing column, (k) Auxiliary column, (l) Separation chamber, (m) Drying column, (n) Pure acid column, (o) Residue column. Adapted from Cheung et al. (2011).	11
Figure 1.5. Propanoic acid BASF process. (a) High-pressure reactor, (b) Heat exchanger, (c) Separator, (d) Expansion vessel, (e) Distillation column. Adapted from Samel et al. (2011).	17
Figure 1.6. World primary energy demand by fuel in the New Policies Scenario defined by the OECD/IEA.	20
Figure 1.7. Biomass conversion systems. Adapted from Demirbas (2009a).....	22
Figure 1.8. Proposed decomposition kinetic model reaction mechanism for gasification of xylose by supercritical water by Goodwin and Rorrer (2010).	23
Figure 1.9. Cyclic dimerization caused by two hydrogen bonds formed by the carboxylic groups of two acid molecules.....	25
Figure 2.1. Raal and Mühlbauer (1998) classification of high-pressure vapour – liquid equilibrium experimental methods.....	29
Figure 2.2. Dohrn et al. (2010) classification of experimental methods for high-pressure phase equilibria.	30
Figure 2.3. Experimental apparatus of Freeman and Wilson for vapour – liquid equilibrium measurements. Taken from Freeman and Wilson (1985).	36
Figure 2.4. Schematic drawing of the static – analytical apparatus. (a) Water supply, (b) Digital liquid-pump, (c) Vacuum-pump, (d) Safety rupture disc, (e) Equilibrium cell, (f) Three-way valve, (g) Magnetic drive, (h) Digital pressure gauge, (i) Air bath, (j) Liquid sampling valve, (k) Vapour sampling valve, (l) Thermocouple data logger.....	42
Figure 2.5. (a) Actual view of the static – analytical apparatus. (b) Close up of sampling valves.	43
Figure 2.6. Original set-up of the Parr 4575 reactor series. Taken from Parr Instrument Company (2014).	44
Figure 2.7. Modified reactor (Equilibrium cell) for the static – analytical measurements.	45



List of Figures

Figure 2.8. Calibration plot for the thermocouple at the interior of the equilibrium cell. T_{calc} is the calculated temperature from the second order polynomial.	48
Figure 2.9. Deviations from the reference temperature, T_{NIST} , by the use of the second order polynomial Equation (2.1). (●) Maximum deviation, (●) minimum deviation.....	49
Figure 2.10. TCD calibration plots for the acetic acid (1) + water (2) system. (a) Low acetic acid concentration range. (b) High acetic acid concentration range.....	52
Figure 2.11. TCD calibration plots for the propanoic acid (1) + water (2) system. (a) Low propanoic acid concentration range. (b) High propanoic acid concentration range.....	53
Figure 2.12. Deviations from the standard acetic acid mass fraction, $w_{1,std}$, by the use of response factor ratio = 2.1077. (●) Maximum deviation, (●) minimum deviation.	54
Figure 2.13. Deviations from the standard propanoic acid mass fraction, $w_{1,std}$, by the use of response factor ratio = 1.6826. (●) Maximum deviation, (●) minimum deviation.	54
Figure 2.14. Vapour – liquid diagram for the acetic acid (1) + water (2) system at $T = 412.6, 443.2$ and 483.2 K. (●) Water vapour pressures from NIST (2011).....	65
Figure 2.15. Vapour – liquid diagram for the acetic acid (1) + water (2) system at 412.6 K. Comparison with literature values of Freeman and Wilson (1985a; 1985l). Figures: experimental data. Lines are used as a guide to the eye. (●) Water vapour pressure from NIST (2011).	66
Figure 2.16. Vapour – liquid diagram for the propanoic acid (1) + water (2) system at $T = 423.2, 453.2$ and 483.2 K. (●) Water vapour pressures from NIST (2011).....	69
Figure 2.17. Positron Emission Particle Tracking (PEPT) is used to locate the vapour – liquid interface of an enclosed equilibrium cell. (a) PEPT detectors, (b) Air bath, (c) Equilibrium cell, (d) radioactive tracer.	81
Figure 2.18. Schematic drawing of the synthetic apparatus. (a) Water supply, (b) Digital liquid-pump, (c) Vacuum-pump, (d) Safety rupture disc, (e) Equilibrium cell, (f) Three-way valve, (g) Magnetic drive, (h) Digital pressure gauge, (i) Air bath, (j) PEPT detectors, (k) Data acquisition unit, (l) Thermocouple data logger.	82
Figure 2.19. Actual view of the synthetic apparatus based on Positron Emission Particle Tracking (PEPT) measurements. The equilibrium cell is inside the oven shown in the centre. PEPT detectors are located either side of the oven.	83
Figure 2.20. Gamma rays trajectories emitted from the radioactive tracer inside the equilibrium cell. ..	83
Figure 2.21. Calibration plot for the total volume of the liquid phase, V_L , as a function of tracer’s position in height, h	89
Figure 2.22. Deviations between the measured, $V_{L,meas}$, and calculated, $V_{L,calc}$, liquid volumes by the use of Equation (2.38). (●) Maximum deviation, (●) minimum deviation.	89
Figure 2.23. Vapour – liquid equilibrium diagram for the acetic acid (1) + water (2) system at 412.6 K obtained with PEPT, the static – analytical method described in Section 2.3.5.4 and literature values of Freeman and Wilson (1985a; 1985l). Figures: experimental data. Lines are used as a guide to the eye. ..	98
Figure 3.1. Equation-of-state tree showing the inter-relationship of different equations of state. Adapted from Wei and Sadus (2000).....	117



Figure 3.2. Interaction plot as a function of Equation of State (EoS), Association type and Temperature (T) of the average deviations in pressure (ΔP) of the acetic acid + water system in predictive mode ($k_{ij} = 0$).	159
Figure 3.3. Interaction plot as a function of Equation of State (EoS), Association type and Temperature (T) of the average deviations in vapour composition (Δy_1) of the acetic acid (1) + water (2) system in predictive mode ($k_{ij} = 0$).	160
Figure 3.4. Interaction plot as a function of Equation of State (EoS), Association type and Temperature (T) of the average deviations in pressure (ΔP) of the propanoic acid + water system in predictive mode ($k_{ij} = 0$).	161
Figure 3.5. Interaction plot as a function of Equation of State (EoS), Association type and Temperature (T) of the average deviations in vapour composition (Δy_1) of the propanoic acid (1) + water (2) system in predictive mode ($k_{ij} = 0$).	162
Figure 3.6. Vapour – liquid diagram for the acetic acid (1) + water (2) system at 293.15 K. Experimental data (●) from Lazeeva and Markuzin (1973). Lines: equation of state predictions ($k_{ij} = 0$).	164
Figure 3.7. Vapour – liquid diagram for the acetic acid (1) + water (2) system at 373.12 K. Experimental data (●) from Achary and Narasingrao (1947). Lines: equation of state predictions ($k_{ij} = 0$).	165
Figure 3.8. Vapour – liquid diagram for the acetic acid (1) + water (2) system at 443.2 K. Experimental data (●) from this work. Lines: equation of state predictions ($k_{ij} = 0$).	166
Figure 3.9. Vapour – liquid diagram for the acetic acid (1) + water (2) system at 502.85 K. Experimental data (●) from (Freeman and Wilson, 1985I). Lines: equation of state predictions ($k_{ij} = 0$).	166
Figure 3.10. Vapour – liquid diagram for the propanoic acid (1) + water (2) system at 343.2 K. Experimental data (●) from Heintz et al. (1986); Miyamoto et al. (2001). Lines: equation of state predictions ($k_{ij} = 0$) and UNIQUAC-HOC correlations.	168
Figure 3.11. Vapour – liquid diagram for the propanoic acid (1) + water (2) system at 453.2 K. Experimental data (●) from this work. Lines: equation of state predictions ($k_{ij} = 0$) and UNIQUAC-HOC correlations.	169
Figure 3.12. Interaction plot as a function of Equation of State (EoS), Association type and Temperature (T) of the average deviations in pressure (ΔP) of the acetic acid + water system in correlative mode ($k_{ij} = k_{ij}^0 + k_{ij}^1 T$).	172
Figure 3.13. Interaction plot as a function of Equation of State (EoS), Association type and Temperature (T) of the average deviations in vapour composition (Δy_1) of the acetic acid (1) + water (2) system in correlative mode ($k_{ij} = k_{ij}^0 + k_{ij}^1 T$).	173
Figure 3.14. Interaction plot as a function of Equation of State (EoS), Association type and Temperature (T) of the average deviations in pressure (ΔP) of the propanoic acid + water system in correlative mode ($k_{ij} = k_{ij}^0 + k_{ij}^1 T$).	174
Figure 3.15. Interaction plot as a function of Equation of State (EoS), Association type and Temperature (T) of the average deviations in vapour composition (Δy_1) of the propanoic acid (1) + water (2) system in correlative mode ($k_{ij} = k_{ij}^0 + k_{ij}^1 T$).	175
Figure 3.16. Vapour – liquid diagram for the acetic acid (1) + water (2) system at 412.6 K. Symbols: experimental data. Lines: equation of state correlations ($k_{ij} = k_{ij}^0 + k_{ij}^1 T$).	177



List of Figures

- Figure 3.17. Vapour – liquid diagram for the acetic acid (1) + water (2) system at 483.2 K. Experimental data (●) from this work. Lines: equation of state correlations ($k_{ij} = k_{ij}^0 + k_{ij}^1 T$). 178
- Figure 3.18. Vapour – liquid diagram for the propanoic acid (1) + water (2) system at 423.2 K. Experimental data (●) from this work. Lines: equation of state correlations ($k_{ij} = k_{ij}^0 + k_{ij}^1 T$). 178
- Figure 3.19. Vapour – liquid diagram for the acetic acid (1) + water (2) system at 7.91 bar. Experimental data (●) from Othmer et al. (1952). Lines: equation of state correlations ($k_{ij} = k_{ij}^0 + k_{ij}^1 T$). 179
- Figure 3.20. Vapour – liquid diagram for the propanoic acid (1) + water (2) system at 1 bar. Experimental data: (■), Rivenq (1961); (▲), Ito and Yoshida (1963); (x), Kushner et al. (1967) and (●), Amer (1975). Lines: equation of state correlation ($k_{ij} = k_{ij}^0 + k_{ij}^1 T$). 179
- Figure 3.21. Vapour – liquid diagram for the acetic acid (1) + water (2) system at 412.6 K. Experimental data (●), with error bars, obtained from the PEPT technique. Lines: equation of state correlation ($k_{ij} = k_{ij}^0 + k_{ij}^1 T$) and UNIQUAC-HOC correlations. 182
- Figure 3.22. Vapour – liquid diagram for the propanoic acid (1) + water (2) system at 453.2 K. Experimental data (●) from this work. Lines: equation of state predictions ($k_{ij} = 0$). 184
- Figure E.1. Spectrophotometer calibration plot. Absorbance vs. concentration of iron (III) solutions. ... 236
- Figure H.1. Phase diagram for the 1-butanol (1) + *n*-hexane (2) system. (a) Original figure in Kontogeorgis et al. (2006a). (b) This work: symbols: experimental data from Berro et al. (1982) and Rodríguez et al. (1993); dash line: 1-butanol as 2B association type; solid line: 1-butanol as 3B. 241
- Figure H.2. Phase diagram for the methanol (1) + *n*-pentane (2) system. (a) Original figure in Kontogeorgis et al. (2006a). (b) This work: symbols: experimental data from Wilsak et al. (1987); dash line: methanol as 2B association type; solid line: methanol as 3B. 242
- Figure H.3. Phase diagram for the acetic acid (1) + 1-butanol (2) system at 308.15 K. (a) Original figure in Kontogeorgis et al. (2006m). (b) This work: symbols: experimental data from Apelblat et al. (1983); lines: correlations with ECR and CR1 combining rule. Acetic acid modelled as 1A and 1-butanol as 2B. 243
- Figure H.4. Phase diagram of the *n*-butane (1) + ethanol (2) system. (a) Original figure in Gross and Sadowski (2002). (b) This work: symbols: experimental data from Deak et al. (1995); lines: correlations with $k_{ij} = 0.028$. Ethanol modelled as 2B. 244
- Figure H.5. Phase diagram of methanol (1) + 1-octanol (2) at 1.013 bar. (a) Original figure in Gross and Sadowski (2002). (b) This work: symbols: experimental data from Arce et al. (1995); line: correlations with $k_{ij} = 0.020$. Both compounds modelled as 2B. 245
- Figure H.6. Phase diagram for the *n*-pentane (1) + acetone (2) system. (a) Original figure in Gross and Vrabec (2006). (b) This work: symbols: experimental data from Campbell et al. (1986); lines: correlations with $k_{ij} = 0.024$. Acetone modelled with dipolar contributions. 246

List of Tables

Table 2.1. Experimental vapour – liquid equilibria for the acetic acid + water system available in the open literature.	34
Table 2.2. Experimental vapour – liquid equilibria for the propanoic acid + water system available in the open literature.	39
Table 2.3. Chemical compounds and purities used in the experiments.	40
Table 2.4. Reading temperatures, T_{read} and reference temperatures, T_{NIST} , at reading vapour pressures of water, P_{read}	48
Table 2.5. GC operating conditions for acetic acid and propanoic acid determination in aqueous mixtures.	51
Table 2.6. Water vapour pressures, P_v , at the temperatures of study.	62
Table 2.7. Experimental vapour – liquid equilibrium data for the acetic acid (1) + water (2) system determined by PEPT at pressure P , liquid mole fraction x , vapour mole fraction y , liquid molar density ρ_L and vapour molar density ρ_V at $T = 412.6$ K.	97
Table 3.1. Association schemes for carboxylic acids, alcohols and water according to the classification of Huang and Radosz (1990).	130
Table 3.2. CPA pure component parameters for acetic acid, propanoic acid and water from the literature.	146
Table 3.3. PC-SAFT pure component parameters for acetic acid, propanoic acid and water from the literature.	147
Table 3.4. Equations of state and association combinations studied.	150
Table 3.5. Pure component properties.	155
Table 3.6. CPA pure component parameters and average deviations in vapour pressures (ΔP_v) and liquid densities ($\Delta \rho_L$).	155
Table 3.7. PC-SAFT and PCP-SAFT pure component parameters and average deviations in vapour pressures (ΔP_v) and liquid densities ($\Delta \rho_L$).	156
Table 3.8. Computed pressures (P), acetic acid vapour compositions (y_1), liquid molar densities (ρ_L) and vapour molar densities (ρ_V), and calculated deviations (Δ) with PCP-SAFT _{2B-4C} and UNIQUAC-HOC.	181
Table 3.9. Non-associating PC-SAFT and PCP-SAFT pure component parameters and average deviations in vapour pressures (ΔP_v) and liquid densities ($\Delta \rho_L$).	184
Table D.1. Experimental vapour – liquid equilibrium data for acetic acid (1) + water (2) system at pressure P , liquid mole fraction x , vapour mole fraction y and temperatures $T = 413.2, 443.2$ and 483.2 K.	233
Table D.2. Experimental vapour – liquid equilibrium data for propanoic acid (1) + water (2) system at pressure P , liquid mole fraction x , vapour mole fraction y and temperatures $T = 423.2, 453.2$ and 483.2 K.	234



List of Tables

Table E.1. Maximum iron content on the organic acid mixtures + water systems.	236
Table G.1. Mass of acetic acid (m_{acetic}), mass of water (m_{water}) and total volume of the liquid phase (V_L) data used in the regression analysis.	239
Table I.1. Average deviations in pressure (ΔP) and acetic acid vapour composition (Δy_1) of the equations of state with different association schemes and $k_{ij} = 0$	247
Table I.2. Average deviations in pressure (ΔP) and propanoic acid vapour composition (Δy_1) of the equations of state with different association schemes and $k_{ij} = 0$	250
Table I.3. Average deviations in pressure (ΔP) and acetic acid vapour composition (Δy_1) of the equations of state with different association schemes and $k_{ij} = k_{ij}^0 + k_{ij}^1 T$	252
Table I.4. Average deviations in pressure (ΔP) and propanoic acid vapour composition (Δy_1) of the equations of state with different association schemes and $k_{ij} = k_{ij}^0 + k_{ij}^1 T$	255
Table J.1. Temperature dependent binary interaction parameters (k_{ij}) for each equation of state and association scheme.	259
Table J.2. Temperature dependent binary interaction parameters (k_{ij}) for each equation of state and association scheme.	262
Table J.3. Parameters k_{ij}^0 and k_{ij}^1 in $k_{ij} = k_{ij}^0 + k_{ij}^1 T$ for the acetic acid (i) + water (j) system.	264
Table J.4. Parameters k_{ij}^0 and k_{ij}^1 in $k_{ij} = k_{ij}^0 + k_{ij}^1 T$ for the propanoic acid (i) + water (j) system.	265

Nomenclature

Abbreviations

CAGR	Compound Annual Growth Rate
CPA	Cubic Plus Association
CR1	Combining Rule 1
ECR	Elliot Combining Rule
EoS	Equation of State
GC	Gas – Chromatography; group contribution method
mb/d	Million barrels per day
Mtoe	Million tonnes of oil equivalent
NIST	National Institute of Standards and Technology
PCP-SAFT	Perturbed-Chain Polar SAFT
PC-SAFT	Perturbed-Chain SAFT
PEPT	Positron Emission Particle Tracking
PR	Peng-Robinson
RK	Redlich-Kwong
SAFT	Statistical Associating Fluid Theory
sPC-SAFT	simplified PC-SAFT
SRK	Soave-Redlich-Kwong
TCD	Thermal Conductivity Detector
vdW	van der Waals
VLE	Vapour – Liquid equilibrium

Symbols

A	Helmholtz free energy; peak area
a	attraction parameter
a_0	characteristic parameter in CPA
b	repulsive parameter
c_1	characteristic parameter in CPA
d	temperature-dependent segment diameter
F	response factor
f	fugacity
g_{ij}	radial distribution function

Nomenclature

h	height
k	Boltzmann's constant
k_{ij}	binary interaction parameter
m	number of segments per chain; mass
n	number of moles
N	number of measurements
N_p	number of experimental points
P	pressure
P_c	critical pressure
P_v	vapour pressure
r	distance between two molecules
R	universal gas constant
T	temperature
T_c	critical temperature
T_r	reduced temperature
u	uncertainty
u_c	combined standard uncertainty
V	total volume
w	mass fraction
x	liquid mole fraction
X^A	fraction of molecules not bonded at site A
y	vapour mole fraction
Z	compressibility factor

Greek letters

β^{AB}	association volume in CPA
Γ	intermolecular potential function
Δ^{AB}	strength of association
ΔP	average deviation in pressure
ΔP_{max}	maximum pressure drop
δx	resolution
Δy	average deviation in composition
ε	depth of the potential well
ε^{AB}	association energy
η	reduced density
θ	quantity or property
κ^{AB}	association volume
μ	chemical potential; dipolar moment
ρ	saturated molar density



σ	temperature-independent segment diameter; standard deviation
ϕ	fugacity coefficient
ω	acentric factor

Subscripts

<i>add</i>	addition
<i>bal</i>	balance
<i>calc</i>	calculated
<i>calib</i>	calibration
<i>cont</i>	control
<i>corr</i>	correlation
<i>EC</i>	equilibrium cell
<i>fitt</i>	fitting
<i>i, j</i>	$i^{\text{th}}, j^{\text{th}}$ component
<i>L</i>	liquid phase
<i>read</i>	reading
<i>rep</i>	repeatability
<i>repr</i>	reproducibility
<i>resl</i>	resolution
<i>sampl</i>	sampling
<i>std</i>	standard
<i>T</i>	total
<i>V</i>	vapour phase

Superscripts

<i>assoc</i>	association
<i>calc</i>	calculated
<i>dip</i>	dipolar
<i>disp</i>	dispersion
<i>exp</i>	experimental
<i>hc</i>	hard-chain
<i>hs</i>	hard-sphere
<i>res</i>	residual

Introduction

Carboxylic acids, the simplest of the organic acids are present in our everyday life. We could find them as food condiments or, once processed, in the form of plastics. They are also found as precursors of hydrogen in the thermochemical treatment of biomass. In recent years, the economic market of two carboxylic acids, the acetic and the propanoic acids, have increased considerably due to their versatile applications. In their production processes, the desired purity is achieved by removing water normally by distillation. Precise knowledge of their properties as pure compounds or in mixture at a wide range of concentrations and temperature and pressure conditions are thus needed. While it is possible to consult such properties at atmospheric pressures, the data at high temperatures and pressures are scarce.

Additionally, a reliable thermodynamic model is needed for simulation purposes. The most widely known are those named classical equations of state or cubic equations of state. Cubic equations have been used for many years in industry. However, these models do not explicitly account for intermolecular interactions such as association and polarity, two phenomena present in carboxylic acids and in water, limiting their predictive capabilities. Modern equations of state which consider explicitly intermolecular interactions are expected to exceed the performance of cubic models. However, their complexity is considerably higher, an aspect that may not be appealing from an engineering point of view.



Every year new thermodynamic models or modifications of the existing ones appear in the literature, creating a vast choice for the engineer interested in phase equilibrium properties. Nevertheless, and despite the current availability, it is somehow necessary to test several models in order to devise the most adequate for the particular requirements.

The focus of this thesis is the experimental and theoretical study of the phase behaviour of acetic acid and propanoic acid + water mixtures.

The aims of the research are:

- i) To obtain new vapour – liquid equilibria data for the acetic acid + water and the propanoic acid + water system.
- ii) To model the experimental data with traditional and modern equations of state in order to determine the best thermodynamic model for such mixtures.

Towards this end, the construction of an experimental apparatus was necessary. During the design process it was envisaged the use of positron emission particle tracking (PEPT) as a tool to locate the vapour – liquid interface inside a close vessel where no direct visual determination is possible.

The classic Peng-Robinson (PR), the modern Cubic Plus Association (CPA) and the Perturbed Chain Statistical Associating Fluid Theory (PC-SAFT) equations of state have been selected as thermodynamic models for comparison. PC-SAFT was chosen since the systems of interest comprise association as well as polar



interactions; CPA to be a cubic model that considers association interactions, and PR for its simplicity and widespread use.

The objectives of the project are:

- i) To design and construct an experimental rig to work at isothermal conditions based on the static-analytical method.
- ii) To design and construct an experimental rig based on the synthetic method using PEPT technology to locate the interface of a two-phase system.
- iii) To compare the performance of classical and modern equations of state in modelling the new and the existing experimental data.
- iv) To determine the effect of different possible association schemes in CPA and PC-SAFT.
- v) To determine the effect of considering dipolar interactions explicitly in PC-SAFT.

The thesis is divided into four main parts: [Chapter 1](#) emphasizes on the acetic acid and propanoic acid current industrial applications, production processes and economic aspects. [Chapter 2](#) is focused on phase equilibria measurement. The chapter provides a classification of experimental methods for phase equilibria determination and is subdivided into two main parts: one for the static-analytical method and the other for the technique employing PEPT (synthetic method). [Chapter 3](#) focuses on the thermodynamic modelling of the mixtures. The chosen thermodynamic models for comparison are detailed as well as a classification of



association schemes, necessary for the understanding of the comparison. Each chapter ends with some concluding remarks. General conclusions and suggestions for future work are given at the end of the Thesis.

1. Carboxylic acids

Organic acids are organic compounds that contain the carboxylic acid group ($COOH$) at least once in their molecule. This can be as simple as formic acid (in fact the simplest one) or more complex as those as fatty acids or the amino acids. Organic acids possess different properties depending on their molecular structure, some are toxic and highly corrosive, e.g. formic and acetic acid, or can be totally edible with fruity aromas, e.g. citric, malic and tartaric acid. Even though they appear naturally in the world they can also be artificially synthesized to produce long chain carboxylic acids (fatty acids) (Fineberg, 1979; Johnson and Daniels, 2000; Blatti et al., 2013). Despite the practically infinite possibility of organic acids, arguably the most commercially important are the ones called carboxylic acids; in particular the first three low molecular weight ones: formic, acetic and propanoic acids. This work is focused on the last two since a proper study of formic acid would involve kinetic studies due to its chemical instability even at room conditions. A summary of physical and chemical properties of acetic and propanoic acid can be found in [Appendix A](#). A brief description of the characteristics, uses, industrial production and economic aspects of acetic and propanoic acids is given below.

1.1 Acetic acid

Also known as ethanoic acid, it receives its name from the Latin word *acetum* meaning sour or sharp wine, probably after being discovered in spoiled wine. It



is a colourless corrosive liquid with a very characteristic odour with the chemical formula CH_3COOH . It is ordinarily known as vinegar although this is actually a dilute mixture of acetic acid in water. Acetic acid has hygroscopic characteristics making it very difficult to find at very high purities. When in pure form, it is called glacial acetic acid for its tendency to form ice-like crystals. In fact, its freezing point (289.81 K) serves as an indicator of purity (Cheung et al., 2011).

1.1.1 Uses

Acetic acid and its derivatives are used in several industries making it one of the major worldwide commodity chemicals. More than 65% of the acetic acid produced in the world ends in the form of polymers, mainly produced as derivatives of vinyl acetate and cellulose acetate (Cheung et al., 2011). Poly-vinyl acetate is used in paint formulations, coatings, safety glass, plastics, adhesives and sealants. Cellulose acetate goes primarily for textile applications (e.g. yarns), solvents, pesticides, insecticides, cigarette filters, cosmetics and detergents. It is used in the production of pharmaceuticals; for instance, acetyl salicylic acid (aspirin) produced from acetic anhydride (Burdick and Leffler, 2001). It is also used as a reaction solvent of purified terephthalic acid (PTA) for further production of polyethylene terephthalate (PET). In the food industry, it serves as an acidulant, preservative and flavouring agent, among other applications (Stratford, 2000). Its most common household usage is in the form of vinegar and as a descaling agent. It cannot be ignored of course, its use as a 'non-brewed condiment' in every fish and chips shop through the UK (Clegg, 2014). Acetic acid volume market share, by application, for 2013 is shown in [Figure 1.1](#).

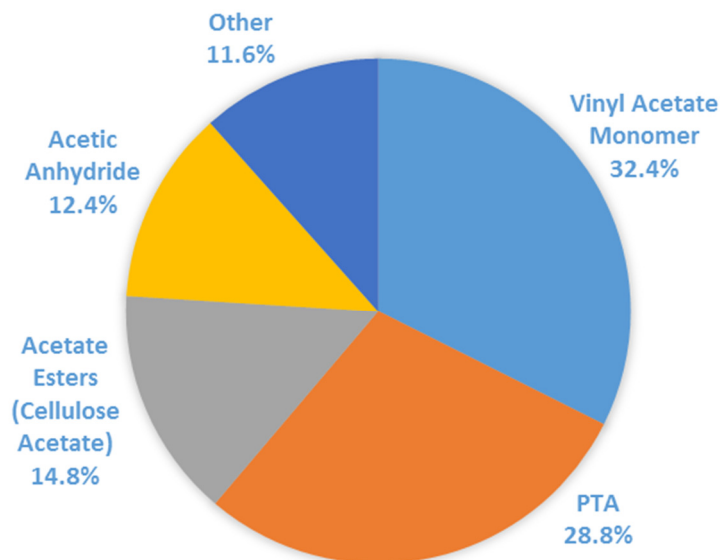


Figure 1.1. Acetic acid market volume share, by application, for 2013. Adapted from Grand View Research (2014).

1.1.2 Production

The ancient method to produce dilute acetic acid or vinegar is through fermentation, probably discovered as a result of spoiled wine and thus dating back to at least 10,000 years ago (Nickol, 1979). The term vinegar is usually reserved for low concentration mixtures (5 – 12% volume acetic acid in water) in which acetic acid is obtained by fermentation, but in some countries as in the UK, it can also refer to mixtures in which acetic acid was obtained from chemical processes (Ebner et al., 1996; Clegg, 2014). Including the ancient method, acetic acid is obtained from any of the processes below.

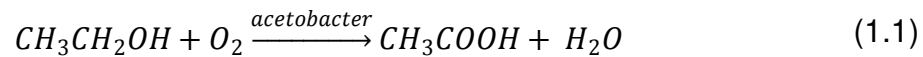
1.1.2.1 Enzymatic oxidation of ethanol (aerobic oxidation)

Used basically to produce vinegar from ciders, wines or yeast-fermented malt (Stratford, 2000). Ethanol is oxidized to acetic acid and water by *acetobacter aceti*



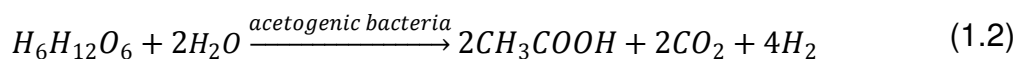
Carboxylic acids

bacteria in presence of oxygen at 300 – 310 K with a yield of about 85% according to the following reaction (Partin and Heise, 1993; Ebner et al., 1996; Beyer and Walter, 1997):



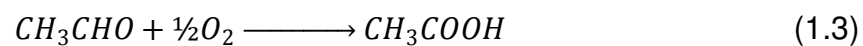
1.1.2.2 Anaerobic oxidation

Glucose is converted into acetic acid by acetogenic bacteria species, e.g. *Clostridium thermoaceticum*, with a yield of about 85% according to the following reaction (Partin and Heise, 1993):



1.1.2.3 Acetaldehyde process

Acetaldehyde is transformed into acetic acid by oxidation (Beyer and Walter, 1997; Burdick and Leffler, 2001):



Common operating conditions are 333 – 353 K and 3 – 10 bar, with yields of around 90%. Water is removed by azeotropic distillation in a final step to achieve purities greater than 99% (Cheung et al., 2011).

1.1.2.4 Oxidation of hydrocarbons

Acetic acid is obtained from oxidation of aliphatic hydrocarbons, the main by-products being formic acid and propanoic acid. Crude acetic acid is purified by fractional distillation operations. Reaction temperature conditions are 423 – 470 K and pressures of 40 – 65 bar, with yields of 75 – 80%, depending on the raw material used. Celanese and Chemische Werke Hüls (Hüls AG, now Evonik Industries; [Figure 1.2](#)) uses *n*-butane as the raw material while British Petroleum Chemicals (BP; [Figure 1.3](#)) employs naphtha (Beyer and Walter, 1997; Burdick and Leffler, 2001; Chiusoli and Maitlis, 2006; Samel et al., 2011).

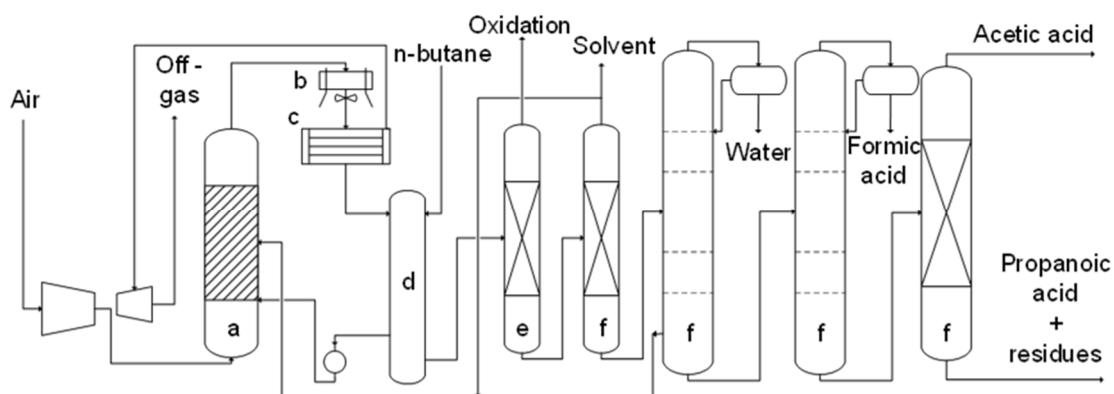


[Figure 1.2](#). Acetic acid Chemische Werke Hüls process. (a) Reactor, (b) Air cooler, (c) Collector, (d) Separation vessel, (e) Pressure column, (f) Distillation column. Adapted from Cheung et al. (2011).

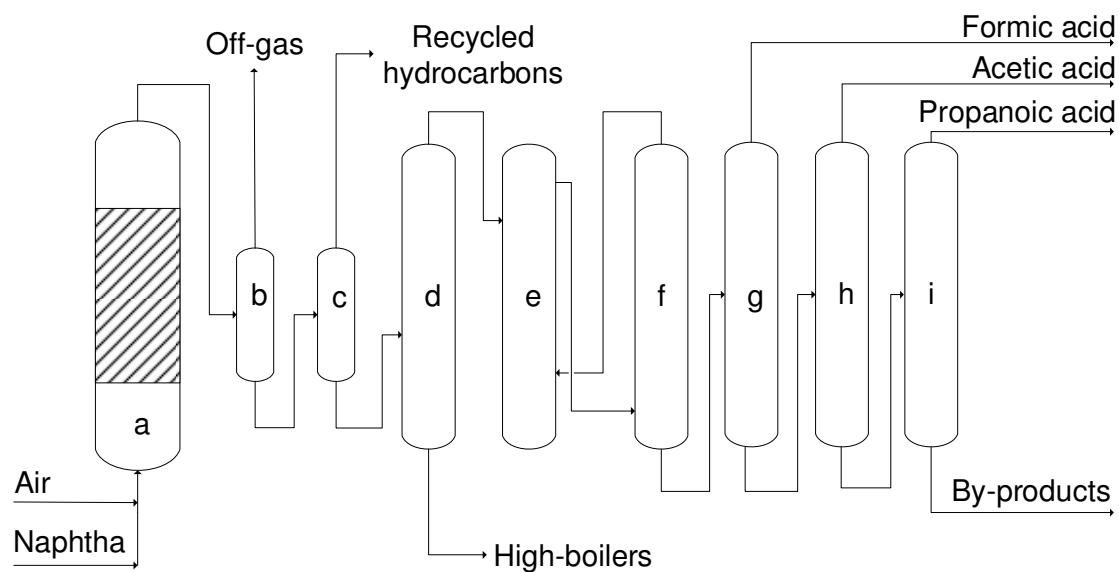
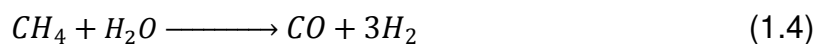


Figure 1.3. Acetic acid BP Chemicals process. (a) Reactor, (b) Gas – liquid separator, (c) Liquid – liquid separator, (d) Distillation column, (e) Extraction, (f) Separation of extraction agent, (g) Formic acid distillation, (h) Acetic acid distillation, (i) Propanoic acid distillation. Adapted from Samel et al. (2011).

1.1.2.5 Carbonylation of methanol

Developed in 1960's by BASF ([Figure 1.4](#)), most of the acetic acid currently produced around the world (about 75%) comes from the catalytic carbonylation of methanol by means of the following set of reactions (Burdick and Leffler, 2001; Chiusoli and Maitlis, 2006):



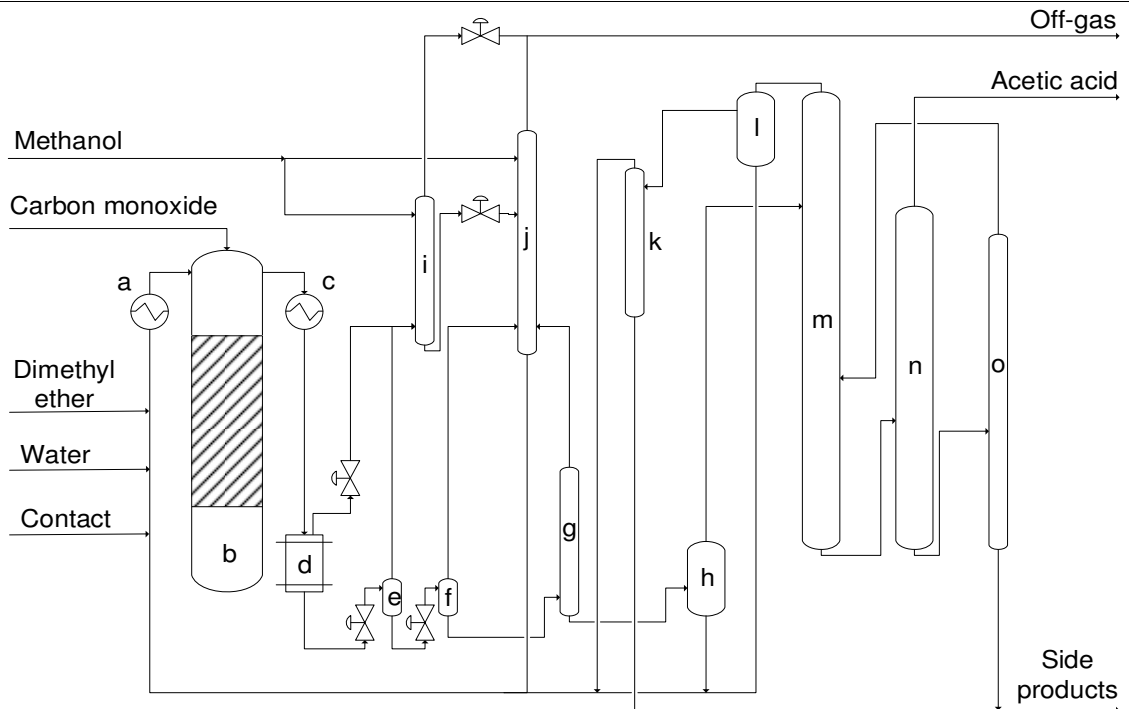
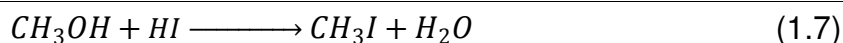


Figure 1.4. Acetic acid BASF process. (a) Preheater, (b) Reactor, (c) Cooler, (d) High-pressure separator, (e) Intermediate pressure separator, (f) Expansion chamber, (g) Degasser column, (h) Catalyst separation column, (i) Wash column, (j) Scrubbing column, (k) Auxiliary column, (l) Separation chamber, (m) Drying column, (n) Pure acid column, (o) Residue column. Adapted from Cheung et al. (2011).

There are two main advantages of this process over the previous ones; first, the use of carbon monoxide as a very cheap raw material and second, the outstanding selectivity of the methanol carbonylation (Chiusoli and Maitlis, 2006). The syngas raw material of the process can be obtained from natural gas or coal (Cheung et al., 2011). Since methanol comes from syngas, both carbons in the final product come from CO .

Common catalysts for the process are cobalt, rhodium and iridium. In any case, a mixture of acetic acid and an iodide co-catalyst is needed to activate the methanol by converting it into iodomethane according to (Chiusoli and Maitlis, 2006):



The acetic acid – HI mixture is highly corrosive and introduces the need of expensive steels. Each catalyst process is discussed extensively by Chiusoli and Maitlis (2006) and summarised below.

1.1.2.5.1 Cobalt catalysed

Developed by BASF in the 1960's, it was the very first carbonylation process. It requires high temperatures and pressures, ca. 390 K and 700 bar, respectively with around 90% selectivity.

1.1.2.5.2 Rhodium catalysed

Developed and introduced by Monsanto in 1970, the process takes place at conditions of up to 470 K and 60 bar, giving an outstanding yield of 99%. The main drawback of the process is the huge amounts of water required to prevent deactivation of the rhodium catalyst. Water as well as by-products such as propanoic acid are removed by distillation from the final product. The process was further improved to work under low water catalysis by Celanese in the 1980's under the patented acetic acid optimization (AO) technology (Cheung et al., 2011).



1.1.2.5.3 Iridium catalysed

Monsanto also developed a process involving iridium as a catalyst but it was not commercialised since it was not optimised for high water content operation. It was not until the 1990's with the BP Cativa™ process that the iridium catalysed route was fully developed. The Cativa™ process uses a ruthenium promoter and requires lower water concentrations to achieve high catalytic rates and therefore reduces operational costs. The BP acetic acid production plant is located in Hull, at the north of the UK and utilizes syngas from the North Sea.

1.1.2.6 BP Saabre™ Technology

BP has recently announced the development of a new technology to produce acetic acid directly from syngas in a three-step process that: '... eliminates the need to purify carbon monoxide, does not require the purchase of methanol and contains no iodides reducing the need for exotic metallurgy...' (BP press office, 2013a). The first industrial scale production is projected to take place at Duqm, Oman (2b1stconsulting, 2014).

1.1.3 Economic aspects

In 2008, the world production capacity of acetic acid was around 10.6 Mt/year (Cheung et al., 2011). The global demand for acetic acid in 2013 was around 10.5 Mt (North America and Europe accounting for 30% of the demand) and it is projected to grow at a Compound Annual Growth Rate (CAGR) of 4.7 – 5.1% from 2011 to 2020 to reach 15.5 Mt/year. Market revenue is estimated to reach



12,190 million USD by 2020 growing at an estimated CAGR of 9.2% from 2014 to 2020. The increase will come primarily from the rise in demand of vinyl acetate monomer and PET in emerging economies and China, but closely followed by the requirements of India and Japan. PET demand is expected to reach 25 Mt by 2020. (Companies and Markets.com; Grand View Research, 2014; Lee, 2014)

The main companies in the production of acetic acid are: BP, Celanese, Eastman Chemical and Jiangsu Sopo, sharing 65% percent of the global market altogether (Grand View Research, 2014). Most of the market, however, is dominated by Celanese and BP; Celanese operating in the American continent while BP predominantly in Europe. Celanese in Asia is based in China and Singapore while BP in Korea, Malaysia and Taiwan (Wagner, 2014). In 1999 and 2000, Celanese stopped acetic acid production in Mexico in its Cangrejera (165 kt/year) and Celaya (65 kt/year) units. Shutting down a total of 410 kt/year including the ceased production of 180 kt/year in Frankfurt, Germany in 1999. At the same time the company announced the opening of a new plant in Singapore with a production of 500 kt/year. The plans being to move from the old less efficient acetaldehyde oxidation process to their more competitive AO process (ICIS, 2000). BP production capacities in US, Europe and Rest of the World at December of 2012 were: 600, 500 and 1,400 kt/year, respectively (BP press office, 2013b). Eastman Chemical has recently announced their plans to expand carboxylic acids production in the Texas and Tennessee facilities by 20 kt/year at the end of 2014 (Chemical Processing, 2014).



1.2 Propanoic acid

Commonly known as propionic acid, it is the third of the carboxylic acids and has a chemical formula CH_3CH_2COOH . Its name comes from the Greek *protos* (first) and *pion* (fat) since it is the first of the organic acids exhibiting the properties of the fatty acids. It was named by the French chemist Jean Baptiste-Dumas in 1847 although it was first described by Johann Gottlieb (Chaput et al., 2011). Propanoic acid is a clear, colourless, corrosive liquid with a pungent characteristic odour. It exhibits intermediate characteristics between the low chain organic acids (formic and acetic acid) and the fatty acids. It appears naturally by the effect of propionic acid bacteria in the stomach of ruminants, sweat glands of humans and in cheeses, contributing to their preservation and taste (Chamba and Irlinger, 2004; Chaput et al., 2011). Propanoic acid had had little attention from industry until recent years, but is now becoming an important chemical due its increasing application as a food preservative. Data for propanoic acid are more scarce compared with that available for acetic acid. Samel et al. (2011) have made a review of the main applications of propanoic acid and its production processes which are briefly presented next.

1.2.1 Uses

In the chemical industry, propanoic acid is mainly used as an intermediate in the production of esters, the most important being cellulose acetate propionate and the vinyl propionate families, from which thermoplastics and dispersions are produced, respectively. Derivatives like the methyl-, ethyl-, propyl-, and butyl-



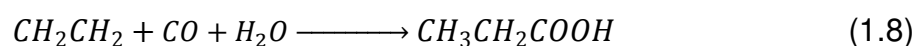
propionates are used as solvents in resins and paints formulations. Propionate ethers are used in the preparation of flavours and fragrances due to their fruity aromas. In the pharmaceutical industry it is used in the production of propionyl chloride, an intermediate for the introduction of the propionyl group in synthesis reactions. Calcium and sodium propionates are preservatives of animal feed, grain and food, mainly due to their bactericidal and fungicidal properties but also because they are cheap environmental friendly agents (Stratford, 2000; Davidson et al., 2013; IHS, 2013). It may also serve as an antiviral and at high concentrations as an acaricida. Chlorinated propionic acid takes part in herbicides. An increasing market for propanoic acid is in vitamin E production, an ingredient used for direct human consumption, in food preparation, beverage formulation, animal nutrition, skin creams, hairsprays and shampoos, among many other applications (BASF, 2006).

1.2.2 Production

Propanoic acid is produced naturally from the action of propanoic acid bacteria, named *propionibacterium* by Orla-Jensen in 1898 (Chamba and Irlinger, 2004). It is also obtained from the dry distillation of wood, nitric oxidation of 1-propanol, as a by-product in acetic acid production by carbonylation of methanol, oxidation of *n*-butene and by the reaction of ethylene, carbon monoxide and water over noble-metal catalysts (Beyer and Walter, 1997; Chiusoli and Maitlis, 2006; Samel et al., 2011). However, these routes are not economically convenient due to the low yields. Industrial production is done by any of the following processes:

1.2.2.1 Ethylene carbonylation

In the BASF process (Figure 1.5), ethylene is reacted with carbon monoxide and water in the presence of nickel propionate; the latter is converted *in situ* into nickel tetracarbonyl according to the Reppe chemistry (Beyer and Walter, 1997; Chiusoli and Maitlis, 2006):



The process takes place at 523 – 593 K and 100 – 300 bar and is characterized by high yields. Water is removed from the crude acid stream by distillation.

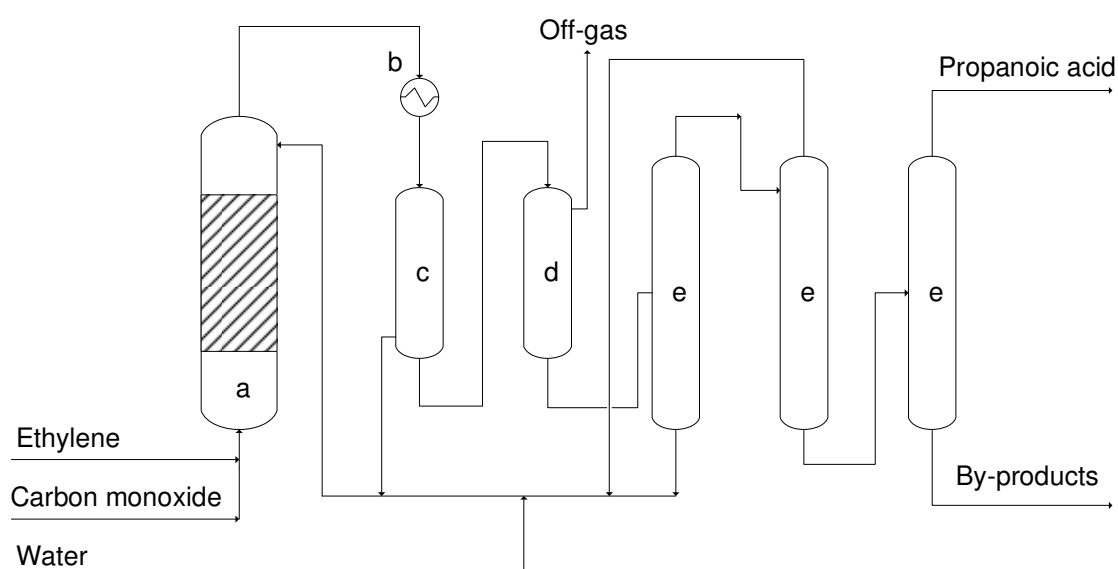


Figure 1.5. Propanoic acid BASF process. (a) High-pressure reactor, (b) Heat exchanger, (c) Separator, (d) Expansion vessel, (e) Distillation column. Adapted from Samel et al. (2011).



1.2.2.2 Oxidation of propanal

It is an economically attractive route, although two different steps are involved: i) production of propanal: by either cobalt catalysed carbonylation (403 – 423 K, 280 – 280 bar) or rhodium (or iridium) catalysed carbonylation (ca. 373 K and ca. 20 bar); and ii) its oxidation, at 313 – 323 K (Chiusoli and Maitlis, 2006).

1.2.2.3 Oxidation of hydrocarbons

The process is essentially centred on naphtha and is primarily used for acetic acid production where propanoic acid alongside other acids like formic and butyric are obtained as by-products. The BP process ([Figure 1.3](#)) takes place above 443 K and up to 45 bar. The desired acids are obtained by extractive dehydration followed by fractional distillation.

1.2.3 Economic aspects

Worldwide production of propanoic acid in 2006 was estimated in 377 kt/year (Samel et al., 2011). By 2012, 78.5% of world consumption was towards its use as a preservative (IHS, 2013). The global market value of propanoic acid and its derivatives was estimated in 944.6 million USD at 2012 and is projected to reach 1,622.2 million USD by 2018 at a CAGR of 7.8% (PR Newswire, 2013). The global market is expected to grow at a faster pace in the next four years mainly driven by the demand as a feed and food preservative in Europe, the most important market (the largest internal market is Germany, followed by the UK),



USA coming next and in developing countries due to the growing awareness of its use (BASF, 2006; Markets and Markets, 2013).

Main producers are BASF (production capacity of 149 kt/year at 2009), Dow Chemical (122.45 kt/year at 2006) and Eastman Chemical (70 kt/year at 2006) (Samel et al., 2011). Other companies are Celanese, Perstorp and Diecel.

1.3 Biofuel context

With a foreseen growth world population of 0.9% per year from 2010 to 2035, reaching an estimated of 8.6 billion people by 2035, the world energy requirements are projected to be 14,922 Mtoe by 2020 and to reach 17,197 Mtoe by 2035; of these, the bioenergy requirements are expected to become 1,881 Mtoe in 2035 (Figure 1.6) under the New Policies Scenario defined by the International Energy Agency (IEA) (OECD/IEA, 2012).

Currently, global energy requirements are mostly fulfilled by the non-renewable fossil sources, namely, petroleum, natural gas and coal. However, increasing political, environmental and economic issues around these sources have made a global priority to look for alternative, sustainable, environmental-friendly and economic sources of energy. Many countries are stabilising targets to increase participation of renewable sources. In the UK, for example, the 2009/28/EC Renewable Energy Directive has set a target of 15% of energy production to come from renewable sources by 2020 (National Renewable Energy Action Plan, 2010). In Mexico, the Secretaría Nacional de Energía through the plan Estrategia

Nacional de Energía 2012-2026 has established the guidelines to increase non-fossil source power generation by 35% (Secretaría de Energía, 2012).

Biofuels are projected to increase their contribution to the transport sector. Indeed, oil will continue to be part as an energy source with a projected world demand of 99.7 mb/d in 2035, but biofuels participation are estimated to grow from 1.3 to 4.5 mb/d (expressed in energy-equivalent volumes of gasoline and diesel) during 2011-2035 period (OECD/IEA, 2012). The participation of biofuels will be more towards their use in blends rather than as a full substitution. Around 1.5 trillion USD investment on biofuels will be needed over the period 2012-2035 (OECD/IEA, 2012). Biofuels mainly comprised bio-alcohols (ethanol and methanol from sugar, cellulose or grains), biodiesel and vegetable oils whose feedstock competes with the food supply, increasing its overall costs besides the controversial aspect (Demirbas, 2011; Nigam and Singh, 2011; Dutta et al., 2014; Yue et al., 2014).

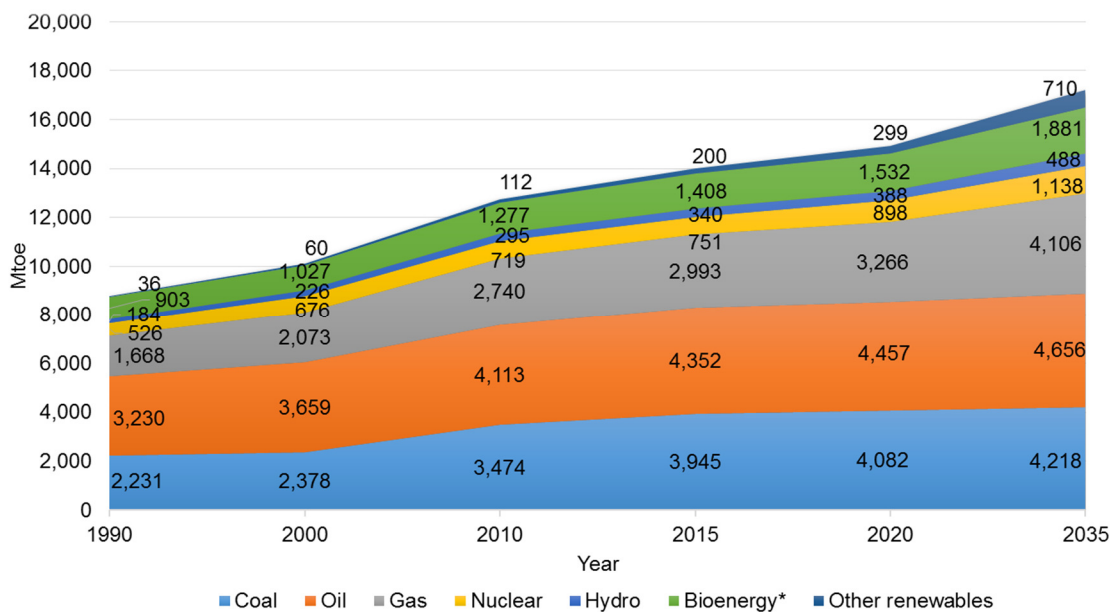


Figure 1.6. World primary energy demand by fuel in the New Policies Scenario defined by the OECD/IEA. *Includes traditional and modern biomass uses. Adapted from OECD/IEA (2012).



In addition to the rise in demand of energy, an increase in demand of commodity chemicals, like acetic acid, will certainly come. In order to diminish fossil fuel dependency, but primarily with the will of not to exceed the global temperature by more than 2°C (relative to pre-industrial levels) in the long term, there is an international focus on biomass as a renewable, environmentally-friendly and economic source of energy that does not compete with food crops. Moreover, among all the possible renewable sources of energy (e.g. wind, hydro, geothermal, solar, etc.), biomass is the only one that can also be used as a source of chemicals.

Biomass can be defined as any vegetation or biological waste whose energy can be harnessed in a fuel (Schaschke, 2014). Biomass conversion systems to produce valuable products can be classified into two main paths (Figure 1.7): Thermochemical Conversion processes or Biochemical Conversion processes. Both routes present their own challenges with no preferable option so far. The challenge in the biomass processes is to be able to produce biomass feedstocks that can be used to make fuels and chemicals that are cost competitive with traditional commodities (Demirbas, 2009b; Demirbas, 2011).

The different Thermochemical Conversion processes can be distinguished based on their temperature and pressure conditions. Liquefaction conditions are between 525 – 600 K, 50 – 200 bar; pyrolysis takes place between 650 – 800 K, 1 – 5 bar without presence of oxygen; whereas gasification takes place at 1250 – 1800 K, 25 – 60 bar without presence of water (Demirbas, 2009a).

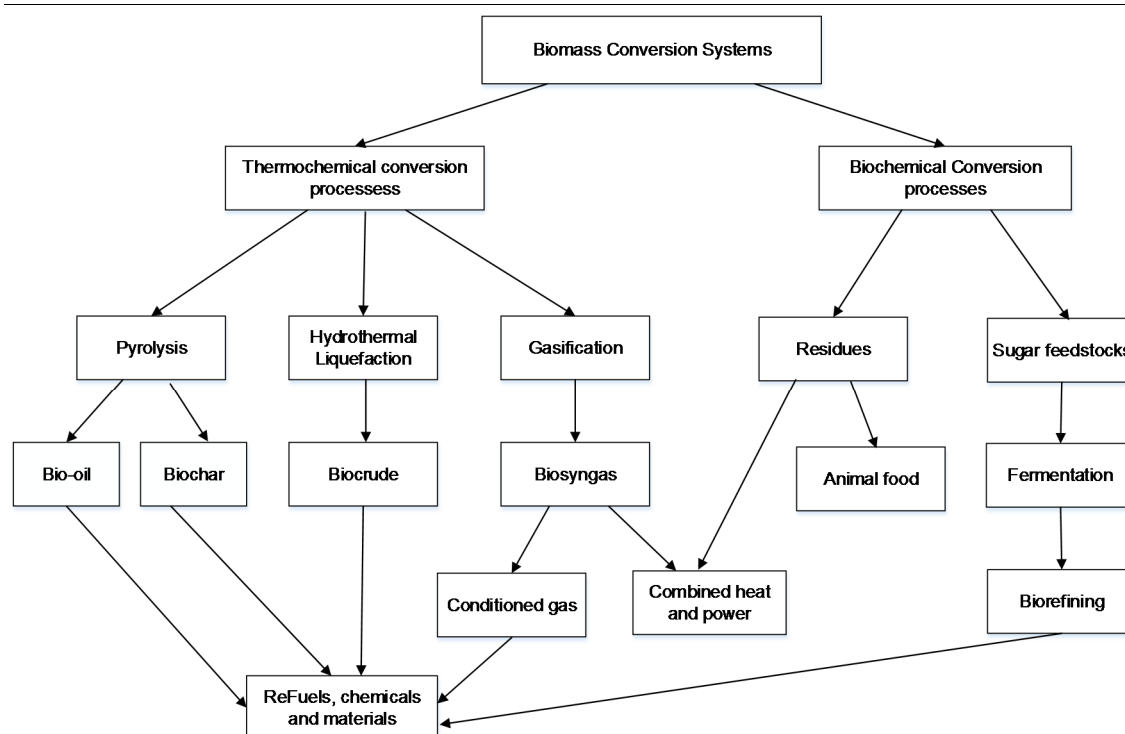


Figure 1.7. Biomass conversion systems. Adapted from Demirbas (2009a).

Bio-oil and biocrude which are the result of the pyrolysis and hydrothermal liquefaction processes (Figure 1.7), respectively, can be seen as possible substitutes of traditional oil (Yue et al., 2014). The main difference compared with traditional oil is their higher oxygen content (>20 wt.%) compared with that of oil (<1 wt.%) (Demirbas, 2011). Bio-oil and biocrude can also be differentiated according to its heating value, 15 – 22 MJ/kg for the former while 30 – 39 MJ/kg to the latter, against 43 – 46 of fossil-derived oil MJ/kg (Demirbas, 2011; Vardon et al., 2011). Bio-oil and biocrude are actually a complex mixture of organic compounds such as organic acids, phenols, alcohols and ketones as exemplified by several studies; the composition of the final mixture depends on the process, temperature, pressure, heating rate, reaction time, catalyst and feedstock (Sinag et al., 2004; Srokol et al., 2004; Asghari and Yoshida, 2006; Sinag et al., 2009; Goodwin and Rorrer, 2010; Klingler and Vogel, 2010; Sinag et al., 2010; Zhou et

al., 2010; Akhtar and Amin, 2011; Moniz et al., 2013; Rasmussen et al., 2014; Tirpanalan et al., 2014). The mixture can be upgraded in order to produce valuable fuels (with less oxygen content) or processed in order to obtain desired chemicals; it has been forecast that facilities analogous to refineries today, called biorefineries, will produce a range of chemicals in the near future (Demirbas, 2011; Yue et al., 2014).

Some investigations have also shown that acetic acid and propanoic acid are intermediates in the formation of hydrogen in the thermochemical treatment of biomass (Figure 1.8). (Goodwin and Rorrer, 2010; Sinag et al., 2010; Tanksale et al., 2010)

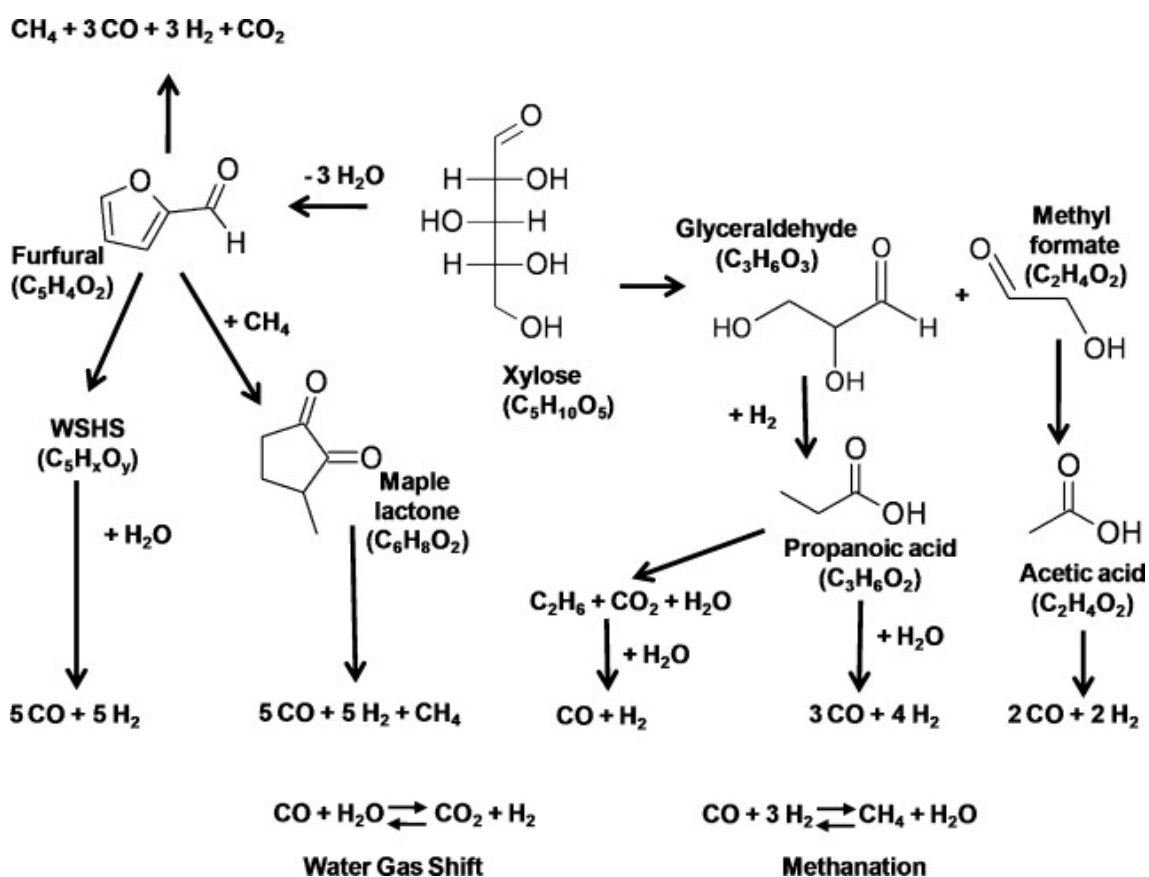


Figure 1.8. Proposed decomposition kinetic model reaction mechanism for gasification of xylose by supercritical water by Goodwin and Rorrer (2010).

1.4 Thermal decomposition

Formic acid decomposes uncatalysed into carbon monoxide, hydrogen and water even at room temperature (Hinshelwood and Topley, 1923; Nelson and Engelder, 1926; Barham and Clark, 1951; Blake et al., 1971; Bjerre and Sorensen, 1992; Yu and Savage, 1998; Yasaka et al., 2006). Studies on acetic acid and propanoic acid, on the other hand, have revealed that the non-catalysed decomposition takes place at elevated temperatures and, apart from temperature, it is a function of reaction time and concentration, in this case of water content (Bamford and Dewar, 1949; Knopp et al., 1962; Child and Hay, 1964; Blake and Hole, 1966; Blake and Jackson, 1968; 1969; Mackie and Doolan, 1984; Doolan et al., 1986). As an example, as much as 0.028% of extremely pure acetic acid taken at its normal boiling point (391.05 K) will decompose into acetic anhydride and water if kept at this condition long enough (Knopp et al., 1962).

Because of phase equilibria studies in this work were carried out at a maximum temperature of 483.2 K and in the presence of water, no effects due to thermal decomposition were foreseen.

1.5 Association

While it is now generally accepted that carboxylic acids have a tendency to form cyclic dimers in the vapour phase through hydrogen bonding ([Figure 1.9](#)) (Bhar and Lindstrom, 1955; Clague and Bernstein, 1969; Lumbroso-Bader et al., 1975; Borschel and Buback, 1988; Crupi et al., 1996), confirmed by molecular

simulations (Chen and Siepmann, 2000); and hydrogen bonded linear chains in the solid phase (Heisler et al., 2011), there is still no universal consensus regarding the predominant form in the liquid phase.

In acetic acid for example, some controversial results showed that the chain-like structure prevails in the liquid state as a result of the solid state (Heisler et al., 2011). Other authors have argued that although cyclic dimers are present in the liquid state at low temperatures, they tend to open when temperature increases (Crupi et al., 1996). Some more recent studies have shown, however, that the prevailing form is, as in the vapour phase, the cyclic dimer, in pure and dilute aqueous solutions (Genin et al., 2001; D'Amico et al., 2010; Heisler et al., 2011); an observation that seems to be confirmed by molecular simulation (Xu and Yang, 2010).

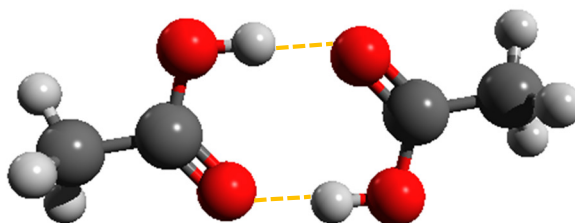


Figure 1.9. Cyclic dimerization caused by two hydrogen bonds formed by the carboxylic groups of two acid molecules.

1.6 Concluding remarks

Acetic acid and propanoic acid are two carboxylic acids positioned nowadays as commodity chemicals serving as a key agents in the formulation and preparation of a broad variety of products in several industries like the pharmaceutical, food



Carboxylic acids

and chemical. Industrial production processes of these compounds involve mixtures with water which have to be removed from the crude streams, usually by distillation. Acetic acid and propanoic acid also appear as some of the many degradation products of the thermochemical treatment of biomass. Knowledge of the properties of such acids at a wide range of temperature and pressure conditions is essential for design and optimization of these processes.

2. Phase Equilibrium Measurements

A robust design of a new chemical plant is possible through chemical process simulators which utterly take into account all sorts of physical, chemical, economic and logistic interactions and their constraints into a superstructure aiming to find the optimum arrangement. Existing plants also benefit from such simulators, typically through optimizing processes in order to reduce costs or to increase production margins. The core module in all of these simulators is the internal properties package. It contains a selection of thermodynamic models for prediction and correlation aims and a somewhat extensive database of experimentally determined thermophysical properties of pure compounds and mixtures. The thermodynamic models would not exist if there were no experimental data to which they can be compared for development or tuning. Therefore, the main prerequisite in any process design and/or optimization is to have reliable experimental data at the conditions required. These conditions can span wide ranges of temperature, pressure and composition and may involve the presence of several fluid phases. Since there are an infinite number of compounds varying in physical and chemical properties, there is thus, a vast number of possibilities regarding experimental systems and conditions that can be measured. It is because of this infinite world of possibilities that there is no universal equipment design for phase equilibrium measurements. Each equipment needs to be designed or adapted to the system and conditions in turn and on the properties sought. Additional design restraints appear when looking at factors such as experimentalist experience, budget and location of the research facility.



This chapter focuses on the design and operation of two experimental rigs for measuring vapour – liquid equilibrium (VLE) properties in the form of P_{xy} data of binary mixtures comprising acetic acid or propanoic acid with water at pressures above atmospheric, based on two different methods, namely the static-analytical and the synthetic method. Regarding the synthetic method, a new experimental technique was developed that uses Positron Emission Particle tracking (PEPT) technology as a tool to locate the vapour – liquid interface.

The chapter starts with an overview of the classification of the experimental equipment for phase equilibrium measurements. It continues with a literature review of the VLE of the acetic acid + water and propanoic acid + water systems. Details of the two designed apparatuses are then presented. Calibrations, experimental techniques, uncertainties estimation and corrosion determination procedures are provided. The experimental results are finally presented and discussed. A general assessment of the results from both techniques concludes the chapter.

2.1 Experimental methods

Two main groups of phase equilibrium measurements based on pressure can basically be distinguish: low-pressure and high-pressure measurements. Where one starts and the other finishes is relative. The criterion of Dohrn et al. (2010) which categorizes measurements as ‘high-pressure’ when at least one experimental point of any given reported data is above 10 bar has been adopted

in this work. Consequently, the data to be presented here are thus of the high-pressure kind.

Deiters and Schneider (1986) distinguish the methods for high-pressure phase behaviour as Analytical methods and Synthetic methods. A somewhat complimentary classification for vapour – liquid determinations is defined by Raal and Mühlbauer (1998) (Figure 2.1), based on if either circulation of a single phase or both phases takes place through the equilibrium cell. It is called Dynamic or Flow method when circulation takes place, and Static method when it is absent. A more broad classification is given by Dohrn et al. (2010) (Figure 2.2), in which methods are classified into two main groups: Analytical and Synthetic, and further subdivisions are made based on: sampling, intensive variable fixed, analysis and detection type.

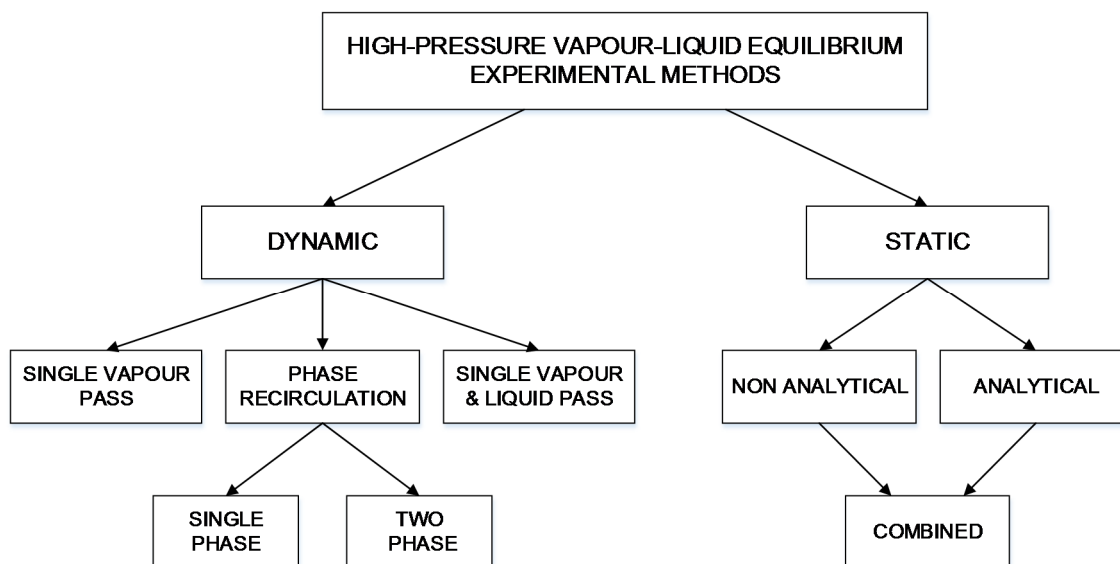


Figure 2.1. Raal and Mühlbauer (1998) classification of high-pressure vapour – liquid equilibrium experimental methods.

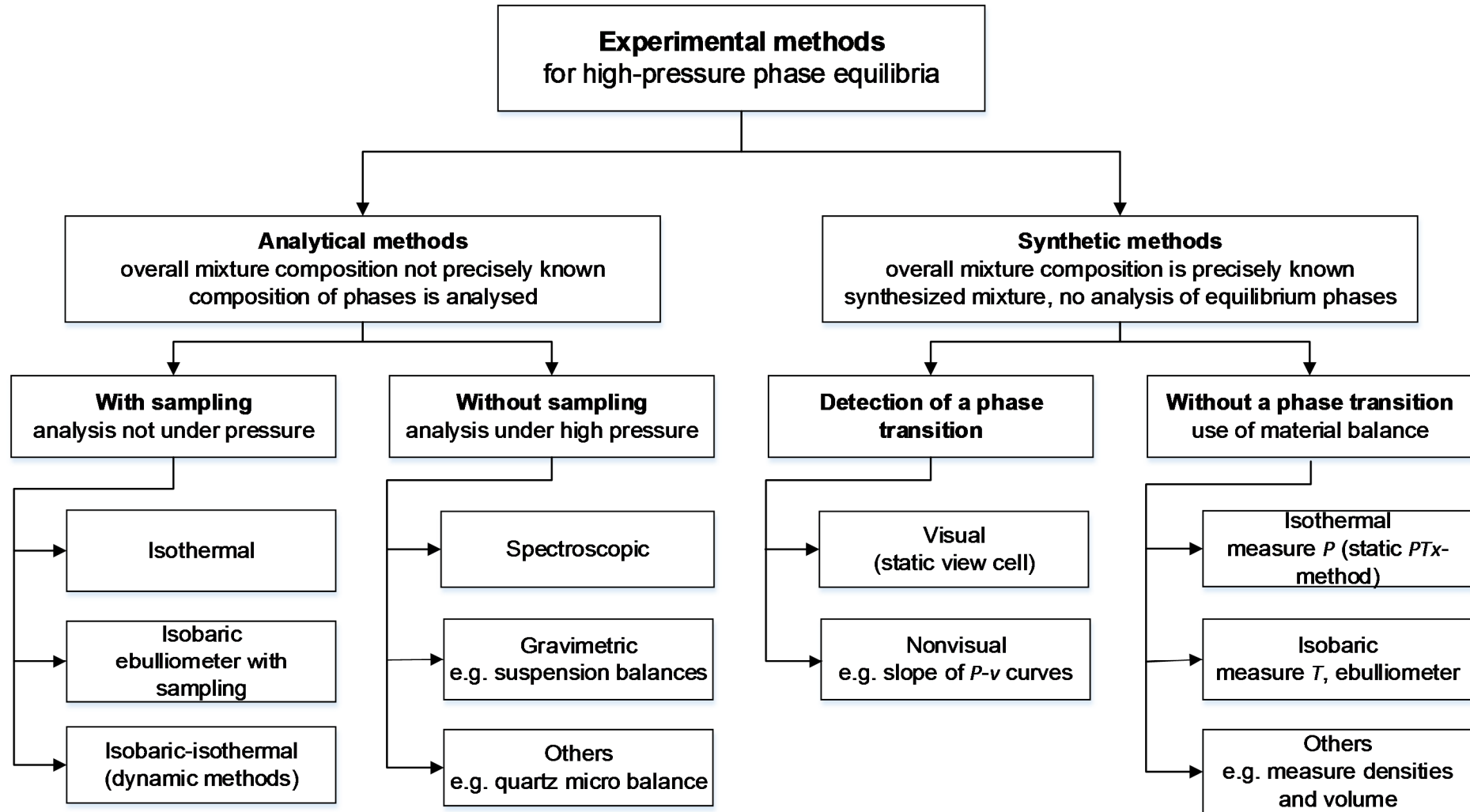


Figure 2.2. Dohrn et al. (2010) classification of experimental methods for high-pressure phase equilibria.



A general overview of the two main classes, i.e. analytical or synthetic, is given below as well as its advantages and disadvantages based on the reviews of Richon (2009); Dohrn et al. (2010); Fonseca et al. (2011) and Peper and Dohrn (2012).

2.1.1 Analytical method

In this method, a mixture of not precisely known overall composition is placed inside the equilibrium cell. Temperature and/or pressure are varied to bring about phase separation. Phase compositions can be determined with or without sampling. The main advantages of the method are that systems with more than two components can be easily studied, as well as multiphase systems. The main disadvantage is the care needed for sample preparation and handling (Deiters and Schneider, 1986). When a sample is withdrawn from the system, perturbation of the equilibrium state is undoubtedly done. How large the perturbation has to be before one may consider it significant and what measures can be taken to reduce it, are aspects that ought to be considered in the equipment design. P_{xy} and T_{xy} diagrams are the common output of this method.

2.1.2 Synthetic method

In this method, a mixture of precisely known composition is prepared and placed into the equilibrium cell. There is no analysis of the equilibrium phases. Synthetic methods can be subdivided into those with phase transitions and without phase transition. In the former case, temperature or pressure is adjusted until phase



separation of a homogeneous mixture takes place; the composition of the first large phase is set to the known overall composition and a point in the PTx diagram is established. In the latter case, properties like pressure, temperature, phase volumes and densities are measured and compositions are calculated solving the material balance. The main advantages of the synthetic methods are that the procedures are generally quick, easy and apparatus with less parts are required. Volumetric properties can also be determined if total phase volumes are measured. The main disadvantages are the precision required in the initial load preparation and that it is less applicable for multicomponent mixtures.

2.2 Literature review

2.2.1 Acetic acid + water

About the carboxylic acids, experimental VLE data for the acetic acid + water are the most readily available, 45 different articles were found reporting isothermal or isobaric data in the open literature ([Table 2.1](#)). The oldest work seems to date back to 1921 (Pascal et al., 1921) while the most recent one to 2012 (Xin et al., 2012). Most of the available data are isobaric, among these the majority is sub-atmospheric measurements. Lowest isobar is 0.01 bar while the highest is 35.48 bar. Wichterle et al. (1973; 1976) and Gmehling and Onken (1977) have compiled most of these works.

The only isobaric high-pressure work found in the open literature is that of Othmer et al. (1952), reporting isobars at 2.73, 7.90, 21.69 and 35.48 bar at temperatures



up to 516 K by means of 4 L, SS-316 static-analytical apparatus. Only five experimental points in the dilute acetic acid region are reported for the 35.48 bar isobar. The data of Othmer et al. at 2.7 bar has been validated by Houzelle et al. (1983) employing a 0.03 L glass dynamic apparatus.

Tsirlin and Vasil'eva (1962; cited in Freeman and Wilson (1985b)) and Ermolaev et al. (1972) also presented early measurements at high pressure conditions, up to 11 and 71 bar respectively; but Freeman and Wilson (1985b) have questioned the reliability of these results.

To date, the most recent paper regarding isobaric data is that of Xin et al. (2012) reporting VLE data at 1.01 bar obtained from a glass recirculating still. Unfortunately, these data do not agree with the values of Othmer et al. (1952) and Conti et al. (1960).

Most of the isothermal data available are at temperatures below 373 K, a temperature below the normal boiling point of acetic acid (391.05 K), mainly because of the corrosive nature of the compounds. The common apparatus for these kind of measurements is made of glass, which is inadequate for handling high pressures. Special alloys are thus required to handle the high pressures and the increasing corrosive conditions encountered at the higher temperatures. A review of glass apparatuses for low-pressure phase equilibria can be found in the review of Raal and Mühlbauer (1998). An exemption of the low isothermal data is that of Freeman and Wilson (1985b) who presented P_{xy} data at 372.77, 412.57, 462.06 and 502.86 K and pressures ranging from 0.56 to 27.78 bar.

**Table 2.1.** Experimental vapour – liquid equilibria for the acetic acid + water system available in the open literature.^a

Year	T range [K]	P range [bar]	Data type	Reference
1921	372 - 390	1.01	Txy	Pascal et al. (1921)
1933	-	1.01	xy	Cornell and Montonna (1933)
1933	322- 355	0.13 - 0.46	Txy	Keyes (1933)
1942	373 - 386	1.01	Txy	York and Holmes (1942)
1944	329 - 391	0.17 - 1.01	Txy	Gilmont and Othmer (1944)
1947	353 - 373	0.55 - 0.70	Pxy	Achary and Narasingrao (1947)
1947	373 - 391	1.01	Txy	Achary and Narasingrao (1947)
1950	373 - 391	1.01	Txy	Brown and Ewald (1950)
1951	-	1.01	xy	Altsheler et al. (1951)
1952	295 - 530	0.03 - 35.48	Txy	Othmer et al. (1952)
1953	373 - 388	1.01	Txy	Garwin and Haddad (1953)
1953	373 - 391	1.01	Txy	Rivenc (1953)
1954	373 - 389	1.01	Txy	Garner et al. (1954)
1956	370 - 371	0.96 - 0.97	Pxy	Ellis and Bahari (1956)
1956	355 - 370	0.53 - 0.99	Txy	Marek (1956)
1957	294 - 391	0.02 - 1.01	Txy	Chalov and Aleksandrova (1957)
1958	342 - 363	0.18 - 0.69	Pxy	Arich and Tagliavini (1958)
1960	373 - 391	1.01	Txy	Conti et al. (1960)
1960	373 - 391	1.01	Txy	Ocon et al. (1960)
1963	298	0.02 - 0.03	Px	Campbell et al. (1963)
1963	317 - 389	0.09 - 1.01	Txy	Ito and Yoshida (1963)
1964	373 - 389	1.01	Txy	Ramalho et al. (1964)
1964	313 - 333	0.05 - 0.19	Pxy	Tsiparis and Smorigai.Ny (1964)
1966	311 - 319	0.06 - 0.07	Txy	Kushner et al. (1966)
1967	373 - 386	1.01	Txy	Sebastiani and Lacquaniti (1967)
1972	342	0.18 - 0.31	Pxy	Haddad and Edmister (1972)
1973	392 - 352	0.01 - 0.47	Pxy	Lazeeva and Markuzin (1973)

Table 2.1. (Continuation)

Year	T range [K]	P range [bar]	Data type	Reference
1974	339 - 344	0.26	Txy	Linek and Wichterle (1974)
1977	339 - 391	0.27 - 1.01	Tx	Tochigi and Kojima (1977)
1979	373 - 373	0.98 - 1.08	$TPxy$	Cruz and Renon (1979)
1983	391 - 421	1.8 - 2.7	Txy	Houzelle et al. (1983)
1985	372 - 502	0.56 - 27.78	Py	Freeman and Wilson (1985a)
1985	372 - 502	0.56 - 27.78	Pxy	Freeman and Wilson (1985b)
1985	372 - 390	0.99	Txy	Narayana et al. (1985)
1985	373	1.01	Txy	Sako et al. (1985)
2001	343	0.19 - 0.30	Pxy	Miyamoto et al. (2001)
2001	372 - 390	1.00	Txy	Vercher et al. (2001)
2005	373 - 386	1.01	Txy	Calvar et al. (2005)
2005	373 - 388	1.01	Txy	Chang et al. (2005)
2006	323	0.07 - 0.12	Pxy	Bernatová et al. (2006)
2006	433 - 573	5.51 - 74.40	$TPxy$	Richardson et al. (2006)
2009	373 - 388	1.01	Txy	Xie et al. (2009)
2010	366 - 370	0.77	Txy	Navarro-Espinosa et al. (2010)
2012	374 - 389	1.01	Txy	Xin et al. (2012)

^a Temperature, T ; pressure, P ; liquid mole fraction x and vapour mole fraction, y .

The equilibrium still of Freeman and Wilson (1985b) deserves special attention since most of the modelling work currently found in the literature use these data sets. Freeman and Wilson's still (Figure 2.3), was designed to carry out VLE studies based on the static-analytical method with sampling of both phases. It was made of Inconel-600 and consisted of a still inside another still, the inner one serving as the actual equilibrium cell while the outer as a 1 L volume adiabatic chamber. The inner tube acted in an analogous way as the Cottrell tube in the glass recirculating stills. Inspection of Figure 2.3, however, reveals some

important drawbacks in the design. The most important being the lack of stirring. Thermal and concentration gradients are not eliminated and thus not allowing the system to reach truly equilibrium conditions. The returning condensate in the inner still, for example, is higher in composition of the more volatile component (in this case water) affecting the concentration of the liquid sample. As a consequence, the liquid sample point may not be the best location as well. Second, the likelihood of thermal gradients, not eliminated by proper stirring, along the upper and bottom heaters resulting in flashing of the compounds during sampling. Finally, the considerably large vapour sample line that in addition with the thermal gradient just mentioned, will most likely lead to poor reproducibility of sample concentrations.

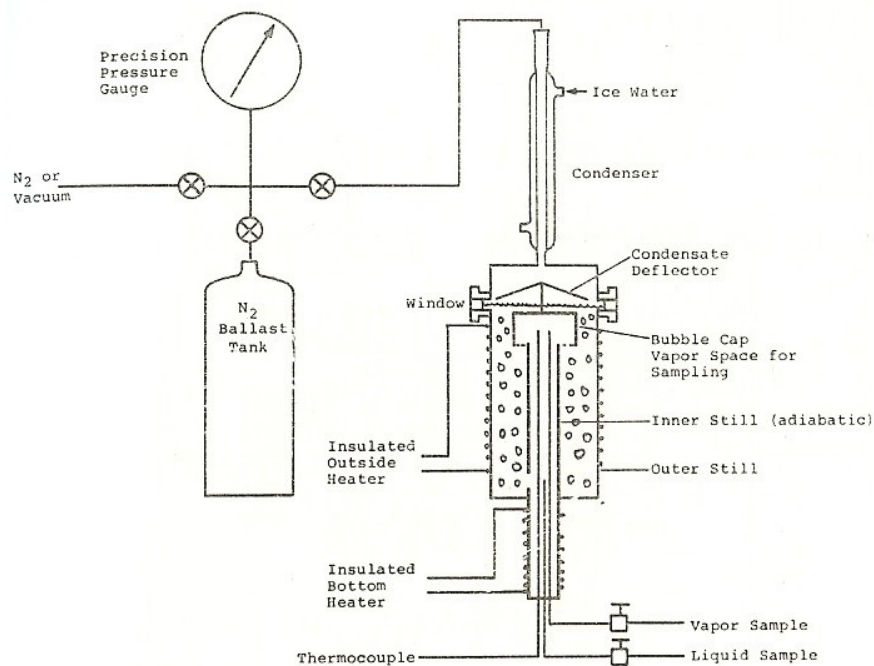


Figure 2.3. Experimental apparatus of Freeman and Wilson for vapour – liquid equilibrium measurements. Taken from Freeman and Wilson (1985b).



In an accompanying paper, Freeman and Wilson (1985a) presented *PVT* data for acetic acid + water at 373.2, 413.2, 463.2 and 503 K measured in two synthetic apparatus involving a 12 L, Inconel-600 vessel and a 26.5 L glass carboy. The last pressure measurement at any given temperature and composition corresponding to the dew point of the mixture. Unfortunately, the dew points do not agree with those reported with the analytical method a few pages later in the same journal.

Richardson et al. (2006) generated isopleths based on the analytical isothermal method (Dohrn et al., 2010; Fonseca et al., 2011) at 10, 20 and 40 wt.% liquid of acetic acid (0.032-0.166 mole fraction) by utilizing a modified 2 L volume, SS-316 Parr 4522 reactor series. Composition analysis was performed by NMR. Temperatures and pressures ranged from 433 – 573 K and 5.51 – 74.4 bar, respectively. The data agree well with that of Othmer et al. (1952) at 10% and 20 wt.% but deviations are observed at 40 wt.%. What does not seem to be consistent, however, is that based on different isobaric and isothermal data, one would expect a decrease in pressure as the amount of acetic acid in the mixture increases at any given temperature; this effect is not observed in their values. The inconsistency might be attributed to large fluctuations in temperature due to the default reactor temperature control unit employed, leading to large fluctuations in pressure. It is worth mentioning that although an uncertainty of 1 °C was reported, assigned to the resolution of the device, manufacturers' control unit manual for this kind of reactor states an accuracy of ± 2 °C. Another important point is that the original work (Richardson, 2003) does not provide any details about the dimensions of the sampling tubing employed.



As in the case of isobaric data, none of the isothermal work has reported azeotropic behaviour of the mixture.

Volumetric properties are also important for the design of process equipment. Unfortunately, literature reporting these kind of properties is rare. Only the paper of Qiao et al. (2010) could be found reporting liquid densities of acetic acid + water at high temperature and pressure conditions, in the ranges of 313 – 473 K and 1 – 32 bar, respectively.

In this thesis, new VLE was generated at 412.6, 443.2 and 483.2 K. The isotherm at 412.6 K from Freeman and Wilson (1985b) is used for comparison of our data. The experimental data at 293.15, 313.15, 343.2, 363.02 and 373.12 K from the open literature ([Table 2.1](#)) (Achary and Narasingrao, 1947; Arich and Tagliavini, 1958; Lazeeva and Markuzin, 1973; Miyamoto et al., 2001), are used for modelling in [Chapter 3](#).

2.2.2 Propanoic acid + water

VLE experimental data for the propanoic acid + water mixture are the scarcest of the three low-chain carboxylic acids. [Table 2.2](#) summarises the data currently available in the open literature. Earlier research on the system dates back to 1942 with Giacalone et al. (1942) who reported bubble-point pressures at 307.58 K and showed what seems to be an azeotrope in the 0.01 – 0.03 propanoic acid mole fraction region. A year later, Othmer (1943) reported azeotropic behaviour at 1 bar near 373 K. Gmehling and Onken (1977) have compiled most of the subsequent work, basically sub- and atmospheric measurements up to 414 K.



More recent studies by Miyamoto et al. (2001) and Olson et al. (2008), reported data at 343.2 K and liquid compositions at or below atmospheric pressure, respectively. Azeotropic behaviour has been reported in most of these publications. It is possible to appreciate from [Table 2.2](#) a lack of high-pressure and high-temperature VLE data of the system.

In this project, VLE at 423.2, 453.2 and 483.2 K were determined to increase the current available data in the open literature. Experimental data at 313.1, 343.2 and 373.1 K (Brazauskiene et al., 1965; Rafflenbeul and Hartmann, 1978; Miyamoto et al., 2001) is used for modelling in [Chapter 3](#).

[Table 2.2](#). Experimental vapour – liquid equilibria for the propanoic acid + water system available in the open literature.^a

Year	T range [K]	P range [bar]	Data type	Reference
1942	307	0.055 - 0.058	Px	Giacalone et al. (1942)
1943	372 - 414	1.01	Txy	Othmer (1943)
1954	371 - 414	1.01	Txy	Johnson et al. (1954)
1961	372 - 401	1.01	Txy	Dakshinamurty et al. (1961)
1961	324 - 414	1.01	Txy	Rivenq (1961)
1962	311 - 373	0.06 - 1.01	TPx	Zheleznyak (1962)
1962	372 - 395	1.01	Txy	Aristovich et al. (1962)
1963	317 - 404	1.01	Txy	Ito and Yoshida (1963)
1965	313 - 333	0.01 - 0.19	Pxy	Brazauskiene et al. (1965)
1967	373 - 401	1.01	Txy	Kushner et al. (1967)
1975	372 - 410	1.01	Txy	Amer (1975)
1978	332 - 372	0.05 - 1.03	Pxy	Rafflenbeul and Hartmann (1978)
1985	373	1.01	Txy	Sako et al. (1985)
2001	343	0.09 - 0.32	Pxy	Miyamoto et al. (2001)
2008	325 - 373	0.13 - 1.01	Tx	Olson et al. (2008)

^a Temperature, T ; pressure, P ; liquid mole fraction x and vapour mole fraction, y .



2.3 Static – Analytical Measurements

The static – analytical measurements were carried out for both the acetic acid + water and for the propanoic acid + water systems. In this section, details about the equipment designed and the methodology employed are given.

2.3.1 Chemical compounds

[Table 2.3](#) summarizes the chemical compounds used in the experiments as well as their corresponding purities. Gas – Chromatography (GC) analysis with a TCD detector of the organic acids revealed two main peaks, one corresponding to the carboxylic acid and the other to water in accordance with their hydrophilic characteristics. A third small peak accounting for 0.028% and 0.030% of the mass sample were unidentified impurities of the acetic acid and propanoic acid reagents, respectively. The impurity was considered to be part of the water content in both cases. Chemicals were used without further purification and were only subjected to a degassing process as described in [Section 2.3.3](#).

[Table 2.3](#). Chemical compounds and purities used in the experiments.

Chemical name	CAS number	Source	Initial mole fraction purity	Purification method	Final mole fraction purity	Analysis method
acetic acid	64-19-7	Sigma-Aldrich	0.9901	-	-	GC ^a
propanoic acid	79-09-4	Sigma-Aldrich	0.9798	-	-	GC
water	7732-18-5	Sigma-Aldrich	1	-	-	-

^a Gas – Chromatography.



2.3.2 Apparatus description

A fit for purpose apparatus was designed and constructed since no trademark equipment is currently available in the laboratory. The following aspects were taken as design basis: working conditions of up to 503 K and 20 bar. Construction material ought to be resistant to corrosion attack at the working conditions and at high organic acid concentrations. Water as the added component for safety and corrosion issues. The liquid state of the chemicals at room conditions.

A schematic view and the actual experimental apparatus constructed is shown in [Figures 2.4](#) and [2.5](#), respectively. It consists mainly of an equilibrium cell (composed of a vessel and its head), a temperature control environment, a liquid feeding pump, a vacuum pump, a pressure gauge, thermocouples, a magnetic-drive stirrer and a gas-chromatograph.

2.3.2.1 Equilibrium cell and fittings

A Parr 4575 reactor series was modified to serve as the equilibrium cell. It is rated to 773 K and 345 bar. It consists of a 250 mL nominal volume, 2.5" internal diameter (ID) and 3.25" outside diameter (OD), cylinder and a movable head. Both bodies as well as all the internals are made of Hastelloy C-276, an alloy capable to resist organic acids corrosive attack (Garverick, 1994). A PTFE gasket seals the cylinder and the head. The original set-up of the reactor consists of six ports: i) pressure gauge and vapour sampling valve, ii) liquid sampling valve, iii) and iv) cooling loop ports, v) thermowell and vi) safety rupture disc.

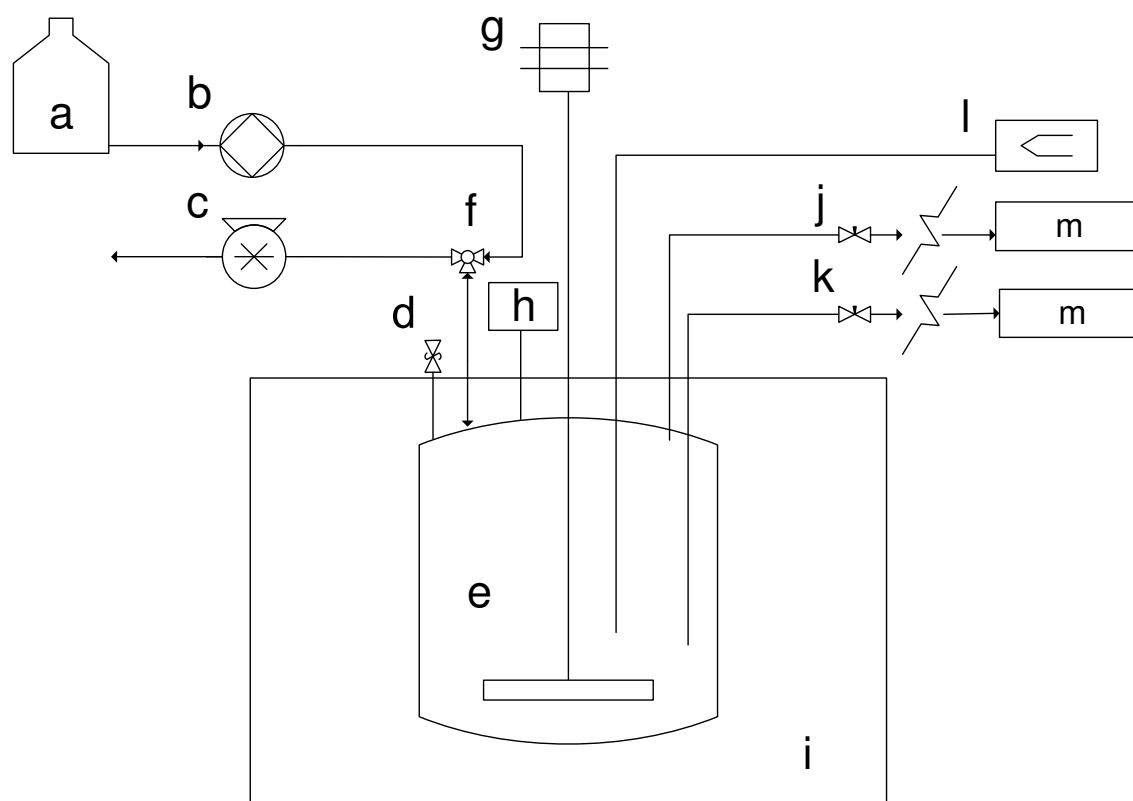


Figure 2.4. Schematic drawing of the static – analytical apparatus. (a) Water supply, (b) Digital liquid-pump, (c) Vacuum-pump, (d) Safety rupture disc, (e) Equilibrium cell, (f) Three-way valve, (g) Magnetic drive, (h) Digital pressure gauge, (i) Air bath, (j) Liquid sampling valve, (k) Vapour sampling valve, (l) Thermocouple data logger.

The cooling loop, liquid sample dip tube and sample valves were removed and replaced by new fittings. [Figures 2.6](#) and [2.7](#) show the original and the modified reactor (equilibrium cell), respectively. The original sampling valves were initially substituted by 1/16", grafoil packing, HIP needle valves. However, during the initial trials, it was observed that the packing tended to fall apart during the course of a few samples, blocking the lines. The valves were then replaced by Swagelok ball valves (SS-41GS1) with modified PTFE packing. SS-316 tubing, 1/16" OD and 0.005" ID was used for the sampling lines. Sampling tubing lengths were of 20 cm and 5 cm for the liquid and vapour lines, respectively. Tubing lengths after the valves were of 5 cm for both lines.

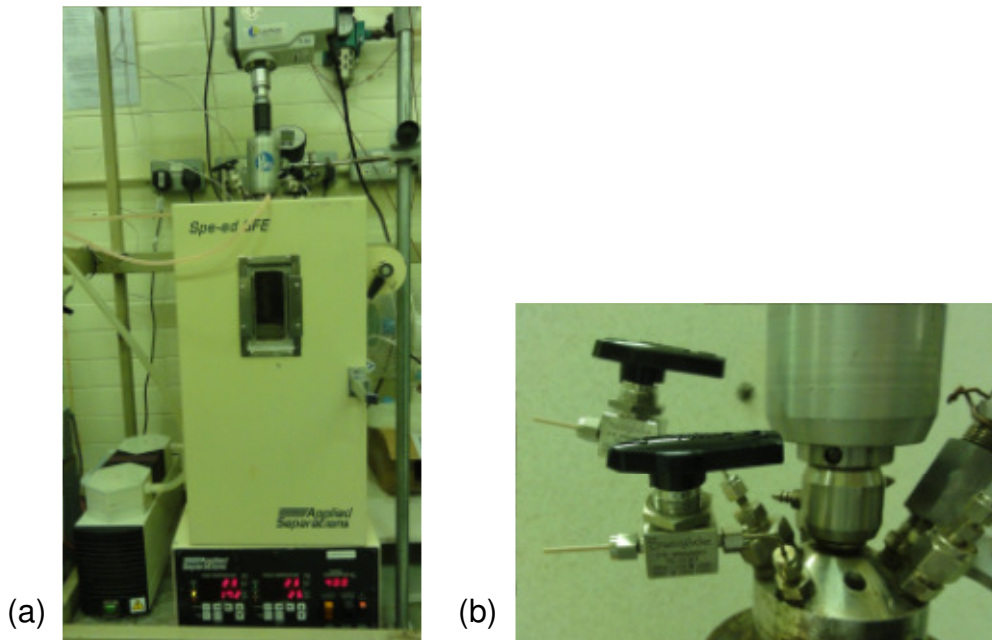


Figure 2.5. (a) Actual view of the static – analytical apparatus. (b) Close up of sampling valves.

For the experiments with propanoic acid, the sampling lines were replaced by 0.004" ID tubing while the downstream tubing was replaced by 0.064 mm nominal ID (0.003"), 3 cm length, PEEK tubing; reducing the dead volume by 60% and 45% for the vapour and liquid lines, respectively. SS-316 tubing was purchased from Swagelok while the PEEK tubing from RESTEK. Custom-made SS-316 reducers were constructed in the Chemical Engineering workshop to shift from the original 1/4" NPT connector to the 1/16" compression ones. In light of the modifications, the vessel would require re-assessment of pressure and temperature to evaluate its rating. It is hard to determine the new rating without proper tests, but the vessel was taken to 100 bar at room temperature without signs of leaking.

A three-way valve attached to one of the original cooling loop ports, selected between water addition and vacuum services. The second cooling loop port connected a digital pressure gauge through a 10 cm length, 0.01" ID, 1/16" OD,

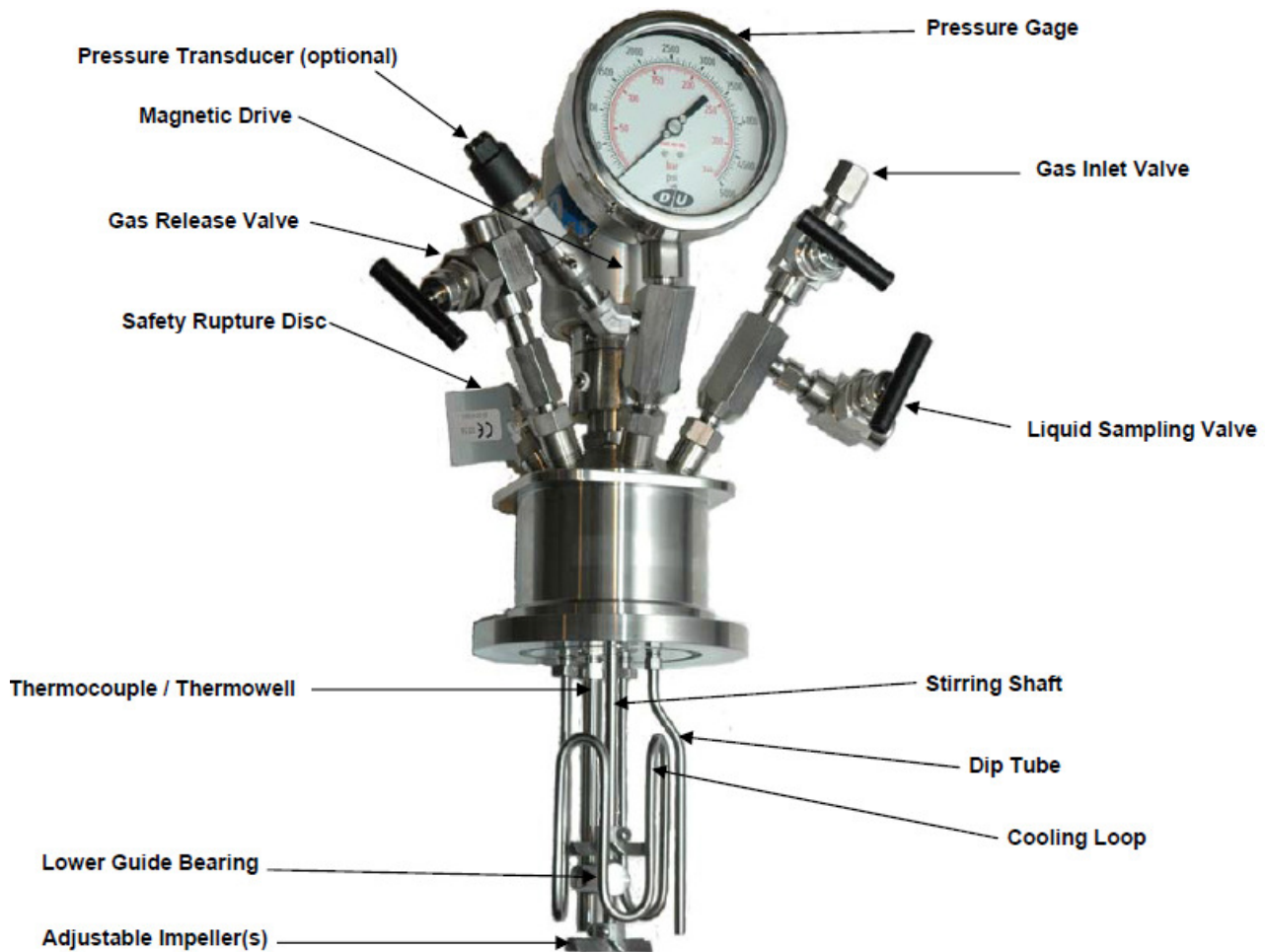


Figure 2.6. Original set-up of the Parr 4575 reactor series. Taken from Parr Instrument Company (2014).

SS-316 tubing. This length was needed in order to reduce the temperature of the fluid in contact with the pressure gauge. A DIN 3869 EPDM (ethylene propylene diene monomer (M-class)) soft seal for G 1/4" size sealed the pressure gauge connector. This material avoided chemical attack of the seal.

The originally supplied type J thermocouple was replaced by a type T (due to its lower tolerance) to measure temperature at the interior of the vessel. It was placed inside the thermowell, so direct contact with the fluid was avoided.

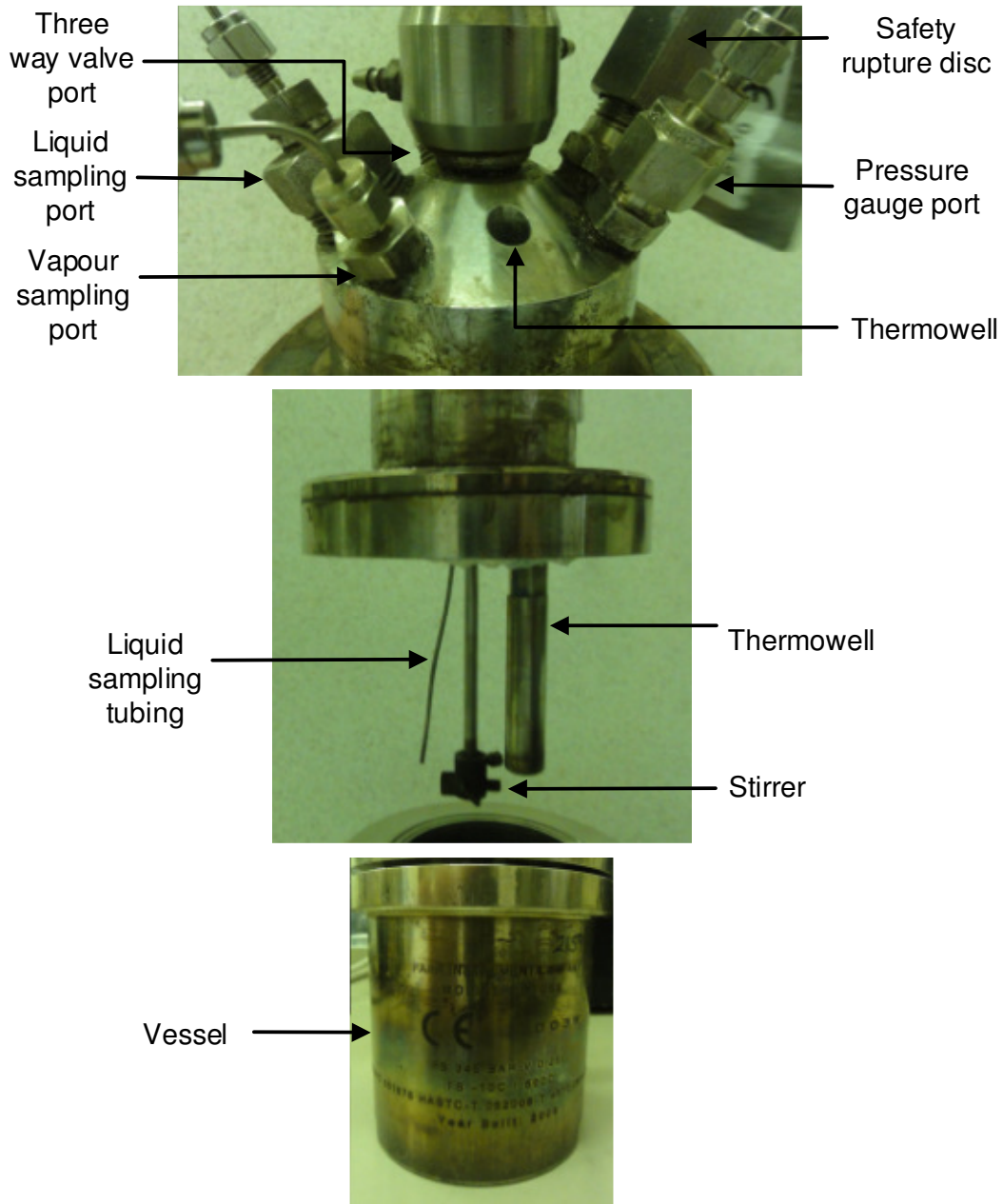


Figure 2.7. Modified reactor (Equilibrium cell) for the static – analytical measurements.

Three other thermocouples (type T), one at the side, one at the outside bottom of the equilibrium cell and one at the middle of the oven helped to produce a temperature profile.

The original port for the rupture disc remain unchanged as well as the stirrer and the lower guide bearing. Stirring was accomplished by the magnetic drive



attached to the head of the vessel. Its internal parts are made of Hastelloy C-276.

Three rubber bushings avoided contact of the fluids with the internal parts of the stirrer.

A digital pressure gauge (Keller-Druck, LEX1), range 0 – 20 bar with 0.001 bar resolution, measured pressure with a ± 0.01 bar accuracy according to manufacturer's calibration certificate ([Appendix B](#)).

An oven (Applied Separations, model Spe-ed SFC) previously used for supercritical extractions was modified to act as the temperature control environment. A hole of 15 cm diameter, wide enough to leave room to place the equilibrium cell, was cut at the top of the oven. In actual operation, a 5 cm thick layer of glass fibre insulation material prevented heat losses from the top. The maximum operating temperature of the oven is 400 °C with a resolution of 1 °C.

2.3.2.2 Peripherals

A data logger (Pico Technology, model TC-08) for up to eight channels, plugged into a PC via USB interface, monitored and recorded temperatures with a resolution of 0.05 K.

A vacuum pump (KNF Neuberger Edwards, model Laboport PM 13196-840.3) vacuumed the cell at the beginning of each experiment.

Water was loaded into the equilibrium cell by means of a liquid high-pressure pump (JASCO, model PU-1586).



Mechanical mixing to induce equilibrium was done by a Hastelloy C-276 internal stirrer attached to a magnetic drive (PARR Instruments, model A1120HC) with internals of the same alloy, and attached to a head stirrer (Heidolph RZR 2020).

Quantitative analysis was done by GC. Details of the analytical equipment are given in the TCD calibration section (2.3.2.4).

2.3.2.3 Thermocouples calibration

The three thermocouples located outside the equilibrium cell were calibrated against mercury thermometers with 0.1 °C graduation by measuring temperatures of water from its normal freezing point up to its normal boiling point. Maximum deviations from the mercury thermometer readings were 0.5 K.

The thermocouple located inside the equilibrium cell was calibrated *in situ* by comparing measured vapour pressures of water from 301 to 487 K against equilibrium data from the National Institute of Standards and Technology (NIST). Table 2.4 shows the vapour pressures readings, P_{read} , the temperatures readings, T_{read} , and the corresponding reference temperatures, T_{NIST} , retrieved from NIST database (NIST, 2011). The following polynomial of second order described the functionality of the readings (Figure 2.8):

$$T_{calc}/K = -3.89 \times 10^{-5} (T_{read}/K)^2 + 1.033 T_{read}/K - 7.89 \quad (2.1)$$

where T_{calc} stands for a calculated temperature. Deviations from the reference temperature given by the use of Equation (2.1) are shown in Figure 2.9. The

maximum and minimum deviations are 0.30 K and 0.04 K, respectively; these values aided in the uncertainty calculation described in [Section 2.3.4](#).

Table 2.4. Reading temperatures, T_{read} and reference temperatures, T_{NIST} , at reading vapour pressures of water, P_{read} .

P_{read} [bar]	T_{read} [K]	T_{NIST} [K] ^a
0.035	301.07	299.82
0.982	372.87	372.24
1.474	384.75	383.98
3.565	413.28	412.65
3.558	413.19	412.59
3.572	413.17	412.72
3.574	413.29	412.74
4.797	423.99	423.43
4.795	423.99	423.41
4.797	424.01	423.43
4.796	423.99	423.42
4.799	424.01	423.44
20.114	486.47	485.81
20.160	486.60	485.93
20.164	486.62	485.94

^a Data from NIST (2011).

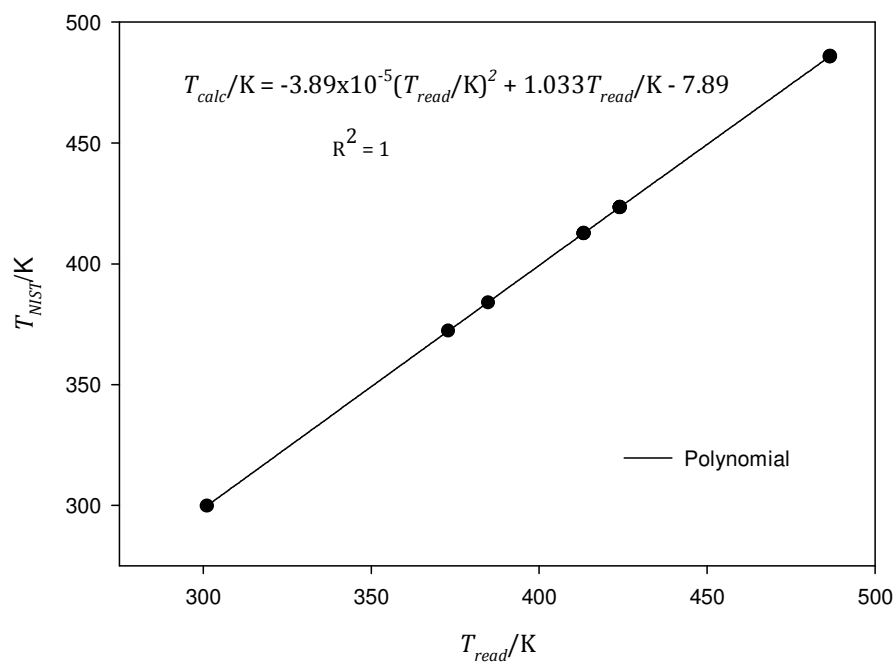


Figure 2.8. Calibration plot for the thermocouple at the interior of the equilibrium cell. T_{calc} is the calculated temperature from the second order polynomial.

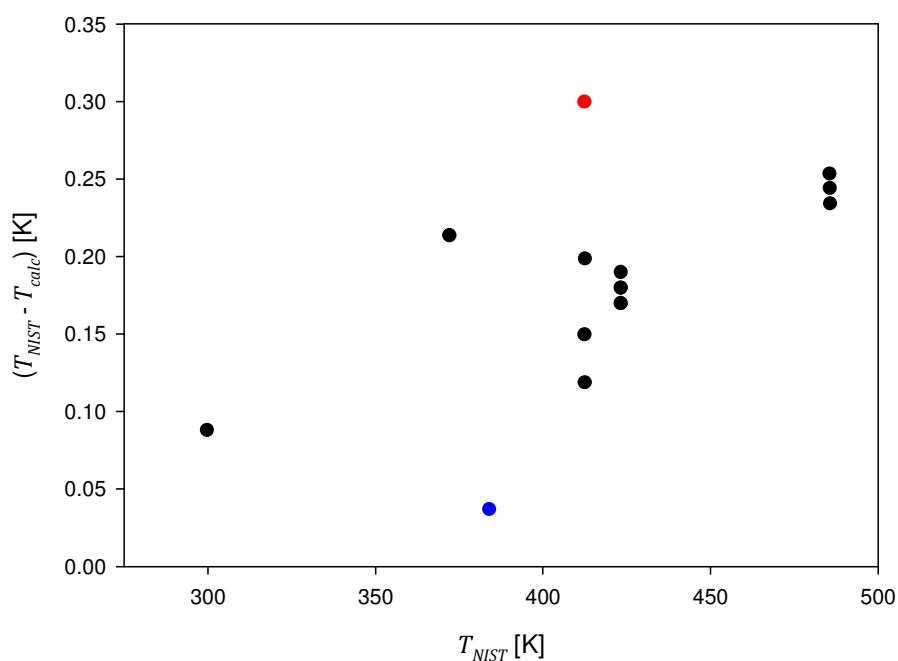


Figure 2.9. Deviations from the reference temperature, T_{NIST} , by the use of the second order polynomial Equation (2.1). (●) Maximum deviation, (●) minimum deviation.

2.3.2.4 TCD calibration

A Gas – Chromatograph (Agilent Technologies, model 6850), analysed the samples. It is equipped with a thermal conductivity detector (TCD) connected to a data acquisition system (Agilent Chem Station, version B.02.01). The TCD was chosen in order to detect the organic compounds as well as water. Carrier gas was Helium obtained from BOC with a certified purity $\geq 99.999\%$. Separation was done by a Porapak N packed column with 80/100 mesh for alumina, 3' x 1/8" SS (Speck and Burke Analytical). An autosampler (Agilent Technologies, model 7683B) injected the samples for precision and reproducibility.



The calibration procedure of Raal and Mühlbauer (1998) for liquid sample injections was adopted in this work. The method consists of injecting gravimetrically prepared samples of known composition (standards) to get the peak area, A , related to the number of moles, n , passing through the detector. The response factor, F , is then defined as the proportionality constant between n and A ; that is, for any i component: $n_i = A_i F_i$. Raal and Mühlbauer have suggested to work with area ratios since the amount of sample injected (and consequently the peak Area) is not very reproducible, thus for a binary system:

$$\frac{n_1}{n_2} = \frac{x_1}{x_2} = \left(\frac{A_1}{A_2}\right) \left(\frac{F_1}{F_2}\right) \quad (2.2)$$

where x is the mole fraction. A plot of the GC area ratios A_1/A_2 , versus mole fraction ratios x_1/x_2 has a slope F_2/F_1 , corresponding to the response factor ratio, which is expected to be constant over the entire composition range. Preliminary results showed a non-constant response factor in terms of molar fractions, but constant in terms of mass fractions, w , for the systems studied here.

In this way, gravimetrically prepared organic acid + water standards were prepared in the range of 0 – 0.99 mole fraction of the organic acid. Desired amounts of the compounds were weighed in an electronic semi-microbalance (Sartorius, model R-160-P) to an accuracy of ± 0.1 mg. 0.2 μL of the standard solutions were injected by the autosampler equipped with a 0.5 μL syringe (SGE). Three sequences of two injections per sample were performed. Specific methods were developed for each mixture to optimize analysis time. [Table 2.5](#) summarizes



the GC operating conditions for the individual methods. Full details can be found in [Appendix C](#).

The mass fraction ratios and the corresponding area ratios for the acetic acid + water standards, for the low and high concentration ranges, are plotted in [Figure 2.10](#), to check for constant response factor ratios. At both limits, the plots

extrapolate to the origin and the slope of $\frac{F_{water}}{F_{acetic\ acid}} = 0.4764 = \frac{1}{2.1077} = \frac{F_{acetic\ acid}}{F_{water}}$.

It is concluded that a single F_2/F_1 can be used in the entire composition range.

Similarly, the calibration plots for propanoic acid + water ([Figure 2.11](#)) show constant F_2/F_1 . Deviations from the standard, w_{std} , and calculated, w_{calc} , mass fractions of the two systems are plotted in [Figures 2.12](#) and [2.13](#). Maximum and minimum deviations for the acetic acid and the propanoic acid mixtures are: 0.010, -0.003 and 0.014, -0.003, respectively. The response factor ratios used in the experimental analysis were finally: 2.1077 and 1.6826, for the acetic acid and the propanoic acid systems, respectively.

Table 2.5. GC operating conditions for acetic acid and propanoic acid determination in aqueous mixtures.

Method	Inlet Temperature [K]	Oven Temperature [K]	Column flow [mL/min]	Detector temperature [K]
acetic acid	503	423	40 (1 min), 60 (4 min) at 10 mL/min	473
propanoic acid	503	453	45	473

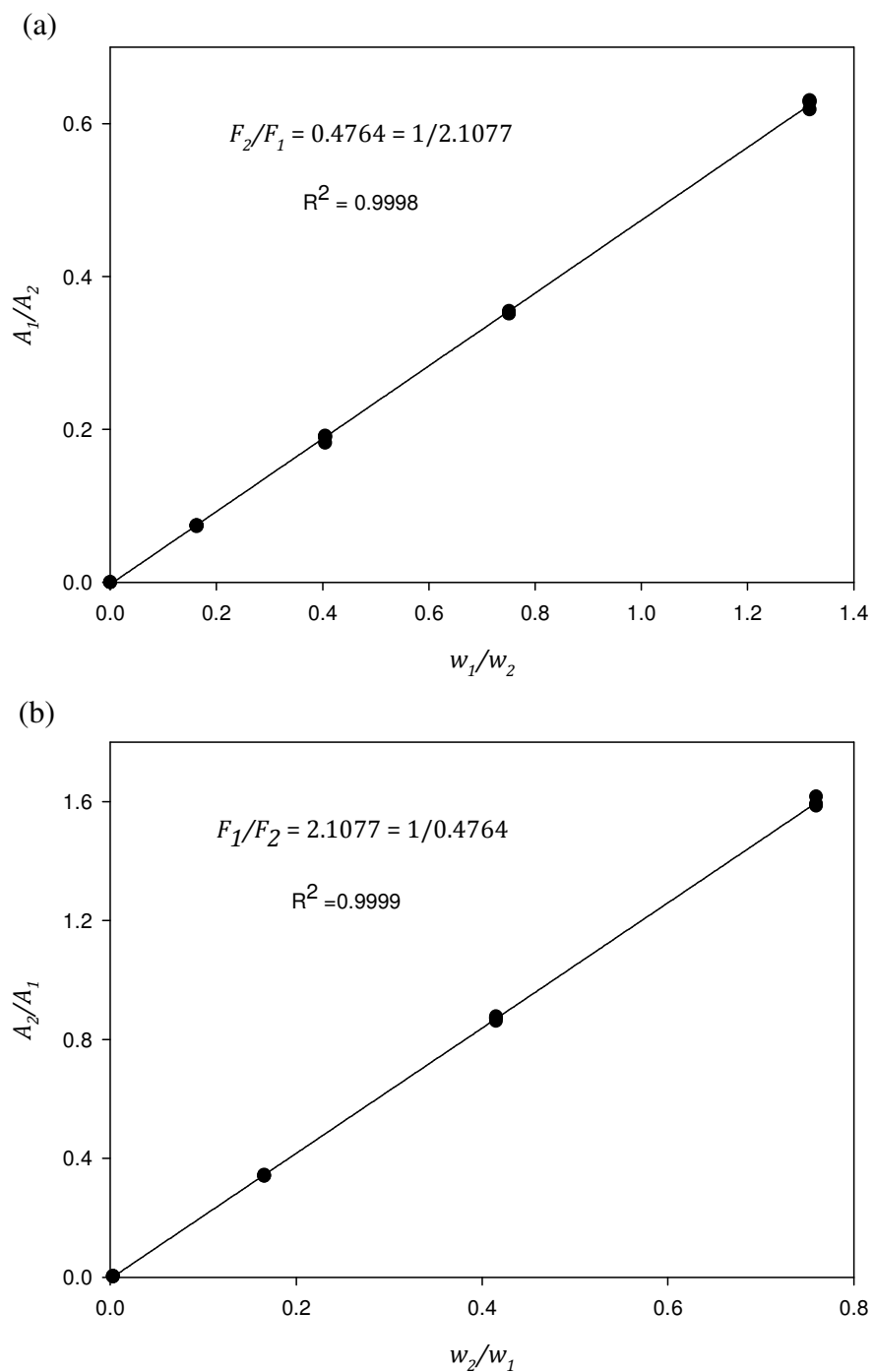


Figure 2.10. TCD calibration plots for the acetic acid (1) + water (2) system. (a) Low acetic acid concentration range. (b) High acetic acid concentration range.

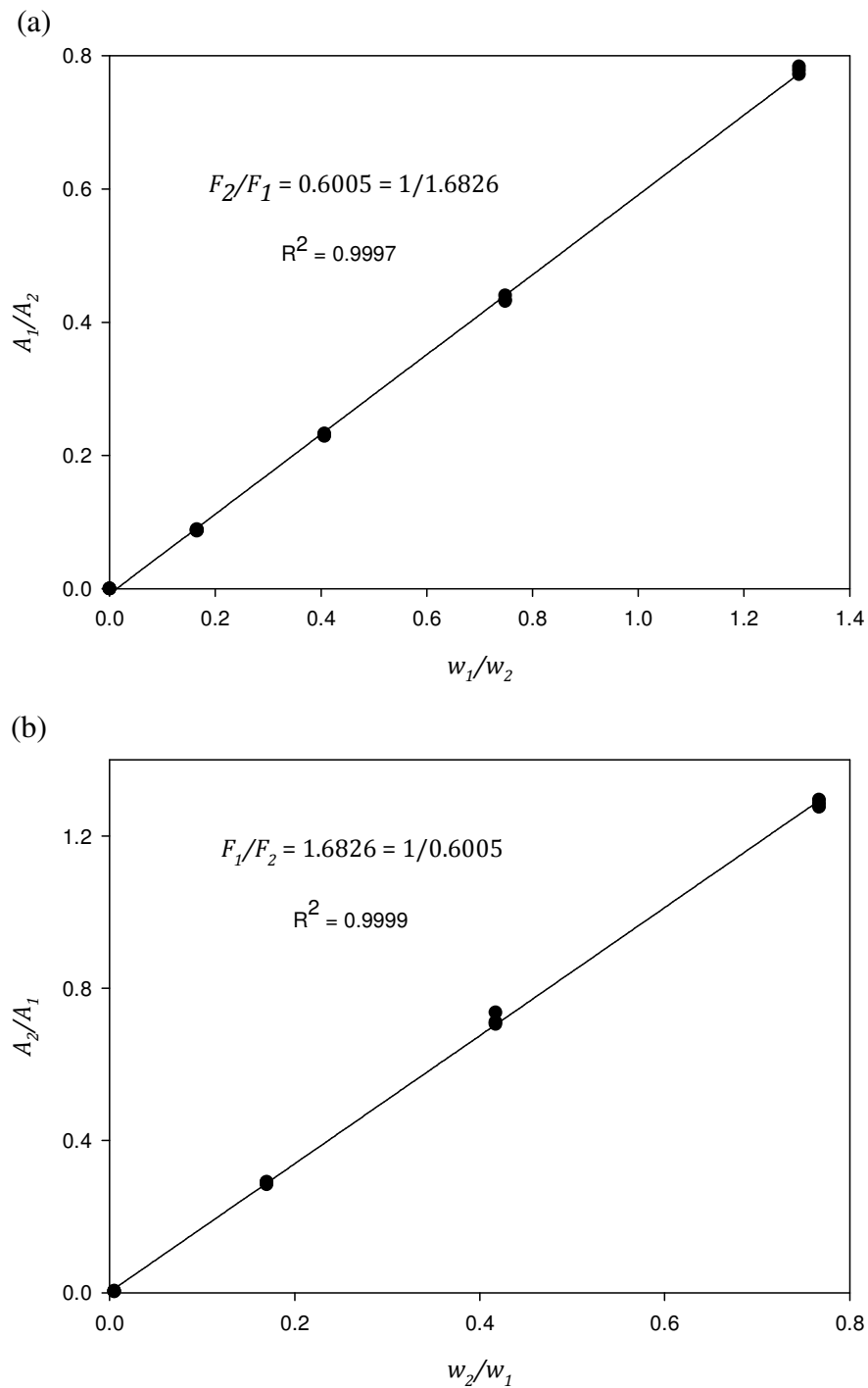


Figure 2.11. TCD calibration plots for the propanoic acid (1) + water (2) system. (a) Low propanoic acid concentration range. (b) High propanoic acid concentration range.

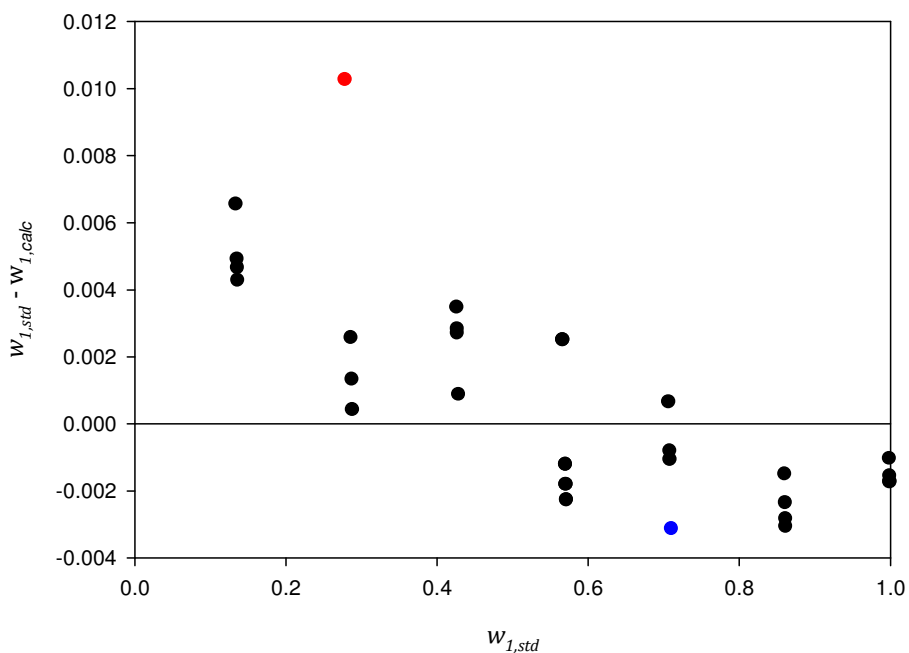


Figure 2.12. Deviations from the standard acetic acid mass fraction, $w_{1,std}$, by the use of response factor ratio = 2.1077. (●) Maximum deviation, (●) minimum deviation.

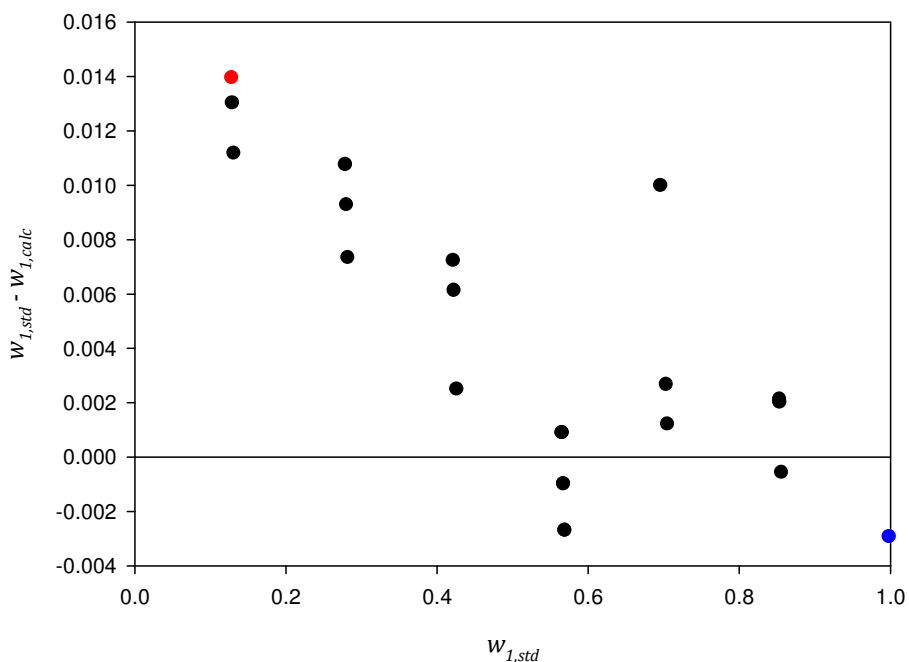


Figure 2.13. Deviations from the standard propanoic acid mass fraction, $w_{1,std}$, by the use of response factor ratio = 1.6826. (●) Maximum deviation, (●) minimum deviation.



2.3.3 Experimental procedure

Before each experimental run, the vessel and head were disassembled and the magnetic drive was disengaged from the head. The head stirring chamber was dismantled to allow a thorough cleaning since small amounts of the compounds from previous runs can reach the top of the magnetic drive.

All the parts disassembled, these and the sample lines were washed and rinsed with ethanol and acetone, and left to dry in an oven for around 4 hours. After this time, the parts were then allowed to cool to room temperature. Visual checks of the PTFE seal were carried out and, if needed, replaced by a new seal. All parts were then purged with nitrogen to remove solvent traces. The cell was assembled and closed using a torque wrench to a bolt torque of 15 ft-lbs. A leak test with compressed nitrogen at 80 bar and room temperature was run overnight.

Approximately 60 mL of the compounds were degassed in an ultrasonic bath degasser (Grant, model XB6) for 1 hour. A mixture of the organic acid and water was immediately loaded into the equilibrium cell, this was closed and vacuumed down to 0.015 – 0.020 bar at room temperature under constant stirring and kept at this condition for 1 hour. The desired equilibrium cell temperature was achieved by manually controlling the temperature of the oven. The system was then allowed to reach equilibrium condition under constant stirring, at 40 rpm, which was assumed when temperature and pressure did not vary within $\pm 0.05\text{K}$ and ± 0.005 bar, respectively, for at least 5 minutes. The thickness of the vessel helped for a favourable control of the temperature.



Once in equilibrium, sampling of the phases took place. A minimum of five samples of each phase, (20 μL volume each), were withdrawn and collected in 250 μL vial inserts (Agilent Technologies) for further analysis by GC. The first three samples were discarded to purge the lines from the previous sample composition. During sampling, the first sample taken was usually from the liquid phase as it induced less pressure drop. For the case of the vapour sampling, it was possible to take advantage of the liquid state condition of the mixtures at ambient conditions, the lines and the valve serving as a condenser. This approach was previously used in the work of Freeman and Wilson (1985b). Sampling was done quick enough to reduce equilibrium perturbation, which was monitored by checking for pressure drops; although not avoidable, these did not exceed 0.01 bar. The relatively large volume of the equilibrium cell and the low dead volume of the sample lines aided to reduce the equilibrium perturbation.

Pressure was then increased by pumping additional water into the cell and a new equilibrium point was then established. An experimental run to get 4 experimental points usually took around 12 hours. Several experiments with different initial overall loadings were needed to complete the full phase diagram.

2.3.4 Uncertainties determination

The Guide to the Expression of Uncertainty in Measurement (GUM, 2008) defines uncertainty as a “parameter, associated with the result of a measurement, that characterizes the dispersion of the values that could reasonably be attributed to the measurand”. When a combination of different sources to the dispersion is included it is called combined uncertainty, u_c , expressed for any θ quantity as:

$$u_c(\theta) = \sqrt{\sum_i u_i(\theta)^2} \quad (2.3)$$

where $u_i(\theta)^2$ are the variances of the different possible sources of uncertainty, determined basically by the experimentalist and believed not to be negligible. The uncertainties in temperature, pressure and composition are the ones of interest in this thesis. The following subsections provide details of the sources of uncertainty considered in the estimation. Most of the uncertainties calculated here belong to those classified as subjective probability or Type B standard uncertainty. The procedure is based on the recommendations of Taylor and Kuyatt (1994); GUM (2008) and Patience (2013).

2.3.4.1 Temperature

The combined standard uncertainty in temperature, $u_c(T)$, is given by the contributions due to the calibration, $u_{calib}(T)$, resolution, $u_{resl}(T)$, and control, $u_{cont}(T)$:

$$u_c(T) = \sqrt{u_{calib}(T)^2 + u_{resl}(T)^2 + u_{cont}(T)^2} \quad (2.4)$$

Assuming rectangular distribution, $u_{calib}(T)^2$ is calculated from:

$$u_{calib}(T)^2 = \frac{(a_+ - a_-)^2}{12} \quad (2.5)$$

where a_+ and a_- are the maximum and minimum deviations retrieved from the calibration equation.

For a given resolution, δx , of a digital device the associated uncertainty is:

$$u_{resl}(T)^2 = \frac{(\delta x)^2}{12} \quad (2.6)$$

Considering rectangular distribution and the temperature to be controlled within a_+ and a_- bounds and their difference expressed as $2a$, Equation (2.5) can be written for the control contribution as:

$$u_{cont}(T)^2 = \frac{a^2}{3} \quad (2.7)$$

2.3.4.2 Pressure

For the pressure uncertainties, the contributions considered to be influential are those of the calibration, $u_{calib}(P)$, repeatability, $u_{rep}(P)$, and pressure drop during sampling, $u_{sampl}(P)$:

$$u_c(P) = \sqrt{u_{calib}(P)^2 + u_{rep}(P)^2 + u_{sampl}(P)^2} \quad (2.8)$$

The calibration uncertainty is in this case calculated from the error, stated by the manufacturer's calibration certificate, $\Delta P_{certificate}$. Assuming an interval of confidence of 95%, the variance is:

$$u_{calib}(P)^2 = \left(\frac{\Delta P_{certificate}}{1.96} \right)^2 \quad (2.9)$$

The variance due to the repeatability can be calculated from the standard deviation, σ , of a series of N measurements according to:

$$u_{rep}(P)^2 = \left(\frac{\sigma}{\sqrt{N}} \right)^2 \quad (2.10)$$

$u_{sampl}(P)$ was considered as the maximum pressure drop, ΔP_{max} , observed during the sampling process. The corresponding variance can be calculated from:

$$u_{sampl}(P)^2 = (\Delta P_{max})^2 \quad (2.11)$$

2.3.4.3 Mole fraction

Combined standard uncertainties in mole fraction, $u_c(x_i)$, were computed assuming two main sources, those generated from the calibration procedure, $u_{calib}(x_i)$, and those of the repeatability, $u_{rep}(x_i)$; thus, for component i :

$$u_c(x_i) = \sqrt{u_{calib}(x_i)^2 + u_{rep}(x_i)^2} \quad (2.12)$$

The calibration uncertainty is the sum of the uncertainties brought about when preparing the standard mixtures by weighing them in the balance, $u_{bal}(x_i)$, and those of the correlation plot, $u_{corr}(x_i)$:



$$u_{calib}(x_i)^2 = \sqrt{u_{bal}(x_i)^2 + u_{corr}(x_i)^2} \quad (2.13)$$

For a two-compound system with masses m_1 and m_2 , and uncertainties $u(m_1)$ and $u(m_2)$, respectively, it can be written that:

$$u_{bal}(x_i)^2 = (x_1 x_2)^2 \left(\frac{u(m_1)^2}{m_1} + \frac{u(m_2)^2}{m_2} \right) \quad (2.14)$$

where $u(m_i)$ is the uncertainty given by the accuracy of the balance.

The $u_{corr}(x_i)$ term in [Equation \(2.13\)](#) is computed from the calibration curve, analogous to temperature, by [Equation \(2.5\)](#). $u_{rep}(x_i)$ can be calculated, similar to the case for P , from [Equation \(2.10\)](#); it is therefore necessary to calculate the standard deviations for any given temperature, pressure and phase.

2.3.5 Results and Discussion

2.3.5.1 Uncertainties

Uncertainties in temperature and pressure for the organic acid + water mixtures computed by the procedure described in [Section 2.3.4](#) were estimated as: $u_c(T) = 0.1$ K and $u_c(P) = 0.01$ bar, respectively. Uncertainties in composition for each experimental point are provided in the corresponding results table ([Appendix D](#)).



The largest contributions to $u_c(T)$ were given by the correlation procedure. Temperature was successfully controlled within ± 0.05 K during the experiments, the relatively thick vessel helped to create a controlled environment. The main contributions to $u_c(P)$ were given by the pressure drop during the sampling process, which varied between 0.005 – 0.01 bar depending on the experimental conditions. For estimation purposes 0.01 bar was assigned for all measurements. For the molar compositions, the major contributions to the uncertainty were those of the repeatability, resulting in final uncertainties as large as $u_c(y) = 0.033$ as in the case of the propanoic acid + water system.

2.3.5.2 Water vapour pressures

Vapour pressures for pure water were measured in the apparatus at the temperatures under study and were compared against literature data from NIST (2011) (Table 2.6). The maximum relative deviation (ΔP_v) computed was 0.40% for the temperature of 483.2 K.

Vapour pressures of the pure organic acids were not measured as these were used at the purchased purity without further purifications. In fact, for the measurements in the high acetic acid concentration region, a few millilitres of water were added in order not to start with a “pure” organic acid mixture. This was done for two main reasons, first to reduce corrosion of the dip tube and second to reduce the time required to achieve an equilibrium temperature due to the exothermic reaction taking place during the addition of water.



Table 2.6. Water vapour pressures, P_v , at the temperatures of study.

T [K]	P_v [bar]		$\Delta P\%$ ^b
	This work	NIST ^a	
412.6	3.56	3.56	0.07
423.2	4.76	4.77	0.21
443.2	7.92	7.93	0.12
453.2	10.03	10.04	0.13
483.2	19.02	19.10	0.40

^a NIST (2011)

$$\text{^b } \Delta P = 100 \cdot \left| \frac{P_{v,NIST} - P_{v,this\ work}}{P_{v,NIST}} \right|$$

2.3.5.3 Corrosion

A yellow-greenish colour liquid remained at the end of the experimental runs with acetic acid evidencing corrosion attack. Coloration is due to the presence of iron in the mixture from the alloy composition. Corrosion was essentially observed in the SS-316 dip tube, that is, the tube for the liquid sampling. No sensitive signs of it were observed in the fittings in contact with the vapour phase nor in the internals of the magnetic drive.

A more intense colour was observed at the maximum run temperature of 483.2 K for a concentrated mixture of acetic acid, for which a 0.01% iron content was determined by spectrophotometry. Othmer et al. (1952) have shown in their studies of acetic acid + water that a presence of 2% content gave no interference to the phase behaviour when testing a 85 wt.% acetic acid solution at 503 K and



21.7 bar (more severe conditions than those studied in this thesis) in their Type SS-316 still.

Experiments with propanoic acid resulted in lighter colorations, and thus, a lower corrosion effect is estimated. [Appendix E](#) details the spectrophotometry method employed.

2.3.5.4 Acetic acid + water

The experimental VLE obtained for the acetic acid + water system at 412.6, 443.2, and 483.2 K as well as the combined uncertainties in composition are shown in [Figure 2.14](#), and are presented in tabulated form in [Appendix D](#).

[Figure 2.15](#) shows a comparison of the newly obtained data against those of Freeman and Wilson (1985a; 1985b) at 412.6 K. The new liquid compositions are comparable to the literature values of Freeman and Wilson (1985b), albeit with some discrepancies. It is, however, necessary to point out some aspects of the literature values. First, the rather “un-natural” shape of the bubble-point curve; this is easier to appreciate above $P = 3$ bar. It exhibits a maximum pressure of $P = 3.59$ bar in the dilute acetic acid region after which the pressure decreases sharply, reaching a vapour pressure of water of 3.502 bar. There is no obvious reason for this maximum to happen. This maximum may be interpreted as an azeotrope in the dilute region but the newly obtained results and previous work do not report azeotropic behaviour for this mixture. Second, it is very likely that repeatability was not easy to achieve due to the likelihood of thermal and composition gradients, as discussed in the analysis of their rig in [Section 2.2.1](#). It



is reasonable to assume that deviations in pressure must be larger than the reported ones since the stated vapour pressure of water at 412.6 K gives a relative error of 1.6% (NIST data as reference) in contrast to that of 0.07% from the measurements of this work (Table 2.6). One can conclude that the experimental values of the liquid compositions obtained in the present work are more reliable than those reported by Freeman and Wilson although the accuracy reported by them is actually lower (0.001 of Freeman and Wilson vs an average of 0.005 in this work).

Nevertheless, large discrepancies are present for the vapour compositions from the three investigations (this work, Freeman and Wilson (1985a) and Freeman and Wilson (1985b)). The newly determined dew-curve is shifted to a higher water content compared with the data of Freeman and Wilson (1985b), in some instances by more than 0.2 in mole fraction. Although the new dew-curve is closer to that from Freeman and Wilson (1985a), their data exhibits pronounced irregularities.

At the beginning of the study it was believed that the new results were more accurate than those of the literature and were, consequently, left as it. However, as will be shown in the modelling section (3.7.2) none of the thermodynamic models employed in this project can correlate the vapour phase experimental values obtained, all models are more in agreement with those of Freeman and Wilson (1985b), a fact that raised the question about the reliability of the new data.

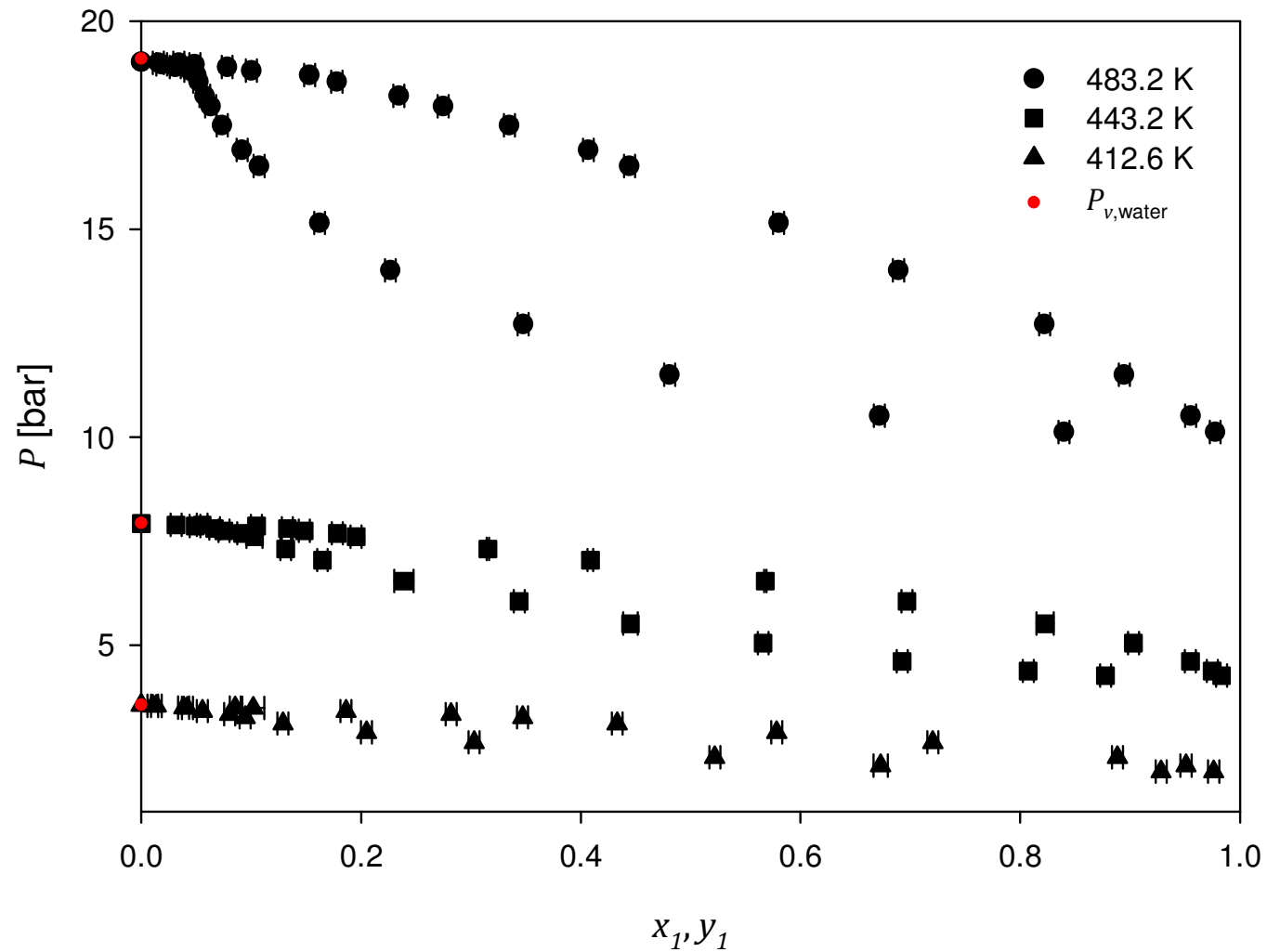


Figure 2.14. Vapour – liquid diagram for the acetic acid (1) + water (2) system at $T = 412.6, 443.2$ and 483.2 K. (•) Water vapour pressures from NIST (2011).

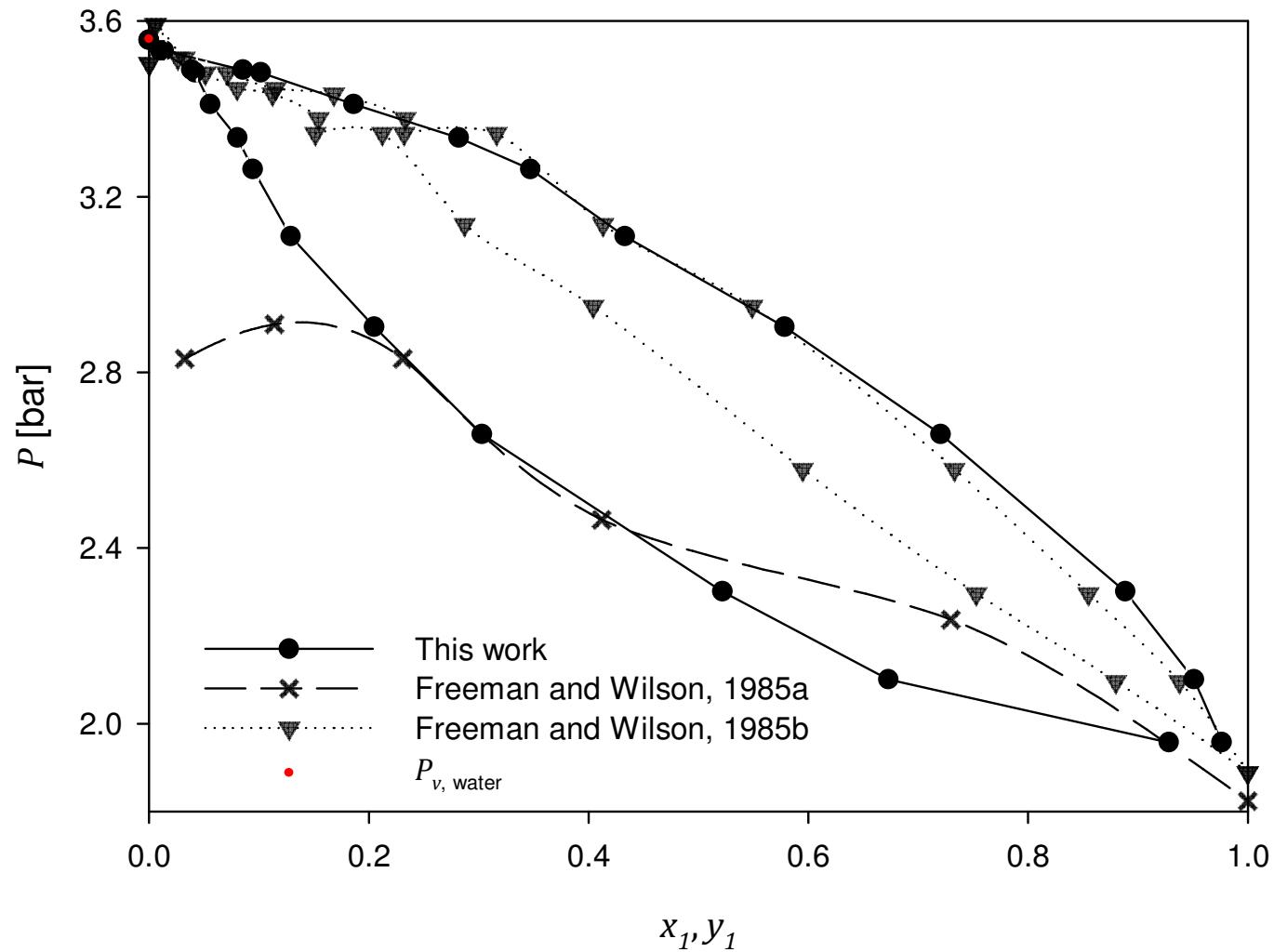


Figure 2.15. Vapour – liquid diagram for the acetic acid (1) + water (2) system at 412.6 K. Comparison with literature values of Freeman and Wilson (1985a; 1985b). Figures: experimental data. Lines are used as a guide to the eye. (●) Water vapour pressure from NIST (2011).



The arguments in favour and in contrast for the reliability of the newly obtained vapour phase compositions are presented below.

The compositions of an experimental run were always a continuation of the compositions of the previous one, e.g. if an experimental run was for the 0.9 to 0.6 acetic acid mole fraction (undertaken in reverse order because water was the component being added), the next experimental run, say for of the $x = 0.6 - 0.2$, resulted in compositions of the phases following the tendency of the previous run. Moreover, it was possible to reproduce the experimental points in different runs, this was not done for all the experimental points due to time restrictions. The cause is not a result of lack of condensation of the sample, if this were the case the samples would have had a higher acetic acid content (the less volatile component). Corrosion affecting the composition is a possibility, but signs of it were not observed in the sample line as was seen for the liquid sample tubing. The possibility of entrainment is also discarded as it would have resulted in compositions shifted to the high-concentration acetic acid rather than the lower-concentration. The possibility of condensation of water in the sampling line is also discarded since it may have resulted in random compositions of the vapour phase.

Based on the fact that the only difference between the acetic acid and the propanoic acid experiments was a lower dead volume in the latter case ([Section 2.3.2.1](#)), a systematic error due to the sampling volume seems to be the cause of the discrepancy in the vapour phase acetic acid concentrations. The sampling technique was chosen to reduce equipment costs taking advantage of the liquid state of the compounds at room conditions.



A consistency test may not necessarily reveal a poor quality of the experimental data (Marcilla et al., 2013) since a thermodynamic model accurate enough to represent the phase behaviour is needed. The acetic acid + water system, and in general the organic acid + water systems, present an important challenge from the thermodynamic point of view.

The results of the vapour phase compositions are presented in conjunction with the liquid ones, but when used should be kept in mind the possibility of a systematic error in the measurements.

2.3.5.5 Propanoic acid + water

Results for the propanoic acid + water mixture at 423.2, 453.2 and 483.2 K are plotted in [Figure 2.16](#), and tabulated in [Appendix D](#). Positive deviation from ideal behaviour with azeotropism is observed in the low propanoic acid concentration region, below 0.1 mole fraction. There are no available experimental data in the literature to compare this system. Nevertheless, as will be shown in [Chapter 3](#), predictions with equations of state and activity coefficient models are in good agreement with the values reported.

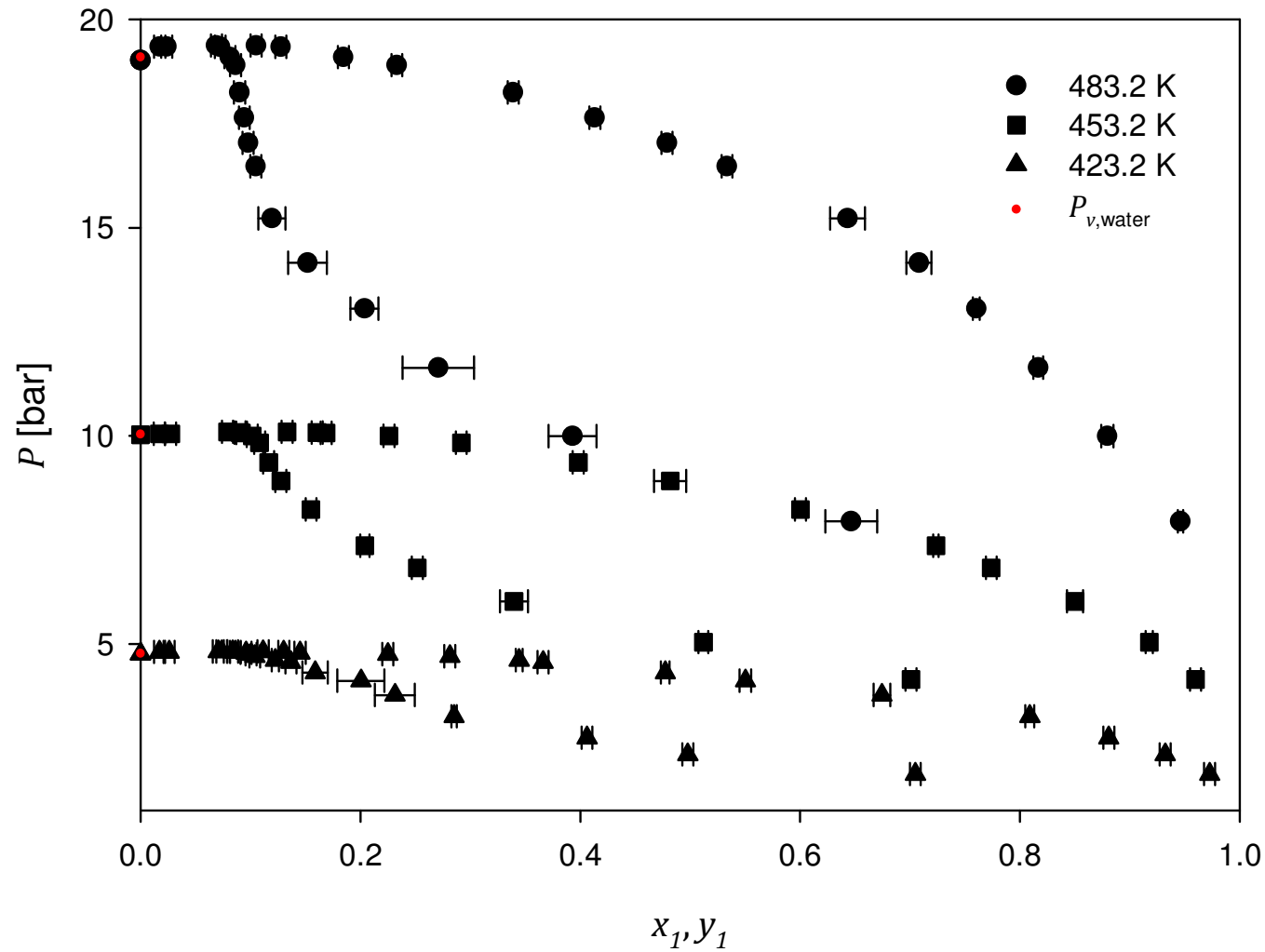


Figure 2.16. Vapour – liquid diagram for the propanoic acid (1) + water (2) system at $T = 423.2, 453.2$ and 483.2 K. (•) Water vapour pressures from NIST (2011).



2.4 Synthetic Measurements

As part of this thesis project, a new experimental technique pertaining to the synthetic class was developed, more specifically to the Other Synthetic methods according to the classification of Dohrn et al. (2010) (SyncOth in [Figure 2.2](#)). The novelty of the technique lies in the application of Positron Emission Particle Tracking (PEPT) technology in locating the vapour – liquid interface at the interior of an enclosed equilibrium cell where direct visual determination is not possible. From the information of the interface location, total cell volume and initial overall loading, phase compositions are evaluated from the mass balance. Furthermore, phase molar densities can be recovered which are valuable for engineering design but seldom published.

Time restrictions in the present project allowed for determinations only for the acetic acid + water system at 412.6 K. The results obtained are compared with those published by Freeman and Wilson (1985b) and the ones obtained from the static-analytical method described in [Section 2.3.5.4](#).

This section starts with an overview of the particularity of the synthetic method used in this project. It is followed by a literature review of articles that have applied synthetic measurements in the determination of phase compositions and volumes. A brief introduction to the PEPT technology is then given. The equipment details as well as the experimental procedure are provided afterwards including an analysis of the possible sources of experimental uncertainty. Finally, the results are presented and discussed.



2.4.1 Overview

A special case in the synthetic method without phase transition (SyncoTh), is that in which phase compositions and molar (or mass) densities are found simultaneously from the mass balance, providing overall compositions and total phase volumes are determined accurately.

For a binary system of n_1 moles of compound 1 and n_2 moles of compound 2 exhibiting a vapour and a liquid phase in equilibrium and no constraints, there are two degrees of freedom according to the Gibbs phase rule. If temperature and pressure are given, the phase compositions as well as the conformable saturated molar densities (ρ_L and ρ_V) are fixed regardless of the overall molar composition. A different overall molar composition at the same conditions will result in a different vaporized fraction but compositions and saturated densities will remain. Consequently, for two different overall loadings (A and B), with total volumes V_V and V_L for the vapour and liquid phases, respectively, the following set of equations can be written:

$$\begin{cases} \rho_{L,1}^A V_L^A + \rho_{V,1}^A V_V^A = n_1^A \\ \rho_{L,2}^A V_L^A + \rho_{V,2}^A V_V^A = n_2^A \\ \rho_{L,1}^B V_L^B + \rho_{V,1}^B V_V^B = n_1^B \\ \rho_{L,2}^B V_L^B + \rho_{V,2}^B V_V^B = n_2^B \end{cases} \quad (2.15)$$

Since:



$$\begin{aligned}\rho_{L,1}^A &= \rho_{L,1}^B \\ \rho_{V,1}^A &= \rho_{V,1}^B \\ \rho_{L,2}^A &= \rho_{L,2}^B \\ \rho_{V,2}^A &= \rho_{V,2}^B\end{aligned}\tag{2.16}$$

the system of equations can be rewritten simply as:

$$\begin{cases} \rho_{L,1}V_L^A + \rho_{V,1}V_V^A = n_1^A \\ \rho_{L,2}V_L^A + \rho_{V,2}V_V^A = n_2^A \\ \rho_{L,1}V_L^B + \rho_{V,1}V_V^B = n_1^B \\ \rho_{L,2}V_L^B + \rho_{V,2}V_V^B = n_2^B \end{cases}\tag{2.17}$$

Which is a system of four linear equations in four unknowns ($\rho_{L,1}$, $\rho_{L,2}$, $\rho_{V,1}$ and $\rho_{V,2}$).

Analogous to the case of the static – analytical method where the challenge is about obtaining a representative sample with the less perturbation possible, in this synthetic technique the challenge is about measuring the total volumes of the phases in equilibrium accurately enough to solve the system of equations. The number of total volumes required to be determined is in reality the number of phases minus one, since the remaining volume is obtained from the subtraction of the total volume of the equilibrium cell. For a variable volume cell, it would be necessary to obtain a correlation of the total cell volume as a function of the volume-change agent.

There are some important aspects that have to be taken into account in this kind of determinations: i) as in any synthetic method, precise preparation of the synthetic mixture; ii) temperature and pressure of the different loadings are to be



reproduced to a high accuracy; and iii) the ability to determine the volumes correctly. (Deiters and Schneider, 1986)

2.4.2 Literature review

The SyncOth method was first applied to measure pure compound orthobaric densities of coexisting liquid and vapour phases by Campbell and Chatterjee (1968) and later generalized for multicomponent-multiphase systems by Knobler and Scott (1980).

Creek et al. (1981) determined with both, the analytical and the synthetic method three-phase curves of the methane + *n*-pentane + 2,3-dimethylbutane and methane + 2,2-dimethylbutane + 2,3-dimethylbutane systems. Only qualitative agreement could be found when comparing the data from both techniques. It is not clear, unfortunately, whether the same or a different apparatus was employed for the synthetic case.

Specovius et al. (1981) studied the multiphase equilibria of ethane containing binary mixtures in a cylindrical equilibrium cell made of Pyrex 2.5 mm wall thickness, the cell was of variable volume with mercury as the compressing fluid. A cathetometer measured the level of mercury and the location of the interphase with ± 0.02 mm accuracy.

Fontalba et al. (1984) designed a more elaborated way to determine the phase volumes. They employed a thermistor probe to detect differences in thermal conductivity and thus establishing the interface level. To compensate for the added



volume of the probe into the cell, they employed a metallic rod, with the same diameter as the probe body, placed inside a pressurizing jacket connected to the equilibrium cell. Changes in the cell volume due to the probe insertion were hence compensated by a change in volume of the same magnitude in the pressurizing jacket. In this form, the authors were able to determine compositions and saturated volumes of the CO₂ + isopentane system. Accuracy of the interface levels were reported to be within 0.1 mm.

The design of Fontalba et al. (1984) is basically restricted to VLE determinations since its application when the phases have similar properties, e.g. near critical points or in some liquid – liquid equilibria (LLE), is limited. For this reason, Laugier et al. (1990) modified the apparatus by using a sapphire variable volume equilibrium cell, thus allowing for visual determination of three phases in equilibrium. A cathetometer measured the interface levels with an accuracy of 0.01 mm. Laugier et al. (1990) studied in this way equilibrium compositions and molar volumes of CO₂ + tetradecane, CO₂ + acetic acid and CO₂ + acetic acid + water mixtures. It is important to mention that the vapour compositions were mostly determined by direct sampling. The justification given was that the number of moles in vapour phase were much lower than those in the liquid phase, resulting in poor conditions for the resolution of the system of equations. This aspect of ill-conditioned systems, inherent to the technique, was previously recognized by Deiters and Schneider (1986) in their review of experimental methods for high pressure phase equilibria.

DiAndreth (1985); DiAndreth and Paulaitis (1987); DiAndreth et al. (1987) and DiAndreth and Paulaitis (1989) measured multiphase equilibria for the alcohol +



water + CO₂ systems in a variable volume equilibrium cell fitted with sapphire windows to visually locate the interfaces. A cathetometer measured the levels within a 0.1 mm accuracy.

Gutiérrez and Luks (2003) also employed a cathetometer in their investigation of vapour – liquid – liquid equilibria (VLLE) of the ternary mixtures of CO₂ + 1-methylnaphthalene + (methanol or *n*-hexane) and CO₂ + tetradecane + *n*-hexane in a visual cell. Volumes were measured to an accuracy of 0.01 cm³.

In a more recent paper, Shiflett and Yokozeki (2006) obtained VLLE compositions and liquid molar volumes of pentafluoroethane (R125) + 1-butyl-3-methylimidazolium hexafluorophosphate ([bmim][PF₆]). The method consisted in placing three different overall loadings in three different borosilicate glass containers for visual determination of the volume heights by an electronic caliper. Heights were measured to an accuracy of 0.01 mm.

2.4.3 Mass balance equations

A corollary of the case exposed in [Section 2.4.1](#) is that comprising two different mass loadings with the same overall composition taken at the same conditions of temperature and pressure. Both loadings will result in a different vaporized fraction but will share the same phase compositions and saturated densities; that is, the set of linear equations given in [Equation \(2.17\)](#) will remain valid.

In theory, only two different experiments are required to solve [Equation \(2.17\)](#) for the molar densities. In practice, however, a larger number is suggested (Knobler



and Scott, 1980). This can be accomplished by a least square analysis involving more than two loadings. The approach, detailed for a ternary system with three coexisting phases by DiAndreth (1985) is applied in this work for a binary system with a vapour and a liquid phase in equilibrium.

The mass balance over any of the components, e.g. component 1, for a given loading i is:

$$\rho_{L,1}V_L^i + \rho_{V,1}V_V^i = n_1^i \quad (2.18)$$

Defining δ^i as the difference between the number of moles loaded and the number of moles computed from the measured total volumes, is possible to write:

$$\delta^i = \rho_{L,1}V_L^i + \rho_{V,1}V_V^i - n_1^i \quad (2.19)$$

Expressing S as the sum of squares of the differences over all of the individual N loadings:

$$S = \sum_{i=1}^N (\delta^i)^2 = \sum_{i=1}^N (\rho_{L,1}V_L^i + \rho_{V,1}V_V^i - n_1^i)^2 \quad (2.20)$$

At the minimum, the derivative of S with respect to the molar density of compound 1 in each phase must be zero:

$$\frac{\partial S}{\partial \rho_{L,1}} = \sum_{i=1}^N 2(\rho_{L,1}V_L^i + \rho_{V,1}V_V^i - n_1^i)V_L^i = 0 \quad (2.21)$$



$$\frac{\partial S}{\partial \rho_{V,1}} = \sum_{i=1}^N 2(\rho_{L,1}V_L^i + \rho_{V,1}V_V^i - n_1^i)V_V^i = 0 \quad (2.22)$$

Rearranging:

$$\rho_{L,1} \sum_{i=1}^N (V_L^i)^2 + \rho_{V,1} \sum_{i=1}^N (V_V^i V_L^i) = \sum_{i=1}^N (n_1^i V_L^i) \quad (2.23)$$

$$\rho_{L,1} \sum_{i=1}^N (V_L^i V_V^i) + \rho_{V,1} \sum_{i=1}^N (V_V^i)^2 = \sum_{i=1}^N (n_1^i V_V^i) \quad (2.24)$$

Equations (2.23) and (2.24) conform a system of two equations in two unknowns.

In matrix notation this is:

$$\mathbf{Ax} = \mathbf{b} \quad (2.25)$$

where:

$$\mathbf{A} = \begin{bmatrix} \sum (V_L^i)^2 & \sum (V_V^i V_L^i) \\ \sum (V_L^i V_V^i) & \sum (V_V^i)^2 \end{bmatrix} \quad (2.26)$$

$$\mathbf{x} = \begin{bmatrix} \rho_{L,1} \\ \rho_{V,1} \end{bmatrix} \quad (2.27)$$

$$\mathbf{b} = \begin{bmatrix} \sum (n_1^i V_L^i) \\ \sum (n_1^i V_V^i) \end{bmatrix} \quad (2.28)$$



A similar set of equations can be written for compound 2 following the same analysis. As noted from [Equations \(2.26\) – \(2.28\)](#), the number of moles of compound 2 are not needed to solve for the molar densities of compound 1 and vice versa.

Molar compositions for the liquid, x , and vapour, y , phases are calculated from the molar densities according to:

$$x_1 = \frac{\rho_{L,1}}{\rho_{L,1} + \rho_{L,2}} \quad (2.29)$$

$$y_1 = \frac{\rho_{V,1}}{\rho_{V,1} + \rho_{V,2}} \quad (2.30)$$

Finally, phase molar densities are computed from:

$$\rho_L = \rho_{L,1} + \rho_{L,2} \quad (2.31)$$

$$\rho_V = \rho_{V,1} + \rho_{V,2} \quad (2.32)$$

2.4.4 PEPT technology

Positron Emission Tomography (PET) is as a radioactive tracer imaging technique used in medicine to produce three-dimensional images from a metabolic fluid which has been labelled with a positron-emitting radionuclide (tracer). The industrial application of PET for flow studies was developed at the



University of Birmingham with the construction of a portable positron camera at the Rutherford Appleton Laboratory (Parker et al., 1994). Positron Emission Particle Tracking (PEPT) has surged as an alternative to PET as a flow tracing technique. In contrast to PET in which a bulk of fluid is labelled, in PEPT, a single particle is labelled, allowing for faster and more accurate trackings since the statistics require to determine the tracer location are significantly lower than the equivalent required for a volume.

The physics principle behind PET and PEPT is briefly described as follows: a short-lived radioactive tracer isotope undergoes positron emission decay followed by positron annihilation in the surrounding material by its interaction with an electron. As a result of the annihilation, a pair of gamma rays are emitted possessing equal momentum but approximately opposite direction (i.e. $180^\circ \pm 0.5^\circ$ apart) (Leadbeater et al., 2012). The detection of both gamma photons defines a line of response in which it is assumed that the annihilation site occurred, therefore establishing the position of the radioisotope source. The gamma rays are detected using high-efficiency scintillators coupled to photomultiplier tubes. The detectors are part of a portable modular positron camera built at the University of Birmingham. The accuracy of the detectors to track the position of the tracer has been estimated to be of 0.1 mm. (Parker et al., 2009; Leadbeater and Parker, 2011)

The image or position of the tracer is reconstructed from a series of detection events. Because some of the detected events are inherently corrupt (e.g due to scattering or random coincidences), an algorithm is used to determine the tracer of the particle using an iterative triangulation approach (Leadbeater et al., 2012).



The tracer should be ideally taken from the bulk material under study or at least to possess similar size and density to the particle of interest. Particle tracers can be labelled by indirect or direct activation. In the former case for example, the tracer is prepared by exposure to an aqueous solution of the isotope, prepared by indirect bombardment of ultrapure water (Fan et al., 2006a). In the direct activation an isotope is generated from direct bombarding of a solid material with ^3He beams produced in a cyclotron (Fan et al., 2006b).

Current applications of PEPT include studies of: fluidised beds, granular gases, stirred tanks, rolling drums, mixing systems and multiphase flows (Bakalis et al., 2006; Guida et al., 2010; Chiti et al., 2011; Guida et al., 2011; Leadbeater et al., 2012; Pérez-Mohedano et al., 2015).

In this thesis, a new application of the PEPT technology was envisaged, that is, as a tool for the determination of vapour – liquid equilibria properties. In the new technique, PEPT is used to locate the vapour – liquid interface at the interior of an enclosed equilibrium cell (Figure 2.17), avoiding the need of direct visual determination. From the information of the interface location, total cell volume and initial overall loading, the phase compositions are evaluated from the mass balance.

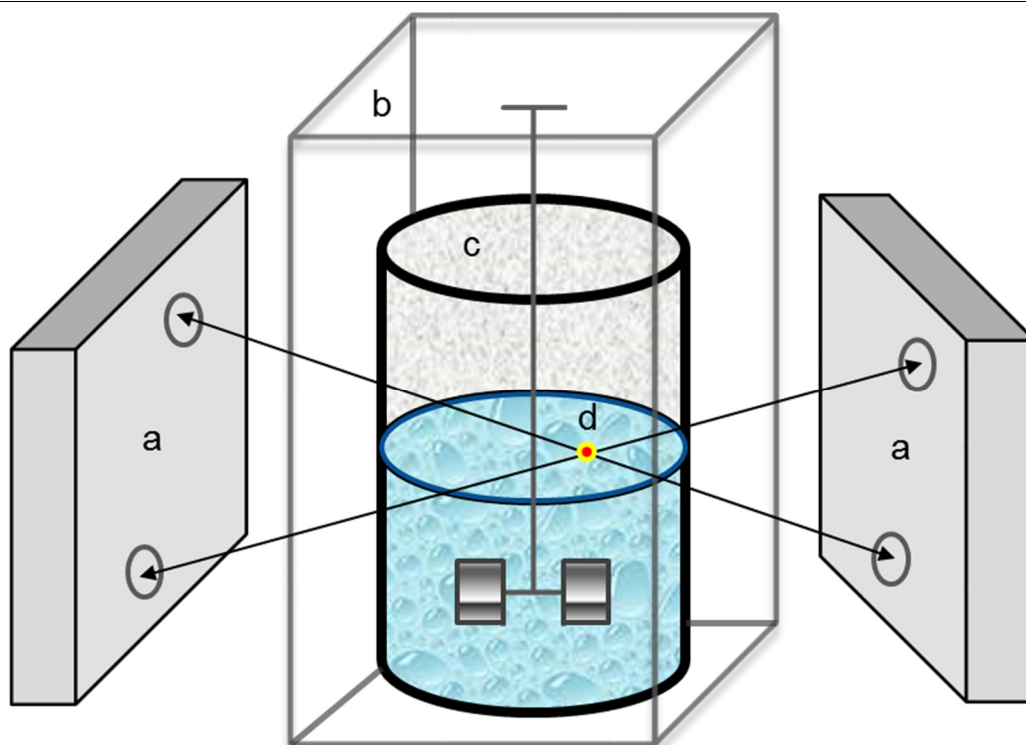


Figure 2.17. Positron Emission Particle Tracking (PEPT) is used to locate the vapour – liquid interface of an enclosed equilibrium cell. (a) PEPT detectors, (b) Air bath, (c) Equilibrium cell, (d) radioactive tracer.

2.4.5 Chemical compounds

Acetic acid and water were used as described in [Section 2.3.1](#) for the static – analytical experiments. The amount of impurity of acetic acid assigned as water was added to the number of moles of water in the final mixture.

2.4.6 Apparatus description

The apparatus used in the synthetic experiments is a modification of the apparatus used in the static – analytical experiments described in [Section 2.3.2](#). [Figures 2.18](#) and [2.19](#) show a schematic diagram and the actual set-up of the equipment, respectively. As sample withdrawing is not needed in this technique,

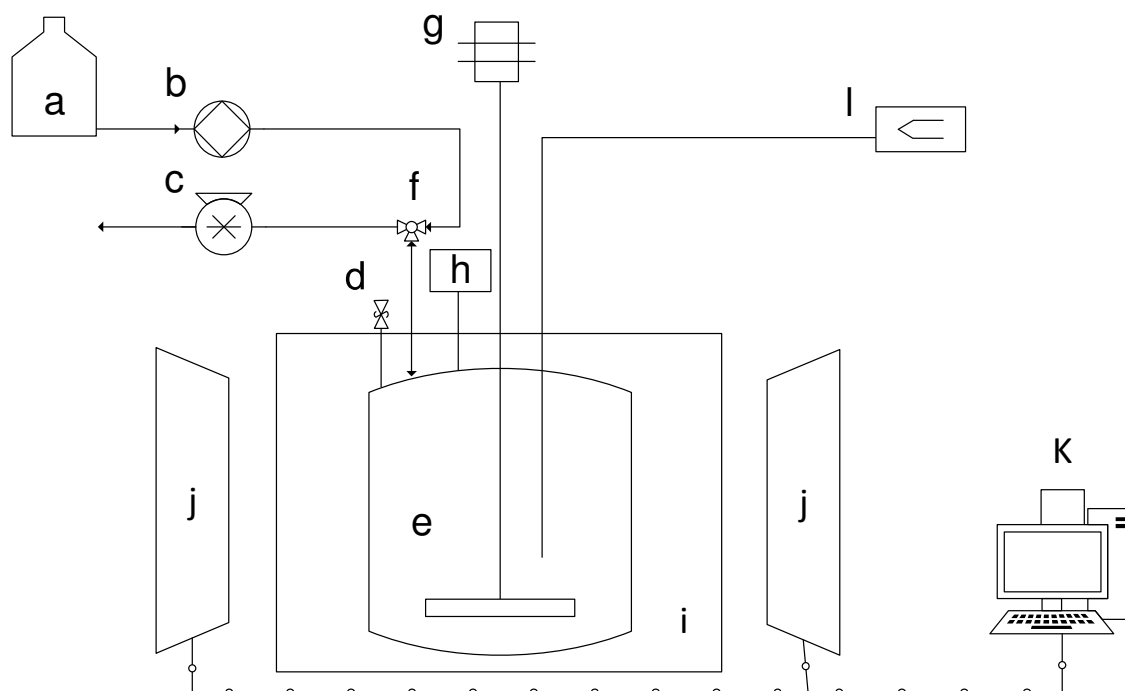


Figure 2.18. Schematic drawing of the synthetic apparatus. (a) Water supply, (b) Digital liquid-pump, (c) Vacuum-pump, (d) Safety rupture disc, (e) Equilibrium cell, (f) Three-way valve, (g) Magnetic drive, (h) Digital pressure gauge, (i) Air bath, (j) PEPT detectors, (k) Data acquisition unit, (l) Thermocouple data logger.

the sampling lines and valves were removed and the ports capped with plugs made of Hastelloy C-276. The three-way valve with the water feeding and vacuum lines, the bursting disc, the digital pressure gauge and the stirrer were kept in place. The temperature control environment and all peripherals were the same as those described in [Sections 2.3.2.1](#) and [2.3.2.2](#), except for the GC which is not necessary in this case.

The special detectors to locate the tracer position were placed at each side of the oven ([Figures 2.18](#) and [2.19](#)). [Figure 2.20](#) shows a number of gamma ray trajectories emitted from the radioactive tracer inside the equilibrium cell.

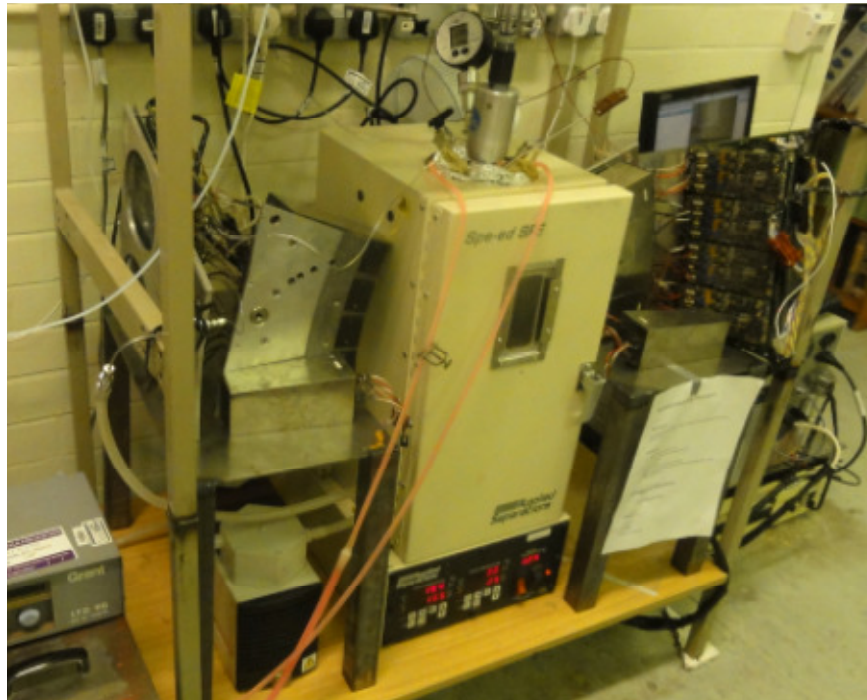


Figure 2.19. Actual view of the synthetic apparatus based on Positron Emission Particle Tracking (PEPT) measurements. The equilibrium cell is inside the oven shown in the centre. PEPT detectors are located either side of the oven.

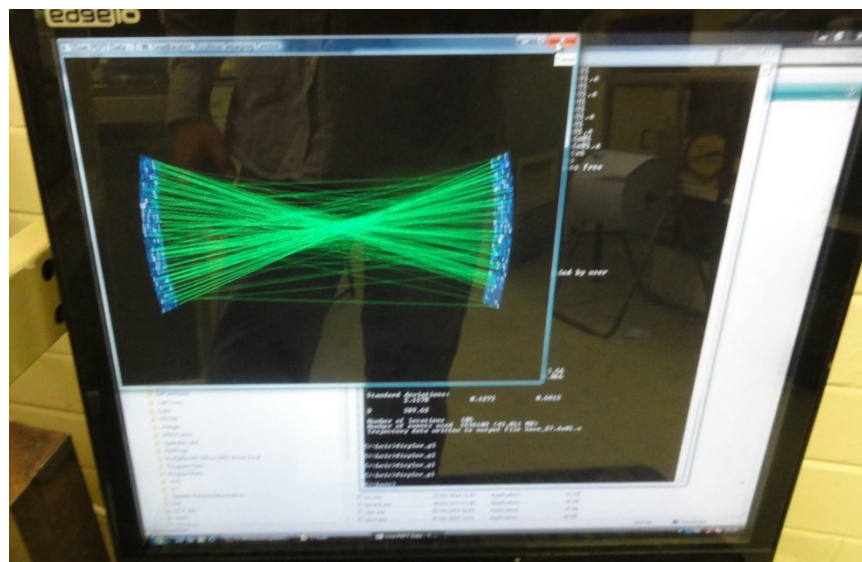


Figure 2.20. Gamma rays trajectories emitted from the radioactive tracer inside the equilibrium cell.



2.4.6.1 Radioactive tracer

The radioactive particle plays an important role in the new apparatus. It consisted of a 500 μm diameter ion-exchange resin keyed to the adsorption of fluorine. The radioisotope ^{18}F (positron emitter, half-life 110 min) was produced in a dilute water solution by the School of Physics and Astronomy in the MC40 cyclotron. The particle was labelled with activity using the indirect technique (Fan et al., 2006a).

Apart from its inherent radioactive properties necessary for its detection, the particle had also to fulfil the requirement of floating at the interface. For this and at the same time to protect it from the corrosive environment, it was necessary to find an appropriate coating material. A polymer emerged as the most suitable option. Its search was constrained in satisfying the following material properties: mechanical strength for up to 20 bar, chemical resistance to high concentrations of acetic acid, and to have a lower density than that of the liquid mixture. The search basically converged to two options: polypropylene (PP) and polystyrene (PS). Two suppliers for PP were considered: Dow Chemical and LyondellBasell. PS was located from Polimeri Europa. Small samples of these polymers were tested inside the equilibrium cell at approximately 0.8 mole fraction of acetic acid, taken up to 417 K and 3.3 bar for a period of 8 hours. Pressure stability was an indication of the absence of polymer degradation at this conditions. The system was then cooled down and the samples removed from the apparatus. A visual inspection revealed deformation in the PS samples. PP from LyondellBasell change in coloration from white clear to opaque. No apparent signs of distortion were observed in the PP from Dow Chemical. This material was then chosen as



the coating for the radioactive particle. A copy of the Material Data sheet of the polymer can be found in [Appendix F](#). With the objective of determining the highest working temperature of the polymer, it was subjected to a temperature of 473 K. The polymer degraded before reaching such temperature, probably around 463 K.

The radioactive particle was inserted into a polymer bead of size range 1.5 – 2 mm diameter. The half-life of the radioactive particle limited the number of experimental runs to only one; this means that a new tracer was needed for each test.

2.4.6.2 Thermocouples and pressure gauge calibration

The pressure gauge and the thermocouples described in [Sections 2.3.2.1](#) and [2.3.2.3](#), were also used in this technique. Calibration checks were performed for the devices by measuring vapour pressures of water, as used during the calibration procedure, for the thermocouples; while for the pressure gauge, its readings were compared against a mercury barometer. All readings were inside their estimated calibration uncertainties (0.076 K and 0.001 bar, computed from [Equations \(2.5\)](#) and [\(2.9\)](#), respectively).

2.4.6.3 Total volume Equilibrium cell

An integral part of the new method is to know accurately the total volume of the equilibrium cell. CP grade carbon dioxide, 99.995% purity, supplied from BOC was used for the volume cell calibration. The procedure was as follows:



The three-way valve (letter f in [Figure 2.18](#)) was attached to a needle valve and connected to a pressurized carbon dioxide cylinder. The equilibrium cell was filled with carbon dioxide to around 28 bar after repetitive flushings with the gas. The three-way valve was closed and the line disconnected from the cylinder and the system was allowed to equilibrate overnight. Temperature and pressure of the equilibrium cell were recorded at the equilibrium state and the mass density of carbon dioxide ($\rho_{CO_2,EC}^{NIST}$) at these conditions were retrieved from NIST database (NIST, 2011).

The volume of carbon dioxide inside the rig was measured by a Wet Test Gas Flow Meter (Alexander Wright & Company, model DM3A) which has a resolution of 0.005 dm³ and was calibrated by the supplier (Alexander Wright & Company). Flow was controlled through the needle valve. The volume of carbon dioxide that passed through the wet meter, V_M , was calculated from the difference of the initial and the last meter readings. Working temperature and pressure conditions of the flow meter were read from its built-in thermometer and from an external mercury barometer, respectively. The mass density of carbon dioxide at these conditions, $\rho_{CO_2,M}^{NIST}$, were retrieved from NIST. The mass that had passed through the flow meter, $m_{CO_2,M}$, was then calculated from:

$$m_{CO_2,M} = V_M \rho_{CO_2,M}^{NIST} \quad (2.33)$$

The total volume of the equilibrium cell, V_{EC} , was finally computed from:

$$V_{EC} = \frac{m_{CO_2,M}}{\rho_{CO_2,EC}^{NIST}} \quad (2.34)$$



After seven different measurements, the total volume of the equilibrium cell was determined to be 289.26 mL with a standard deviation of 0.35 mL (variance 0.12 mL).

2.4.6.4 Phase volume – height calibration

Although the position of the tracer can be known in a three-dimensional space, its position related to the vertical axis is actually the only one needed. This position represents the height (level) of the liquid phase, which in turn can be related to the liquid phase volume by a proper calibration. The calibration procedure in this case consisted on tracking the vertical position of the radioactive particle for a series of liquid volumes of pure water laying on its vapour pressure curve as follows:

A gravimetric amount of pure water (ACS reagent from Sigma Aldrich), measured in an electronic semi-microbalance (Sartorius, model R-160-P) to an accuracy of ± 0.1 mg, was placed inside the equilibrium cell and the amount recorded (m_T). The amount of water had to be large enough to cover the impeller and the lower guide bearing in order to avoid nonlinearities due to the amorphous shapes of the parts. That is, to have liquid volumes lying in the symmetric part of the vessel. With the radioactive tracer placed in the vessel, the equilibrium cell was assembled and vacuumed down to 0.015 bar at room temperature. The cell was then taken to the desired temperature by adjusting the oven temperature. The system was allowed to reach equilibrium under constant stirring, which was assumed when temperature and pressure did not vary between ± 0.05 K and ± 0.005 bar for 5 minutes. Once in equilibrium, the PEPT scanners tracked the



tracer's position in height, h , for at least 2 minutes. At this condition, specific volumes of the saturated liquid (v_L) and vapour (v_V) phases were retrieved from the NIST database. The equilibrium pressure was compared against the data from NIST, serving in a way to corroborate the calibration procedure of the thermocouples. Total volume of the liquid phase, V_L , was then calculated from the following set of equations:

$$m_L v_L + m_V v_V = V_{EC} \quad (2.35)$$

$$m_V + m_L = m_T \quad (2.36)$$

$$V_L = m_L v_L \quad (2.37)$$

The position of the tracer is relative to an arbitrary origin, in this case, it was set to the bottom of the vessel. Additional water was added into the cell by means of the high pressure liquid pump. The mass of water was computed from volumetric readings of a burette class A, 0.01 mL resolution, and the density of water at 25°C, the average temperature in the laboratory. A new temperature was set and thus a new point in the calibration plot. This is shown in [Figure 2.21](#) alongside the trendline for a linear correlation. It is important to point out, that a polynomial of second or higher order would not have led to a better R^2 coefficient in the plot. The total liquid volume as a function of height is finally determined by the following equation:

$$V_L = 3.0512h + 26.50 \quad (2.38)$$

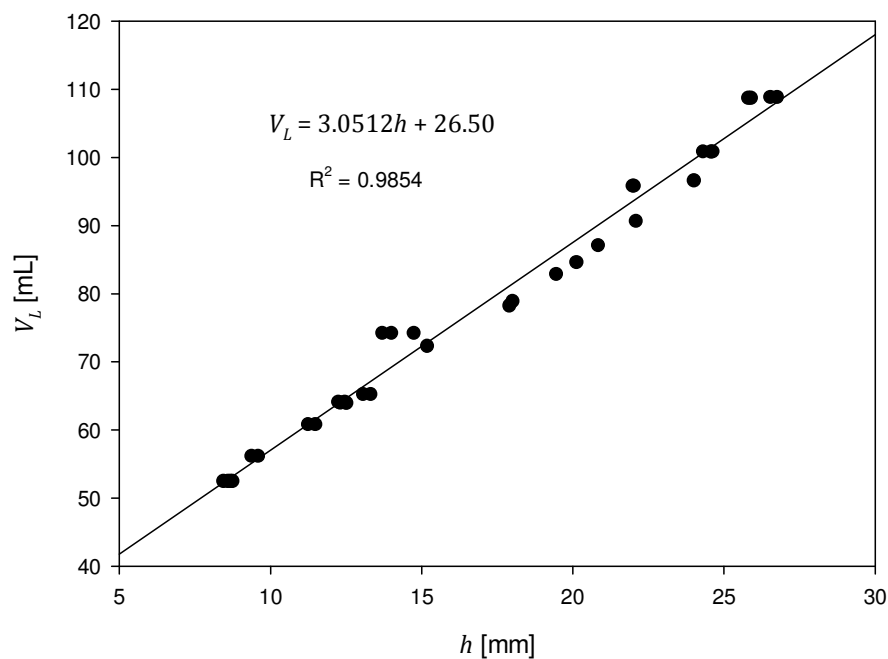


Figure 2.21. Calibration plot for the total volume of the liquid phase, V_L , as a function of tracer's position in height, h .

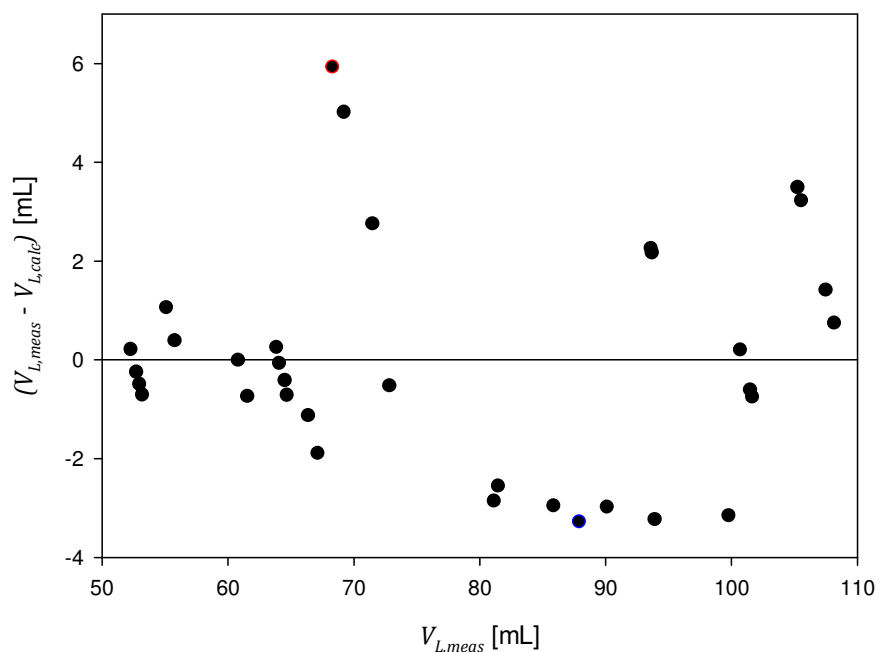


Figure 2.22. Deviations between the measured, $V_{L,meas}$, and calculated, $V_{L,calc}$, liquid volumes by the use of Equation (2.38). (●) Maximum deviation, (●) minimum deviation.



Deviations between the measured liquid volumes, $V_{L,meas}$, and those calculated with Equation (2.38) are plotted in Figure 2.22. Maximum and minimum deviations are 5.93 and -3.27 mL, respectively.

No corrections due to thermal expansion were made, these were assumed to be captured by the calibration process.

2.4.7 Experimental procedure

The procedure is similar to that described in Section 2.3.3 for the static – analytical measurements, except for the sampling method that is replaced in this case by the PEPT tracking technique. Nevertheless, for the sake of clarity, the steps of the method are described in detail, which unavoidably results in some repetitions of the earlier text.

Before each experimental run, the vessel and head were disassembled and the magnetic drive was disengaged from the head. The head stirring chamber was dismantled to allow a thorough cleaning since small amounts of the compounds from previous runs can reach the top of the magnetic drive. All the internals of the magnetic drive are made of Hastelloy C-276.

After all the parts were disassembled, these and the sample lines were washed and rinsed with ethanol and acetone, and left to dry in an oven for around 4 hours. After this time, the parts were then allowed to cool to room temperature. Visual checks of the PTFE seal were carried out and, if needed, a new seal was fitted. All parts were then purged with nitrogen to remove solvent traces. The cell was



assembled and closed using a torque wrench to a bolt torque of 15 ft-lbs. A pressure test with compressed nitrogen at 80 bar and room temperature was run overnight.

Desired amounts of acetic acid and water were degassed in an ultrasonic bath degasser (Grant, model XB6) for 1 hour. A gravimetric mixture of acetic acid + water was prepared by means of an electronic semi-microbalance (Sartorius, model R-160-P) to an accuracy of ± 0.1 mg and placed into the cell. The cell was closed and vacuumed down to 0.015 – 0.020 bar at room temperature under constant stirring and kept at this condition for 1 hour. The desired equilibrium cell temperature was achieved by manually controlling the temperature of the oven. The system was then allowed to reach equilibrium condition under constant stirring, at 40 rpm, which was assumed when temperature and pressure did not vary within ± 0.05 K and ± 0.005 bar, respectively, during at least 5 minutes. The thickness of the vessel helped for a favourable control of the temperature.

Once in equilibrium, stirring was stopped and particle tracking procedure was initialized. Each tracking recording (sampling) was done for at least 2 minutes. The wall thickness of the vessel although helpful for the temperature stability, resulted in scattered data for the tracer position, particularly when the tracer moved outside the centreline of the detection range. In these cases the standard deviation was usually above 0.9 mm. Standard deviations above 0.6 mm were disregarded and a new track-sampling performed. This was repeated until at least two consecutive trackings resulted in similar values of the height.



Pressure was then increased by pumping additional water into the cell and a new equilibrium point was then established. Near the desired pressure, water was added in volumetric flows as low as 0.05 mL/min to attain, as accurately as possible, the desired pressure. In accordance with the technique, several loadings with different amounts of the mixture, but with the same overall composition were loaded into the cell to solve the system of linear equations given by [Equation \(2.25\)](#).

The half-life of the tracer limited the number of experimental points to be obtained in a single run to three.

2.4.8 Uncertainties determination

Combined standard uncertainties in temperature, pressure, composition and molar density were computed with a similar procedure as that described for the static – analytical measurements ([Section 2.3.4](#)). The uncertainty due to sampling is replaced in this case by the uncertainty generated from the reproducibility of the pressure and temperature conditions in the experimental runs. The following subsections show the considerations used in the uncertainty determinations for the properties stated above.

2.4.8.1 Temperature

The combined standard uncertainties in temperature, $u_c(T)$, are given by the contributions due to the calibration, $u_{calib}(T)$, resolution, $u_{resl}(T)$, control, $u_{cont}(T)$, and reproducibility, $u_{repr}(T)$:

$$u_c(T) = \sqrt{u_{calib}(T)^2 + u_{resl}(T)^2 + u_{cont}(T)^2 + u_{repr}(T)^2} \quad (2.39)$$

The expressions for $u_{calib}(T)$, $u_{resl}(T)$, and $u_{cont}(T)$, are those previously given by [Equations \(2.5\) – \(2.7\)](#). $u_{repr}(T)$ is computed from:

$$u_{repr}(T)^2 = \left(\frac{\sigma}{\sqrt{N}}\right)^2 \quad (2.40)$$

where σ is the standard deviations of a N number of determinations.

2.4.8.2 Pressure

The combined standard uncertainties in pressure, $u_c(P)$, are given by the contributions due to the calibration, $u_{calib}(P)$, repeatability, $u_{rep}(P)$ and reproducibility, $u_{repr}(P)$:

$$u_c(P) = \sqrt{u_{calib}(P)^2 + u_{rep}(P)^2 + u_{repr}(P)^2} \quad (2.41)$$

The expressions for $u_{calib}(P)$ and $u_{rep}(P)$ are taken from [Equations \(2.9\) and \(2.10\)](#), respectively. $u_{repr}(P)$ is computed from:

$$u_{repr}(P)^2 = \left(\frac{\sigma}{\sqrt{N}}\right)^2 \quad (2.42)$$

**2.4.8.3 Molar density and mole fraction**

The combined standards uncertainties for the molar densities and mole fractions can be computed from the following general expression that comprises the contributions due to temperature, T , pressure, P , number of moles, n , volume of the liquid phase, V_L , and the height, h :

$$\frac{u_c(\theta)^2}{(\theta)^2} = \left(\frac{u_c(T)}{T}\right)^2 + \left(\frac{u_c(P)}{P}\right)^2 + \left(\frac{u_c(n)}{n}\right)^2 + \left(\frac{u_c(V_L)}{V_L}\right)^2 + \left(\frac{u_c(h)}{h}\right)^2 \quad (2.43)$$

where θ can be either ρ_L , ρ_V , x_1 , or y_1 .

$u_c(n)$ is given by the uncertainty contributions due to the fitting procedure, $u_{fitt}(n)$, those created when preparing the initial loadings by weighing them in the balance, $u_{bal}(n)$, and those due to the addition of water during the experiments, $u_{add}(n)$:

$$u_c(n) = \sqrt{u_{fitt}(n)^2 + u_{bal}(n)^2 + u_{add}(n)^2} \quad (2.44)$$

$u_{fitt}(n)$ is computed from the standard error of the fitted curve when solving the mass balance where ρ_L and ρ_V can be seen as coefficients of the curve. Therefore, for the N number of measurements:

$$u_{fitt}(n)^2 = \frac{1}{N-2} \sum_{i=1}^N (n_i - \rho_L V_L^i - \rho_V V_V^i)^2 \quad (2.45)$$



$u_{bal}(n)$ is computed by first setting the uncertainty of the masses m_1 and m_2 for the compounds 1 and 2, respectively, as that given by the accuracy of the balance, that is $u(m_1)^2 = u(m_2)^2 = \text{balance accuracy}$, and with the following expression:

$$u_{bal}(n)^2 = \frac{u(m_1)^2}{M_1} + \frac{u(m_2)^2}{M_2} \quad (2.46)$$

where M_1 and M_2 are the molecular weights of compounds 1 and 2, respectively.

Assuming a 5% error in the mass of water added during the experiments and a rectangular distribution, $u_{add}(n)$ is obtained from:

$$u_{add}(n)^2 = \frac{\left(0.05 \frac{m_{wat}}{M_{wat}}\right)^2}{3} \quad (2.47)$$

The uncertainty in volume is that given primarily by the calibration procedure. It is computed from:

$$u_c(V_L)^2 = u_{calib}(V_L)^2 = \frac{a^2}{3} \quad (2.48)$$

The uncertainties in height were estimated by assuming that the detectors can track the position of the tracer to an accuracy of 0.1 mm. Therefore:

$$u_c(h)^2 = (0.1)^2 \quad (2.49)$$



2.4.9 Results

The experimental VLE for the synthetic method is presented in [Table 2.7](#) as well as the estimated uncertainties. Only three experimental points were obtained with the use of the new technique, mainly limited by the half-life of the tracer. [Appendix G](#) contains the data sets used in the regression analysis. No signs of corrosion were observed in any of the experimental runs.

A graphical comparison of the new data with those from the static-analytical method and from the literature values of Freeman and Wilson (1985a) and Freeman and Wilson (1985b) is given in [Figure 2.23](#). All three data sources agree relatively well in regard to the liquid compositions. Discrepancies between the sources are for the vapour compositions. The new data are closer to the values reported by Freeman and Wilson (1985a) supporting the idea of a systematic error in the analytical measurements in [Section 2.3.5.4](#). Unfortunately, it is not possible to rule out the presence of a systematic error in the synthetic determinations as well. The disagreement between the phase compositions can be explained by accepting a source of error in the tracked position.

Several trials were needed before gathering valuable data. At the end, only four of nine experiments were of sufficient quality to be used in the fitting analysis. A possible source of error is the thickness of the coating material for the tracer. The coating process was done as consistent as possible for the different tracers but there is no way to guarantee that the same layer thickness was made in all cases. Insufficient coating material resulted in sinking of the particle. Another possible source of error is the scattering due to the wall thickness. This was an issue in

some of the measurements since it resulted in positions estimated with an error higher than 1 mm; such cases were eliminated.

Table 2.7. Experimental vapour – liquid equilibrium data for the acetic acid (1) + water (2) system determined by PEPT at pressure P , liquid mole fraction x , vapour mole fraction y , liquid molar density ρ_L and vapour molar density ρ_V at $T = 412.6$ K.^a

P [bar]	$u_c(P)$ [bar]	x_1	$u_c(x_1)$	y_1	$u_c(y_1)$	ρ_L [mol/L]	$u_c(\rho_L)$ [mol/L]	ρ_V [mol/L]	$u_c(\rho_V)$ [mol/L]
2.389	0.008	0.82	0.04	0.61	0.03	16.5	0.8	0.67	0.03
2.661	0.006	0.72	0.04	0.45	0.02	17.6	0.9	0.77	0.04
3.136	0.007	0.42	0.02	0.21	0.01	23.2	1.1	1.40	0.07

^a Combined standard uncertainties, u_c , for temperature are $u_c(T) = 0.1$ K. $u_c(P)$, $u_c(x_1)$, $u_c(y_1)$, $u_c(\rho_L)$ and $u_c(\rho_V)$ are display for each pressure.

The lack of experimental data for the phase molar densities at the conditions studied limited the assessment of the quality of the new data. It is possible to compare the obtained densities with simulations and only for the case of vapour densities to compare them with the literature values of Freeman and Wilson (1985a). The experimental values for the liquid phase compare well with modelling data, as will be shown in [Section 3.7.2.3 \(Table 3.8\)](#). On the other hand, experimental vapour densities are unphysical with one order of magnitude higher than those achieved from the modelling. The resulting system of linear equations [Equation \(2.25\)](#) used in the analysis had a conditioned number of around 300, meaning a loss of accuracy of 2 decimal places. It cannot be fully concluded, therefore, that the system is ill-conditioned and discard the results.

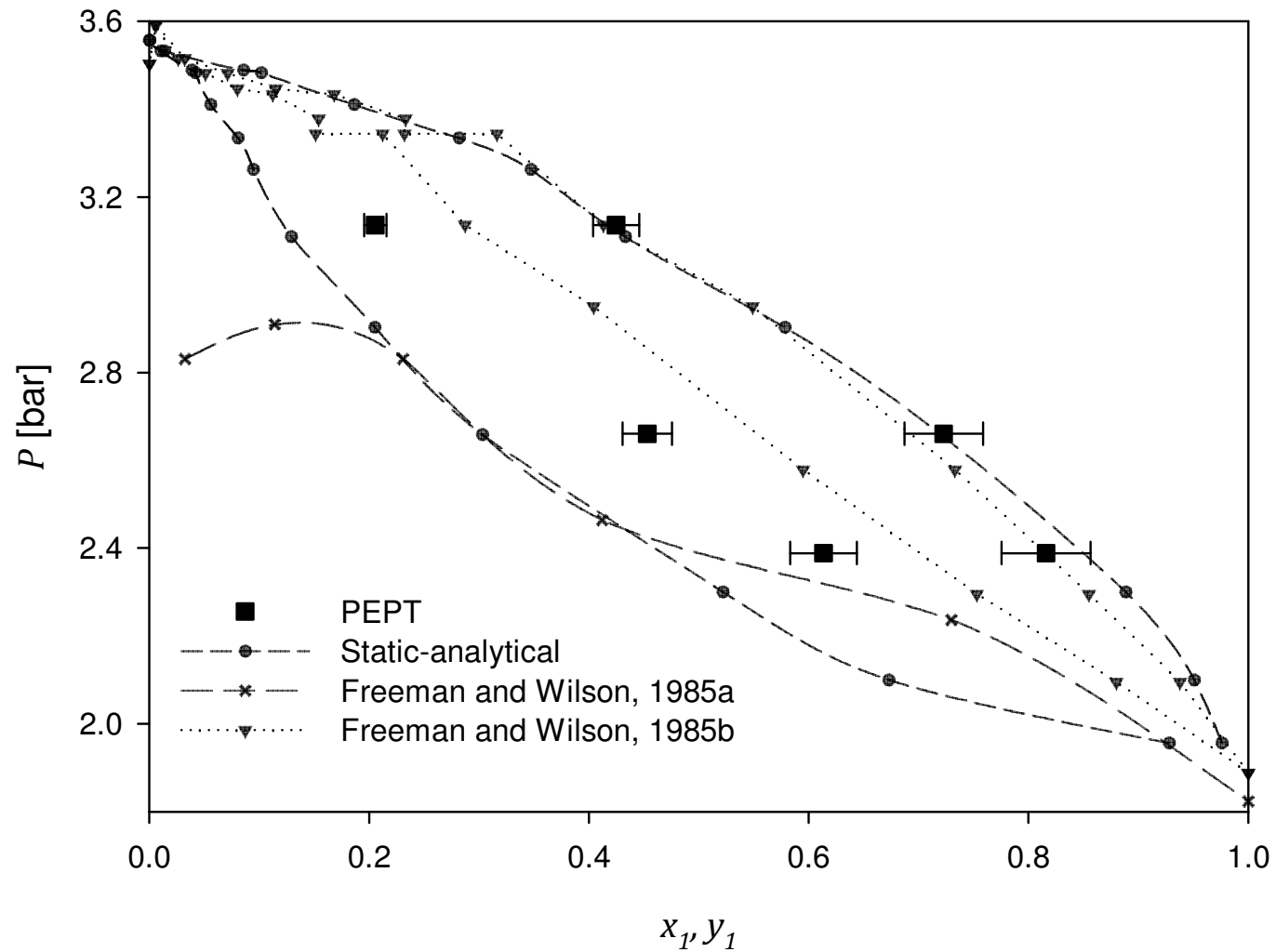


Figure 2.23. Vapour – liquid equilibrium diagram for the acetic acid (1) + water (2) system at 412.6 K obtained with PEPT, the static – analytical method described in Section 2.3.5.4 and literature values of Freeman and Wilson (1985a; 1985b). Figures: experimental data. Lines are used as a guide to the eye.



From the compressibility factors reported by Freeman and Wilson (1985a) it is possible to calculate the vapour phase molar densities. The computed densities are of the same order of magnitude than those obtained from the predictions of the equations of state, however, and as shown in [Figure 2.23](#), the vapour phase compositions display some erratic behaviour. It is not sensible, therefore, to use these data as a reference of comparison.

2.5 Concluding remarks

Two experimental rigs were designed and built based on the static-analytical and the synthetic methods to perform measurements for mixtures of acetic acid + water and propanoic acid + water. Analytical measurements were done by gas-chromatography. For the synthetic method, a new technique was established which uses PEPT technology to gather information of the interface location.

Experimental data was generated for the acetic acid + water at 412.6 K with the two methods. When compared with literature data both techniques gave similar results in the liquid compositions. Discrepancies are observed for the vapour phase between the different techniques. Compositions determined by the PEPT technique are closer to the literature values of Freeman and Wilson (1985b) than the ones obtained from the analytical method. The cause of the discrepancies for the case of the analytical method seems to be a possible systematic error in the sampling procedure. In the case of the synthetic method, the deviations are generated from the uncertainty in locating the tracer accurately. Despite these issues, valuable data have been generated for the acetic acid + water system at



412.6, 443.2 and 483.2 K for the liquid phase. The PEPT technique also allowed for molar densities determination of the phases. The determined vapour phase molar densities are unphysical with one order of magnitude higher than those reported in the literature or from equations of state calculations. The lack of experimental data in the open literature for the liquid densities limited the comparison.

Experimental data for the propanoic acid + water system were obtained from analytical measurements at 423.2, 453.2 and 483.2 K. The vapour sampling line had a lower dead volume compared with the experiments for acetic acid, resulting in more reliable measurements. The system exhibits azeotropic behaviour at the conditions studied, in agreement with previous observations at lower temperatures available in the open literature.

The new developed technique with use of PEPT technology will be valuable in measuring VLE at the interior of an enclosed equilibrium cell where direct visual determination of the interface is not possible.

3. Phase Equilibria Modelling

The governing equations of phase equilibria thermodynamics are well established and have been known for a long time (as early as 1876 with the work of Gibbs (cf. Prausnitz et al. (1999)). Equation (3.16) provides an exact solution for the fugacity term required in phase equilibria computations. The problem (challenge) in phase equilibrium modelling is not to solve the expressions for phase equilibrium per se but to account for volumetric properties of the pure compound or mixture in a pressure explicit form in order to calculate the term $\left(\frac{\partial P}{\partial n_i}\right)_{T,V,n_j}$. While such volumetric properties may be available in a tabulated experimental form, it is more useful to have them in the form of a mathematical expression such as an equation of state (EoS). An equation of state relates pressure, temperature, volume and composition properties. Experimental data are fitted to an EoS in order to obtain its characteristic parameters and, under pertinent considerations, to interpolate or extrapolate their applicability beyond the correlated conditions. To date there is no universal EoS that can be applicable to any system, pure component or mixture, simple or complex, from the low to the high density region without some degree of uncertainty. Even though many theories have been developed through the years towards a “universal” EoS, there is still a gap between theory and real application. The reason behind this, is due to the lack of knowledge at the molecular level. It is still not known how molecules of different substances or even of the same species interact with each other under different conditions. As Prausnitz et al. (1999) have pointed out: “progress in applications of phase equilibrium thermodynamics is possible only with increased



knowledge of intermolecular forces". The understanding of intermolecular forces is important in many aspects (Kontogeorgis and Folas, 2010): i) to interpret and understand phase behaviour, ii) to understand the molecular background of certain thermodynamic models and principles, iii) to choose thermodynamic models in particular applications, and iv) for thermodynamic model development, including mixing and combining rules.

This chapter focuses on the study of the thermodynamic modelling of the acetic acid + water and propanoic acid + water systems. For this purpose, the experimental data obtained in [Chapter 2](#) as well as data available from the open literature is included in the modelling. The chapter begins with providing some preliminary background about equilibrium modelling, starting with the topic of molecular forces in nature. A succinct introduction to intermolecular potential functions as a way to modelled intermolecular forces is given, mostly based on the review of Prausnitz et al. (1999). The criteria for phase equilibria is given next and the role of the Helmholtz free energy in deriving thermodynamic properties at equilibrium. The chapter continues by covering the mathematical expressions of the thermodynamic models chosen for the computations, namely, the Peng-Robinson (PR), the Cubic Plus Association (CPA), the Perturbed Chain Statistical Associating Fluid Theory (PC-SAFT) and the PC polar SAFT (PCP-SAFT); as well as the available methods for gathering information about their pure component parameters. The topic of association schemes in SAFT-type equations of state is introduced and a literature review of previous considerations on the association schemes for organic acids and water is given.



A comparison of the accuracy of the models in predicting and correlating the experimental data of the systems under study are presented and discussed in the [Results and Discussion](#) section. The analysis involves the different possible association schemes for organic acids and water.

The chapter ends with some general conclusions about the most suitable thermodynamic model for phase equilibrium computations and the role of the association scheme.

3.1 Preliminary background

3.1.1 Intermolecular forces

The force, F , acting between two molecules is related to the intermolecular potential energy function, Γ , according to:

$$F(r, \theta, \phi, \dots) = -\nabla\Gamma(r, \theta, \phi, \dots) \quad (3.1)$$

where r is the distance between the molecules and θ , ϕ , etc., are additional coordinates to fully specify the potential energy. Commonly, F is simplified and expressed only in terms of the distance r :

$$F = -\frac{d\Gamma}{dr} \quad (3.2)$$



Expressions for Γ are dependent upon the actual intermolecular (and interparticle) interactions. The negative sign in the potential energy function indicates attractive forces (work must be done to separate two molecules), and a positive sign repulsive forces (work to bring together two molecules).

Among the several intermolecular forces, in non-ionic liquids, the most important are the dispersion (London), dipolar (Keesom) and induction (Debye) forces.

Dispersion forces are always present, are quantum mechanical in origin and temperature independent ([Equation \(3.3\)](#)) (Israelachvili, 2011).

$$\Gamma_{12} = -\frac{3\alpha_1\alpha_2}{2(4\pi\epsilon_0)^2r^6} \left(\frac{I_1I_2}{I_1 + I_2} \right) \quad (3.3)$$

In [Equation \(3.3\)](#), α is the electronic polarizability, ϵ_0 is the dielectric permittivity of vacuum and I is the first ionization potential.

Dipolar forces appear in particles without a net electric charge but with an uneven spatial distribution of electronic charges about the nuclei. The potential energy is a function of the distance and orientation of the dipole moment, μ . This orientation is in turn a result of two factors: an electric field tending to align the dipoles, and the kinetic energy allocating them randomly. At high temperatures, as orientations are increasingly random, the potential energy diminishes. Keesom (1922) showed that orientations leading to negative potential energies are more likely to appear at moderate and high temperatures. The potential energy after averaging over all orientations is:



$$\Gamma_{12} = -\frac{\mu_1^2 \mu_2^2}{3kT(4\pi\epsilon_0)^2 r^6} \quad (3.4)$$

in which k is the Boltzmann's constant and T the temperature. Polar forces are important when modelling molecules with a dipole moment above 1 D (Kontogeorgis and Folas, 2010).

Molecules can also exhibit quadrupole moment as a result of concentration of electric charge at four different points. Quadrupolar forces, although important as they provide special characteristics to the molecules containing them (e.g. carbon dioxide) are not as well studied as dipolar forces. Quadrupolar and higher multipoles have less effect on the thermodynamic properties than the dipoles.

Furthermore, polar as well as non-polar molecules can exhibit a dipolar moment when subjected to an electric field that changes its electron orientations, creating an induce dipole. The induce dipole moment, μ^i , is proportional to the field strength E :

$$\mu^i = \alpha E \quad (3.5)$$

where the proportionality factor, α , is known as the polarizability of the molecule. The resultant potential energy was first calculated by Debye and the general equation is:

$$\Gamma_{12} = -\frac{\alpha_1 \mu_2^2 + \alpha_2 \mu_1^2}{(4\pi\epsilon_0)^2 r^6} \quad (3.6)$$



Induce polar interactions are the weakest of the van der Waals forces.

A special kind of force that can be classified as an attractive quasi-chemical force is the so-called hydrogen bonding. It is quantum mechanical in origin and its bonds are formed by the attraction of hydrogen atoms attached to nitrogen or oxygen atoms. Hydrogen bonds are not true bonds and as such, are weaker than the covalent (chemical) bonds, but stronger than van der Waal forces. Hexamer structures in hydrogen fluoride, crystal structure of ice and dimerization in organic acids are all examples of hydrogen bonding. In relation to hydrogen bonding in solutions, it is possible to distinguish between two effects: association and solvation. Association (self-association) refers to the tendency of molecules to form polymers while solvation (cross-association) to molecules of different species to form complexes. For the cross-association effects there are the following possibilities (Kontogeorgis and Folas, 2010):

- i) Cross-association between two self-associating compounds. For example, water – methanol.
- ii) Solvation where only one of the compounds is self-associating. For example water – acetone.
- iii) Solvation where none of the compounds is self-associating but cross associate. For example, chloroform – acetone.

Functions for the potential energy due to hydrogen bonding are complex (Israelachvili, 2011) and for the case of those applied in equations of state, are vast simplifications.



3.1.2 Intermolecular potential functions

London (1937) calculated potential energies for a few simple molecules in the form:

$$\Gamma = -\frac{B}{r^6} \quad (3.7)$$

where B was either a contribution of dispersion, dipole or induction interactions. London showed in this form the relative contribution of these forces to the potential energy. It was observed that [Equation \(3.7\)](#) did not hold at small distances; i.e., when repulsive forces become more dominant than attractive forces. Conveniently, repulsive forces are expressed to vary as a function of an inverse-power law according to:

$$\Gamma = \frac{A}{r^m} \quad (3.8)$$

Mie (1903), assumed that the total potential energy could be expressed as the addition of the attractive and repulsive potentials:

$$\Gamma = \Gamma_{repulsive} + \Gamma_{attractive} = \frac{A}{r^m} - \frac{B}{r^n} \quad (3.9)$$

where A , B , m and n are positive constants.

[Equation \(3.9\)](#) has served as the basis for the development of several intermolecular functions aiming to improve the modelling of intermolecular forces.



The most representative intermolecular functions, at least in the context of this thesis, are: the Hard Sphere potential, the Lennard-Jones, the Square Well and the Chen-Kreglewski potential, which have also served as the basis for the development of modern equations of state. A profound description of these and other intermolecular potentials as well as their graphical representation can be found in the reviews of Prausnitz et al. (1999) and Kontogeorgis and Folas (2010).

3.1.3 Thermodynamic treatment of VLE

The equilibrium state can be defined as the state in which there is no driving force for a change of the intensive variables within the system (Elliott and Lira, 2012); that is, a system without tendency to depart spontaneously.

For an isolated non-reacting system, consisting of π phases (heterogeneous system) and C components, for which the individual phases are considered open systems, the set of equations defining the equilibrium criteria are:

$$T^{(1)} = T^{(2)} = \dots T^{(\pi)} \quad (3.10)$$

$$P^{(1)} = P^{(2)} = \dots P^{(\pi)} \quad (3.11)$$

$$\mu_i^{(1)} = \mu_i^{(2)} = \dots \mu_i^{(\pi)} \quad i = 1, \dots, C \quad (3.12)$$

where T is temperature, P pressure and μ the chemical potential (defined first by J.W. Gibbs (1876)). The objective of phase equilibrium thermodynamics is to



establish the magnitudes of P , T and μ at the equilibrium state. Four equivalent expressions for the chemical potential are possible in terms of the thermodynamic variables of Internal energy (U), Enthalpy (H), Helmholtz free energy (A) and Gibbs free energy (G):

$$\mu_i = \left(\frac{\partial U}{\partial n_i} \right)_{S,V} = \left(\frac{\partial H}{\partial n_i} \right)_{S,P} = \left(\frac{\partial A}{\partial n_i} \right)_{T,V} = \left(\frac{\partial G}{\partial n_i} \right)_{T,P} \quad (3.13)$$

Variable S in Equation (3.13) is the Entropy of the system. To relate the chemical potential to quantifiable variables such as T , P and V , G.N Lewis introduced the concept of fugacity, f . The relationship between fugacity and chemical potential for an isothermal change, for any component in any system is given by:

$$\mu_i - \mu_i^0 = RT \ln \frac{f_i}{f_i^0} \quad (3.14)$$

where μ_i^0 and f_i^0 are the chemical potential and the fugacity in the standard state, respectively. At equilibrium, the fugacity for each phase and component must be equal:

$$f_i^{(1)} = f_i^{(2)} = \dots = f_i^{(\pi)} \quad i = 1, \dots, C \quad (3.15)$$

From relationships of the classical thermodynamics and by defining an additional variable, the fugacity coefficient, as $\varphi_i = \frac{f_i}{y_i P}$, it is possible to relate f with the volumetric properties according to (Michelsen and Mollerup, 2007):



$$RT \ln \varphi_i = RT \ln \frac{f_i}{y_i P} = - \int_{\infty}^V \left[\left(\frac{\partial P}{\partial n_i} \right)_{T, V, n_j} - \frac{RT}{V} \right] dV - RT \ln Z \quad (3.16)$$

From a mathematical point of view, it is more convenient to differentiate rather than integrate. By interchanging the order of integration and differentiation in [Equation \(3.16\)](#) a more useful expression is derived (Michelsen and Mollerup, 2007):

$$RT \ln \varphi_i = \left(\frac{\partial A^{res}(T, V, n)}{\partial n_i} \right)_{T, V, n_j} - RT \ln Z \quad (3.17)$$

where A^{res} is the residual Helmholtz function, defined as the difference between the total Helmholtz free energy of the mixture at conditions T , V and n , and that of the ideal gas mixture at the same state variables T , V and n :

$$\frac{A^{res}(T, V, n)}{RT} = \frac{A(T, V, n)}{RT} - \frac{A^{ideal}(T, V, n)}{RT} \quad (3.18)$$

A thermodynamic model for computing the volumetric properties can, therefore, be defined in terms of its residual Helmholtz free energy. Other thermodynamic properties can be calculated as partial derivatives of A^{res} :

Pressure:

$$P = - \left(\frac{\partial A^{res}(T, V, n)}{\partial V} \right)_{T, n} + \frac{nRT}{V} \quad (3.19)$$



Compressibility factor, Z :

$$Z = 1 - \frac{V}{nRT} \left(\frac{\partial A^{res}(T, V, n)}{\partial V} \right)_{T, n} \quad (3.20)$$

Residual chemical potential, μ^{res} :

$$\mu_i^{res}(T, V, n) = \left(\frac{\partial A^{res}(T, V, n)}{\partial n_i} \right)_{T, V} \quad (3.21)$$

In practice, there are two methods for the application of [Equation \(3.17\)](#) in the modelling of the VLE of non-ideal systems. The first method, named equation of state method or φ - φ method, relates the fugacity and the volumetric properties of the different phases. [Equation \(3.15\)](#) can be rewritten for the i^{th} component as:

$$\varphi_i^L x_i = \varphi_i^V y_i \quad (3.22)$$

Where φ is the fugacity coefficient, x and y are the molar fractions in the liquid and vapour phases, respectively. Both fugacity coefficients are computed through equations of state.

The second method is the activity coefficient method or γ - φ method. In this case, the liquid phase non-ideality is treated through the activity coefficient (γ) and the vapour phase through the fugacity coefficient. [Equation \(3.15\)](#) is rewritten as:

$$\gamma_i x_i f_i^0 = \varphi_i^V y_i P \quad (3.23)$$



where f_i^0 is the fugacity of the i^{th} component in the standard state. γ is calculated from a local composition activity model and φ by an EoS. The most popular activity models are perhaps the models of Wilson, NRTL, UNIQUAC, UNIFAC and more recently COSMO-RS/SAC (Prausnitz et al., 1999; Elliott and Lira, 2012). Although easy and fast calculations can be obtained with this method, the main disadvantage is that it is only appropriate from low to moderate pressures (<10 bar).

The advantages of the φ - φ over the γ - φ method is that a single thermodynamic model can represent all the phases involved, is applicable over a wider range of temperatures and pressures, and besides volumetric properties, calorific properties can also be obtained. Solution of [Equation \(3.22\)](#) is an iterative process that requires an algorithm for its acceleration.

It is worth mentioning that, although the equality of fugacities is a necessary condition at equilibrium, it does not guarantee the stability of the system. The solution may correspond to local minima, maxima or saddle points of the Gibbs free energy. Baker et al. (1982) demonstrated theoretically that a necessary and sufficient condition for stability is that at any given temperature and pressure, the tangent plane to the Gibbs free energy surface at a given overall composition should not intersect the surface at another point. The problem was studied numerically by Michelsen (1982b; 1982a) who provided algorithms for its solution.

Stability analysis is a rigorous task in phase equilibrium calculations that guarantees truly equilibrium stages, usually accomplished by minimization techniques. If the number of phases at equilibrium are known or assumed,



equation solving methods (Wakeham and Stateva, 2004) can also be applied in the solution of the equilibrium problem. In this sense, the algorithm of Sandler (1998) for bubble-point calculations has been implemented in this project for the solution of [Equation \(3.22\)](#), i.e., following the method of equations of state. The necessary routines were implemented in Matlab (The MathWorks Inc., 2013).

The next section presents an overview of equations of state and focuses on the selected models showing their mathematical expressions.

3.1.4 Equations of state

An equation of state is a thermodynamic model that relates the T , P and V state functions. The first equation of state able to predict the coexistence of a liquid and vapour phase was proposed by van der Waals in 1873 which carries its name. The van der Waals equation (vdW) ([Equation \(3.24\)](#)) was also the first to consider separately attractive and repulsive forces. V in [Equation \(3.24\)](#) is the molar volume, R is the gas constant, a , the attraction or energy parameter and b the repulsion or co-volume parameter.

$$P = \frac{nRT}{V - nb} - \frac{n^2a}{V^2} \quad (3.24)$$

It is thanks to this pioneering work that today there is a vast selection of equations of state to choose from depending on the industrial needs. Although important for its breakthrough development, the van der Waals equation is no longer in use other than as historical reference. It provides only qualitative descriptions of the



PVT relationships. In this manner, Vankonyenburg and Scott (1980) applied the equation in developing the classification system of binary mixtures according to their *PT* projections.

The vdW EoS has been the subject of hundreds of modifications, and because when rearranged in terms of volume Equation (3.24) is a polynomial of third order, it has given rise to the well-known cubic equations of state family (sometimes also called empirical or semi-empirical) (Kontogeorgis and Folas, 2010). Reviews about the modifications of the vdW equation can be found in the papers of Abbott (1979); Wei and Sadus (2000); Poling et al. (2001); Valderrama (2003) and Economou (2010).

Undoubtedly, the most popular modifications of the vdW equation among academia and industry are the Soave-Redlich-Kwong (SRK) (Soave, 1972) and the Peng-Robinson (PR) (Peng and Robinson, 1976) EoS. They have been widely applied in modelling systems encountered in the oil and gas industry, but also in modelling complex mixtures including polymer systems (Leeke et al., 2001; Economou, 2010) under certain modifications, e.g. using different mixing and combining rules (Goodwin and Sandler, 2010). Cubic equations of state have been widely studied and their pitfalls are well understood nowadays. For example, the inaccuracy of the repulsive term was established a long time ago (Henderson, 1979) and that the attractive term serves somehow to correct for its inaccuracies. Some of the disadvantages of the cubic EoS are (Valderrama, 2003; Kontogeorgis and Folas, 2010):



- i) The attractive and repulsive term are both inaccurate, as shown by molecular simulation.
- ii) In most cases, predictions (interaction parameters set to zero) are not possible.
- iii) Often, a temperature-dependent interaction parameter is needed.
- iv) Poor correlations of complex mixtures (e.g. polar and associating) are usually obtained.
- v) When two interaction parameters are used (k_{ij} and l_{ij}), they cannot be easily generalized as a function of some characteristics of the compounds involved (e.g. molecular weight, polarity, etc.).
- vi) Liquid – liquid equilibria is in general not well correlated.
- vii) Cannot be easily extended to electrolyte systems or biomolecules.

Despite these limitations, some of the main advantages are (Valderrama, 2003; Kontogeorgis and Folas, 2010):

- i) Simple mathematical models resulting in fast computations.
- ii) Applicable over a wide range of T and P
- iii) Usually a single binary interaction parameter is needed for modelling hydrocarbon systems.



- iv) Satisfactory results for low- and high-pressure VLE.

- v) Vast databases and correlations for k_{ij} .

A different group of EoS is that classified as theoretical equations. Such equations are developed based on a more theoretical sound basis (e.g. based on perturbation theory). The main advantages of the theoretical EoS over the empirical are (von Solms et al., 2005):

- i) The model can be tested against molecular simulation results.

- ii) The model can be improved by extending the theory.

- iii) Equation parameters have a physical meaning.

Wei and Sadus (2000) have presented an equation of state tree to visualize the distinction between the empirical and the theoretical EoS (Figure 3.1). The van der Waals branch corresponds to those of the empirical group, while those of the Thermodynamic Perturbation Theory to the theoretical.

Based on theoretical considerations on theory of hard bodies, Carnahan and Starling (1969; 1972) developed a term for a hard-sphere fluid and introduced it as a substitution of the repulsive term in the Redlich-Kwong (RK) equation. It proved to be an improvement over the RK model. The Carnahan and Starling (CS) repulsive term was not the first modification to the term (Wei and Sadus, 2000), but it is perhaps the most popular.

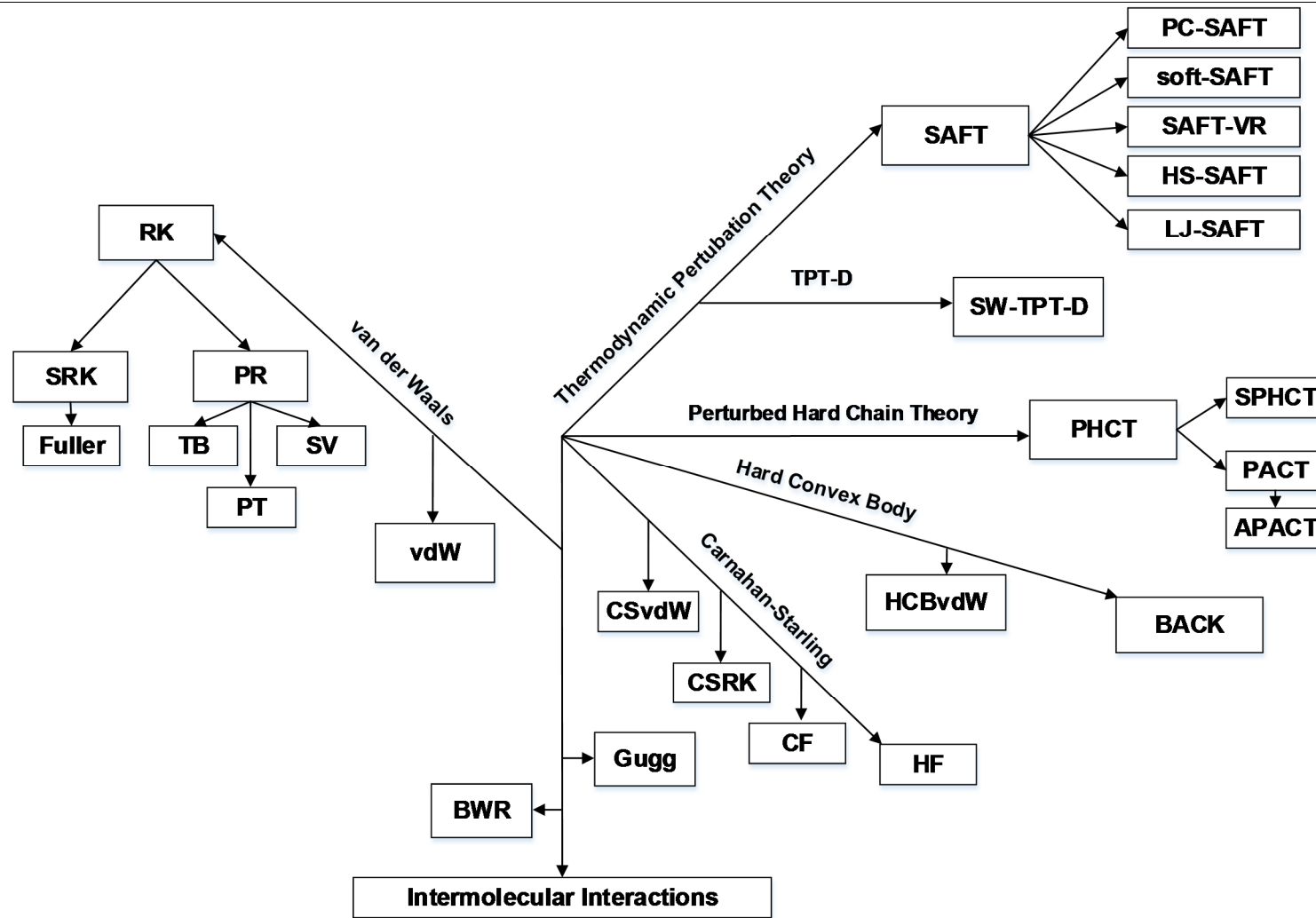


Figure 3.1. Equation-of-state tree showing the inter-relationship of different equations of state. Adapted from Wei and Sadus (2000).



Further improvements can be done if the attractive term is also modified. In fact, and as was observed by Henderson (1979), the attractive term in the RK was developed to compensate the limitations of the repulsive term in the VdW equation, and therefore not necessarily the best choice if a different expression is used. In light of this, Chen and Kreglewski proposed a term for the attractive part based on simulation data of Alder (Wei and Sadus, 2000); the equation was termed BACK.

Beret and Prausnitz (1975) developed an equation of state based on perturbed hard-sphere theory for chain molecules and Prigogine's theory for chain molecules. The equation was named PHCT (Perturbed Hard Chain Theory) and has led to further developments to make it simpler (simplified PHCT) (Kim et al., 1986), to include polar (Perturbed Anisotropic Chain Theory, PACT) (Vimalchand and Donohue, 1985), as well as association interactions (Associated-PACT, APACT) (Ikonomou and Donohue, 1986).

A large step towards more accurate equations of state was done with the development of the Statistical Associating Fluid Theory (SAFT) methodology (Chapman et al., 1988; Chapman et al., 1989; 1990) based on the Perturbation Theory of Wertheim (Wertheim, 1984a; b; 1986a; b). In SAFT, the residual Helmholtz energy is given as a sum of contributions due to the hard-sphere reference fluid (A^{hs}), dispersion forces (A^{disp}), chain formation (A^{chain}) and association (A^{assoc}) interactions. The model has been extended also to treat polar as well as electrolyte interactions (McCabe and Galindo, 2010). Several versions of the original model exist nowadays, starting with the version of Huang and Radosz (SAFT-HR) (Huang and Radosz, 1990; 1991; 1993) which has given path



to the now known as SAFT-type family equations of state. Economou (2002) has made a review of the first modifications of the SAFT model. More recent publications are those of McCabe and Galindo (2010) and Kontogeorgis and Folas (2010).

Among the many SAFT versions, it is possible to highlight the SAFT-HR (Huang and Radosz, 1990; 1991; 1993), Lennard-Jones (LJ)-SAFT (Kraska and Gubbins, 1996a; b), SAFT- variable range (VR) (Gil-Villegas et al., 1997), Soft-SAFT (Blas and Vega, 1997; 1998) and Perturbed Chain (PC)-SAFT (Gross and Sadowski, 2000; 2001; 2002). SAFT and its variants have been applied successfully in modelling simple to complex mixtures (Economou, 2002; Kontogeorgis and Folas, 2010; McCabe and Galindo, 2010).

One of the modifications of SAFT that has gained particular popularity is the PC-SAFT model (Gross and Sadowski, 2001; 2002), being itself the subject of several modifications which will be mentioned in [Section 3.3](#).

An aspect linked with the use of SAFT-type EoS is the acquisition of the pure component parameters of the model. Different techniques have been proposed to determine pure component parameters as an alternative to the common fitting procedure of saturated properties, in order to reduce or even to eliminate the number of adjustable parameters (Kouskoumvekaki et al., 2004b; McCabe and Galindo, 2010; Albers et al., 2012; Umer et al., 2014). However, there is not yet absolute proof that these techniques work better than the traditional fitting; of course, providing these data are available and of quality.



Group contribution methods can also be used to determine pure component parameters and even binary parameters, which have given rise to the SAFT group contribution (GC) equations of state: the GCA (Gros et al., 1996), GC-SAFT (Tamouza et al., 2004), GC-polar SAFT (Nguyen-Huynh et al., 2008), GC-sPC-SAFT (Tihic et al., 2008), the GC-SAFT-VR (Peng et al., 2009) and the GC-PPC-SAFT (Nguyen-Huynh et al., 2011; Rozmus et al., 2011). Preliminary versions of GC + SAFT methods can be found in the reviews of McCabe and Galindo (2010) and in Kontogeorgis and Folas (2010).

An equation presenting a balance between simplicity and reliability is desirable for engineering practical applications. With this objective in mind, Kontogeorgis et al. (1996) developed the Cubic Plus Association (CPA) EoS, that is a practical approach to improve the capability of a cubic equation of state (representing the physical forces) by coupling it with a term to account for the association forces. In its development, Kontogeorgis et al. (1996) decided to use the SRK equation with the association model of Wertheim; i.e. the same association term as in the SAFT-type equations. An advantage of the CPA model is that in case no association interactions are required, e.g. in modelling hydrocarbons, the user can easily recover the SRK equation.

The physical part in CPA is not restricted to SRK, it can be handled by any cubic model, for instance the PR (Pfohl et al., 1999; Huang et al., 2007), or by a new expression as recently done by Polishuk (2011a; 2011b; 2011c).

It is also possible to name “CPA” equations that are not necessary cubic but that present three real roots (Kontogeorgis et al., 2006a), as is the case of the Elliot-



Suresh-Donohue (ESD) equation (Elliott Jr et al., 1990; Suresh and Elliott, 1992).

An interesting feature of ESD is that the association contributions are modelled by a reaction equilibrium approach instead of a potential function.

Recently, De Villiers et al. (2011) have modified CPA to account for dipolar interactions, testing the dipolar terms of Jog and Chapman (1999) and Gross and Vrabec (2006). The VLE of several mixtures were tested showing the improvements of the polar CPA.

In this work, the PR, the CPA model of Kontogeorgis et al. (1996) and the PC-SAFT models have been selected to model the experimental data. The next sections deal with their mathematical expressions.

3.2 The Peng-Robinson equation of state

It is worth mentioning what Gray (1979) stated regarding his experience in applying the Redlich-Kwong (RK) equation, which can be extended in general to the cubic equations: "... Regardless of which of the new methods [he was referring partially to the promising Perturbed Hard-Chain model of Donohue and Prausnitz] ultimately find wide use in industrial applications, the process of selecting, adapting, and testing them for this purpose will take years. During this period RK [cubic] methods will provide the benchmark by which the emerging methods are judged..."

It is in this sense that the results of the modelling with the Peng-Robinson (PR) EoS are presented in this thesis. In other words, we know its flawless, we know it will fail but we need a basis to compare with.

The Soave-Redlich-Kwong (SRK) (Soave, 1972) and the PR (Peng and Robinson, 1976) equations can be written in a general form in terms of the residual Helmholtz free energy as (Michelsen and Mollerup, 2007):

$$\frac{A^{res}(T, V, n)}{RT} = -n \ln(1 - B/V) - \frac{D(T)}{RTB(\delta_1 - \delta_2)} \ln \left(\frac{1 + \delta_1 B/V}{1 + \delta_2 B/V} \right) \quad (3.25)$$

The PR equation is recovered by setting $\delta_1 = 1 + \sqrt{2}$ and $\delta_2 = 1 - \sqrt{2}$. $D(T)$ and B are computed from van der Waals one-fluid mixing rules according to:

$$D(T) = n^2 a_{mix} = \sum_i \sum_j n_i n_j a_{ij}(T) \quad (3.26)$$

$$nB = n^2 b_{mix} = \sum_i \sum_j n_i n_j b_{ij} \quad (3.27)$$

with the following classical combining rules:

$$a_{ij}(T) = \sqrt{a_i a_j} (1 - k_{ij}) \quad (3.28)$$

$$b_{ij} = \frac{(b_i + b_j)}{2} (1 - l_{ij}) \quad (3.29)$$



where k_{ij} and l_{ij} are binary interaction parameters. For the case in which $l_{ij} = 0$, as it is often assumed, Equation (3.27) reduces to:

$$B = \sum_i n_i b_i \quad (3.30)$$

Parameters a and b are commonly obtained from correlations of critical properties (T_c , P_c) and acentric factor (ω) (Equations (3.72) and (3.73) in Section 3.6), but they can also be obtained from fitting vapour pressures and liquid density data (Voutsas et al., 2006; Alfradique and Castier, 2007).

3.3 The PC-SAFT equation of state

The Perturbed Chain Statistical Associating Fluid Theory (PC-SAFT) (Gross and Sadowski, 2001) was developed based on perturbation theories of statistical thermodynamics. The underlying idea consists in dividing the intermolecular forces in a reference term and a perturbation term. The reference term comprises the repulsion interactions while the perturbation the attraction interactions. In contrast to SAFT for which the reference fluid is a hard-sphere, in PC-SAFT the reference system is a hard-chain fluid and the perturbation is given by the attractive dispersion, association and polar interactions (dipolar, quadrupolar, induced-dipolar, etc.) (Tumakaka et al., 2005; Kleiner, 2008). These contributions add to the residual Helmholtz free energy of the system:

$$\frac{A^{res}(T, V, n)}{RT} = \frac{A^{hc}(T, V, n)}{RT} + \frac{A^{disp}(T, V, n)}{RT} + \frac{A^{assoc}(T, V, n)}{RT} + \frac{A^{polar}(T, V, n)}{RT} \quad (3.31)$$



PC-SAFT has been applied successfully in modelling from simple hydrocarbons to complex mixtures, e.g. ionic liquids, polymer and electrolyte systems, in a wide range of conditions, including supercritical conditions (Arce and Aznar, 2010; Justo-García et al., 2010; McCabe and Galindo, 2010; Naeem and Sadowski, 2010; Román-Ramírez et al., 2010; Costa et al., 2011; Naeem and Sadowski, 2011; Sadowski, 2011; Bamgbade et al., 2012; Maity, 2012; Xu et al., 2012; Leekumjorn and Krejbjerg, 2013; Carneiro et al., 2014; Liang et al., 2014b; Sedghi and Goual, 2014; Zuñiga-Hinojosa et al., 2014). However, and despite this success, it has been shown the limitations of the model under certain conditions, for example, two regions of two-phases for pure compounds and negative values of critical points for long chain values ($m > 210$) possible in polymers (Yelash et al., 2005; Privat et al., 2010).

3.3.1 Hard Chain Fluid reference term

The reference fluid consists of chain molecules of spherical freely jointed hard-sphere segments lacking of attraction interactions. The reference system is described by the equation of state for the hard-chain fluid developed by Chapman et al. (1988). The intermolecular potential function describing the interactions between the chain segments is given by a modified square well potential proposed by Chen and Kreglewski (1977) for non-associating molecules, that takes into account the soft-repulsion. In contrast to the work of Chen and Kreglewski no temperature correction was introduced in the depth of the potential well. As a result, non-associating molecules can be characterized by three parameters: the number of segments per chain (m), the temperature-



independent segment diameter (σ) and the depth of the potential well (ε); usually obtained from fitting vapour pressures and saturated liquid density data. The Helmholtz energy due to chain formation for mixtures is given as:

$$\frac{A^{hc}(T, V, n)}{RT} = \bar{m} \frac{A^{hs}(T, V, n)}{RT} - \sum_i n_i (m_i - 1) \ln g_{ii}^{hs}(d_{ii}) \quad (3.32)$$

where n_i is the number of moles of compound i . \bar{m} is the mean segment number in the mixture, computed from:

$$\bar{m} = \sum_i n_i m_i \quad (3.33)$$

The radial distribution function for the hard-sphere fluid is given by:

$$g_{ij}^{hs}(d_{ij}) = \frac{1}{1 - \zeta_3} + \left(\frac{d_i d_j}{d_i + d_j} \right) \frac{3\zeta_2}{(1 - \zeta_3)^2} + \left(\frac{d_i d_j}{d_i + d_j} \right)^2 \frac{2\zeta_2^2}{(1 - \zeta_3)^3} \quad (3.34)$$

And the Helmholtz free energy due to the hard-sphere segments by:

$$\frac{A^{hs}(T, V, n)}{RT} = \frac{1}{\zeta_0} \left[\frac{3\zeta_1\zeta_2}{1 - \zeta_3} + \frac{\zeta_2^3}{\zeta_3(1 - \zeta_3)^2} + \left(\frac{\zeta_2^3}{\zeta_3^2} - \zeta_0 \right) \ln(1 - \zeta_3) \right] \quad (3.35)$$

with

$$\zeta_l = \frac{\pi}{6} \rho \sum_i n_i m_i d_i^l \quad l = (0, 1, 2, 3) \quad (3.36)$$

ρ in the equation above is defined as the total number density of molecules. The temperature-dependent segment diameter is obtained from:

$$d_i = \sigma_i \left[1 - 0.12 \exp \left(-3 \frac{\varepsilon_i}{kT} \right) \right] \quad (3.37)$$

3.3.2 Dispersion term

The expression for the dispersive interaction was derived by applying the perturbation theory of Barker and Henderson (Gross and Sadowski, 2000; 2001) for the hard-chain fluid:

$$\begin{aligned} \frac{A^{disp}(T, V, n)}{RT} = & -2\pi\rho I_1(\eta, \bar{m}) \sum_i \sum_j n_i n_j m_i m_j \left(\frac{\varepsilon_{ij}}{kT} \right) \sigma_{ij}^3 \\ & - \pi\rho \bar{m} C_1 I_2(\eta, \bar{m}) \sum_i \sum_j n_i n_j m_i m_j \left(\frac{\varepsilon_{ij}}{kT} \right)^2 \sigma_{ij}^3 \end{aligned} \quad (3.38)$$

with

$$C_1 = \left(1 + \bar{m} \frac{8\eta - 2\eta^2}{(1 - \eta)^4} + (1 - \bar{m}) \frac{20\eta - 27\eta^2 + 12\eta^3 - 2\eta^4}{[(1 - \eta)(2 - \eta)]^2} \right)^{-1} \quad (3.39)$$

and the following power series function of reduced density, η , and the mean segment number:

$$I_1(\eta, \bar{m}) = \sum_{i=0}^6 a_i(\bar{m}) \eta^i \quad (3.40)$$

$$I_2(\eta, \bar{m}) = \sum_{i=0}^6 b_i(\bar{m})\eta^i \quad (3.41)$$

The coefficients a_i and b_i are functions of \bar{m} according to:

$$a_i(\bar{m}) = a_{0i} + \frac{\bar{m} - 1}{\bar{m}} a_{1i} + \frac{\bar{m} - 1}{\bar{m}} \frac{\bar{m} - 2}{\bar{m}} a_{2i} \quad (3.42)$$

$$b_i(\bar{m}) = b_{0i} + \frac{\bar{m} - 1}{\bar{m}} b_{1i} + \frac{\bar{m} - 1}{\bar{m}} \frac{\bar{m} - 2}{\bar{m}} b_{2i} \quad (3.43)$$

Values for the coefficients in [Equations \(3.42\)](#) and [\(3.43\)](#) are reported in the original publication of Gross and Sadowski (2001).

For mixtures, conventional Berthelot-Lorenz combining rules are employed introducing one adjustable interaction parameter, k_{ij} , to correct for the mixture dispersion energy:

$$\sigma_{ij} = \frac{(\sigma_i + \sigma_j)}{2} \quad (3.44)$$

$$\varepsilon_{ij} = \sqrt{\varepsilon_i \varepsilon_j} (1 - k_{ij}) \quad (3.45)$$

3.3.3 Association contribution

Based on Wertheims's first order perturbation theory Chapman et al. (1988); Chapman et al. (1989; 1990) derived an expression to account for association contributions which was implemented in the SAFT model (Chapman et al., 1989;

Huang and Radosz, 1990; 1991; 1993) and later in PC-SAFT (Gross and Sadowski, 2002). The association term allows the PC-SAFT model to be applicable to mixtures exhibiting hydrogen bonding, e.g. aqueous, organic acids, alcohols, polymers, etc. It is a linear average with respect to the number of moles according to:

$$\frac{A^{assoc}(T, V, n)}{RT} = \sum_i n_i \sum_{A_i} \left(\ln X^{A_i} - \frac{X^{A_i}}{2} + \frac{1}{2} \right) \quad (3.46)$$

where X^{A_i} is the fraction of molecules of component i that are not bonded at the association site A , and is given by the following implicit equation:

$$X^{A_i} = \frac{1}{1 + \frac{1}{V} \sum_j n_j \sum_{B_j} X^{B_j} \Delta^{A_i B_j}} \quad (3.47)$$

The term $\Delta^{A_i B_j}$ can be seen as a strength of association computed by:

$$\Delta^{A_i B_j} = g_{ij}^{seg}(d_{ij}) \kappa^{A_i B_j} \sigma_{ij}^3 \left[\exp\left(\frac{\varepsilon^{A_i B_j}}{kT}\right) - 1 \right] \quad (3.48)$$

The radial distribution function for the segments, $g_{ij}^{seg}(d_{ij})$, in Equation (3.48) is approximated by that of the hard-sphere fluid expression, i.e.:

$$\begin{aligned} g_{ij}^{seg}(d_{ij}) &\approx g_{ij}^{hs}(d_{ij}) \\ &= \frac{1}{1 - \zeta_3} + \left(\frac{d_i d_j}{d_i + d_j} \right) \frac{3\zeta_2}{(1 - \zeta_3)^2} + \left(\frac{d_i d_j}{d_i + d_j} \right)^2 \frac{2\zeta_2^2}{(1 - \zeta_3)^3} \end{aligned} \quad (3.49)$$



The association term introduces two additional pure component parameters, the association volume, $\kappa^{A_i B_i}$, and the association energy, $\varepsilon^{A_i B_i}$, between site A and site B of component i , also treated as adjustable parameters. Combining rules of Wolbach and Sandler are used for mixtures (Gross and Sadowski, 2002).

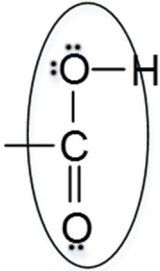
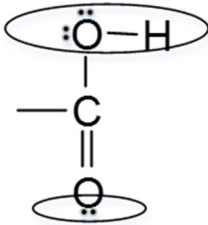
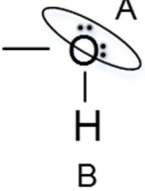
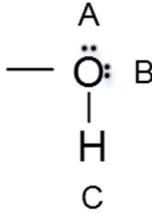
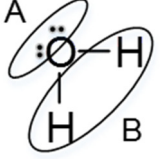
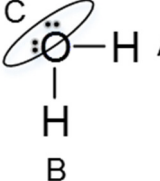
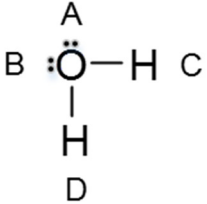
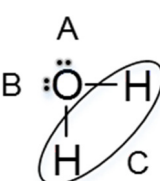
$$\kappa^{A_i B_j} = \sqrt{\kappa^{A_i B_i} \kappa^{A_j B_j}} \left(\frac{\sqrt{\sigma_i \sigma_j}}{(\sigma_i + \sigma_j)/2} \right)^3 \quad (3.50)$$

$$\varepsilon^{A_i B_j} = \frac{\varepsilon^{A_i B_i} + \varepsilon^{A_j B_j}}{2} \quad (3.51)$$

The association term is actually the most mathematically and computationally demanding of the PC-SAFT terms. The monomer fraction X^{A_i} needs to be solved iteratively for all sites. A system of non-linear equations is created whose number depends on the number of compounds and association sites per molecule. The numerical challenge increases if it is considered that first order partial derivatives are needed to compute certain thermodynamic properties (e.g. fugacity). Huang and Radosz (1990) have presented a classification of association types for some functional groups showing their allocated number of association sites and possible types under which they may be modelled. [Table 3.1](#) summarizes the cases for carboxylic acids, alcohols and water. For instance, in modelling water with a 2B association scheme, both pairs of electrons are assumed to conform one single association site A , and both hydrogen atoms a second independent association site B . Combinations $A_i A_i$ and $B_i B_i$ will result in a zero magnitude in the association strength and the contributions are given by the $A_i B_i$ combinations solely.

Numerical guidance for the solution of X^{A_i} can be found in the publication of Michelsen and Mollerup (2007) while analytical solutions for some instances in the work of Kraska (1998).

Table 3.1. Association schemes for carboxylic acids, alcohols and water according to the classification of Huang and Radosz (1990).

Species	Type			
Acids		1A		2B
	Alcohols		2B	
Water		2B		3B
			4C	



3.3.4 Dipolar contribution

The original version of PC-SAFT did not consider the polar interactions explicitly, these were assumed to be accounted for by the rest of the terms. Indeed, association and polarity are related (Smith, 1955). However, it is expected that considering the dipole moment explicitly would result in better approximations to experimental data of polar molecules.

The first attempt to include a dipolar term within the PC-SAFT framework was the work of Tumakaka and Sadowski (2004) who modelled satisfactorily VLE and LLE of binary systems comprising low molecular weight polar compounds as well as polar copolymer systems. For the implementation of the dipolar term, Tumakaka and Sadowski used the dipolar term proposed by Jog and Chapman (1999); Jog et al. (2001) (JC). The model is hereafter referred as PC-SAFT-JC. In addition to the pure component parameters m , σ and ε , for non-associating molecules, the dipole moment, μ , as well as the fraction of dipolar segments in the molecule, x_p , are needed. Usually μ is taken from experimental data while x_p is treated as an additional adjustable parameter.

Dominik et al. (2005) compared PC-SAFT-JC against another possible dipolar term, the one proposed by Saager and Fischer (SF), developed from empirical expressions fitted to VLE simulation data. PC-SAFT-SF also requires an additional pure component parameter (x_p). The authors concluded that although both models yield similar results for the systems studied, the parameters of PC-SAFT-JC are more physically meaningful. Moreover, Gross and Vrabec (2006)



have pointed out that the PC-SAFT-SF model produces similar results as the non-polar PC-SAFT model, the only advantage being a lower k_{ij} .

Similar to the approach of Saager and Fischer of using molecular simulation data, Gross and Vrabec (2006) proposed expressions to account for the dipolar interactions. The model is referred as PCP-SAFT. An important feature of PCP-SAFT is that it does not introduce the need of an additional pure component parameter and that the values of the dipole moment can be taken either from independently determined experimental data or adjusted if needed.

In the development of PCP-SAFT the authors claimed the model to be more accurate than the PC-SAFT-JC and the PCP-SAFT-SF models. In a later study, however, Alsaifi et al. (2008) found the model of JC to be superior (at least for the water-alcohol-hydrocarbon systems considered). In a more recent study, although using the simplified version of PC-SAFT (sPC-SAFT) (von Solms et al., 2003) De Villiers et al. (2014) obtained similar results between PC-SAFT-JC and PCP-SAFT in modelling binary systems involving alcohols. These studies show that the outcome in any comparison will depend on the compounds and the conditions under study.

An important restriction of PCP-SAFT is that it only considers aligned dipoles in the molecules, that is, it does not take into account different orientations. Korden et al. (2012) have investigated orientational effects of the dipole moment in the PCP-SAFT model employing molecular simulation data. However, the original PCP-SAFT when applied to real substances, resulted in better correlations (Schäfer and Sadowski, 2012; Schäfer et al., 2014).



As discussed in [Section 3.1.1](#), polar and even non-polar molecules can exhibit a temporary dipole moment in the presence of dipolar compounds. An effect that is not explicitly considered in PCP-SAFT. For this reason, Kleiner and Gross (2006); Kleiner (2008) proposed expressions to include induce-dipole interactions, naming the equation PCIP-SAFT. Modelling of actual mixtures resulted only in minor improvements compared with the PCP-SAFT model.

Quadrupole moments and even quadrupole-dipole interactions have also been included in PC-SAFT (Gross, 2005; Vrabec and Gross, 2008). Modelling mixtures involving carbon dioxide, for example, have shown to improve when its quadrupolar moment is considered (Román-Ramírez et al., 2010; Tang and Gross, 2010).

Leonhard et al. (2007a) enhanced the predictive capabilities of PCP-SAFT (that also considers quadrupolar interactions) by introducing a modified combining rule for the dispersion energy. Furthermore, new expressions for the polar interactions (Leonhard et al., 2007b) were developed, yielding better results compared with the original PCP-SAFT, at least for the system studied. The model, however, has not being tested widely yet.

As an alternative to the PC-SAFT polar models exposed above, Karakatsani et al. (2005) proposed a PC-SAFT polar model for dipolar interactions, the equation was termed PC-polar SAFT (PC-PSAFT) and was later extended to account for quadrupole-quadrupole, dipole-quadrupole, and dipole-induce dipole interactions (Karakatsani and Economou, 2006; Karakatsani et al., 2006; Karakatsani and Economou, 2007). For practical reasons the resulted complex model had to be



truncated in their expressions, and is the reason why it is referred to as truncated-PC-PSAFT (tPC-PSAFT). While the PC-PSAFT model does not introduce an additional adjustable parameter, the tPC-PSAFT model does it in order to maintain its accuracy.

In this work, the dipolar term of Gross and Vrabec (2006) is employed since it does not introduce an adjustable parameter, keeping a more predictive approach of the model. No induced-dipole interactions were considered explicitly in the model. Values of the dipolar moments were taken from reported experimental data. It is important to note that usually, the reported experimental dipolar values correspond to those for the gas phase in vacuum and would not capture the actual values. As pointed out by McCabe and Galindo (2010), even if the dipolar moments are obtained from *ab initio* calculations, “they will always limit the predictive capability of the approach since the effect of changes in temperature and state conditions on changes in the multipole moments is not captured”.

The dipolar contribution to the Helmholtz free energy (A^{dip}) in PCP-SAFT is given by Gross and Vrabec (2006):

$$\frac{A^{dip}(T, V, n)}{RT} = \frac{\frac{A_2}{RT}}{1 - \frac{A_3}{A_2}} \quad (3.52)$$

where A_2 and A_3 are second and third-order perturbation terms given by:

$$\frac{A_2}{RT} = -\pi \frac{\rho}{(kT)^2} \sum_i \sum_j n_i n_j \frac{\mu_i^2 \mu_j^2}{\sigma_{ij}^3} \frac{n_{\mu,i}}{m_i} \frac{n_{\mu,j}}{m_j} J_{2,ij}^{DD} \quad (3.53)$$

$$\frac{A_3}{RT} = -\frac{4}{3} \pi^2 \frac{\rho^2}{(kT)^3} \sum_i \sum_j \sum_k n_i n_j n_k \frac{\mu_i^2 \mu_j^2 \mu_k^2}{\sigma_{ij} \sigma_{ik} \sigma_{jk}} \frac{n_{\mu,i}}{m_i} \frac{n_{\mu,j}}{m_j} \frac{n_{\mu,k}}{m_k} J_{3,ijk}^{DD} \quad (3.54)$$

where $n_{\mu,i}$ is the number of dipolar segments in a molecule i . $J_{2,ij}^{DD}$ and $J_{3,ijk}^{DD}$ are power series of the reduced density, according to:

$$J_{2,ij}^{DD} = \sum_{n=0}^4 \left(a_{n,ij} + b_{n,ij} \frac{\varepsilon_{ij}}{kT} \right) \eta^n \quad (3.55)$$

$$J_{3,ijk}^{DD} = \sum_{n=0}^4 c_{n,ijk} \eta^n \quad (3.56)$$

The coefficients $a_{n,ij}$, $b_{n,ij}$ and $c_{n,ijk}$ depend on the chain length as:

$$a_{n,ij} = a_{0n} + \frac{m_{ij} - 1}{m_{ij}} a_{1n} + \frac{m_{ij} - 1}{m_{ij}} \frac{m_{ij} - 2}{m_{ij}} a_{2n} \quad (3.57)$$

$$b_{n,ij} = b_{0n} + \frac{m_{ij} - 1}{m_{ij}} b_{1n} + \frac{m_{ij} - 1}{m_{ij}} \frac{m_{ij} - 2}{m_{ij}} b_{2n} \quad (3.58)$$

$$c_{n,ijk} = c_{0n} + \frac{m_{ijk} - 1}{m_{ijk}} c_{1n} + \frac{m_{ijk} - 1}{m_{ijk}} \frac{m_{ijk} - 2}{m_{ijk}} c_{2n} \quad (3.59)$$

$$m_{ij} = (m_i m_j)^{1/2} \quad (3.60)$$

$$m_{ijk} = (m_i m_j m_k)^{1/3} \quad (3.61)$$

The values of m_{ij} and m_{ijk} in [Equations \(3.60\)](#) and [\(3.61\)](#) are restricted to values ≤ 2 since the model constants in [Equations \(3.57\) – \(3.59\)](#) were obtained from fitting simulation data of molecules with $m = 2$, but this does not imply that the model is limited to molecules with 2 segments (Gross and Vrabec, 2006). The constants of [Equations \(3.57\) – \(3.59\)](#) are reported in the original publication (Gross and Vrabec, 2006).

3.4 The CPA equation of state

An intermediate equation between PR and PC-SAFT is the Cubic Plus Association (CPA) EoS (Kontogeorgis et al., 1996). Developed by coupling a cubic EoS with an association term, it retains most of the simplicity of an empirical model but with increased accuracy. The cubic equation of state handles the physical intermolecular interactions while the association the quasi-chemical ones.

The CPA EoS in terms of the residual Helmholtz free energy is (Kontogeorgis and Folas, 2010):



$$\frac{A^{res}(T, V, n)}{RT} = \frac{A_{SRK}^{res}(T, V, n)}{RT} + \frac{A^{assoc}(T, V, n)}{RT} \quad (3.62)$$

where the expression for A_{SRK}^{res} can be retrieved by substituting $\delta_1 = 1$ and $\delta_2 = 0$ in [Equation \(3.25\)](#). In CPA the energy parameter a is computed from:

$$a_i = a_{0,i} [1 + c_{1,i} (1 - \sqrt{T_{r,i}})]^2 \quad (3.63)$$

where a_0 and c_1 , as well as b (previously defined in [Equation \(3.30\)](#)) are characteristic parameters for a given compound.

The association term is similar as the one use in PC-SAFT, but in this case the association strength is computed from:

$$\Delta^{A_i B_j} = g(V, n) b_{ij} \beta^{A_i B_j} \left[\exp\left(\frac{\varepsilon^{A_i B_j}}{RT}\right) - 1 \right] \quad (3.64)$$

where the simplified radial distribution function (Kontogeorgis et al., 1999; Kontogeorgis et al., 2006a) is:

$$g(V, n) = \frac{1}{1 - 1.9\eta} \quad (3.65)$$

and

$$\eta = \frac{B}{4V} \quad (3.66)$$

with B as defined by Equation (3.30).

$\varepsilon^{A_i B_j}$ and $\beta^{A_i B_j}$ are the association energy and association volume parameters respectively. Thus for an associating molecule, five pure component parameters are needed: a_0 , b , c_1 , $\varepsilon^{A_i B_j}$ and $\beta^{A_i B_j}$, which are usually obtained from fitting vapour pressures and liquid density data.

The combining rules for a and b are those defined in Equations (3.28) and (3.29). Several combining rules have been proposed for the association strength in the CPA framework, but the so called Elliot combining rule (ECR) and the CR1 have been the most successful (Folas, 2006; Kontogeorgis et al., 2006a; b):

ECR:

$$\Delta^{A_i B_j} = \sqrt{\Delta^{A_i B_i} \Delta^{A_j B_j}} \quad (3.67)$$

CR1:

$$\varepsilon^{A_i B_j} = \frac{\varepsilon^{A_i B_i} + \varepsilon^{A_j B_j}}{2} \quad (3.68)$$

$$\beta^{A_i B_j} = \sqrt{\beta^{A_i B_i} \beta^{A_j B_j}} \quad (3.69)$$

It has been shown that the equivalent expressions of ECR in terms of $\varepsilon^{A_i B_j}$ and $\beta^{A_i B_j}$ by assuming $\exp\left(\frac{\varepsilon^{A_i B_j}}{RT}\right) \gg 1$ are (Kontogeorgis et al., 2006a):



$$\varepsilon^{A_i B_j} = \frac{\varepsilon^{A_i B_i} + \varepsilon^{A_j B_j}}{2} \quad (3.70)$$

$$\beta^{A_i B_j} = \sqrt{\beta^{A_i B_i} \beta^{A_j B_j}} \frac{b_i b_j}{b_{ij}} \quad (3.71)$$

3.5 Organic acids and water within CPA and PC-SAFT

Choice of the association scheme plays an important role in SAFT-type EoS such as CPA and PC-SAFT. Dimerization in organic acids is caused by the formation of two hydrogen bonds between the carboxylic groups of two acid molecules. This can be captured by applying the rigorous 1A association type according to the classification of Huang and Radosz (1990) (Table 3.1), in which only dimers are allowed to form. However, and as mentioned in Section 1.5, the fact that chain-monomers may appear in the liquid phase also allows for a 2B association model.

Kleiner (2008) has shown for PC-SAFT the 1A scheme represents better pure compound properties compared with the 2B association scheme for organic acids (from formic acid to decanoic acid). Derawi et al. (2004) arrived at the same conclusion for CPA when testing types 1A, 2B and even 4C in predicting vapour pressures and equilibrium constants of formic, acetic and propanoic acids. More recently, Janecek and Paricaud (2012) have tested the 1A, 2B and the doubly bounded dimer (DBD) scheme of Sear and Jackson (1994a; 1994b) in the modelling of the formic acid to pentanoic acid series with PC-SAFT. The reported deviations of the saturated properties of the 1A and 2B schemes did not reveal a



preferred scheme. Saturated pressures, for example, were correlated better with the 2B type for the formic and acetic acids, whereas for propanoic acid the deviations were lower with the 1A. The DBD scheme resulted in the highest deviations of saturated properties.

Aqueous mixtures have been modelled successfully within the SAFT framework in the literature, see e.g. (Huang and Radosz, 1990; Gross and Sadowski, 2002; Kouskoumvekaki et al., 2004b; Kontogeorgis et al., 2006a; von Solms et al., 2006; Aparicio-Martínez and Hall, 2007; Kleiner, 2008; McCabe and Galindo, 2010; Forte et al., 2011; Soo, 2011; Forte et al., 2013). Although the 4C rigorous type for water is more in line with experimental spectroscopy data (Kontogeorgis et al., 2006a; von Solms et al., 2006; Kontogeorgis and Folas, 2010), there is no general agreement on the best association model especially when applied to real mixtures. A 3B and even a 2B assignment could be justified and also lead to satisfactory results. In the original publication of PC-SAFT, for instance, Gross and Sadowski (2002) modelled satisfactorily the system water + 1-pentanol with water as 2B. Similarly, Kleiner and Sadowski (2007), Alsaifi et al. (2008) and Soo (2011) have shown the accuracy of the 2B scheme in modelling aqueous mixtures involving polar and non-polar compounds.

Previously, in their comparison of the three association sites, Suresh and Elliott (1992) found better results with the 2B and 3B types but in particular with the 2B.

Aparicio-Martínez and Hall (2007) modelled binary systems comprising water + carbon dioxide, nitrogen or *n*-alkanes with water as 3B in PC-SAFT. During the process of selecting the best association scheme the authors mentioned that the



2B seems to be the most appropriate for modelling water pure component properties.

Kleiner (2008) compared pure component parameters of water as 2B, 3B and 4C obtaining slightly better representations of the saturated liquid densities with the 3B type, whereas the 4C gave the best results for the vapour pressures. Kleiner concluded that, for mixtures with hydrocarbons, the mutual solubilities can only be described by the 4C scheme. It was also noted that, for other mixtures rather than hydrocarbons, the 2B type is superior than the 4C if the other compound has a functional group, as e.g. polar or associating. This is in agreement with previous observations of Perakis et al. (2007). Moreover, Kleiner also concluded that the phase behaviour is very sensitive to the chosen parameters by comparing results employing three different sources (sets) of pure component parameters for water modelled as 4C. A similar conclusion was reached by von Solms et al. (2006) in their comparison of different sets for water as 4C.

On the other hand, Kontogeorgis et al. (2010) have shown that (for CPA and sPC-SAFT) the 4C model is superior in representing properties of pure water, in particular with CPA. In addition to vapour pressures and liquid densities, the authors also included experimental monomer fraction data in the fitting procedure. Liang et al. (2014a) have arrived to the same conclusion by comparing in addition to saturated properties, isochoric and isobaric heat capacities and speed of sound.

In respect to the modelling of organic acid + water mixtures, it is pertinent to mention the studies of Kouskoumvekaki et al. (2004a) who studied the acetic acid



+ water at 502.9 K with sPC-SAFT assuming both compounds as 2B correlating the experimental data with a $k_{ij} = -0.07$.

Chen et al. (2012) employed PC-SAFT in modelling organic acids (acetic, propionic and acrylic) + water mixtures defining both compounds as 2B. In a more recent study Janecek and Paricaud (2013) have modelled the acetic acid + water and the propanoic acid + water systems for pressures up to 1 bar and compared the cases of the organic acids modelled either as 2B or DBD and water as 4C (the 2B type was also investigated for the case with acetic acid). Predictions with water modelled as 2B were superior to the 4C cases, but the 4C showed improved correlations. In general, the DBD cases resulted in lower, though similar deviations to the 2B scheme, as well as similar magnitudes of the binary interaction parameters.

Kontogeorgis et al. (2007) modelled the formic acid + water and the propanoic acid + water systems at 1 bar with CPA and the CR1 combining rule. For the former system only qualitative results were obtained, while for the latter, the experimental data were fitted at the expense of a large negative binary interaction parameter ($k_{ij} = -0.21$). Both acids were modelled as 1A. In contrast, Kontogeorgis and Folas (2010) have reported that better results could be obtained by considering acetic acid as 2B in the acetic acid + water mixture.

Muro-Suné et al. (2008) modified CPA by introducing the Huron-Vidal mixing rule with a modified non-random two-liquid expression (NRTL) to improve its capabilities in modelling the acetic acid + water mixture. The model was deeply studied by Breil et al. (2011) who compared different data sets in correlating



enthalpies of vaporization and compressibility factors of pure acetic acid and in mixtures with water.

Using a CPA conformed by the PR instead of the SRK equation, Perakis et al. (2007) concluded that for the acetic acid + water, modelling improves by shifting from the 4C to the 3B model for water when acetic acid is 1A. The authors used the geometric rule for both, the association energy and the association volume, as well as a second binary interaction parameter.

Organic acids and water are both dipolar compounds. It is therefore appealing to model these systems by considering the association and polar terms explicitly in the Helmholtz expansion. This approach, however, might not be necessarily in agreement with the actual phenomenon since both interactions are not independent of one another (Smith, 1955; Soo, 2011). It may in some cases improve the fitting as found for CO₂ + alkanol mixtures (Alsaifi et al., 2008; Román-Ramírez et al., 2010) or it could also lead to worse results, as shown for the acetone + water system (Kleiner and Sadowski, 2007). Of the studies involving organic acids, only Soo (2011) has included polar contributions in modelling the formic to *n*-hexanoic acid series. No comparison of the performance of PC-SAFT and that of PCP-SAFT was performed.

The different conclusions from the different research groups about the best association scheme is a consequence of several aspects: the equation of state used, the set of parameters used, the system under study and also of the conditions studied.



It has been discussed so far only one dimension of the problem, that of the association scheme, but another important aspect is the value of the pure component parameters. Multiplicity of pure component parameters is well known in EoS like CPA and PC-SAFT (Kontogeorgis et al., 1996; Alsaifi et al., 2008). The resulting values from the fitting procedure will depend on aspects such as the temperature range used in the fitting, source of experimental data and search algorithm.

In an effort to obtain a unique set of reliable pure component parameters, some researchers have also used information of experimental association energies (Derawi et al., 2004; Grenner et al., 2006), enthalpies of vaporization (Breil et al., 2011) or monomer fraction data (Kontogeorgis et al., 2010; Tsvintzelis et al., 2014). Unfortunately, inclusion of these data is not guarantee of a unique optimum set; besides, the consistency of some of these experimental data, such as the monomer fraction, has been questioned (Kontogeorgis, 2013; Tsvintzelis et al., 2014). Furthermore, a single set of parameters may not be enough to correctly predict equilibrium properties of pure compounds and/or mixtures in a wide range of conditions and equilibrium types as has been demonstrated in the comparisons of Kontogeorgis et al. (1996); von Solms et al. (2006); Kleiner (2008); Tsvintzelis et al. (2014) and recently by Liang et al. (2014a).

Other authors (Albers et al., 2012; Umer et al., 2014) have incorporated quantum mechanical calculations for the estimation of some or all of the parameters but this does not seem to provide any advantage over the common fitting procedure of evoking vapour pressures and liquid densities only.



Values of CPA and PC-SAFT (or its modifications) pure component parameters for acetic acid, propanoic acid and water from different researchers are presented in [Tables 3.2](#) and [3.3](#). In some of these sets, some parameters have been fixed to reduce the number of adjustable parameters and/or to fulfil physical requirements, e.g. values of m close to unity, or values of the association energy near 1813 K for water (Kontogeorgis et al., 1996).

In this work, the phase equilibrium data obtained in [Chapter 2](#) is modelled with the PR, CPA and PC-SAFT EoS. Comparisons of predictive and correlative performance are made. Association types 1A and 2B were tested for the organic acids, whereas types 2B, 3B and 4C for water. Additionally, the case with polar contributions in PC-SAFT, i.e. PCP-SAFT, is also studied with the aim to determine the effect of including both terms simultaneously in the Helmholtz expansion. Pure component parameters were refitted in each case. For CPA, the performance of the ECR and CR1 combining rules were also tested. As a result of these combinations, the actual number of equations being compared is 25. [Table 3.4](#) aids to visualize this information.

Validation plots for the CPA, PC-SAFT and PCP-SAFT programs are provided in [Appendix H](#).

Table 3.2. CPA pure component parameters for acetic acid, propanoic acid and water from the literature.

Compound	Association scheme	a_0 [bar L ² mol ⁻²]	b [L mol ⁻¹]	c_1	ε^{AB} [K]	β^{AB}	T [K]	Reference
acetic acid	1A	9.11960	0.04680	0.46440	4849.779	0.00450	296 - 533	Derawi et al. (2004)
	1A	8.29623	0.04551	0.49462	5788.596	0.00157	293 - 503	Breil et al. (2011)
	1A	8.19937	0.04537	0.50602	5867.591	0.00150	300 - 550	Breil et al. (2011)
	2B	7.05920	0.04780	0.88080	2262.821	0.14080	296 - 533	Derawi et al. (2004)
propanoic acid	1A	13.26760	0.06410	0.68910	4807.924	0.00210	300 - 541	Derawi et al. (2004)
	2B	9.30900	0.06330	1.05740	2749.326	0.05440	300 - 541	Derawi et al. (2004)
water	2B	2.98130	0.01475	0.00001	3439.770	0.01300	-	Kontogeorgis et al. (2010)
	3B	2.55470	0.01520	0.76540	2093.100	0.05950	356 - 582	Kontogeorgis et al. (1996)
	3B	1.86657	0.01316	0.01070	3367.651	0.01490	-	von Solms et al. (2006)
	3B	3.00596	0.01497	0.35928	2501.304	0.02130	356 - 582	Kontogeorgis et al. (2006a)
	3B	3.24211	0.01537	0.70174	1702.455	0.06190	356 - 582	Kontogeorgis et al. (2006a)
	3B	2.87881	0.01463	0.07873	3006.809	0.01080	356 - 582	Kontogeorgis et al. (2006a)
	3B	1.50960	0.01414	1.55530	1924.580	0.21900	-	Kontogeorgis et al. (2010)
	4C	1.22770	0.01452	0.67359	2003.151	0.06920	-	Kontogeorgis et al. (1999)
	4C	2.25190	0.01556	0.61080	1700.400	0.06080	-	Kontogeorgis et al. (2010)
	4C	1.22570	0.01483	1.46791	1574.200	0.14190	298 - 595	Tybjerg et al. (2010)
	4C	1.21324	0.01450	0.67000	1996.500	0.07093	272 - 641	Abolala and Varaminian (2013)



Table 3.3. PC-SAFT pure component parameters for acetic acid, propanoic acid and water from the literature.

Compound	Association scheme	m	σ [Å]	ϵ/k [K]	κ^{AB}	ϵ^{AB}/κ [K]	μ [D]	T [K]	Reference
acetic acid									
	1A ^a	1.6450	3.5782	270.93	0.008400	5184.32	1.74	349 - 586	Karakatsani et al. (2005)
	1A	1.4517	3.7379	286.61	0.002000	5958.40		290 - 580	Kleiner (2008)
	1A	1.9826	3.3094	238.75	0.001000	7133.50		298 - 583	Soo (2011)
	1A	1.8702	3.3816	234.74	0.001000	7067.80	1.70	298 - 583	Soo (2011)
	1A	2.7556	2.9961	230.70	0.366300	3047.30		290 - 590	Janecek and Paricaud (2012)
	2B	1.3403	3.8582	211.59	0.075550	3044.40		302 - 592	Gross and Sadowski (2002)
	2B	2.3420	3.1850	199.90	0.259900	2756.70		300 - 570	Kouskoumvekaki et al. (2004a)
	2B	1.0487	4.1862	205.36	0.060000	3208.40		290 - 580	Kleiner (2008)
	2B	2.7556	2.9777	186.30	0.428600	2336.70		290 - 590	Janecek and Paricaud (2012)
	2B	1.4690	3.9252	365.56	0.020000	2099.40		290 - 570	Albers et al. (2012)
	2B	2.4299	3.2682	289.75	0.020000	2099.40		290 - 570	Albers et al. (2012)
propanoic acid									
	1A	4.0330	2.9071	221.85	0.245100	2627.90		260 - 600	Kleiner (2008)
	1A	2.2147	3.5296	245.33	0.001000	6368.80		273 - 493	Soo (2011)
	1A	2.1246	3.5857	245.31	0.001000	6309.50	1.75	273 - 493	Soo (2011)
	1A	3.0940	3.1541	225.70	0.047790	4097.20		290 - 600	Janecek and Paricaud (2012)
	2B	3.7069	2.9937	200.73	0.320500	2173.40		260 - 600	Kleiner (2008)
	2B	2.5200	3.3900	204.70	0.075550	3044.40		-	Chen et al. (2012)
	2B	3.0940	3.1561	191.80	0.158500	2782.30		290 - 600	Janecek and Paricaud (2012)
	2B	3.2461	3.2162	273.02	0.020000	1961.60		252 - 587	Albers et al. (2012)
	2B	3.1373	3.2437	277.16	0.020000	1961.60		252 - 587	Albers et al. (2012)

Table 3.3. (Continuation)

Compound	Association scheme	m	σ [Å]	ε/k [K]	κ^{AB}	ε^{AB}/κ [K]	μ [D]	T [K]	Reference
water									
	2B	1.0656	3.0007	366.51	0.034868	2500.70		273 - 647	Gross and Sadowski (2002)
	2B	1.3112	2.7613	372.37	0.048987	2123.10		273 - 634	Aparicio-Martínez and Hall (2007)
	2B	1.6963	2.5144	311.19	0.063500	1469.10	1.85	-	Kleiner and Sadowski (2007)
	2B ^b	1.0405	2.9657	175.15	0.089240	2706.70	1.85	273 - 634	Alsaifi et al. (2008)
	2B	1.2255	2.7920	203.00	0.071720	2406.70	1.85	273 - 634	Alsaifi et al. (2008)
	2B	2.5398	2.0790	207.55	0.432700	2335.46		-582	Kontogeorgis et al. (2010)
	2B	1.9599	2.3620	279.42	0.175000	2059.28		275 - 640	Diamantonis and Economou (2011)
	3B	1.7960	2.4697	327.62	0.068277	1558.40		273 - 634	Aparicio-Martínez and Hall (2007)
	3B	2.3753	2.5609	275.81	0.068277	1558.40		273 - 634	Aparicio-Martínez and Hall (2007)
	3B	3.2542	1.9181	196.21	0.046000	1800.60		273 - 647	Kleiner (2008)
	3B	3.3731	1.8670	182.13	0.444000	2019.93		-582	Kontogeorgis et al. (2010)
	4C ^c	1.0000	3.1097	42.77	0.070600	1973.72	1.85	278 - 641	Karakatsani et al. (2005)
	4C	2.0000	2.3533	207.84	0.155000	1506.40		324 - 582	von Solms et al. (2006)
	4C	2.2500	2.2462	194.20	0.205000	1479.60		324 - 582	von Solms et al. (2006)
	4C	2.5000	2.1562	187.06	0.264600	1427.20		324 - 582	von Solms et al. (2006)
	4C	2.7500	2.0794	183.61	0.337400	1354.10		324 - 582	von Solms et al. (2006)
	4C	3.0000	2.0135	182.92	0.428700	1259.00		324 - 582	von Solms et al. (2006)
	4C	3.2500	1.9570	185.46	0.551300	1128.80		324 - 582	von Solms et al. (2006)
	4C	3.5000	1.9134	199.88	0.790100	839.00		324 - 582	von Solms et al. (2006)
	4C	1.5000	2.6273	180.30	0.094200	1804.22		324 - 582	Grenner et al. (2006)
	4C ^d	2.8150	2.0374	150.71	0.351800	1575.20	1.85	278 - 641	Karakatsani and Economou (2007)
	4C	1.5725	2.6270	291.13	0.074347	1334.20		273 - 634	Aparicio-Martínez and Hall (2007)
	4C	3.7923	2.1054	138.60	0.029100	1718.20		273 - 647	Kleiner (2008)
	4C	0.8148	3.3660	388.51	0.018400	1552.34		-582	Kontogeorgis et al. (2010)



Table 3.3. (Continuation)

Compound	Association scheme	m	σ [Å]	ε/k [K]	κ^{AB}	ε^{AB}/k [K]	μ [D]	T [K]	Reference
	4C	2.5967	2.0764	136.76	0.584500	1720.01		298 - 595	Tybjerg et al. (2010)
	4C ^e	0.8096	3.3845	218.79	0.035600	1813.00	1.85	-	Nguyen-Huynh et al. (2011)
	4C	2.1945	2.2290	141.66	0.203900	1804.17		275 - 640	Diamantonis and Economou (2011)
	4C	1.0656	3.0007	366.51	0.010000	1800.00		-	Niño-Amézquita et al. (2012)
	4C	2.5210	2.1328	163.94	0.271200	1575.73		272 - 641	Abolala and Varaminian (2013)
	4C	1.0000	3.0130	44.38	0.048100	2357.10		275 - 450	Janecek and Paricaud (2013)
	4C	1.0000	3.0650	441.70	0.021300	1262.20		275 - 450	Janecek and Paricaud (2013)
	4C	1.0000	3.0556	273.05	0.035150	1749.30		303 - 363	Janecek and Paricaud (2013)
	4C	2.0000	2.3449	171.67	0.159600	1704.06		280 - 620	Liang et al. (2014a)

^a $\sigma^{dd} = 4.749$ [Å]. ^b $x_p = 0.66245$. ^c $\sigma^{dd} = 3.398$ [Å]. ^d $\sigma^{dd} = 6.568$ [Å], $\alpha = 1.49$ [Å³], $Q = 2.69$ [DÅ]. ^e $x_p = 0.295/m$.

Table 3.4. Equations of state and association combinations studied.

EoS	Association scheme ^a						
	Non-associating	1A-2B	1A-3B	1A-4C	2B-2B	2B-3B	2B-4C
PR	*						
CPA ECR		*	*	*	*	*	*
CPA CR1		*	*	*	*	*	*
PC-SAFT		*	*	*	*	*	*
PCP-SAFT		*	*	*	*	*	*

^a The first position is for the organic acid while the second for water

3.6 Parameters estimation

Parameters a and b for the PR equation were estimated from correlations of critical properties (T_c and P_c) and acentric factor (ω) according to the following equations:

$$a_i = \frac{\Omega_a R^2 T_{c,i}^2 \alpha_i}{P_{c,i}} \quad (3.72)$$

$$b_i = \frac{\Omega_b R T_{c,i}}{P_{c,i}} \quad (3.73)$$

with

$$\alpha_i = [1 + m_i(1 - \sqrt{T_{r,i}})]^2 \quad (3.74)$$

and

$$m_i = 0.37464 + 1.5422\omega_i - 0.2699\omega_i^2 \quad (3.75)$$

T_r is the reduced temperature defined as: $T_r = T/T_c$. For PR, $\Omega_a = 0.45724$ and $\Omega_b = 0.07780$.

CPA, PC-SAFT and PCP-SAFT pure component parameters were obtained by fitting vapour pressure (P_V) and liquid density data (ρ_L) with Equation (3.76) as the objective function. Multiplicity of optimum parameters in multiparameter-models is well known (Kontogeorgis et al., 1996; Alsaifi et al., 2008), hence a simplex algorithm was applied in the optimization since it seems to be less sensitive to the initial guesses (Alsaifi et al., 2008).

$$OF_1 = \sum_{i=1}^{Np} \left[\left(\frac{P_{V,i}^{exp} - P_{V,i}^{calc}}{P_{V,i}^{exp}} \right)^2 + \left(\frac{\rho_{L,i}^{exp} - \rho_{L,i}^{calc}}{\rho_{L,i}^{exp}} \right)^2 \right] \quad (3.76)$$

Superscripts *exp* and *calc* stand for an experimental and a calculated property, respectively. Np is the number of experimental points used in the optimization. Average deviations from calculated and experimental saturated properties were computed according to:

$$\Delta\theta = \frac{100}{Np} \sum_{i=1}^{Np} \left| \frac{\theta_i^{exp} - \theta_i^{calc}}{\theta_i^{exp}} \right| \quad (3.77)$$

where θ stands either for P_V or ρ_L .



For mixtures, a single binary interaction parameters (k_{ij}) was used in all equations. Calculations with $k_{ij} = 0$ and a temperature-dependent k_{ij} were carried out for comparison. The optimum binary interaction parameter was obtained by regressing experimental data of bubble-point pressures (P) and vapour compositions (y) simultaneously, according to the following objective function:

$$OF_2 = \sum_{i=1}^{Np} \left[\left(\frac{P_i^{exp} - P_i^{calc}}{P_i^{exp}} \right)^2 + (y_{1,i}^{exp} - y_{1,i}^{calc})^2 \right] \quad (3.78)$$

Fifty experimental points were used for the regression in the temperature range from the triple point up to $0.99T_c$. The experimental data were taken from the Design Institute for Physical Properties (DIPPR) 801 database (DIPPR, 2012). Average deviations between experimental and modelling bubble pressures and vapour compositions were computed according to:

$$\Delta P = \frac{100}{Np} \sum_{i=1}^{Np} \left| \frac{P_i^{exp} - P_i^{calc}}{P_i^{exp}} \right| \quad (3.79)$$

$$\Delta y_1 = \frac{1}{Np} \sum_{i=1}^{Np} |y_{1,i}^{exp} - y_{1,i}^{calc}| \quad (3.80)$$

3.7 Results and Discussion

3.7.1 Pure component parameters

[Table 3.5](#) contains the critical properties and acentric factors for the estimation of PR parameters according to [Equations \(3.72\)](#) and [\(3.73\)](#).

The fitting procedure for the CPA, PC-SAFT and PCP-SAFT parameters involved trying several initial intuitive guesses with the aim to locate all local minima of the objective function. The reported values are those that converged to the same minimum of the objective function ([Equation \(3.76\)](#)) after different initial guesses. Practically all the cases converged to a unique solution, with a few exceptions that gave unphysical parameters such as negative values. No previous information about their magnitude was used in the regression.

Pure component parameters for CPA from the optimization are reported in [Table 3.6](#). The new obtained parameters for the organic acids are comparable in magnitude to those of the literature ([Table 3.2](#)). For acetic acid, the 2B set results in better fitting of both saturated properties, but as a whole the deviations are similar to those of the 1A scheme not leading to the preference of one scheme over another. For the case of propanoic acid, the best fitting is given by the 1A scheme, in agreement with previous studies ([Derawi et al., 2004](#); [Breil et al., 2011](#)).

For the case of water, the vapour pressures are better correlated with the 4C model with deviations almost 50% lower than the 2B (the highest encountered),



with liquid densities equally correlated in both schemes. Additionally, the values of the energy of association with both schemes are closer to the expected experimental range of 1660 – 1860 K (Kontogeorgis et al., 1996; Liang et al., 2014a) than the 3B set. Looking at the correlation of both properties, the hierarchical position according to their performance is $4C > 3B > 2B$; which confirms previous conclusions of the 4C model as the best choice for water with CPA (Kontogeorgis et al., 2006a).

In respect to PC-SAFT and PCP-SAFT (Table 3.7), the 1A scheme results in lower deviations compared with the 2B for the organic acids. When the dipole moment is included in PC-SAFT (i.e. PCP-SAFT), deviations in liquid density decrease but the ones for the vapour pressure increase. Pondering both properties, there is practically no difference in considering or not the polar contributions.

Table 3.5. Pure component properties.^a

Compound	M [g mol ⁻¹]	P_c [bar]	T_c [K]	ω
acetic acid	60.05	57.86	591.95	0.467
propanoic acid	74.08	46.68	600.81	0.580
water	18.02	220.64	647.10	0.345

^a Molar mass (M), critical pressure (P_c), critical temperature (T_c) and acentric factor (ω).
Data from DIPPR (2012) database.

Table 3.6. CPA pure component parameters and average deviations in vapour pressures (ΔP_v) and liquid densities ($\Delta \rho_L$).^a

Compound	Association scheme	a_0 [bar L ² mol ⁻²]	b [L mol ⁻¹]	c_1	ε^{AB} [K]	β^{AB}	T [K]	ΔP_v [%]	$\Delta \rho_L$ [%]
acetic acid	1A	8.4754	0.0459	0.4976	5453.7	0.0025	289.81 - 586.03	0.68	1.04
	2B	6.5145	0.0473	1.0015	2209.0	0.1864		0.64	0.94
propanoic acid	1A	12.1348	0.0628	0.7544	4900.9	0.0035	252.45 - 594.80	0.57	0.54
	2B	9.4034	0.0635	1.0730	2695.9	0.0588		0.47	0.66
	2B	2.5108	0.0150	1.0049	1817.6	0.2882		0.81	1.66
water	3B	2.2150	0.0151	1.2596	1525.7	0.2300	273.16 - 640.63	0.50	1.74
	4C	0.9036	0.0144	1.4898	1796.8	0.1188		0.44	1.68

^a Vapour pressure and liquid density data from DIPPR (2012).

Table 3.7. PC-SAFT and PCP-SAFT pure component parameters and average deviations in vapour pressures (ΔP_v) and liquid densities ($\Delta \rho_L$).^a

Compound	Association scheme	m	σ [Å]	ε/k [K]	κ^{AB}	ε^{AB}/k [K]	μ [D]	T [K]	ΔP_v [%]	$\Delta \rho_L$ [%]
acetic acid	1A	1.5286	3.6681	279.91	0.003102	5778.9		289.81 - 586.03	0.52	0.63
		1.3869	3.8145	279.65	0.003294	5634.4	1.739		0.56	0.60
	2B	2.5969	3.0474	190.22	0.368320	2379.0			0.83	0.96
		2.3857	3.1464	188.31	0.309125	2413.2	1.739		0.87	0.94
propanoic acid	1A	2.8793	3.2416	233.37	0.030267	4261.1		252.45 - 594.80	0.46	0.32
		2.8316	3.2633	232.62	0.029629	4229.5	1.751		0.46	0.34
	2B	3.2579	3.1047	192.67	0.192751	2647.5			0.55	0.40
		3.1508	3.1436	192.01	0.179171	2664.4	1.751		0.52	0.40
water	2B	2.7028	2.0526	218.96	0.561417	2045.0		273.16 - 640.63	0.61	2.01
		2.6206	2.1120	211.82	0.635842	1394.5	1.85		0.58	1.74
	3B	3.5642	1.8609	198.07	0.675246	1546.0			0.48	2.19
		3.1392	1.9769	194.36	0.721409	1073.6	1.85		0.67	1.92
	4C	3.0639	1.9701	150.10	0.429973	1523.7			0.75	2.00
		2.7801	2.0840	146.26	0.445384	1140.6	1.85		0.84	1.74

^a Vapour pressure, liquid density and dipolar moment (μ) data from DIPPR (2012).



For water, the best correlation is given by the 2B scheme with polar contributions, but the results are closely followed by 4C polar. In general, regardless of the association adopted for water, modelling of the dipolar moment improves the fitting. Based on their performance, the association scheme selection order would be 2B > 4C > 3B. It is important to note, however, the unusual values of m (>1) and σ (<3). Water is almost a spherical molecule and a value of m close to 1 is thus expected; on the other hand, values for σ are normally higher than 3 Å. Clearly the values reported here do not lie in this range. Nevertheless, values out of this range have been previously reported with satisfactory results (see e.g. von Solms et al. (2006); Karakatsani and Economou (2007) and Tybjerg et al. (2010) in [Table 3.3](#)). Arguably, the polar and association interactions taking place might be affecting the shape of the molecule, but it can also be attributed to the capabilities of the model recalling the simplifications under it has been developed. Even if the values of the parameters are constrained to strictly fulfil physical values there is no guarantee that these will result in the best set of parameters for any condition, system and type of equilibrium as demonstrated for water (Liang et al., 2014a). Determination of the optimum set of parameters is a complex problem not really studied and out of the scope of this work.

3.7.2 Mixtures

In order to test the capabilities of the selected equations at conditions other than those studied experimentally in this work, data from the open literature at 293.15, 313.15, 343.2, 363.02 and 373.12 K (Achary and Narasingrao, 1947; Arich and Tagliavini, 1958; Lazeeva and Markuzin, 1973; Miyamoto et al., 2001) for acetic



acid + water and at 313.1, 343.2 and 373.1 K (Brazauskiene et al., 1965; Rafflenbeul and Hartmann, 1978; Miyamoto et al., 2001) for propanoic acid + water were included in the modelling. The analysis is done based on the performance of two settings, a predictive mode ($k_{ij} = 0$) and a correlative mode, i.e. ($k_{ij} = k_{ij}^0 + k_{ij}^1 T$).

The notation to be used in the rest of the text is as follows: the first position of the subscript next to the equation is the association scheme for the organic acid and the second position is the association scheme for water. For example, PCP-SAFT_{1A-2B}, means that the PCP-SAFT equation of state is used with the organic acid modelled as 1A, whereas water as 2B. A subscript ECR or CR1 means that either the ECR combining rule or the CR1 rule are being used in CPA.

3.7.2.1 Predictive mode

The deviations from the experimental data and the modelling with the EoS in predictive mode are presented in tabulated form in [Appendix I.1](#). To visualize some trends in the predictive results, [Figures 3.2 – 3.5](#) show the interaction plots for the acetic acid and propanoic acid mixtures. Deviations in pressure (ΔP) and vapour composition of the organic acid (Δy_1) are shown as a function of the equation of state, association type and temperature. For the acetic acid system ([Figure 3.2](#)), for instance, the best predictions in pressure over the whole temperature range are given by the PC-SAFT equations, only exceeded by PCP-SAFT at the 443.2 and 483.2 K. The overall minimum deviation is given by the PC-SAFT_{2B-4C} (6.5%). A clear tendency observed in all models is that higher the temperature the better the pressure predictions.

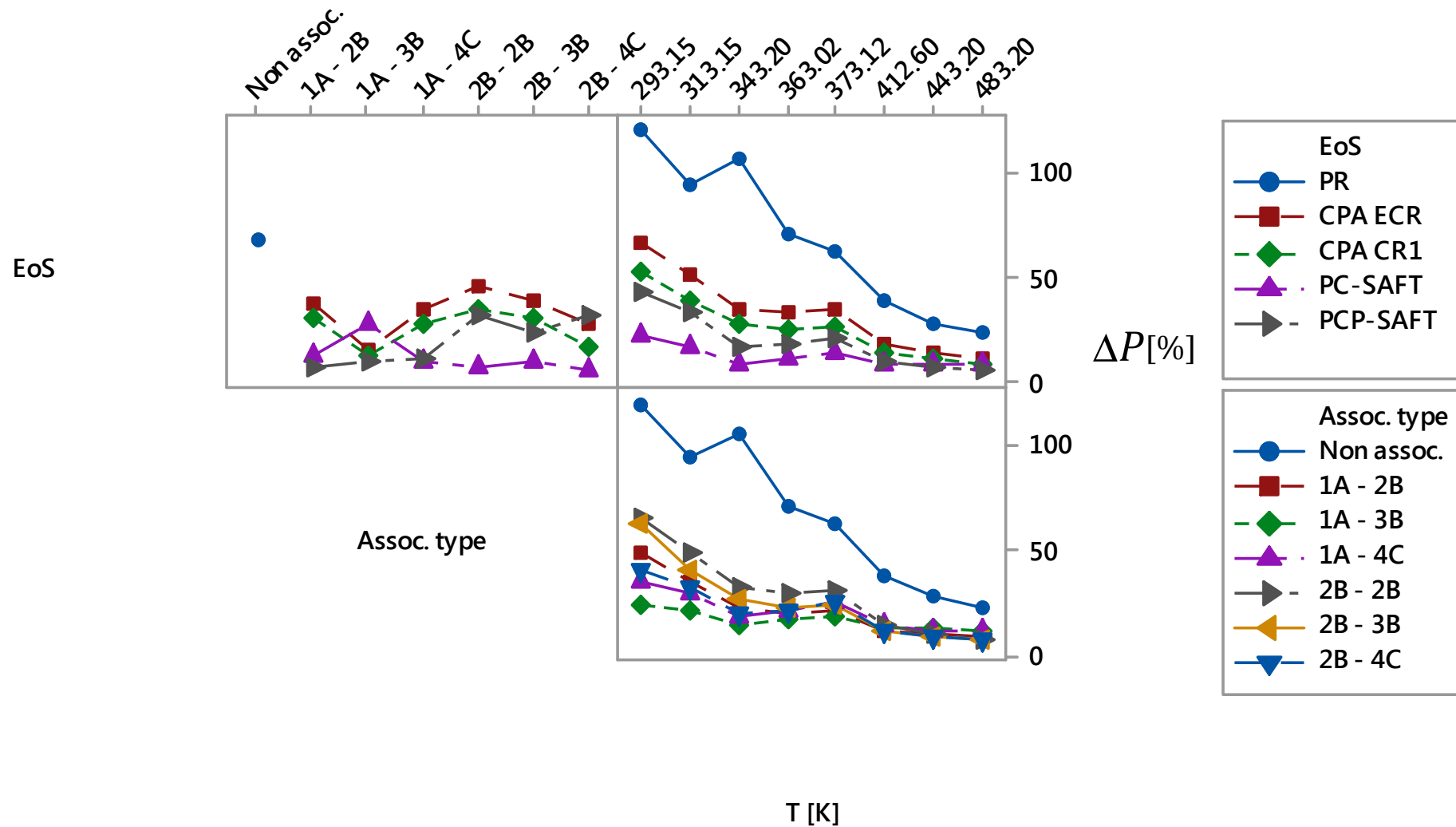


Figure 3.2. Interaction plot as a function of Equation of State (EoS), Association type and Temperature (T) of the average deviations in pressure (ΔP) of the acetic acid + water system in predictive mode ($k_{ij} = 0$).

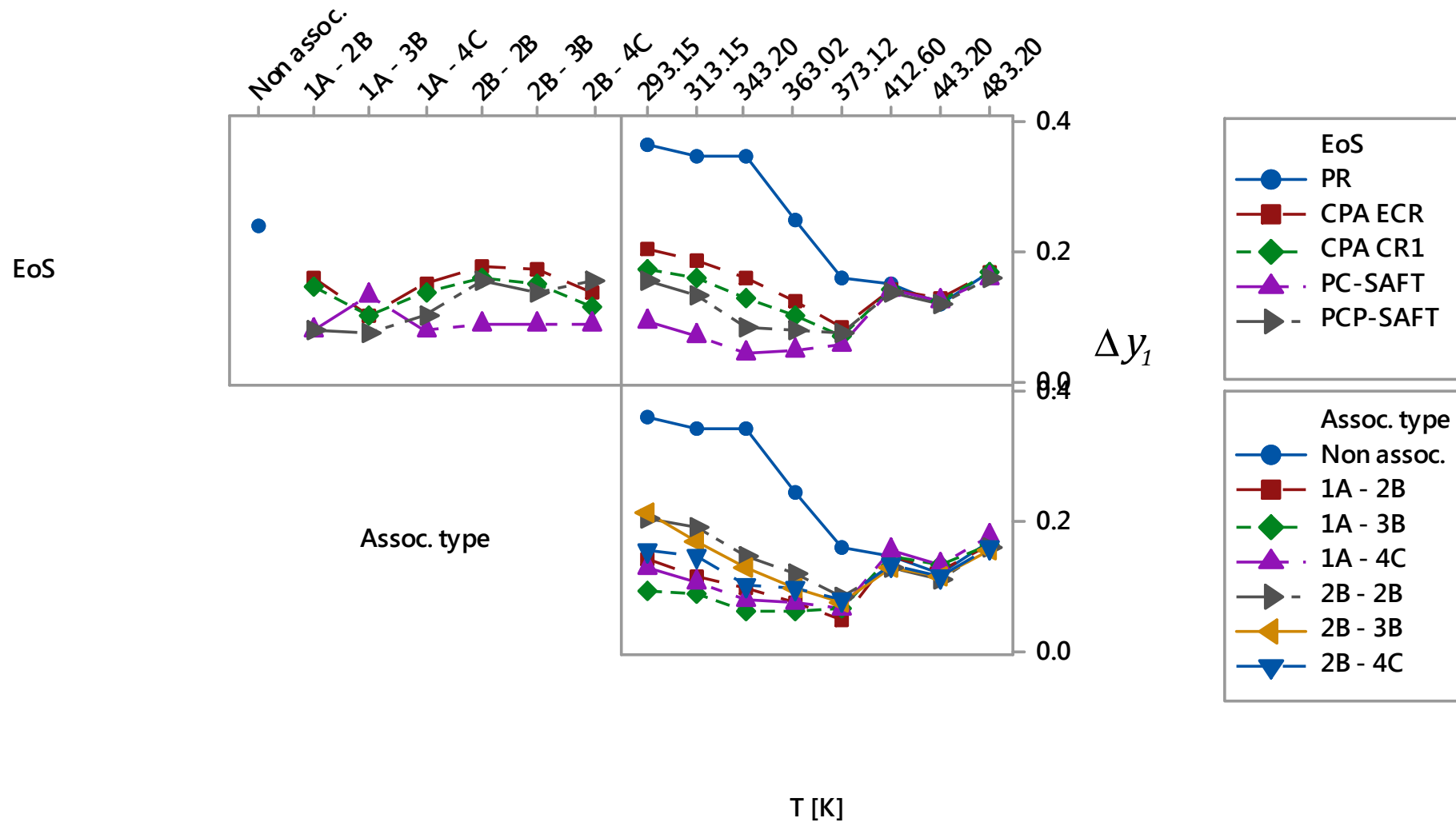


Figure 3.3. Interaction plot as a function of Equation of State (EoS), Association type and Temperature (T) of the average deviations in vapour composition (Δy_1) of the acetic acid (1) + water (2) system in predictive mode ($k_{ij} = 0$).

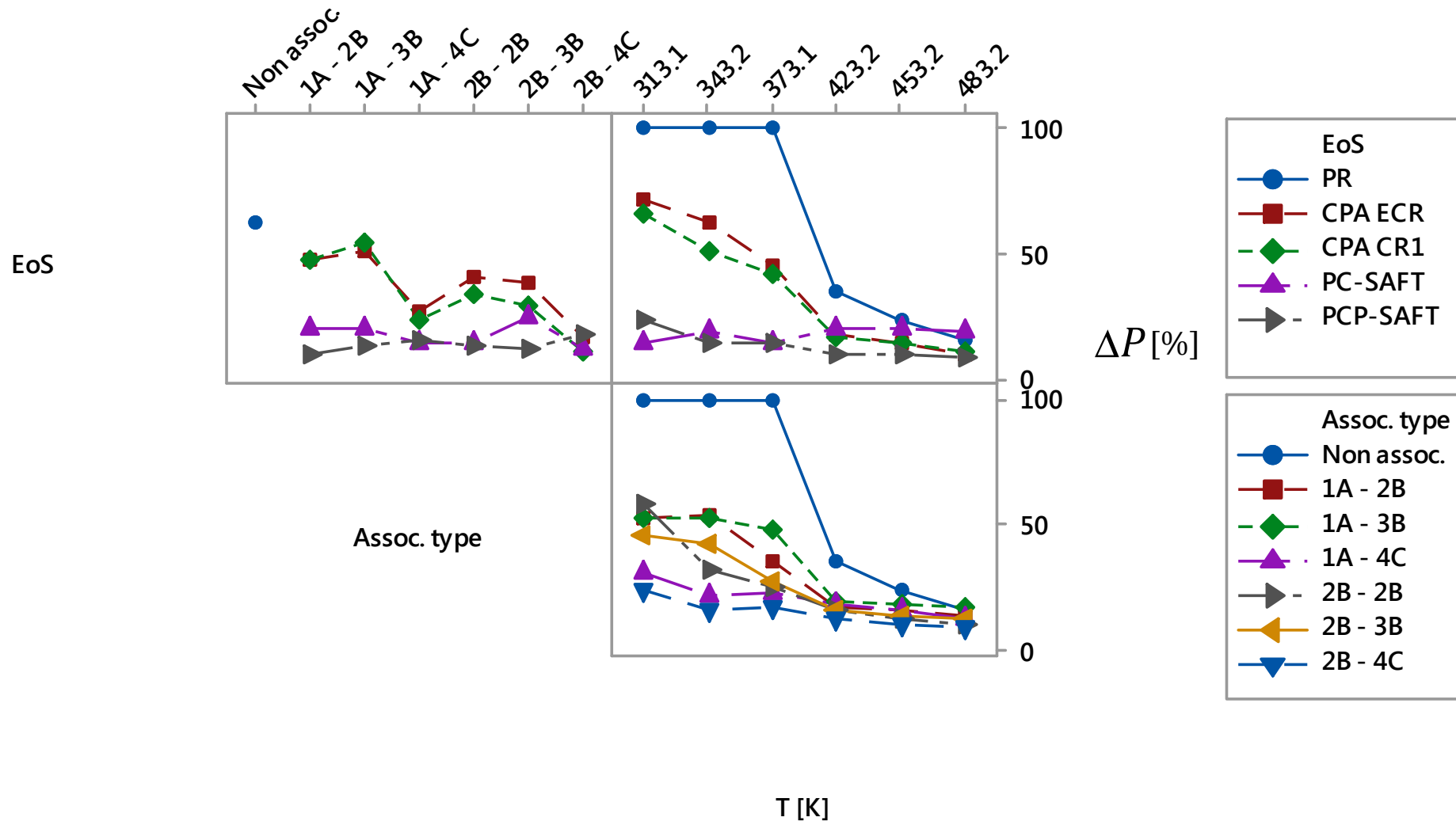


Figure 3.4. Interaction plot as a function of Equation of State (EoS), Association type and Temperature (T) of the average deviations in pressure (ΔP) of the propanoic acid + water system in predictive mode ($k_{ij} = 0$).

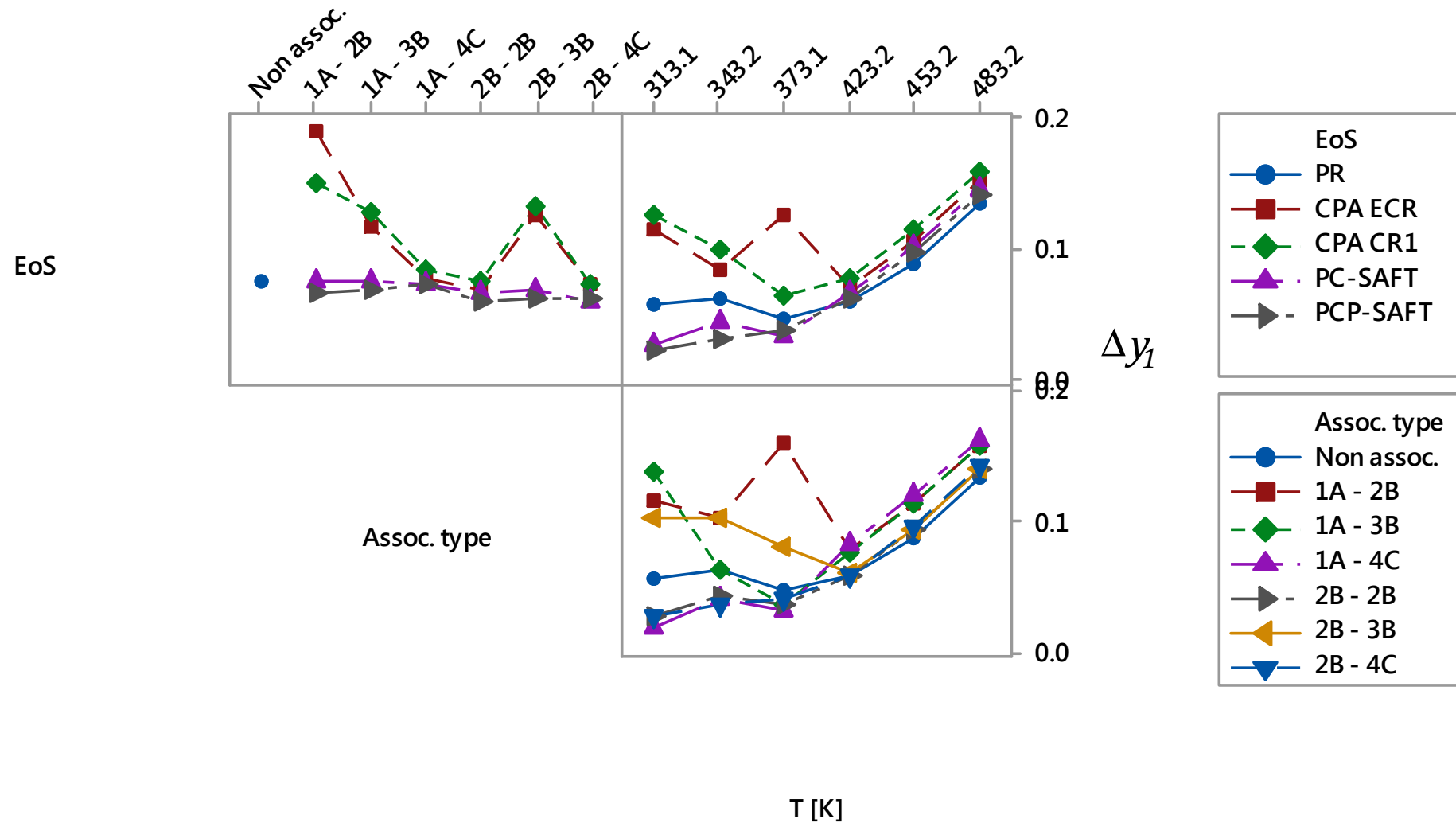


Figure 3.5. Interaction plot as a function of Equation of State (EoS), Association type and Temperature (T) of the average deviations in vapour composition (Δy_1) of the propanoic acid (1) + water (2) system in predictive mode ($k_{ij} = 0$).



In CPA, regardless of the combining rule, the best combination is given by 1A-3B. In general, the results with CPA are intermediate between those of the SAFT models and those of PR. It is reasonable to assume that the cubic part (SRK) is being improved by the inclusion of the association term, but it may also be possible to attribute the success to the fitting of the pure component parameters, i.e., SRK may also result in acceptable correlations if the pure component parameters are also fitted instead of being estimated from [Equations \(3.72\) and \(3.73\)](#). Overall, the results with the CR1 combining rule overcome those of the ECR rule. Nevertheless, predictions with CPA are in general rather poor, especially for some combinations such as 1A-4C or 2B-2B, in agreement with previous observations of Kontogeorgis et al. (2007).

Although the 1A-3B provides the best prediction in CPA, the model is either unable to give a representation or predicts experimentally unobserved azeotropic behaviour. At 293.15 K for example ([Figure 3.6](#)), CPA_{CR1 1A-3B} cannot handle the strong non-ideality without using a binary interaction parameter. Breil et al. (2011) have found it necessary to use CPA coupled with the Huron-Vidal mixing rule to obtain a reasonable representation. PC-SAFT_{2B-4C} predicts erroneously an azeotrope at this temperature. In contrast, while the 1A-3B is not the best overall best combination in PCP-SAFT (this is the 1A-2B), it is slightly closer to the experimental data at this condition.

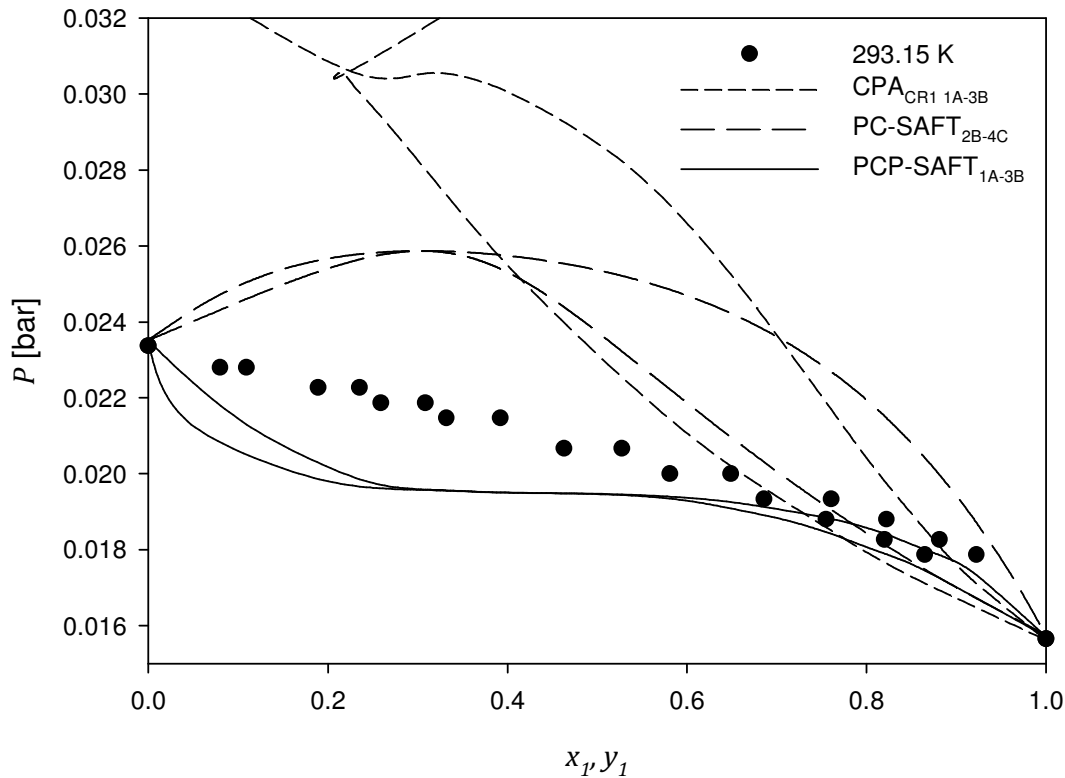


Figure 3.6. Vapour – liquid diagram for the acetic acid (1) + water (2) system at 293.15 K. Experimental data (●) from Lazeeva and Markuzin (1973). Lines: equation of state predictions ($k_{ij} = 0$).

For the vapour compositions of the acetic acid mixture (Figure 3.3), the satisfactory predictions of PC-SAFT are corroborated over the rest of the models. Once more the overall minimum is given by PCP-SAFT, in this case with the 1A-3B combination. It is important to point out at the prediction at the three highest temperatures (the temperatures studied experimentally in this thesis); as discussed in Section 2.3.5.4, a systematic error is very likely, but as can be seen in Figure 3.3, errors of the same magnitude appear for the literature values. Previous to the 373.12 K isotherm there seems to be a tendency of the error to decrease with temperature (as observed for the errors in pressure). It is possible to confirm, consequently, the existence of a systematic error in the measurements.

PR is not able to predict the behaviour at the lowest temperatures. As temperature increases, deviations decrease but the model tends to over predict the bubble-point pressures.

The overall best models for the acetic acid mixture, in order of accuracy among the CPA, PC-SAFT and PCP-SAFT groups are $\text{PC-SAFT}_{2\text{B-4C}} > \text{PCP-SAFT}_{1\text{A-2B}} > \text{CPA}_{\text{CR1 1A-3B}} > \text{CPA}_{\text{ECR 1A-3B}} > \text{PR}$. Typical predictions with these models are plotted in Figures 3.7 – 3.9, showing the phase behaviour at 373.12, 443.2 K and 502.85 K. PR predictions are only shown at 373.12 as a common example of the inaccuracy of the model for this mixture. The higher predictive capabilities of $\text{PC-SAFT}_{2\text{B-4C}}$, in particular at the highest temperatures, are evidenced in all these Figures.

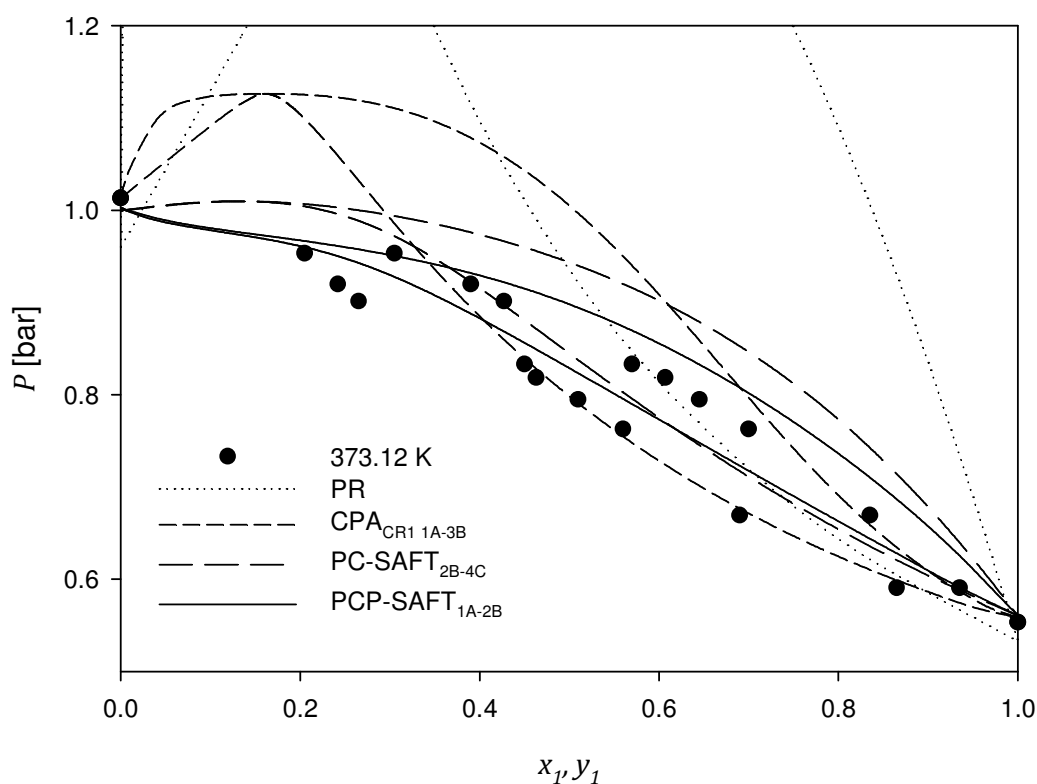


Figure 3.7. Vapour – liquid diagram for the acetic acid (1) + water (2) system at 373.12 K. Experimental data (●) from Achary and Narasingrao (1947). Lines: equation of state predictions ($k_{ij} = 0$).

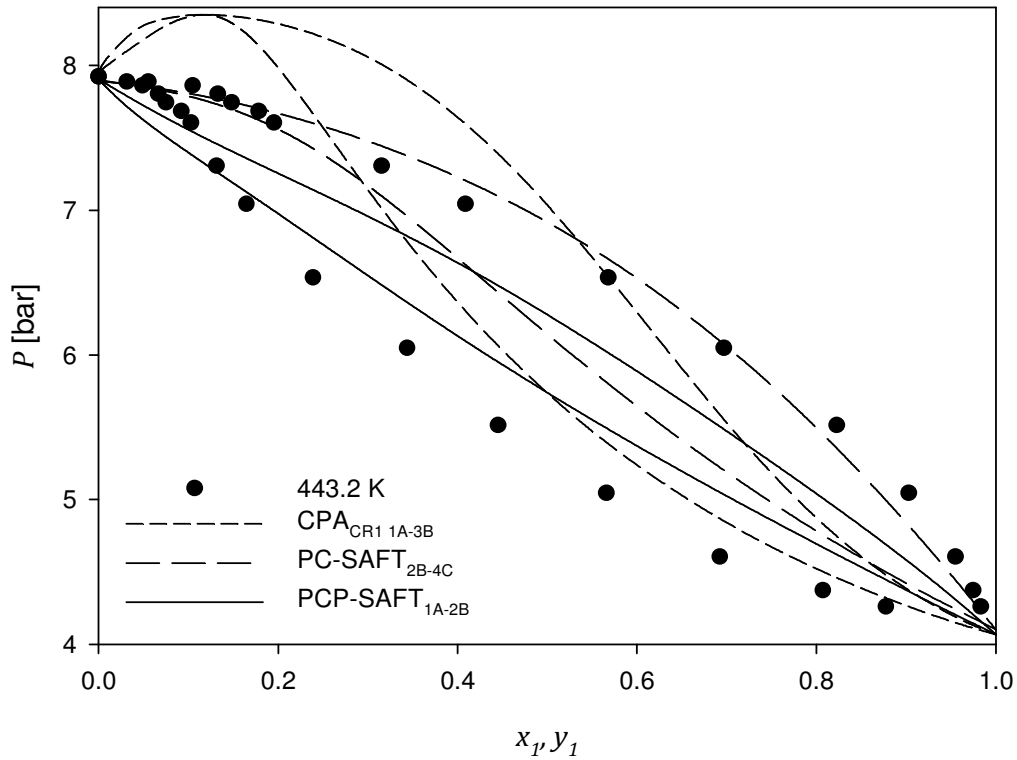


Figure 3.8. Vapour – liquid diagram for the acetic acid (1) + water (2) system at 443.2 K. Experimental data (●) from this work. Lines: equation of state predictions ($k_{ij} = 0$).

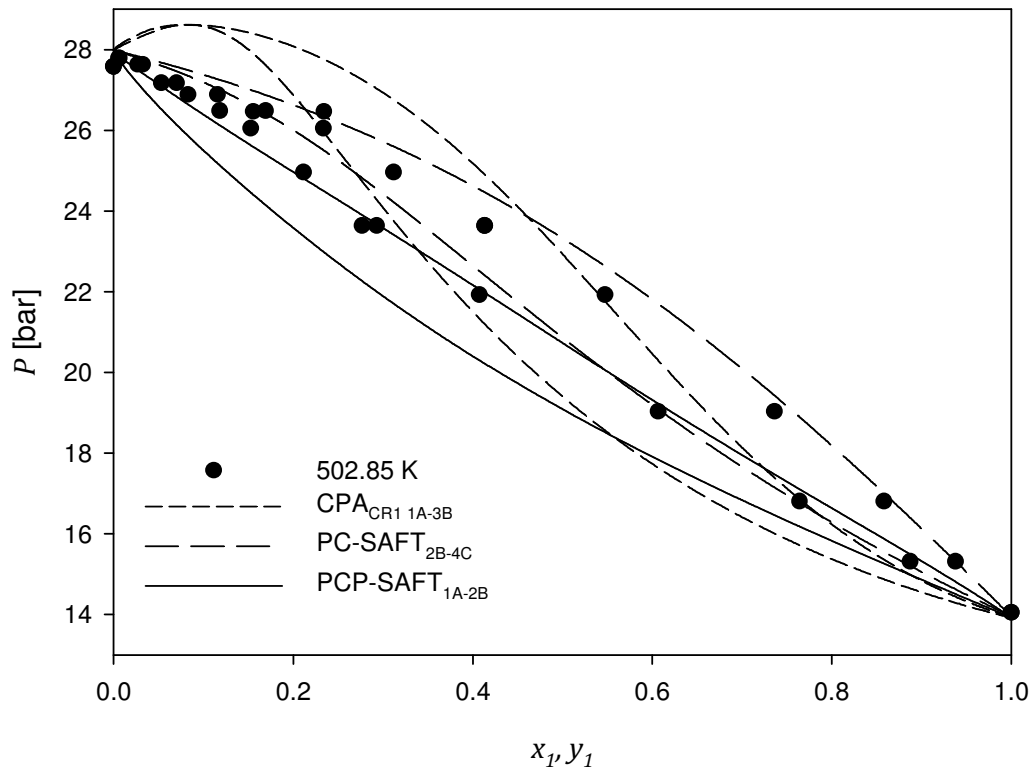


Figure 3.9. Vapour – liquid diagram for the acetic acid (1) + water (2) system at 502.85 K. Experimental data (●) from (Freeman and Wilson, 1985b). Lines: equation of state predictions ($k_{ij} = 0$).



For the propanoic acid + water system (Figures 3.4 – 3.5), the very best predictions in pressure over the whole range of temperatures are obtained with PCP-SAFT ($\Delta P = 13.33\%$), particularly with the 1A-2B (9.13%) scheme. The second best overall predictions are given by CPA_{CR1 2B-4C} (11.29%) closely followed by PC-SAFT_{2B-4C} (11.43%). PR is the worst predictor (62.42%) as expected.

Predictions are quite difficult to obtain with CPA, particularly at the lowest temperatures below 373.1 K. Similar to the case of acetic acid, CR1 shows an improvement in the predictions on pressure compared with the ECR rule, practically for all of the association schemes and in the whole range of temperatures. Regardless of the combining rule employed, CPA shows a better performance than PR but worse than the PC-SAFT and PCP-SAFT models.

Among PC-SAFT and CPA (both CR1 and ECR) the lowest deviations are given by the 2B-4C association. The PC-SAFT model however is not able to capture the azeotropic behaviour of the system as shown at 343.2 K and 453.2 K (Figures 3.10 and 3.11, respectively).

As a comparison, Figures 3.10 and 3.11, include the calculations done with the UNIQUAC (Abrams and Prausnitz, 1975) activity coefficient model coupled with the Hayden-O'Connell term (Hayden and O'Connell, 1975) (UNIQUAC-HOC), which considers the dimerization of carboxylic acids in the vapour phase. The calculations with UNIQUAC-HOC were done in Aspen with the following default pure component and binary parameters: association parameter (η) set to 4.5, 1.7 and 2.5 for the propanoic acid, water and cross-interactions, respectively; $a_{ij} =$

0.7555, $a_{ji} = -0.0992$, $b_{ij} = -599.915$ and $b_{ji} = 123.4991$. UNIQUAC-HOC is

employed here as a benchmark since it was developed to handle the non-ideality of the vapour phase.

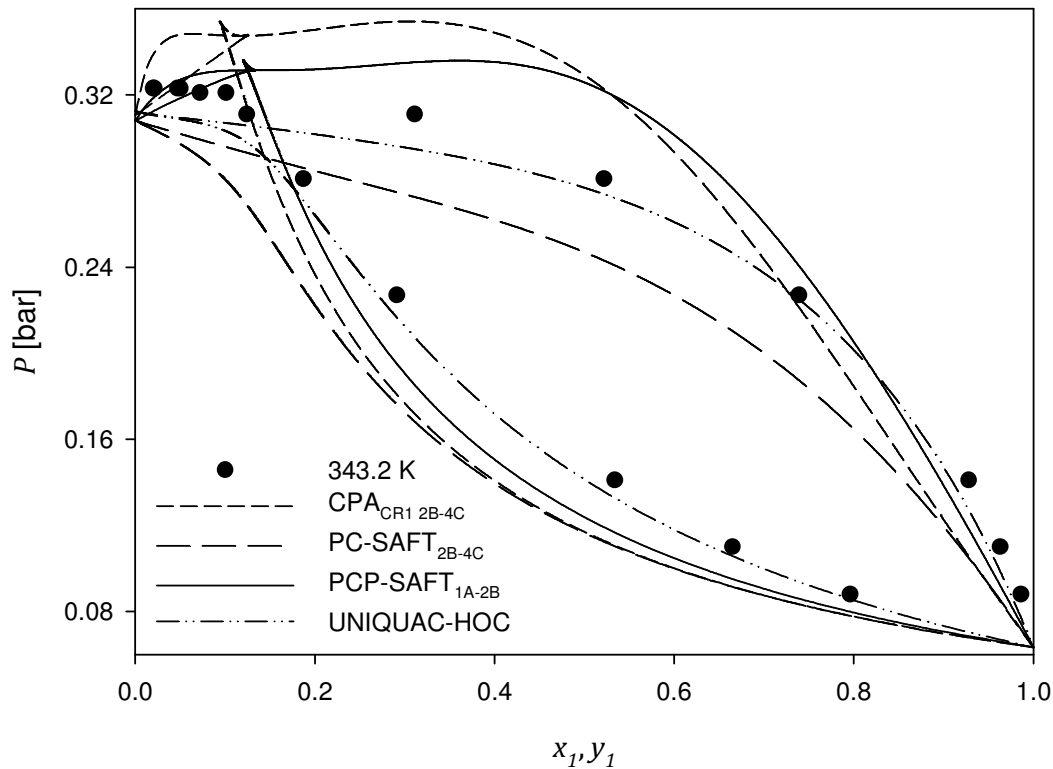


Figure 3.10. Vapour – liquid diagram for the propanoic acid (1) + water (2) system at 343.2 K. Experimental data (●) from Heintz et al. (1986); Miyamoto et al. (2001). Lines: equation of state predictions ($k_{ij} = 0$) and UNIQUAC-HOC correlations.

Not surprisingly, the worst predictions are given by PR, but interestingly, as temperature increases, its performance become closer to the ones of the average of PC-SAFT, in such a way that at 483.2 K, PR becomes first in the overall predictions. Evidently this is partially true, because looking at the association combinations individually, the PC-SAFT_{1A-4C} and the PC-SAFT_{2B-4C} give better performance.

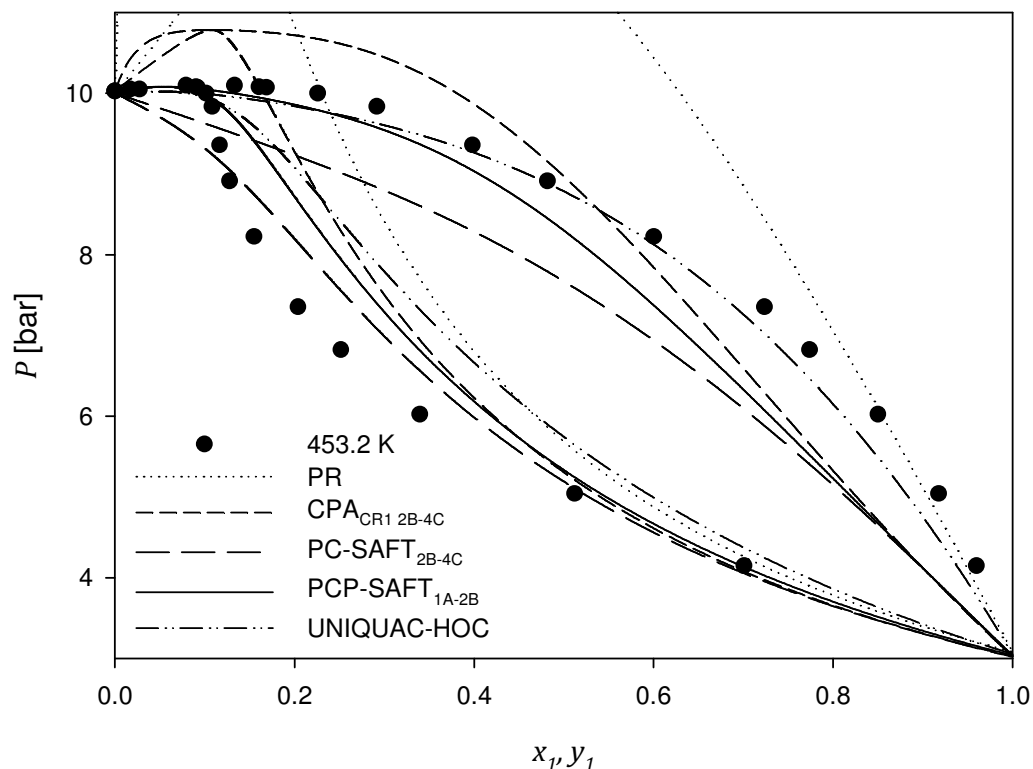


Figure 3.11. Vapour – liquid diagram for the propanoic acid (1) + water (2) system at 453.2 K. Experimental data (●) from this work. Lines: equation of state predictions ($k_{ij} = 0$) and UNIQUAC-HOC correlations.

Deviations in composition are lower with PC-SAFT and PCP-SAFT compared with the rest of the equations, with practically no difference between one another. The same can be said about the ECR and CR1 combining rules. Noticeably, the predictions with PR are in some cases lower than some of the CPA association combinations, e.g. the 1A-3B; and at the highest temperatures, even lower than some of the average deviations of the PC-SAFT and PCP-SAFT models.

The order of accuracy in the predictions for the propanoic acid mixture among each of the CPA, PC-SAFT and PCP-SAFT groups is $\text{PCP-SAFT}_{1\text{A-2B}} > \text{PC-SAFT}_{2\text{B-4C}} > \text{CPA}_{\text{CR1 2B-4C}} > \text{CPA}_{\text{ECR 2B-4C}} > \text{PR}$.

3.7.2.2 Correlative mode

Values of the binary interaction parameter at each temperature and for each system are presented in [Appendix J.1](#). Since a linear temperature dependency was observed, a single temperature-dependent binary interaction parameter with the form $k_{ij} = k_{ij}^0 + k_{ij}^1 T$ was fitted. Parameters k_{ij}^0 and k_{ij}^1 and the corresponding calculated deviations for each model are presented in [Appendices J.2](#) and [I.2](#) respectively. The analysis of the correlative capabilities is done based on this temperature-dependent parameter.

The lowest values of k_{ij} are observed for the PCP-SAFT model for both systems, which for most of the cases are negative. Actually, only the 1A-3B scheme is positive for both mixtures at all temperatures. The very lowest k_{ij} are with the 1A-2B combination, corroborating in some way its highest predictive capabilities. Within PC-SAFT there is no evident trend in the values and sign, which can be as large as 0.12 and as low as -0.0016 depending on the system, temperature and association scheme. For CPA, the magnitude of k_{ij} are negative regardless of the combining rule and system, except for the propanoic acid mixture at 483.2 K with $CPA_{CR1\ 2B-3B}$ ($k_{ij} = 0.010$) and $CPA_{CR1\ 2B-4C}$ ($k_{ij} = 0.007$). Magnitudes as large as -0.26 for the 1A-4C scheme with the ECR combining rule are observed and are in agreement with previous publications (Kontogeorgis et al., 2007).

[Figures 3.12](#) and [3.14](#) contain the interaction plots on bubble-point pressure of the acetic acid and propanoic acid systems, respectively. In this mode, the best correlations in pressure for the acetic acid mixture are given by $PC-SAFT_{1A-3B}$



($\Delta P = 1.32\%$), whereas for the propanoic acid mixture these are given by the PC-SAFT_{2B-4C} (4.24%).

Contrary to the predictive mode, the ECR combining rule exhibits higher correlative capabilities compared to CR1, which are more noticeable with the 2B-4C combination for both systems.

Interestingly, the PR correlations are not the worst case. Depending on the system and temperature, it gives in some instances better correlations than some of the CPA association combinations, besides lower magnitudes of the k_{ij} . For the propanoic acid system, the correlations with PR are close to those produced from PC-SAFT.

In relation to the vapour phase compositions (Figures 3.13 and 3.15), these are better correlated with the PCP-SAFT models but closely followed by the PC-SAFT ones. In CPA, the ECR rule results in slightly lower deviations than the CR1. For the acetic acid system, CPA overcomes the correlations of PR, but for the propanoic acid system it is the opposite order. Recalling the experimental error in the vapour compositions (Section 2.3.5.4), is not surprising to find a dramatic shift in the deviations for all the models at 412.6 K (Figure 3.13).

For the acetic acid mixture the order of accuracy for each group of equations according to their correlative results is PC-SAFT_{1A-3B} > PCP-SAFT_{1A-2B} > CPA_{ECR 2B-4C} > CPA_{CR1 2B-4C} > PR. Whereas for the propanoic acid mixture this is PC-SAFT_{2B-4C} > PCP-SAFT_{2B-2B} > CPA_{ECR 2B-4C} > CPA_{CR1 1A-4C} > PR.

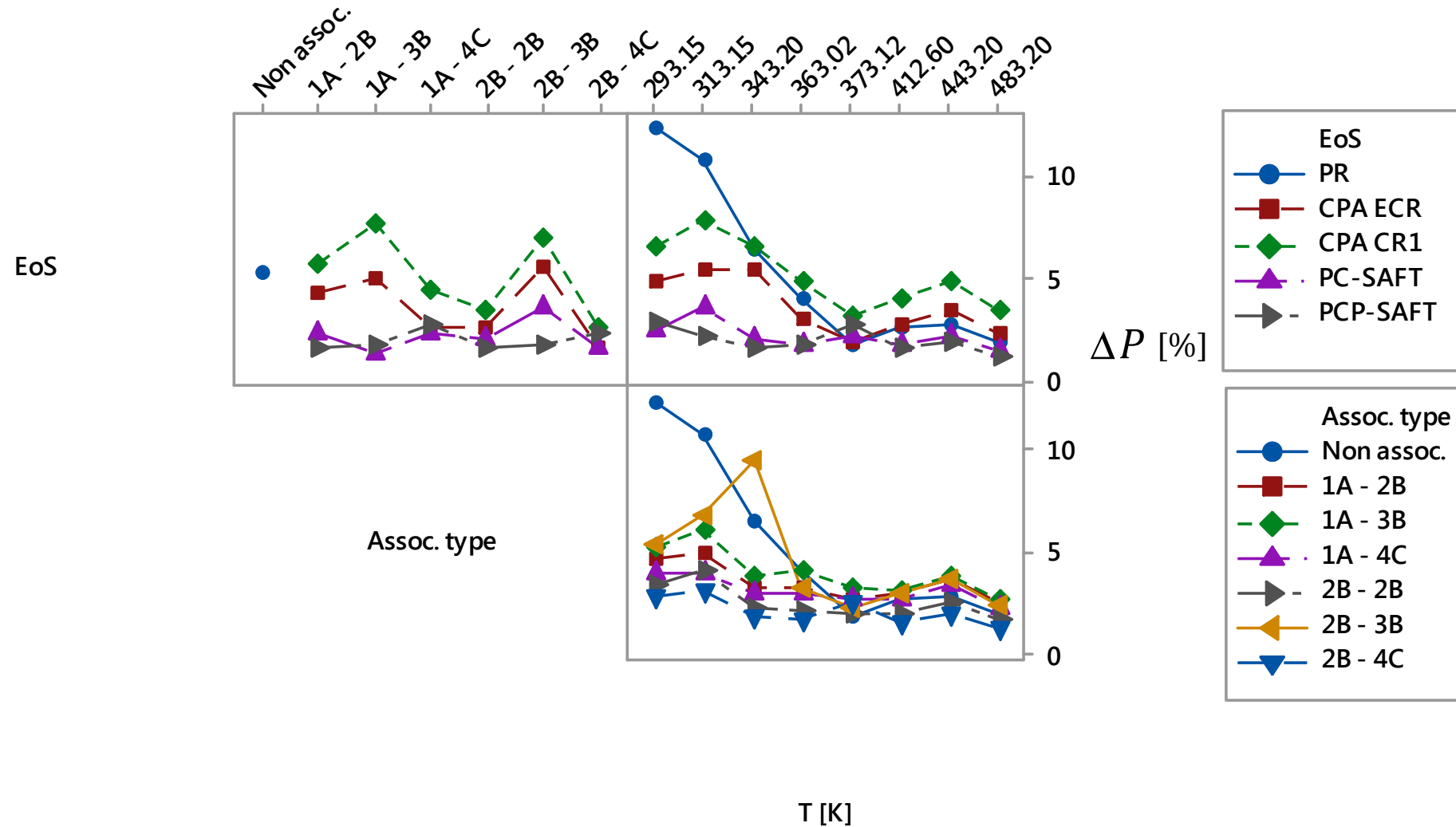


Figure 3.12. Interaction plot as a function of Equation of State (EoS), Association type and Temperature (T) of the average deviations in pressure (ΔP) of the acetic acid + water system in correlative mode ($k_{ij} = k_{ij}^0 + k_{ij}^1 T$).

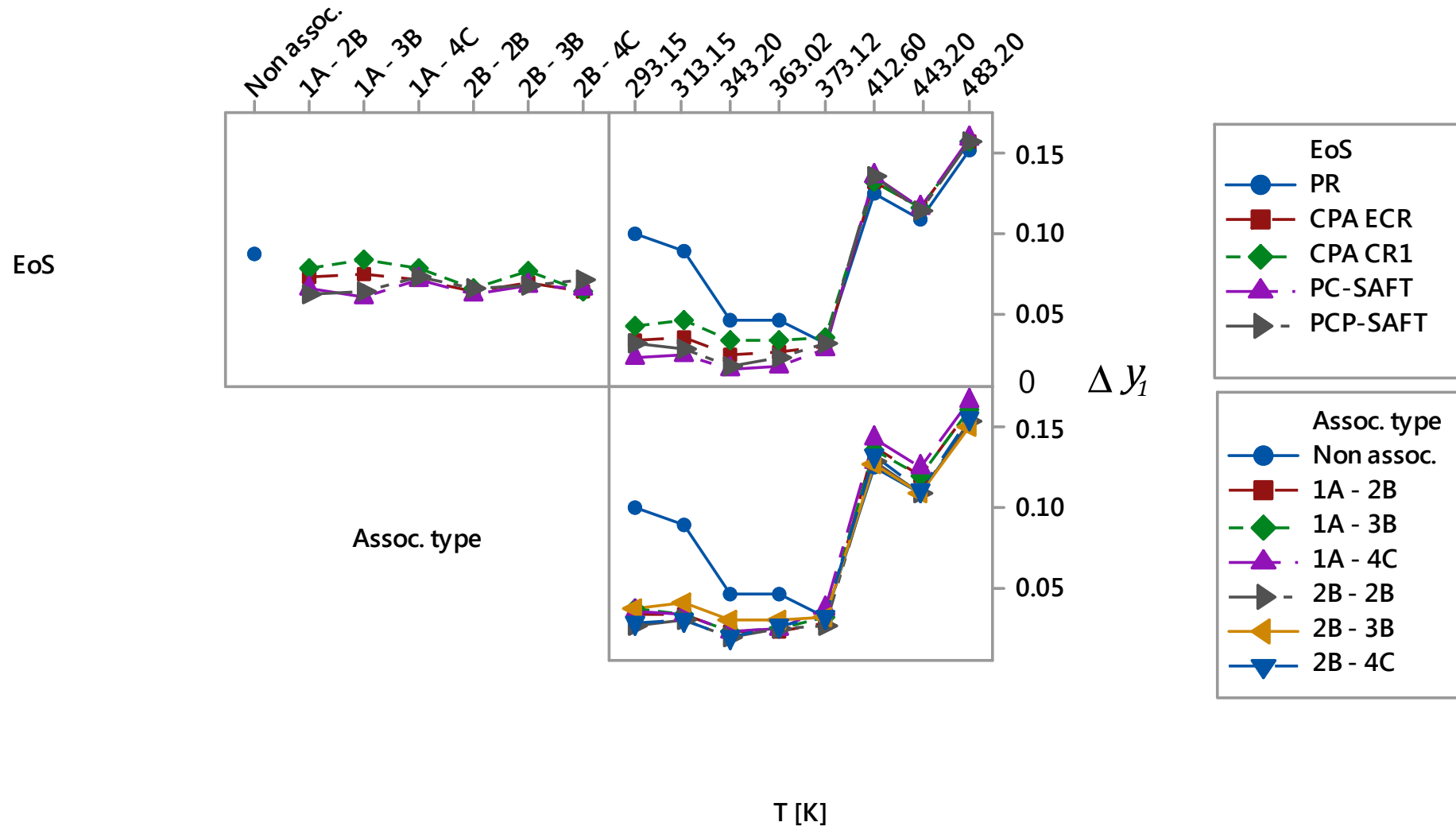


Figure 3.13. Interaction plot as a function of Equation of State (EoS), Association type and Temperature (T) of the average deviations in vapour composition (Δy_1) of the acetic acid (1) + water (2) system in correlative mode ($k_{ij} = k_{ij}^0 + k_{ij}^1 T$).

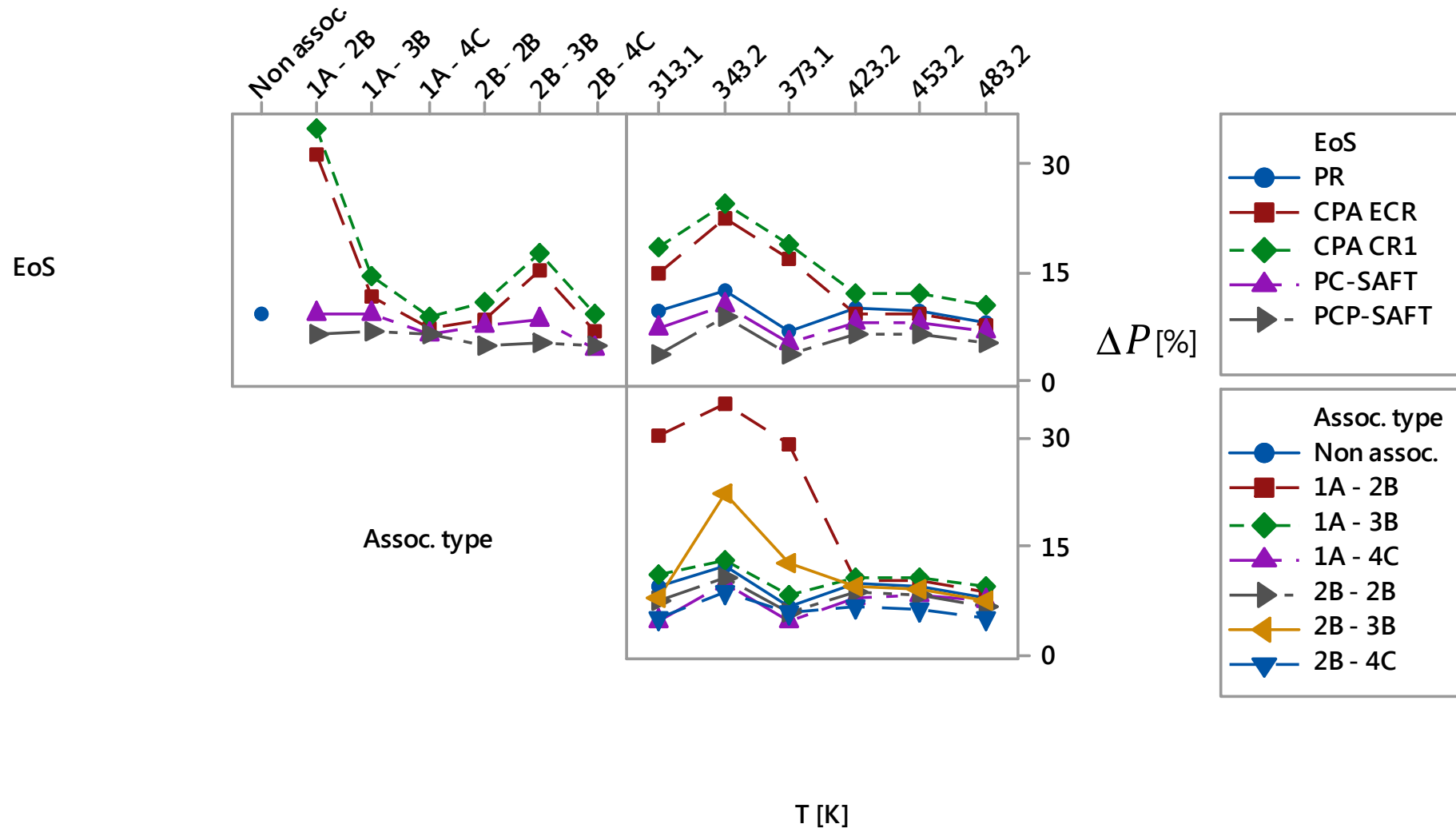


Figure 3.14. Interaction plot as a function of Equation of State (EoS), Association type and Temperature (T) of the average deviations in pressure (ΔP) of the propanoic acid + water system in correlative mode ($k_{ij} = k_{ij}^0 + k_{ij}^1 T$).

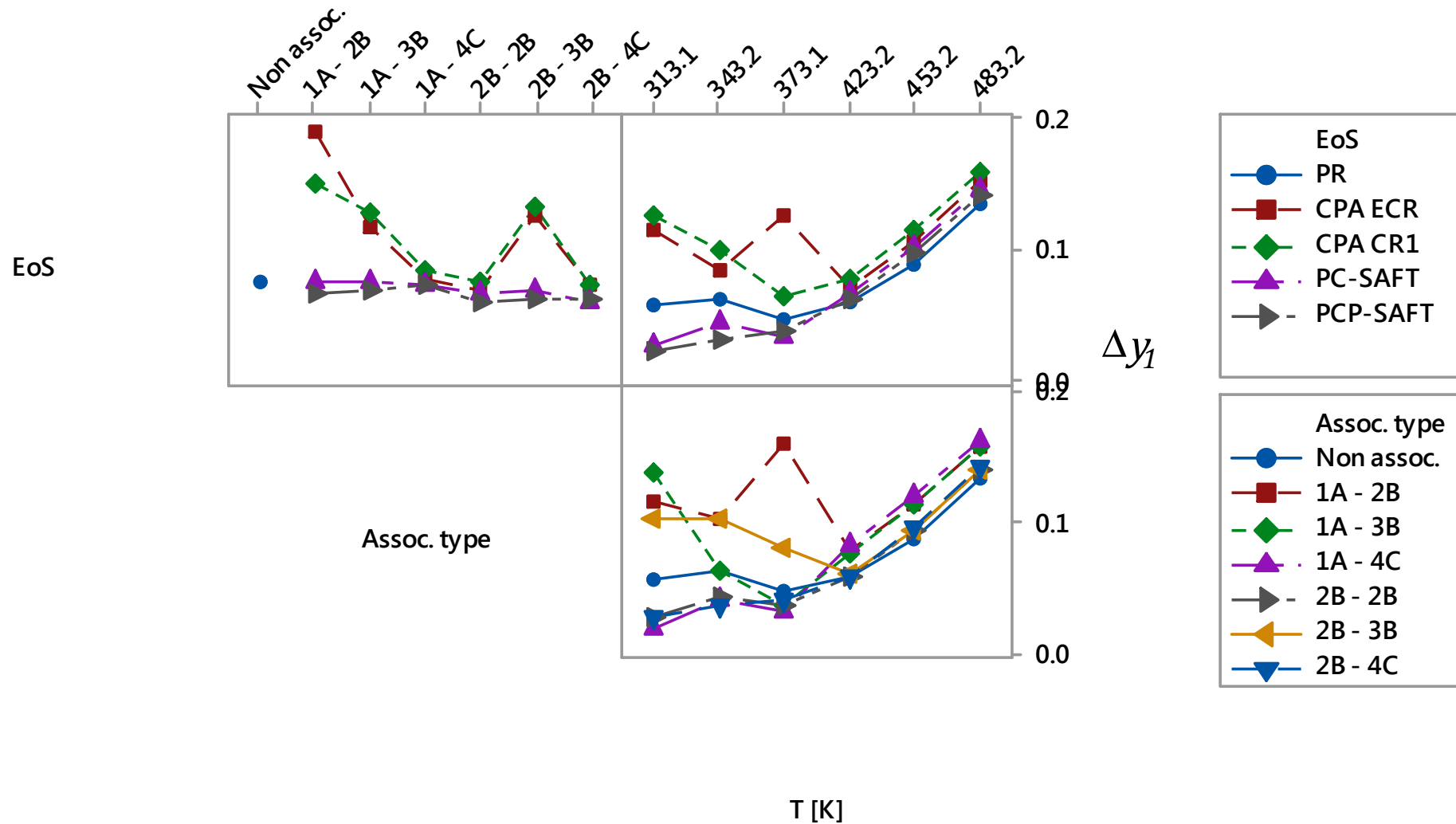


Figure 3.15. Interaction plot as a function of Equation of State (EoS), Association type and Temperature (T) of the average deviations in vapour composition (Δy_1) of the propanoic acid (1) + water (2) system in correlative mode ($k_{ij} = k_{ij}^0 + k_{ij}^1 T$).



From [Figures 3.2 – 3.5](#) and [3.12 – 3.15](#), it is clear that the choice of the best equation will depend on the system under study and temperature. There is no obvious trend for a specific model applicable in the whole range of temperatures and for both systems. In most of the cases modelling of the dipolar moments explicitly in PC-SAFT improves the predictions and correlations. CPA with CR1 has higher predictive capabilities but ECR correlative ones. PR results in the largest deviations in the predictions but in many cases gives better correlations than CPA, and even results in lower magnitudes of the binary interaction parameter.

As a whole, considering the results from both systems and both modes, the best choice of equations among each of the EoS groups are: $PCP-SAFT_{1A-2B} > PC-SAFT_{2B-4C} > CPA_{CR1\ 2B-4C}$. As examples of the accuracy of these models, [Figures 3.16](#) and [3.17](#) show the modelling at 412.6 K and 483.2 K, respectively, for the acetic acid mixture; whereas [Figure 3.18](#) the modelling at 423.2 K for the propanoic acid mixture. [Figures 3.16](#) and [3.17](#) show the satisfactory correlations for the liquid phase compositions with all models and the notably large discrepancies for the vapour experimental data obtained in this work.

The correlation of isobaric data at 7.91 bar for the acetic acid + water system ([Figure 3.19](#)) displays the inaccuracy of the models at some temperatures as was observed in the isothermal analysis. The $PCP-SAFT_{1A-2B}$ model, for instance, underpredicts the dew-line at the lowest temperatures. It is important to note the correlations given by PR, which are comparable to those of CPA.

Figure 3.20 shows isobaric data at 1 bar for the propanoic acid + water system from different sources and the modelling with the selected EoS. As shown, the PCP-SAFT_{1A-2B} correlation is the closest to the average experimental data. PC-SAFT_{2B-4C} curves are comparable with those previously reported by Janecek and Paricaud (2013) and Chen et al. (2012), but in contrast, a lower positive binary interaction parameter ($k_{ij} \approx 0.025$) is required in this case. The largest deviations from the experimental data are encountered with CPA. Even with a large negative value of the binary parameter (≈ -0.09), it is not possible to get a satisfactory representation of the phase behaviour, particularly of the dew-line. PR correlations are satisfactory considering it provides similar results as CPA, although at the expense of a larger $k_{ij} (\approx -0.13)$.

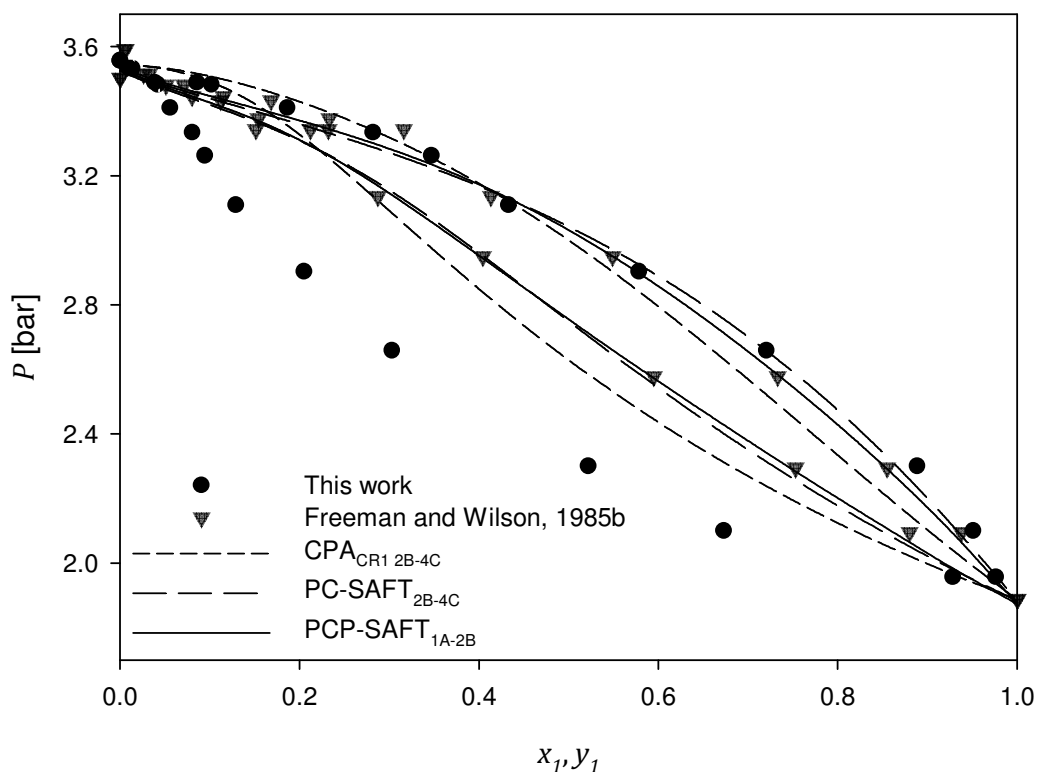


Figure 3.16. Vapour – liquid diagram for the acetic acid (1) + water (2) system at 412.6 K. Symbols: experimental data. Lines: equation of state correlations ($k_{ij} = k_{ij}^0 + k_{ij}^1 T$).

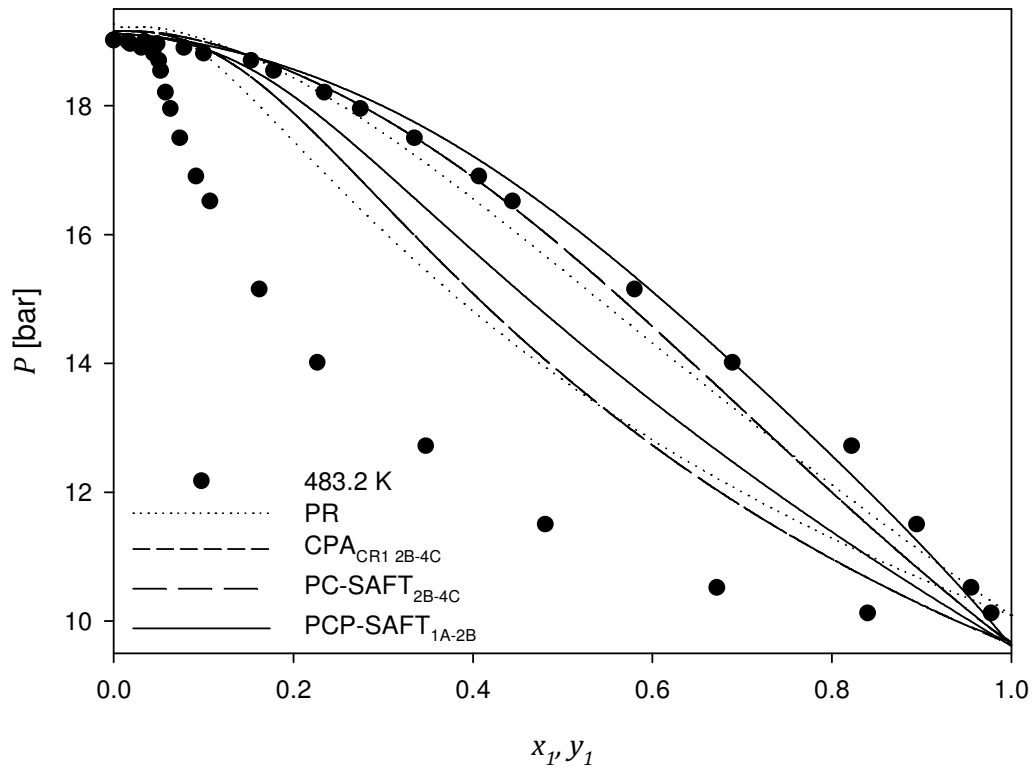


Figure 3.17. Vapour – liquid diagram for the acetic acid (1) + water (2) system at 483.2 K. Experimental data (●) from this work. Lines: equation of state correlations ($k_{ij} = k_{ij}^0 + k_{ij}^1 T$).

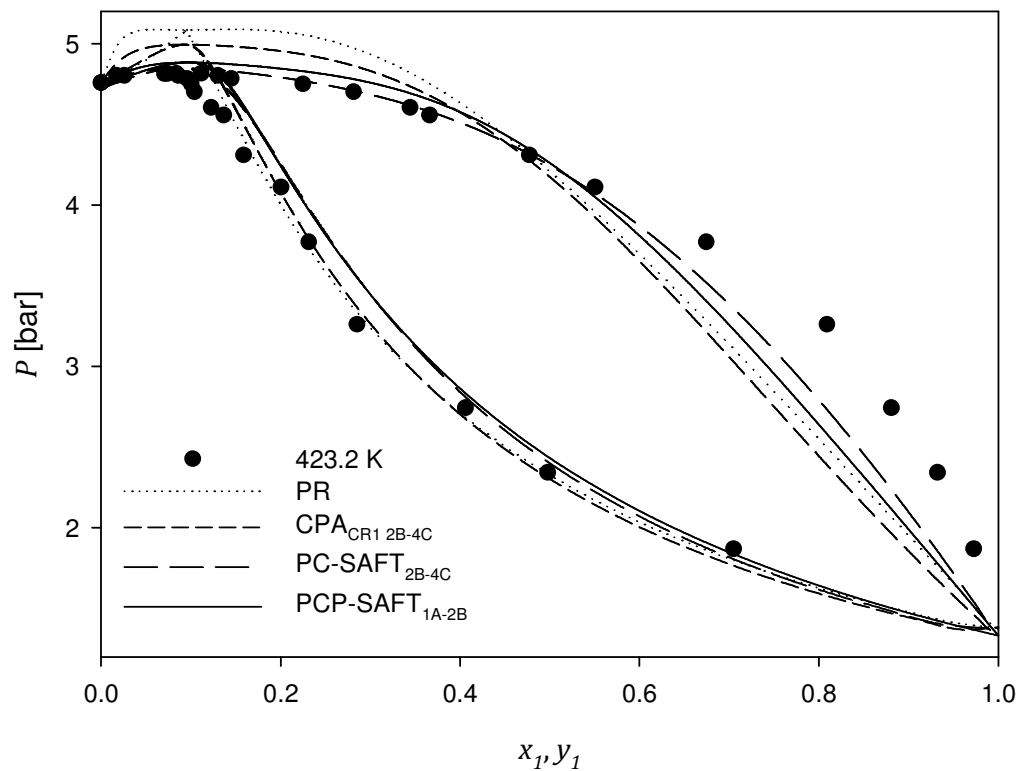


Figure 3.18. Vapour – liquid diagram for the propanoic acid (1) + water (2) system at 423.2 K. Experimental data (●) from this work. Lines: equation of state correlations ($k_{ij} = k_{ij}^0 + k_{ij}^1 T$).

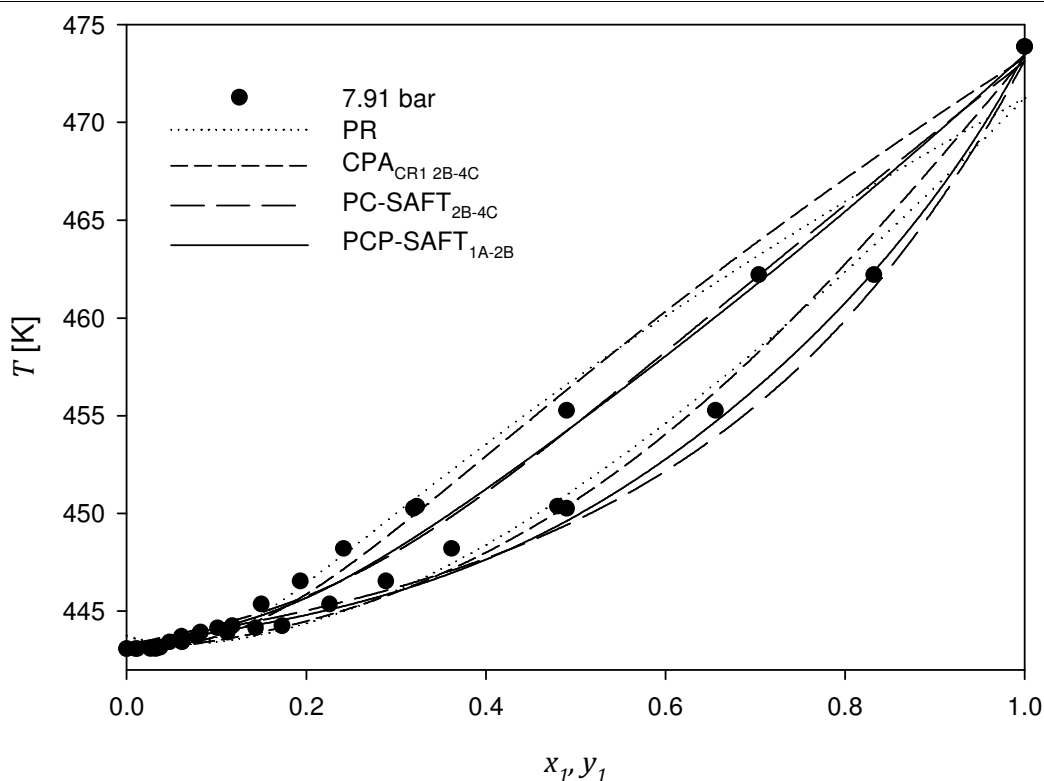


Figure 3.19. Vapour – liquid diagram for the acetic acid (1) + water (2) system at 7.91 bar. Experimental data (●) from Othmer et al. (1952). Lines: equation of state correlations ($k_{ij} = k_{ij}^0 + k_{ij}^1 T$).

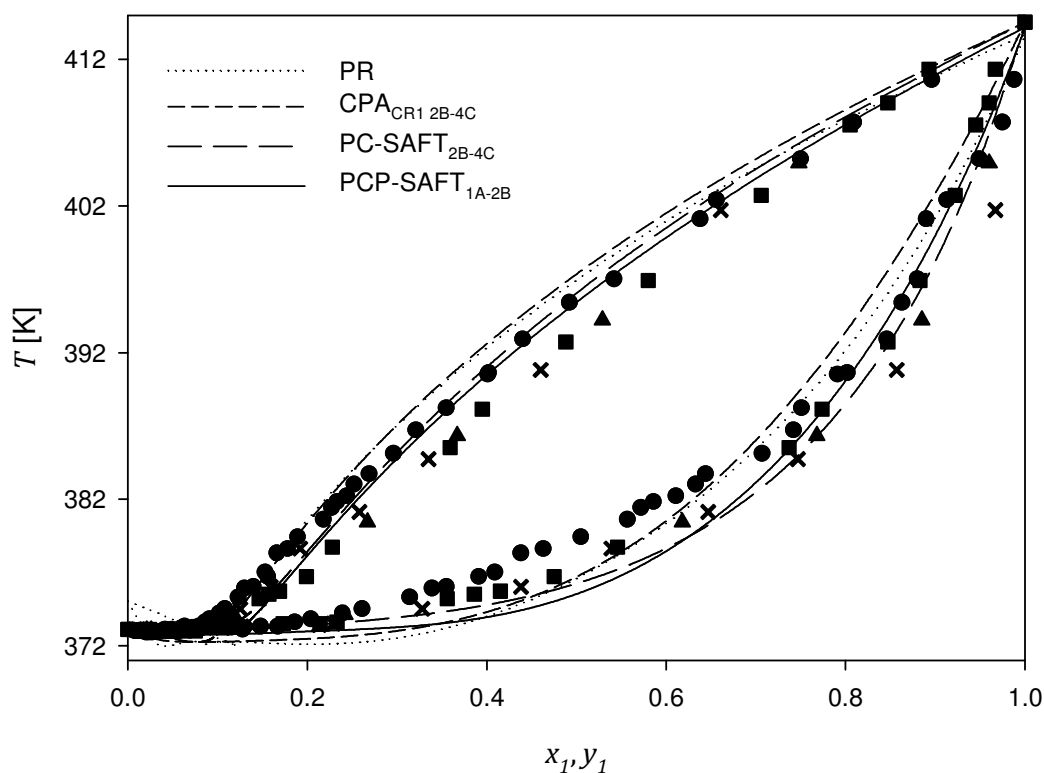


Figure 3.20. Vapour – liquid diagram for the propanoic acid (1) + water (2) system at 1 bar. Experimental data: (■), Rivenq (1961); (▲), Ito and Yoshida (1963); (x), Kushner et al. (1967) and (●), Amer (1975). Lines: equation of state correlation ($k_{ij} = k_{ij}^0 + k_{ij}^1 T$).



3.7.2.3 Synthetic measurements

The experimental data for the acetic acid + water system obtained at 412.6 K with the PEPT technique discussed in [Section 2.4](#), were compared against modelling with the PC-SAFT_{2B-4C} EoS. The binary interaction parameter is retrieved from [Appendix J.2.1](#), i.e. no attempt to find the optimum binary interaction parameter for the data was performed. For comparison, calculations were also made with UNIQUAC-HOC in Aspen with the following default pure compound and binary interaction parameters: association parameter (η) set to 4.5, 1.7 and 2.5 for the acetic acid, water and cross-interactions, respectively; $a_{ij} = 0.7446$, $a_{ji} = 0.0042$, $b_{ij} = -615.264$ and $b_{ji} = 196.899$. The modelling results are presented in [Table 3.8](#) as well as the estimated deviations in pressure, vapour composition and vapour and liquid molar densities. [Figure 3.21](#) shows the VLE diagram with the models.

While the pressures and liquid phase molar densities are well correlated with the two models, the significantly large deviations are for the vapour phase compositions and their densities. Vapour densities are one order of magnitude higher than the estimated with both, the EoS and the activity coefficient model. However, this is not necessarily indicative of inaccurate experimental results. High deviations between experimental and modelling vapour densities have also been observed for other systems such as the carbon dioxide + ethanol, 1-octanol, 1-nonanol and acetone (Chang et al., 1998).



Table 3.8. Computed pressures (P), acetic acid vapour compositions (y_1), liquid molar densities (ρ_L) and vapour molar densities (ρ_V), and calculated deviations (Δ) with PCP-SAFT_{2B-4C} and UNIQUAC-HOC.

PCP-SAFT _{2B-4C}				UNIQUAC-HOC				Deviations ^{a,b}							
P [bar]	y_1	ρ_L [mol L ⁻¹]	ρ_V [mol L ⁻¹]	P [bar]	y_1	ρ_L [mol L ⁻¹]	ρ_V [mol L ⁻¹]	PCP-SAFT _{2B-4C}				UNIQUAC-HOC			
								ΔP [%]	Δy_1	$\Delta \rho_L$ [%]	$\Delta \rho_V$ [%]	ΔP [%]	Δy_1	$\Delta \rho_L$ [%]	$\Delta \rho_V$ [%]
2.433	0.66	17.8	0.08	2.406	0.69	17.5	0.10	1.86	0.04	7.82	88.27	0.72	0.07	6.36	85.09
2.653	0.55	19.4	0.08	2.634	0.56	18.7	0.10	0.29	0.09	9.87	88.97	1.00	0.11	6.32	86.63
3.139	0.31	26.7	0.10	3.135	0.29	21.9	0.10	0.10	0.10	15.04	93.00	0.02	0.08	5.52	92.88

^a Experimental data from PEPT measurements (Section 2.4.9, Table 2.7).

^b $\Delta\theta = \frac{100}{Np} \sum_{i=1}^{Np} \left| \frac{\theta_i^{exp} - \theta_i^{calc}}{\theta_i^{exp}} \right|$, for θ either P , ρ_L or ρ_V . $\Delta y_1 = \frac{1}{Np} \sum_{i=1}^{Np} |y_{1,i}^{exp} - y_{1,i}^{calc}|$.

^c PCP-SAFT binary interaction parameters from Appendix J.2.1.

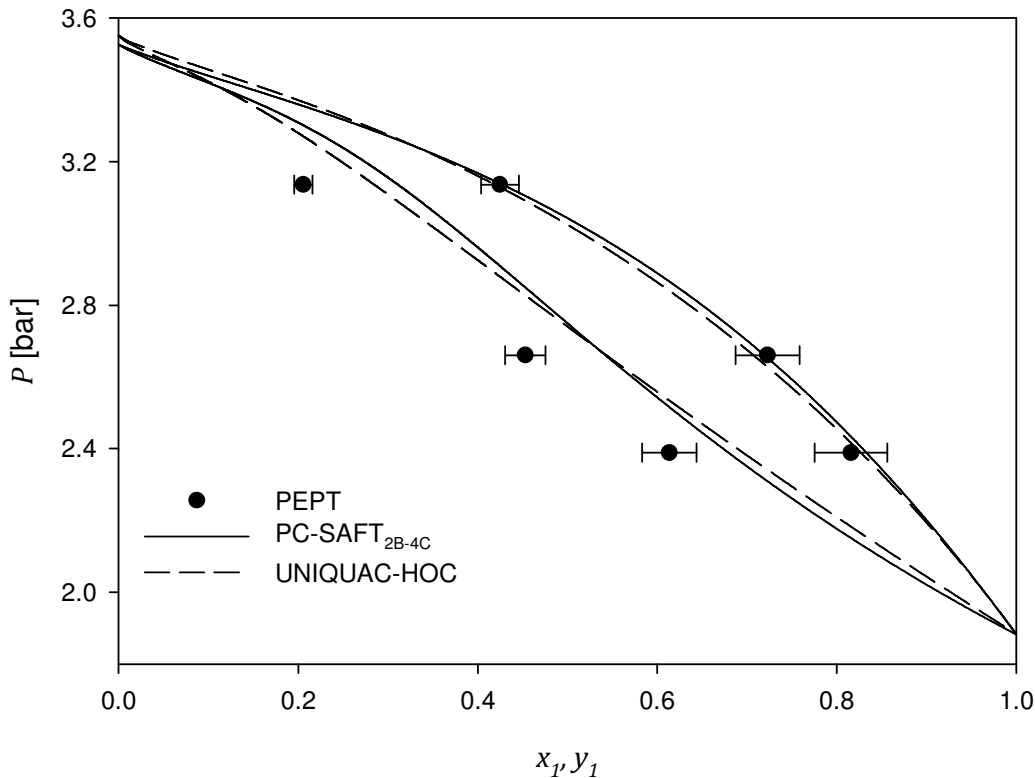


Figure 3.21. Vapour – liquid diagram for the acetic acid (1) + water (2) system at 412.6 K. Experimental data (●), with error bars, obtained from the PEPT technique. Lines: equation of state correlation ($k_{ij} = k_{ij}^0 + k_{ij}^1 T$) and UNIQUAC-HOC correlations.

The synthetic measurements of the vapour phase compositions seem to be more reliable than the analytical ones, since these are closer to the modelling results with both thermodynamic models (Figure 3.21).

It is clear that the highly non-ideal behaviour of the acetic + water system, represents a true challenge from both, the experimental and modelling point of view. More experimental data is needed at this and other conditions to either totally validate or totally discard the vapour phase measurements presented in this work.

3.7.2.4 Non-association scenario

In order to test the effect of the association term in modelling the association interactions in PC-SAFT and PCP-SAFT, it was decided to perform the modelling ignoring association contributions. Pure component parameters for acetic acid, propanoic acid and water without association were fitted as described in [Section 3.6](#) and are presented in [Table 3.9](#). The computed deviations in vapour pressures and saturated liquid densities are larger compared when association is included. However, this does not necessarily lead to a poor representation of mixture properties as has been shown in recent studies (Liang et al., 2014a).

[Figure 3.22](#) shows the Pxy diagram for propanoic acid + water at 453.2 K predicted with PC-SAFT_{2B-4C}, PCP-SAFT_{1A-2B} and the non-associating cases of PC-SAFT and PCP-SAFT (PC-SAFT_{non-assoc} and PCP-SAFT_{non-assoc}). Poor predictions would have been expected when the association interactions are not considered explicitly in the model, but as shown in [Figure 3.22](#), this is not case. PC-SAFT_{non-assoc} is able to capture the azeotrope of the mixture, at least qualitatively, and is closer to the experimental compositions. In contrast, PC-SAFT_{2B-4C} (the best association combination based on the analysis of [Section 3.7.2.2](#)), fails to represent the azeotropic behaviour. On the other hand, PCP-SAFT_{1A-2B} predicts correctly the azeotropic composition, but compositions of the liquid phase are much better predicted with PCP-SAFT_{non-assoc}. Even though at this temperature the polar equations give more accurate representations of the phase behaviour, this cannot be generalized for both systems and for the whole range of temperatures. In fact, PC-SAFT_{non-assoc} results generally in lower deviations than PCP-SAFT_{non-assoc} in predictive mode, as can be seen in

Appendix I.1 containing the computed deviations from the experimental data. In correlative mode the deviations are lower with PCP-SAFT_{non-assoc}. Evidently, the results will also depend on the system under consideration.

Table 3.9. Non-associating PC-SAFT and PCP-SAFT pure component parameters and average deviations in vapour pressures (ΔP_v) and liquid densities ($\Delta \rho_L$).^a

Compound	m	σ [Å]	ε/k [K]	μ [D]	T [K]	ΔP_v [%]	$\Delta \rho_L$ [%]
acetic acid	3.2544	2.9205	283.20		289.81 -	2.88	3.59
	3.2001	2.9373	282.28	1.739	586.03	2.89	3.47
propanoic acid	4.4934	2.8404	248.19		252.45 -	4.80	2.54
	4.4552	2.8490	247.92	1.751	594.80	4.86	2.50
water	2.7528	2.0879	328.03		273.16 -	2.19	3.29
	2.7515	2.0737	288.15	1.85	640.63	0.49	1.95

^a Vapour pressure and liquid density data from DIPPR (2012).

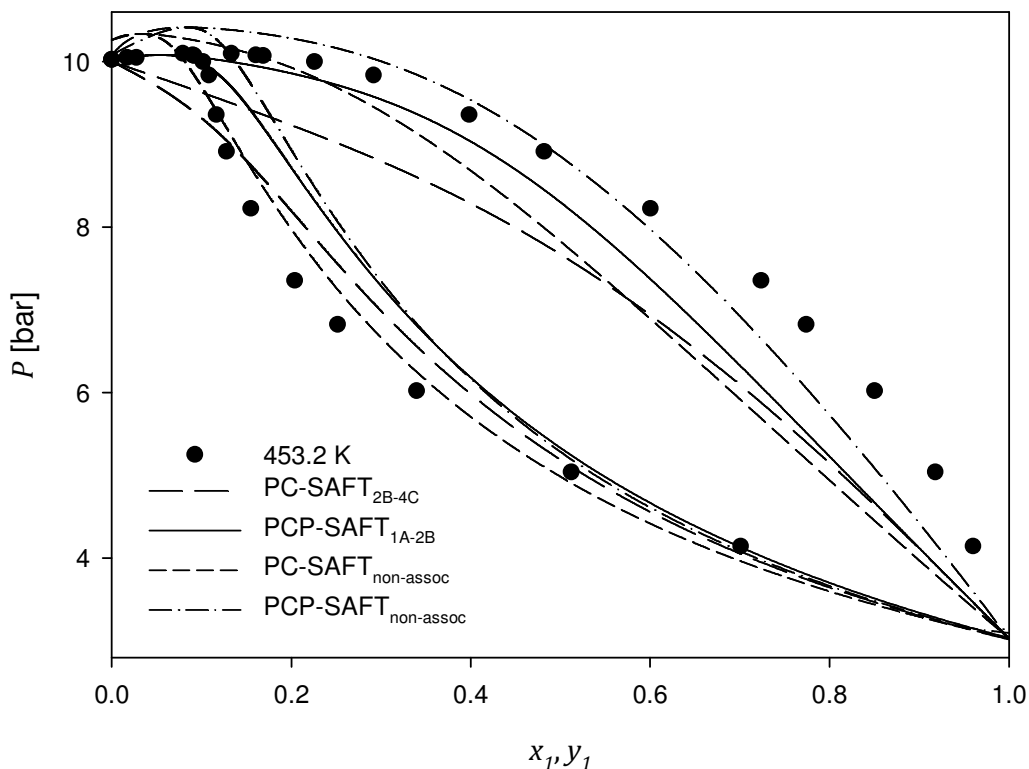


Figure 3.22. Vapour – liquid diagram for the propanoic acid (1) + water (2) system at 453.2 K. Experimental data (●) from this work. Lines: equation of state predictions ($k_{ij} = 0$).



In some instances the resulted deviations with PC-SAFT_{non-assoc} and PCP-SAFT_{non-assoc} are lower than some of the association combinations and perhaps unexpectedly, results in better modelling than any of the CPA equations.

This can be attributable in large part to the pure component parameters employed, but it is interesting to note that it is possible to ignore the association term and yet still obtain acceptable estimations. It is important to keep in mind that the association term in SAFT equations of state has been constructed based on different simplifications and that it would be naive not to expect some inaccuracies in actual applications.

3.8 Concluding remarks

The phase equilibria modelling of acetic acid + water and propanoic acid + water systems were performed with 25 different equations of state, as a product of the combination of the main equations of state: PR, CPA, PCSAFT and PCP-SAFT; the ECR and CR1 combining rules in CPA; the association schemes 1A and 2B for the carboxylic acids and the 2B, 3B and 4C for water.

For the acetic acid mixture, the overall best results were obtained by the PC-SAFT model where the acid was considered as 2B and water as 4C; whereas for the propanoic acid mixture these were given by the 1A scheme for the acid and 2B for water. Considering both systems, PCP-SAFT_{1A-2B} showed the best prediction and correlation capabilities and also resulted in the lowest magnitudes of the binary interaction parameter. The accuracy of PC-SAFT_{1A-2B} is in general closely followed by that of PC-SAFT_{2B-4C}.



Explicitly accounting for the dipolar term in PC-SAFT does not necessarily improve its modelling capabilities, as observed in the results for pure compound properties and for mixtures. PCP-SAFT did not always result in lower deviations than PC-SAFT when comparing the same association scheme (including the non-associating scenario). One reason for this inaccuracy may be due to the fact that the dipole moment is taken from experimental measurements at vacuum, but also that it is assumed constant over the entire temperature range.

Regarding the association interactions, it seems that the association scheme has to be chosen properly in order to obtain satisfactory predictions and/or correlations. It should also be contemplated, the possible inaccuracy of the association term to capture the strong interactions of these systems, as illustrated by the results with the non-association scenario. However, the problem is obscured by the presence of multiplicity of parameters. Moreover, it has been shown, that different conditions and systems require different association combinations for a satisfactory outcome. More experimental data for these and other systems are necessary to arrive at a better conclusion on this aspect.

CPA with the CR1 combining rule with the acid modelled as 2B and water as 4C resulted in the best performance of the CPA equations. The accuracy of the model is intermediate between the PC-SAFT / PCP-SAFT models and PR. PR predictions were rather poor but correlations were comparable to those of CPA, at the expense of a larger k_{ij} .

Conclusions and Suggestions for future work

Vapour – liquid equilibria data for acetic acid and propanoic acid in mixture with water has been measured in the range of 412.6 to 483.2 K, based on a static – analytical apparatus. The 412.6 K isotherm of the acetic acid system was compared with literature values resulting in good agreement of the bubble-point line. Disagreement was found for the vapour phase. A systematic error due to the sampling procedure seems to be the source of the inaccuracies.

The analytical measurements can largely be improved by on-line sampling, either using six-port valves or patented high-pressure samplers such as the ROLSI™ samplers (Guilbot et al., 2000; Richon, 2009). On-line sampling will result in faster and more reliable analyses.

A limiting factor in the present study was also the manual control of the air bath temperature. An automated system is highly recommended that in addition to speed up analyses, it will result in lower uncertainties.

A new technique that avoids sampling by using PEPT technology was developed and applied to determine the phase equilibrium at 412.6 K for the acetic acid + water system. While satisfactory agreement was found for the liquid compositions, the vapour phase data laid between the results of the analytical measurements and those of the literature. A systematic error due to the use of different radioactive tracers for each experiment appeared to be the source of the disagreement. Such error can be avoided by a standardizing the coating layer. Moreover, it is recommended the use of a single particle for the entire



experimental study. To achieve this, a tracer with a longer half-life will be needed.

The use of a variable-volume cell with automated heating control would allow to increase the number of data gathered in a single experimental run.

The current technique is limited by the thermal properties of the polymer used as coating of the radioactive tracer, to temperatures of around 453 K. Different materials with higher thermal and mechanical properties can be used as tracers or coatings, but they need to satisfy the more stringent requirement of be able to float on the liquid phase. The technique can be used for phase equilibria and volumetric properties of other organic acids + water systems from low to high pressures, including sub-atmospheric pressures. It can easily be used for studies on other aqueous mixtures at high pressures and low temperatures, for instance, mixtures with carbon dioxide.

A promising technology that can be used in phase equilibria studies is that involving Neutron Radiography as demonstrated in the study of supercritical water (Balaskó et al., 2009). This technology coupled with imaging processing techniques could be valuable for investigations of multiphase equilibria involving high temperatures and pressures of multicomponent systems.

The modelling has shown that predictions with a thermodynamic molecular model such as PC-SAFT are better compared with a classical cubic model. However, the results for the non-associating cases as well as the results for some of the association combinations have exposed the need for a revision of the theory. It appears that only proper choice of the association scheme will result in satisfactory results; and that the best association scheme for pure compound



properties may not necessarily be the best in mixture. The dipolar term also seems to improve the modelling only when coupled with the proper association scheme. The implication of this, is the need to test different possible association schemes in order to find the most suitable for the system and conditions in turn, and that it may be difficult to generalize about a best association scheme for a compound. The problem is also related to the multiplicity of parameters, a problem not truly studied in the literature and that may be the topic of a research.

Modern equations although theoretical in their development, in their application are still rather empirical since for example the number of association sites per molecule has to be chosen with profound implications in the outcome.

The PC-SAFT model with polar contributions and with the 1A and 2B association schemes for the carboxylic acid and water, respectively, resulted in the best overall average predictions and correlations, when assessing both systems and the whole range of temperatures.

It may be possible to obtain improved correlations if induce-polar interactions are considered explicitly in the PC-SAFT model. Additionally, it would be interesting to model the new experimental data with an equilibrium approach to handle the association interactions, such as in the ESD equation of state.

CPA provided slightly better predictions than a normal cubic equation of state, but the correlations on the other hand, were similar to those obtained with PR. PR was used in this work with parameters correlated to the critical properties, but it has been suggested in the literature that improved results could be obtained if



Conclusions and Suggestions for future work

the parameters are also adjusted from vapour pressures and liquid density data.

This will result in a fairer comparison of the model.

The present work was focused only on acetic acid and propanoic acid, but it would be interesting to study the formic acid + water mixture which requires the consideration of kinetic studies due to the thermal instability of formic acid.

References

2b1stconsulting (2014). **BP mulls over world-scale petrochemical complex in Oman** [online]. Available from: <http://www.2b1stconsulting.com/bp-mulls-over-world-scale-petrochemical-complex-in-oman/> [Accessed October 2014].

Abbott, M.M. (1979) "Cubic equations of state: An interpretive review". In Kwang Chu, C. & Robert, L.R. (Eds.) **Equations of state in engineering and research**. Advances in chemistry. 182. Washington, D.C.: American Chemical Society. pp. 47-70.

Abolala, M. and Varaminian, F. (2013) Modeling the solubility of light reservoir components, HCFCs and HFCs in water using the CPA and sPC-SAFT equations of state. **Journal of Molecular Liquids**, 187: 359-367.

Abrams, D.S. and Prausnitz, J.M. (1975) Statistical thermodynamics of liquid mixtures: A new expression for excess Gibbs energy of partly or completely miscible systems. **AIChE Journal**, 21 (1): 116-128.

Achary, M.V.R. and Narasingrao, M. (1947) Vapour–liquid equilibria of non-ideal solutions - I. **Transactions of the Indian Institute of Chemical Engineers**, 1: 29-37.

Akhtar, J. and Amin, N.A.S. (2011) A review on process conditions for optimum bio-oil yield in hydrothermal liquefaction of biomass. **Renewable Sustainable Energy Reviews**, 15: 1615-1624.

Albers, K., Heilig, M. and Sadowski, G. (2012) Reducing the amount of PCP-SAFT fitting parameters. 2. Associating components. **Fluid Phase Equilibria**, 326: 31-44.

Alfradique, M.F. and Castier, M. (2007) Calculation of phase equilibrium of natural gases with the Peng-Robinson and PC-SAFT equations of state. **Oil & Gas Science and Technology - Revue d'IFP Energies Nouvelles**, 62 (5): 707-714.

Alsaifi, N.M., Hamad, E.Z. and Englezos, P. (2008) Prediction of vapor–liquid equilibrium in water–alcohol–hydrocarbon systems with the dipolar perturbed-chain SAFT equation of state. **Fluid Phase Equilibria**, 271 (1-2): 82-93.



Altsheler, W.B., Unger, E.D. and Kolachov, P. (1951) Improved still for liquid–vapor equilibria. Data on systems: Ethanol–water and acetic acid–water. **Industrial and Engineering Chemistry**, 43 (11): 2559-2564.

Amer, S. (1975) Vapor–liquid equilibrium in binary systems formed by propionic acid with water and amyl alcohol, isoamyl alcohol, secondary amyl alcohol, tertiary amyl alcohol and hexanol at 760 mmHg. **Anales de Quimica**, 71 (2): 127-135.

Aparicio-Martínez, S. and Hall, K.R. (2007) Phase equilibria in water containing binary systems from molecular based equations of state. **Fluid Phase Equilibria**, 254 (1-2): 112-125.

Apelblat, A., Tamir, A. and Wagner, M. (1983) Association in carboxylic acid aliphatic alcohol mixtures. The binary mixtures of acetic acid with *n*-butanol, *n*-hexanol, *n*-octanol and *n*-dodecanol. **Zeitschrift Fur Physikalische Chemie-Wiesbaden**, 137 (2): 129-137.

Arce, A., Blanco, A., Soto, A., et al. (1995) Isobaric vapor–liquid equilibria of methanol + 1-octanol and ethanol + 1-octanol mixtures. **Journal of Chemical and Engineering Data**, 40 (4): 1011-1014.

Arce, P.F. and Aznar, M. (2010) Thermodynamic modeling of liquid–fluid phase equilibrium in supercritical ethylene + copolymer + co-solvent systems using the PC-SAFT equation of state. **Journal of Supercritical Fluids**, 52 (1): 18-29.

Arich, G. and Tagliavini, G. (1958) Liquid–vapor equilibrium isotherms for the water–acetic acid system. **La Ricerca Scientifica**, 28: 2493-2500.

Aristovich, V.Y., Levin, A.I. and Morachevskii, A.G. (1962) Vapor–liquid equilibrium in low molecular weight fatty acids–water systems. **Tr. Vses. Nauchno-Issled. Inst. Neftekhim. Protsesov**, 5: 84.

Asghari, F.S. and Yoshida, H. (2006) Acid-catalyzed production of 5-hydroxymethyl furfural from d-fructose in subcritical water. **Industrial and Engineering Chemistry Research**, 45 (7): 2163-2173.

Bakalis, S., Cox, P.W., Russell, A.B., et al. (2006) Development and use of positron emitting particle tracking (PEPT) for velocity measurements in viscous fluids in pilot scale equipment. **Chemical Engineering Science**, 61 (6): 1864-1877.



Baker, L.E., Pierce, A.C. and Luks, K.D. (1982) Gibbs energy analysis of phase equilibria. **Society of Petroleum Engineers Journal**, 22 (5): 731-742.

Balaskó, M., Horváth, L., Horváth, Á., et al. (2009) Study of the behavior of supercritical water by dynamic neutron radiography. **Nuclear Instruments and Methods in Physics Research Section A: Accelerators, Spectrometers, Detectors and Associated Equipment**, 605 (1–2): 138-141.

Bamford, C.H. and Dewar, M.J.S. (1949) The thermal decomposition of acetic acid. **Journal of the Chemical Society**: 2877-2882.

Bamgbade, B.A., Wu, Y., Burgess, W.A., et al. (2012) Experimental density and PC-SAFT modeling of Krytox (R) (perfluoropolyether) at pressures to 275 MPa and temperatures to 533 K. **Fluid Phase Equilibria**, 332: 159-164.

Barham, H.N. and Clark, L.W. (1951) The decomposition of formic acid at low temperatures. **Journal of the American Chemical Society**, 73 (10): 4638-4640.

BASF (2006) Propionic acid protects food and animal feed from mold – rising demand. **The great preserver** [online]. Available from: <http://www.intermediates.basf.com/chemicals/topstory/propionsaeure> May 2006 [Accessed 08 August 2014].

Beret, S. and Prausnitz, J.M. (1975) Perturbed hard-chain theory: An equation of state for fluids containing small or large molecules. **AIChE Journal**, 21 (6): 1123-1132.

Bernatová, S., Aim, K. and Wichterle, I. (2006) Isothermal vapour–liquid equilibrium with chemical reaction in the quaternary water + methanol + acetic acid + methyl acetate system, and in five binary subsystems. **Fluid Phase Equilibria**, 247 (1-2): 96-101.

Berro, C., Rogalski, M. and Peneloux, A. (1982) Excess Gibbs energies and excess volumes of 1-butanol–*n*-hexane and 2-methyl-1-propanol–*n*-hexane binary systems. **Journal of Chemical and Engineering Data**, 27 (3): 352-355.

Beyer, H. and Walter, W. (1997) "Organic chemistry: A comprehensive degree text and source book". [online]. Woodhead Publishing. pp. 229-268. Available from: Knovel. <http://app.knovel.com/hotlink/toc/id:kpOCACDTS1/organic-chemistry-comprehensive/organic-chemistry-comprehensive>. [Accessed 30 July 2014].



Bhar, B.N. and Lindstrom, G. (1955) Molecular association and proton resonance in propionic acid. **Journal of Chemical Physics**, 23 (10): 1958-1959.

Bjerre, A.B. and Sorensen, E. (1992) Thermal decomposition of dilute aqueous formic acid solutions. **Industrial and Engineering Chemistry Research**, 31 (6): 1574-1577.

Blake, P.G., Davies, H.H. and Jackson, G.E. (1971) Dehydration mechanisms in the thermal decomposition of gaseous formic acid. **Journal of the Chemical Society B: Physical Organic**, (10): 1923-1925.

Blake, P.G. and Hole, K.J. (1966) The thermal decomposition of propionic acid. **Journal of the Chemical Society B: Physical Organic**, (6): 577-579.

Blake, P.G. and Jackson, G.E. (1968) The thermal decomposition of acetic acid. **Journal of the Chemical Society B: Physical Organic**, (10): 1153-1155.

Blake, P.G. and Jackson, G.E. (1969) High- and low-temperature mechanisms in the thermal decomposition of acetic acid. **Journal of the Chemical Society B: Physical Organic**, (2): 94-96.

Blas, F.J. and Vega, L.F. (1997) Thermodynamic behaviour of homonuclear and heteronuclear Lennard–Jones chains with association sites from simulation and theory. **Molecular Physics**, 92 (1): 135-150.

Blas, F.J. and Vega, L.F. (1998) Prediction of binary and ternary diagrams using the statistical associating fluid theory (SAFT) equation of state. **Industrial and Engineering Chemistry Research**, 37 (2): 660-674.

Blatti, J.L., Michaud, J. and Burkart, M.D. (2013) Engineering fatty acid biosynthesis in microalgae for sustainable biodiesel. **Current Opinion in Chemical Biology**, 17 (3): 496-505.

Borschel, E.M. and Buback, M. (1988) Dimerization of carboxylic acids in solution up to high pressures and temperatures. 3. Acetic acid. **Zeitschrift Fur Naturforschung A. A Journal of Physical Sciences**, 43 (3): 207-214.

BP press office (2013a). **BP reveals step-out routes to acetic acid and ethylene with all-new technologies** [online]. Available from: <http://www.bp.com/en/global/corporate/press/press-releases/BP-reveals-new-technologies.html> 07 November 2013 [Accessed 01 August 2014].



BP press office (2013b). **Global petrochemicals media backgrounder** [online]. Available from: <http://www.bp.com/content/dam/bp/pdf/Media-backgrounder-PetrochemicalsL.pdf> November 2013 [Accessed 01 August 2014].

Brazauskiene, J., Mishchenko, K.P. and Ciparis, J. (1965) The liquid–vapor equilibrium in the propionic acid–water system under isothermal conditions (40, 50, 60 °C). **Lietuvos TSR Aukštųjų Mokyklų Mokslo Darbai. Chem. Chem. Technol.**, 6: 141.

Breil, M.P., Kontogeorgis, G.M., Behrens, P.K., et al. (2011) Modeling of the thermodynamics of the acetic acid–water mixture using the cubic-plus-association equation of state. **Industrial and Engineering Chemistry Research**, 50 (9): 5795-5805.

Brown, I. and Ewald, A.H. (1950) Liquid–vapour equilibria. 1. The systems carbon tetrachloride–cyclohexane and water–acetic acid. **Australian Journal of Scientific Research, Series A: Physical Sciences**, 3 (2): 306-323.

Burdick, D.L. and Leffler, W.L. (2001) "Petrochemicals in nontechnical language". 3rd ed. [online]. PennWell. pp. 256-261. Available from: Knovel. <http://app.knovel.com/hotlink/toc/id:kpPNTLE002/petrochemicals-in-nontechnical/petrochemicals-in-nontechnical>. [Accessed 30 July 2014].

Calvar, N., Domínguez, A. and Tojo, J. (2005) Vapor–liquid equilibria for the quaternary reactive system ethyl acetate + ethanol + water + acetic acid and some of the constituent binary systems at 101.3 kPa. **Fluid Phase Equilibria**, 235 (2): 215-222.

Campbell, A.N. and Chatterjee, R.M. (1968) Orthobaric data of certain pure liquids in the neighborhood of the critical point. **Canadian Journal of Chemistry**, 46 (4): 575-581.

Campbell, A.N., Kartzmark, E.M. and Gieskes, J.M.T.M. (1963) Vapor–liquid equilibria, densities, and refractivities in the system acetic acid–chloroform–water at 25 °C. **Canadian Journal of Chemistry**, 41 (2): 407-429.

Campbell, S.W., Wilsak, R.A. and Thodos, G. (1986) Isothermal vapor–liquid equilibrium measurements for the *n*-pentane–acetone system at 372.7, 397.7 and 422.6 K. **Journal of Chemical and Engineering Data**, 31 (4): 424-430.

Carnahan, N.F. and Starling, K.E. (1969) Equation of state for nonattracting rigid spheres. **The Journal of Chemical Physics**, 51 (2): 635-636.



References

Carnahan, N.F. and Starling, K.E. (1972) Intermolecular repulsions and the equation of state for fluids. **AIChE Journal**, 18 (6): 1184-1189.

Carneiro, A.P., Rodríguez, O., Held, C., et al. (2014) Density of mixtures containing sugars and ionic liquids: Experimental data and PC-SAFT modeling. **Journal of Chemical and Engineering Data**, 59 (10): 2942-2954.

Chalov, N.V. and Aleksandrova, O.A. (1957) Liquid–vapor phase equilibrium of acetic acid–water system at atmospheric and lower pressures. **Gidroliz. i Lesokhim. Prom.**, 10: 10.

Chamba, J.-F. and Irlinger, F. (2004) "Secondary and adjunct cultures". In Fox, P.F.; McSweeney, P.L.H.; Cogan, T.M. & Guinee, T.P. (Eds.) **Cheese - Chemistry, Physics and Microbiology**. 3rd ed. [online]. Elsevier. pp. 191-206. Available from: <http://app.knovel.com/hotlink/toc/id:kpCCPME001/cheese-chemistry-physics/cheese-chemistry-physics>. [Accessed 07 August 2014].

Chang, C.M.J., Chiu, K.L. and Day, C.Y. (1998) A new apparatus for the determination of *P*-*x*-*y* diagrams and Henry's constants in high pressure alcohols with critical carbon dioxide. **Journal of Supercritical Fluids**, 12 (3): 223-237.

Chang, W., Guan, G., Li, X., et al. (2005) Isobaric vapor–liquid equilibria for water + acetic acid + (*n*-pentyl acetate or isopropyl acetate). **Journal of Chemical and Engineering Data**, 50 (4): 1129-1133.

Chapman, W.G., Gubbins, K.E., Jackson, G., et al. (1989) SAFT: Equation of state solution model for associating fluids. **Fluid Phase Equilibria**, 52: 31-38.

Chapman, W.G., Gubbins, K.E., Jackson, G., et al. (1990) New reference equation of state for associating liquids. **Industrial and Engineering Chemistry Research**, 29 (8): 1709-1721.

Chapman, W.G., Jackson, G. and Gubbins, K.E. (1988) Phase equilibria of associating fluids. Chain molecules with multiple bonding sites. **Molecular Physics**, 65 (5): 1057-1079.

Chaput, J.-P., Jensen, M.G., Thivierge, M.C., et al. (2011) "Metabolic effects of propionic acid-enriched breads". In Preedy, V.R.; Watson, R.R. & Patel, V.B. (Eds.) **Flour and Breads and their Fortification in Health and Disease Prevention**. [online]. Elsevier. pp. 475-484. Available from: <http://app.knovel.com/hotlink/toc/id:kpFBFHDP03/flour-breads-their-fortification/flour-breads-their-fortification>. [Accessed 07 August 2014].



Chemical Processing (2014). **Eastman Chemical expands capacity of carboxylic acids production in Texas and Tennessee** [online]. Available from: <http://www.chemicalprocessing.com/vendor-news/2014/eastman-chemical-expands-capacity-of-carboxylic-acids-production-in-texas-and-tennessee/> 02 March 2014 Chemical Processing [Accessed 01 August 2014].

Chen, B. and Siepmann, J.I. (2000) A novel Monte Carlo algorithm for simulating strongly associating fluids: Applications to water, hydrogen fluoride, and acetic acid. **Journal of Physical Chemistry B**, 104 (36): 8725-8734.

Chen, S.S. and Kreglewski, A. (1977) Applications of the augmented van der Waals theory of fluids. I. Pure fluids. **Berichte der Bunsengesellschaft für physikalische Chemie**, 81 (10): 1048-1052.

Chen, Y., Afef, A., Fabrice, M., et al. (2012) Thermodynamic modeling of mixtures containing carboxylic acids using the PC-SAFT equation of state. **Industrial and Engineering Chemistry Research**, 51 (42): 13846-13852.

Cheung, H., Tanke, R.S. and Torrence, G.P. (2011) "Acetic acid". **Ullmann's Encyclopedia of Industrial Chemistry**. [online]. Wiley-VCH. pp. 209-237. http://dx.doi.org/10.1002/14356007.a01_045.pub2. [Accessed 30 July 2014].

Child, W.C. and Hay, A.J. (1964) The thermodynamics of the thermal decomposition of acetic acid in vapor phase. **Journal of the American Chemical Society**, 86 (2): 182-187.

Chiti, F., Bakalis, S., Bujalski, W., et al. (2011) Using positron emission particle tracking (PEPT) to study the turbulent flow in a baffled vessel agitated by a Rushton turbine: Improving data treatment and validation. **Chemical Engineering Research and Design**, 89 (10): 1947-1960.

Chiusoli, G.P. and Maitlis, P.M. (2006) "Metal-catalysis in industrial organic processes". [online]. Royal Society of Chemistry. pp. 119-120. <http://app.knovel.com/hotlink/toc/id:kpMCIOP001/metal-catalysis-in-industrial/metal-catalysis-in-industrial>. [Accessed July 2014].

Clague, A.D.H. and Bernstein, H.J. (1969) The heat of dimerization of some carboxylic acids in the vapour phase determined by a spectroscopic method. **Spectrochimica Acta Part A: Molecular Spectroscopy**, 25 (3): 593-596.

Clegg, B. (2014) **Vinegar** [podcast]. Chemistry in its element: compounds. Royal Society of Chemistry.



References

<http://www.rsc.org/chemistryworld/podcast/CIEcompounds/transcripts/vinegar.asp>. [Accessed 30 July 2014].

Companies and Markets.com (2013). **Acetic acid global market to 2020** [online]. Available from: <http://www.companiesandmarkets.com/Market/Chemicals/Market-Research/Acetic-Acid-Global-Market-to-2020/RPT1134064?aCode=b665b089-afc2-4102-9abd-a47c38e3ae3c> [Accessed 30 July 2014].

Conti, J.J., Othmer, D.F. and Gilmont, R. (1960) Composition of vapors from boiling binary solutions. Systems containing formic acid, acetic acid, water, and chloroform. **Journal of Chemical and Engineering Data**, 5 (3): 301-307.

Cornell, L.W. and Montonna, R.E. (1933) Studies in distillation. II. Liquid–vapor equilibria in the systems ethanol–water, methanol–water, and acetic acid–water. **Industrial and Engineering Chemistry**, 25: 1331-1335.

Costa, G.M.N., Kislansky, S., Oliveira, L.C., et al. (2011) Modeling of solid–liquid equilibria for polyethylene and polypropylene solutions with equations of state. **Journal of Applied Polymer Science**, 121 (3): 1832-1849.

Creek, J.L., Knobler, C.M. and Scott, R.L. (1981) Tricritical phenomena in "quasibinary" mixtures of hydrocarbons. I. Methane systems. **The Journal of Chemical Physics**, 74 (6): 3489-3499.

Crupi, V., Magazu, S., Maisano, G., et al. (1996) Hydrogen bonding and the ultrafast time response in carboxylic acids. **Journal of Molecular Structure**, 381 (1-3): 219-226.

Cruz, J.L. and Renon, H. (1979) Nonideality in weak binary electrolytic solutions. Vapor–liquid equilibrium data and discussion of the system water–acetic acid. **Industrial and Engineering Chemistry Fundamentals**, 18 (2): 168-174.

D'Amico, F., Bencivenga, F., Gessini, A., et al. (2010) Temperature dependence of hydrogen-bond dynamics in acetic acid–water solutions. **Journal of Physical Chemistry B**, 114 (32): 10628-10633.

Dakshinamurty, P., Rao, G.J. and Rao, C.V. (1961) Vapor–liquid equilibrium in the system water + propionic acid system. **Journal of Applied Chemistry**, 11: 226.



Davidson, P.M., Taylor, T.M. and Schmidt, S.E. (2013) "Chemical preservatives and natural antimicrobial compounds". In Doyle, M.P. & Buchanan, R.L. (Eds.) **Food Microbiology - Fundamentals and Frontiers**. 4th ed. [online]. American Society for Microbiology (ASM). pp. 765-781. Available from: Knovel. <http://app.knovel.com/hotlink/toc/id:kpFMFFE001/food-microbiology-fundamentals/food-microbiology-fundamentals>. [Accessed 07 August 2014].

De Villiers, A.J., Schwarz, C.E. and Burger, A.J. (2011) Extension of the CPA equation of state with dipolar theories to improve vapour–liquid-equilibria predictions. **Fluid Phase Equilibria**, 312: 66-78.

De Villiers, A.J., Schwarz, C.E., Chobanov, K.G., et al. (2014) Application of sPC-SAFT-JC and sPC-SAFT-GV to phase equilibria predictions of alkane/alcohol, alcohol/alcohol, and water/alcohol binary systems. **Industrial and Engineering Chemistry Research**, 53 (14): 6065-6075.

Deak, A., Victorov, A.I. and de Loos, T.W. (1995) High pressure VLE in alkanol + alkane mixtures. Experimental results for *n*-butane + ethanol, + 1-propanol, + 1-butanol systems and calculations with three EOS methods. **Fluid Phase Equilibria**, 107 (2): 277-301.

Deiters, U.K. and Schneider, G.M. (1986) High pressure phase equilibria: Experimental methods. **Fluid Phase Equilibria**, 29: 145-160.

Demirbas, A. (2009a) Biorefineries: Current activities and future developments. **Energy Conversion and Management**, 50: 2782-2801.

Demirbas, A. (2011) Competitive liquid biofuels from biomass. **Applied Energy**, 88 (1): 17-28.

Demirbas, M.F. (2009b) Biorefineries for biofuel upgrading: A critical review. **Applied Energy**, 86: S151-S161.

Derawi, S.O., Zeuthen, J., Michelsen, M.L., et al. (2004) Application of the CPA equation of state to organic acids. **Fluid Phase Equilibria**, 225: 107-113.

Diamantonis, N.I. and Economou, I.G. (2011) Evaluation of statistical associating fluid theory (SAFT) and perturbed chain-SAFT equations of state for the calculation of thermodynamic derivative properties of fluids related to carbon capture and sequestration. **Energy & Fuels**, 25 (7): 3334-3343.

DiAndreth, J.R. (1985) **Multiphase behavior in ternary fluid mixtures**. PhD Thesis, University of Delaware, Delaware, USA



References

DiAndreth, J.R. and Paulaitis, M.E. (1987) An experimental study of three- and four-phase equilibria for isopropanol–water–carbon dioxide mixtures at elevated pressures. **Fluid Phase Equilibria**, 32 (3): 261-271.

DiAndreth, J.R. and Paulaitis, M.E. (1989) Multiphase behavior in ternary fluid mixtures: A case study of the isopropanol–water–CO₂ system at elevated pressures. **Chemical Engineering Science**, 44 (5): 1061-1069.

DiAndreth, J.R., Ritter, J.M. and Paulaitis, M.E. (1987) Experimental technique for determining mixture compositions and molar volumes of three or more equilibrium phases at elevated pressures. **Industrial and Engineering Chemistry Research**, 26 (2): 337-343.

DIPPR (2012) **801 database. Data compilation of pure compound properties.** AIChE.

Dohrn, R., Peper, S. and Fonseca, J.M.S. (2010) High-pressure fluid-phase equilibria: Experimental methods and systems investigated (2000-2004). **Fluid Phase Equilibria**, 288 (1-2): 1-54.

Dominik, A., Chapman, W.G., Kleiner, M., et al. (2005) Modeling of polar systems with the perturbed-chain SAFT equation of state. Investigation of the performance of two polar terms. **Industrial and Engineering Chemistry Research**, 44 (17): 6928-6938.

Doolan, K.R., Mackie, J.C. and Reid, C.R. (1986) High temperature kinetics of the thermal decomposition of the lower alkanolic acids. **International Journal of Chemical Kinetics**, 18 (5): 575-596.

Dutta, K., Daverey, A. and Lin, J.-G. (2014) Evolution retrospective for alternative fuels: First to fourth generation. **Renewable Energy**, 69: 114-122.

Ebner, H., Sellmer, S. and Follmann, H. (1996) "Acetic acid". In Rehm, H.-J. & Reed, G. (Eds.) **Biotechnology set**. 2nd ed. Weinheim, Germany: VCH Verlagsgesellschaft. pp. 381-401.

Economou, I.G. (2002) Statistical associating fluid theory: A successful model for the calculation of thermodynamic and phase equilibrium properties of complex fluid mixtures. **Industrial and Engineering Chemistry Research**, 41 (5): 953-962.



Economou, I.G. (2010) "Cubic and generalized van der Waals equations of state". In Goodwin, A.R.H.; Sengers, J.V. & Peters, C.J. (Eds.) **Applied thermodynamics of fluids**. Royal Society of Chemistry.

Elliott Jr, J.R., Jayaraman Suresh, S. and Donohue, M.D. (1990) Simple equation of state for nonspherical and associating molecules. **Industrial and Engineering Chemistry Research**, 29 (7): 1476-1485.

Elliott, J.R. and Lira, C.T. (2012) **Introductory chemical engineering thermodynamics**. 2nd ed. USA: Pearson.

Ellis, S.R.M. and Bahari, E.P. (1956) Vapor-liquid equilibrium at low concentrations; acetic acid-water; nitric acid-water. **British Chemical Engineering**, 1: 210-211.

Ermolaev, M.I., Kapitanov, V.F. and Nesterova, A.K. (1972) H₂O-HCOOH, H₂O-CH₃COOH systems. **Zhurnal Fizicheskoi Khimii**, 46 (3): 808.

Fan, X., Parker, D.J. and Smith, M.D. (2006a) Enhancing ¹⁸F uptake in a single particle for positron emission particle tracking through modification of solid surface chemistry. **Nuclear Instruments and Methods in Physics Research Section A: Accelerators, Spectrometers, Detectors and Associated Equipment**, 558 (2): 542-546.

Fan, X., Parker, D.J. and Smith, M.D. (2006b) Labelling a single particle for positron emission particle tracking using direct activation and ion-exchange techniques. **Nuclear Instruments and Methods in Physics Research Section A: Accelerators, Spectrometers, Detectors and Associated Equipment**, 562 (1): 345-350.

Fineberg, H. (1979) Synthetic fatty acids. **Journal of the American Oil Chemists Society**, 56: 805A-809A.

Folas, G.K. (2006) **Modeling of complex mixtures containing hydrogen bonding molecules**. PhD Thesis, Technical University of Denmark, Lyngby, Denmark

Fonseca, J.M.S., Dohrn, R. and Peper, S. (2011) High-pressure fluid-phase equilibria: Experimental methods and systems investigated (2005-2008). **Fluid Phase Equilibria**, 300 (1-2): 1-69.



References

Fontalba, F., Richon, D. and Renon, H. (1984) Simultaneous determination of vapor–liquid equilibria and saturated densities up to 45 MPa and 433 K. **Review of Scientific Instruments**, 55 (6): 944-951.

Forte, E., Galindo, A. and Trusler, J.P.M. (2011) Experimental and molecular modeling study of the three-phase behavior of (*n*-decane + carbon dioxide + water) at reservoir conditions. **Journal of Physical Chemistry B**, 115 (49): 14591-14609.

Forte, E., Galindo, A. and Trusler, J.P.M. (2013) Experimental and molecular modelling study of the three-phase behaviour of (propane + carbon dioxide + water) at reservoir conditions. **Journal of Supercritical Fluids**, 75: 30-42.

Freeman, J.R. and Wilson, G.M. (1985a) "High temperature PVT properties of acetic acid/water mixtures". In Benson, M.S. & Zudkevitch, D. (Eds.) **AIChE symposium series 244**. New York: American Institute of Chemical Engineers. pp. 1-13.

Freeman, J.R. and Wilson, G.M. (1985b) "High temperature vapor–liquid equilibrium measurements on acetic acid/water mixtures". In Benson, M.S. & Zudkevitch, D. (Eds.) **AIChE symposium series 244**. New York: American Institute of Chemical Engineers. pp. 14-25.

Garner, F.H., Ellis, S.R.M. and Pearce, C.J. (1954) Extraction of acetic acid from water. 3. Binary vapour–liquid equilibrium data. **Chemical Engineering Science**, 3 (2): 48-54.

Garverick, L. (1994) **Corrosion in the petrochemical industry**. [online]. ASM International. <http://app.knovel.com/hotlink/toc/id:kpCPI00002/corrosion-in-petrochemical>. [Accessed January 2013].

Garwin, L. and Haddad, P.O. (1953) Dimethylaniline as an aid in acetic acid–water separation. **Industrial and Engineering Chemistry**, 45 (7): 1558-1562.

Genin, F., Quiles, F. and Burneau, A. (2001) Infrared and Raman spectroscopic study of carboxylic acids in heavy water. **Physical Chemistry Chemical Physics**, 3 (6): 932-942.

Giacalone, A., Accascina, F. and Carnesi, G. (1942) Surface activity VIII. Surface activity and vapor pressure of aqueous solutions of aliphatic acids. **Gazzetta Chimica Italiana**, 72: 109.



Gil-Villegas, A., Galindo, A., Whitehead, P.J., et al. (1997) Statistical associating fluid theory for chain molecules with attractive potentials of variable range. **Journal of Chemical Physics**, 106 (10): 4168-4186.

Gilmont, R. and Othmer, D.F. (1944) Composition of vapors from boiling binary solutions. Water–acetic acid system at atmospheric and subatmospheric pressures. **Industrial and Engineering Chemistry**, 36: 1061-1064.

Gmehling, J. and Onken, U. (1977) **Vapor–liquid equilibrium data collection: Aqueous–organic systems**. Chemistry data series. Vol. 1. Part 1. Frankfurt, Germany: DECHEMA.

Goodwin, A.K. and Rorrer, G.L. (2010) Reaction rates for supercritical water gasification of xylose in a micro-tubular reactor. **Chemical Engineering Journal**, 163 (1-2): 10-21.

Goodwin, A.R.H. and Sandler, S.I. (2010) "Mixing and combining rules". In Goodwin, A.R.H.; Sengers, J.V. & Peters, C.J. (Eds.) **Applied thermodynamics of fluids**. Royal Society of Chemistry.

Grand View Research (2014) Market Research and Consulting. **Acetic acid market analysis and segment forecasts to 2020** [online]. Available from: <http://www.grandviewresearch.com/industry-analysis/acetic-acid-market> [Accessed 7 August 2014].

Gray, R.D. (1979) "Industrial experience in applying the Redlich-Kwong equation to vapor–liquid equilibria". In Kwang Chu, C. & Robert, L.R. (Eds.) **Equations of state in engineering and research**. Advances in chemistry. 182. Washington, D.C.: American Chemical Society. pp. 253-270.

Grenner, A., Schmelzer, J., von Solms, N., et al. (2006) Comparison of two association models (Elliott–Suresh–Donohue and simplified PC-SAFT) for complex phase equilibria of hydrocarbon–water and amine-containing mixtures. **Industrial and Engineering Chemistry Research**, 45 (24): 8170-8179.

Gros, H.P., Bottini, S. and Brignole, E.A. (1996) A group contribution equation of state for associating mixtures. **Fluid Phase Equilibria**, 116: 537-544.

Gross, J. (2005) An equation-of-state contribution for polar components: Quadrupolar molecules. **AIChE Journal**, 51 (9): 2556-2568.



References

Gross, J. and Sadowski, G. (2000) Application of perturbation theory to a hard-chain reference fluid: An equation of state for square-well chains. **Fluid Phase Equilibria**, 168 (2): 183-199.

Gross, J. and Sadowski, G. (2001) Perturbed-chain SAFT: An equation of state based on a perturbation theory for chain molecules. **Industrial and Engineering Chemistry Research**, 40 (4): 1244-1260.

Gross, J. and Sadowski, G. (2002) Application of the perturbed-chain SAFT equation of state to associating systems. **Industrial and Engineering Chemistry Research**, 41 (22): 5510-5515.

Gross, J. and Vrabec, J. (2006) An equation-of-state contribution for polar components: Dipolar molecules. **AIChE Journal**, 52 (3): 1194-1204.

Guida, A., Nienow, A.W. and Barigou, M. (2010) PEPT measurements of solid-liquid flow field and spatial phase distribution in concentrated monodisperse stirred suspensions. **Chemical Engineering Science**, 65 (6): 1905-1914.

Guida, A., Nienow, A.W. and Barigou, M. (2011) Mixing of dense binary suspensions: Multi-component hydrodynamics and spatial phase distribution by PEPT. **AIChE Journal**, 57 (9): 2302-2315.

Guilbot, P., Valtz, A., Legendre, H., et al. (2000) Rapid on-line sampler-injector: A reliable tool for HT-HP sampling and on-line GC analysis. **Analusis**, 28 (5): 426-431.

GUM (2008) "Evaluation of measurement data: Guide to the expression of uncertainty in measurement". JCGM 100:2008 (GUM 1995 with minor corrections). <http://www.bipm.org/en/publications/guides/gum.html>.

Gutiérrez, L.E. and Luks, K.D. (2003) Effect of cosolvents on solute separability between liquid phases in liquid-liquid-vapor ternary mixtures. **Fluid Phase Equilibria**, 205 (1): 89-102.

Haddad, P.O. and Edmister, W.C. (1972) Phase equilibria in acetic acid-diethylketone-water system. **Journal of Chemical and Engineering Data**, 17 (3): 275-278.

Hayden, J.G. and O'Connell, J.P. (1975) A generalized method for predicting second virial coefficients. **Industrial and Engineering Chemistry Process Design and Development**, 14 (3): 209-216.



Heintz, A., Dolch, E. and Lichtenthaler, R.N. (1986) New experimental VLE-data for alkanol/alkane mixtures and their description by an extended real association (ERAS) model. **Fluid Phase Equilibria**, 27: 61-79.

Heisler, I.A., Mazur, K., Yamaguchi, S., et al. (2011) Measuring acetic acid dimer modes by ultrafast time-domain Raman spectroscopy. **Physical Chemistry Chemical Physics**, 13 (34): 15573-15579.

Henderson, D. (1979) "Practical calculations of the equation of state of fluids and fluid mixtures using perturbation theory and related theories". In Kwang Chu, C. & Robert, L.R. (Eds.) **Equations of state in engineering and research**. Advances in chemistry. 182. Washington, D.C.: American Chemical Society. pp. 1-30.

Hinshelwood, C.N. and Topley, B. (1923) The energy of activation in heterogeneous gas reactions with relation to the thermal decomposition of formic acid vapour. **Journal of the Chemical Society**, 123: 1014-1025.

Houzelle, C., Legret, D., Richon, D., et al. (1983) Vapour-liquid equilibria of corrosive components using a dynamic method: A new flow apparatus. **Fluid Phase Equilibria**, 11 (2): 179-185.

Huang, S.H. and Radosz, M. (1990) Equation of state for small, large, polydisperse, and associating molecules. **Industrial and Engineering Chemistry Research**, 29 (11): 2284-2294.

Huang, S.H. and Radosz, M. (1991) Equation of state for small, large, polydisperse, and associating molecules: Extension to fluid mixtures. **Industrial and Engineering Chemistry Research**, 30 (8): 1994-2005.

Huang, S.H. and Radosz, M. (1993) Equation of state for small, large, polydisperse, and associating molecules: Extension to fluid mixtures. [erratum]. **Industrial and Engineering Chemistry Research**, 32 (4): 762-762.

Huang, Z., Chiew, Y.C., Feng, M., et al. (2007) Modeling aspirin and naproxen ternary solubility in supercritical CO₂/alcohol with a new Peng-Robinson EOS plus association model. **Journal of Supercritical Fluids**, 43 (2): 259-266.

ICIS (2000). **Celanese to stop acetic acid output in Mexico** [online]. Available from: <http://www.icis.com/Articles/2000/05/01/117074/celanese-to-stop-acetic-acid-output-in-mexico.html> 01 May 2000 [Accessed 31 July 2014].



References

IHS (2013). **Propionic acid** [online]. Available from: <http://www.ihs.com/products/chemical/planning/ceh/propionic-acid.aspx> March 2013 [Accessed 08 August 2014].

Ikonomou, G.D. and Donohue, M.D. (1986) Thermodynamics of hydrogen-bonded molecules: The associated perturbed anisotropic chain theory. **AIChE Journal**, 32 (10): 1716-1725.

Ishibashi, M., Sigematsu, T., Yamamoto, Y., et al. (1956) Ultraviolet spectrophotometric determination of iron. **Bulletin of the Chemical Society of Japan**, 29 (1): 57-60.

Ishibashi, M., Sigematsu, T., Yamamoto, Y., et al. (1957) Ultraviolet spectrophotometric determination of iron (III) as acetato-complex. **Bulletin of the Institute for Chemical Research, Kyoto University**, 35 (1-2): 10.

Israelachvili, J.N. (2011) **Intermolecular and surface forces**. 3rd ed. USA: Elsevier.

Ito, T. and Yoshida, F. (1963) Vapor-liquid equilibria of water-lower fatty acid systems: Water-formic acid, water-acetic acid and water-propionic acid. **Journal of Chemical and Engineering Data**, 8 (3): 315-320.

Janecek, J. and Paricaud, P. (2012) Influence of cyclic dimer formation on the phase behavior of carboxylic acids. **Journal of Physical Chemistry B**, 116 (27): 7874-7882.

Janecek, J. and Paricaud, P. (2013) Influence of cyclic dimer formation on the phase behavior of carboxylic acids. II. Cross-associating systems. **Journal of Physical Chemistry B**, 117 (32): 9430-9438.

Jog, P.K. and Chapman, W.G. (1999) Application of Wertheim's thermodynamic perturbation theory to dipolar hard sphere chains. **Molecular Physics**, 97 (3): 307-319.

Jog, P.K., Sauer, S.G., Blaesing, J., et al. (2001) Application of dipolar chain theory to the phase behavior of polar fluids and mixtures. **Industrial and Engineering Chemistry Research**, 40 (21): 4641-4648.

Johnson, A.I., Furter, W.F. and Barry, T.W. (1954) A phase equilibrium study of the system *n*-octane-water-propionic acid. **Canadian Journal of Technology**, 32 (5): 179-186.



Johnson, R.W. and Daniels, R.W. (2000) "Carboxylic acids, manufacture". **Kirk-Othmer Encyclopedia of Chemical Technology**. [online]. John Wiley & Sons, Inc. <http://dx.doi.org/10.1002/0471238961.1301142110150814.a01>. [Accessed 07 August 2014].

Justo-García, D.N., García-Sánchez, F., Díaz-Ramírez, N.L., et al. (2010) Modeling of three-phase vapor–liquid–liquid equilibria for a natural-gas system rich in nitrogen with the SRK and PC-SAFT EoS. **Fluid Phase Equilibria**, 298 (1): 92-96.

Karakatsani, E.K. and Economou, I.G. (2006) Perturbed chain-statistical associating fluid theory extended to dipolar and quadrupolar molecular fluids. **Journal of Physical Chemistry B**, 110 (18): 9252-9261.

Karakatsani, E.K. and Economou, I.G. (2007) Phase equilibrium calculations for multi-component polar fluid mixtures with tPC-PSAFT. **Fluid Phase Equilibria**, 261 (1-2): 265-271.

Karakatsani, E.K., Kontogeorgis, G.M. and Economou, I.G. (2006) Evaluation of the truncated perturbed chain-polar statistical associating fluid theory for complex mixture fluid phase equilibria. **Industrial and Engineering Chemistry Research**, 45 (17): 6063-6074.

Karakatsani, E.K., Spyriouni, T. and Economou, I.G. (2005) Extended statistical associating fluid theory (SAFT) equations of state for dipolar fluids. **AIChE Journal**, 51 (8): 2328-2342.

Keyes, D.B. (1933) Liquid–vapor composition curves of acetic acid and water at subatmospheric pressures. **Industrial and Engineering Chemistry**, 25: 569-569.

Kim, C.-H., Vimalchand, P., Donohue, M.D., et al. (1986) Local composition model for chainlike molecules: A new simplified version of the perturbed hard chain theory. **AIChE Journal**, 32 (10): 1726-1734.

Kleiner, M. (2008) **Thermodynamic modeling of complex systems: Polar and associating fluids and mixtures**. Doctoral Dissertation, Dortmund University of Technology, Dortmund, Germany

Kleiner, M. and Gross, J. (2006) An equation of state contribution for polar components: Polarizable dipoles. **AIChE Journal**, 52 (5): 1951-1961.



Kleiner, M. and Sadowski, G. (2007) Modeling of polar systems using PCP-SAFT: An approach to account for induced-association interactions. **Journal of Physical Chemistry C**, 111 (43): 15544-15553.

Klingler, D. and Vogel, H. (2010) Influence of process parameters on the hydrothermal decomposition and oxidation of glucose in sub- and supercritical water. **Journal of Supercritical Fluids**, 55 (1): 259-270.

Knobler, C.M. and Scott, R.L. (1980) Indirect determination of concentrations in coexisting phases. **Journal of Chemical Physics**, 73 (10): 5390-5391.

Knopp, J.A., Linnell, W.S. and Child, W.C. (1962) The thermodynamics of the thermal decomposition of acetic acid in the liquid phase. **Journal of Physical Chemistry**, 66 (8): 1513-1516.

Kontogeorgis, G.M. (2013) Association theories for complex thermodynamics. **Chemical Engineering Research and Design**, 91 (10): 1840-1858.

Kontogeorgis, G.M. and Folas, G.K. (2010) **Thermodynamic models for industrial applications**. West Sussex, United Kingdom: John Wiley and Sons.

Kontogeorgis, G.M., Folas, G.K., Muro-Suñé, N., et al. (2007) Modelling of associating mixtures for applications in the oil & gas and chemical industries. **Fluid Phase Equilibria**, 261 (1-2): 205-211.

Kontogeorgis, G.M., Michelsen, M.L., Folas, G.K., et al. (2006a) Ten years with the CPA (cubic-plus-association) equation of state. Part 1. Pure compounds and self-associating systems. **Industrial and Engineering Chemistry Research**, 45 (14): 4855-4868.

Kontogeorgis, G.M., Michelsen, M.L., Folas, G.K., et al. (2006b) Ten years with the CPA (cubic-plus-association) equation of state. Part 2. Cross-associating and multicomponent systems. **Industrial and Engineering Chemistry Research**, 45 (14): 4869-4878.

Kontogeorgis, G.M., Tsvintzelis, I., von Solms, N., et al. (2010) Use of monomer fraction data in the parametrization of association theories. **Fluid Phase Equilibria**, 296 (2): 219-229.



Kontogeorgis, G.M., V. Yakoumis, I., Meijer, H., et al. (1999) Multicomponent phase equilibrium calculations for water–methanol–alkane mixtures. **Fluid Phase Equilibria**, 158–160: 201-209.

Kontogeorgis, G.M., Voutsas, E.C., Yakoumis, I.V., et al. (1996) An equation of state for associating fluids. **Industrial and Engineering Chemistry Research**, 35 (11): 4310-4318.

Korden, S., Van Nhu, N., Vrabec, J., et al. (2012) On the treatment of electrostatic interactions of non-spherical molecules in equation of state models. **Soft Materials**, 10 (1-3): 81-105.

Kouskoumvekaki, I.A., Krooshof, G.J.P., Michelsen, M.L., et al. (2004a) Application of the simplified PC-SAFT equation of state to the vapor–liquid equilibria of binary and ternary mixtures of polyamide 6 with several solvents. **Industrial and Engineering Chemistry Research**, 43 (3): 826-834.

Kouskoumvekaki, I.A., Von Solms, N., Lindvig, T., et al. (2004b) Novel method for estimating pure-component parameters for polymers: Application to the PC-SAFT equation of state. **Industrial and Engineering Chemistry Research**, 43 (11): 2830-2838.

Kraska, T. (1998) Analytic and fast numerical solutions and approximations for cross-association models within statistical association fluid theory. **Industrial and Engineering Chemistry Research**, 37 (12): 4889-4892.

Kraska, T. and Gubbins, K.E. (1996a) Phase equilibria calculations with a modified SAFT equation of state. 1. Pure alkanes, alkanols, and water. **Industrial and Engineering Chemistry Research**, 35 (12): 4727-4737.

Kraska, T. and Gubbins, K.E. (1996b) Phase equilibria calculations with a modified SAFT equation of state. 2. Binary mixtures of *n*-alkanes, 1-alkanols, and water. **Industrial and Engineering Chemistry Research**, 35 (12): 4738-4746.

Kushner, T.M., Tatsievskaya, G.I., Irzun, V.A., et al. (1966) Liquid–vapour phase equilibrium in the system water–formic acid–acetic acid at 50 and 200 mmHg. **Zhurnal Fizicheskoi Khimii**, 40 (12): 3010-3017.

Kushner, T.M., Tatsievskaya, G.I. and Serafimov, L.A. (1967) Liquid–vapor phase equilibrium in the water–formic acid–propionic acid system under atmospheric pressure. **Zhurnal Fizicheskoi Khimii**, 41: 237.



References

Laugier, S., Richon, D. and Renon, H. (1990) Simultaneous determination of vapor–liquid equilibria and volumetric properties of ternary systems with a new experimental apparatus. **Fluid Phase Equilibria**, 54: 19-34.

Lazeeva, M.S. and Markuzin, N.P. (1973) Experimental data on equilibrium between phases and chemical equilibrium in vapor in acetic acid–water system at 20, 40 and 80 °C. **Zhurnal Prikladnoi Khimii**, 46 (2): 360-363.

Leadbeater, T.W. and Parker, D.J. (2011) A modular positron camera for the study of industrial processes. **Nuclear Instruments and Methods in Physics Research Section A: Accelerators, Spectrometers, Detectors and Associated Equipment**, 652 (1): 646-649.

Leadbeater, T.W., Parker, D.J. and Gargiuli, J. (2012) Positron imaging systems for studying particulate, granular and multiphase flows. **Particuology**, 10 (2): 146-153.

Lee, H. (2014) ICIS Chemical Business. **Asia acetic acid to track firmer feed** [online]. Available from: EBSCOhost <http://search.ebscohost.com/login.aspx?direct=true&db=buh&AN=93880143&site=e-host-live> Reed Business Information Limited [Accessed August 2014].

Leeke, G.A., Santos, R. and King, M.B. (2001) Vapor–liquid equilibria for the carbon dioxide + carvacrol system at elevated pressures. **Journal of Chemical and Engineering Data**, 46 (3): 541-545.

Leekumjorn, S. and Krejbjerg, K. (2013) Phase behavior of reservoir fluids: Comparisons of PC-SAFT and cubic EOS simulations. **Fluid Phase Equilibria**, 359: 17-23.

Leonhard, K., Van Nhu, N. and Lucas, K. (2007a) Making equation of state models predictive. Part 2: An improved PCP-SAFT equation of state. **Fluid Phase Equilibria**, 258 (1): 41-50.

Leonhard, K., Van Nhu, N. and Lucas, K. (2007b) Making equation of state models predictive. Part 3: Improved treatment of multipolar interactions in a PC-SAFT based equation of state. **Journal of Physical Chemistry C**, 111 (43): 15533-15543.

Liang, X., Tsivintzelis, I. and Kontogeorgis, G.M. (2014a) Modeling water containing systems with the simplified PC-SAFT and CPA equations of state. **Industrial and Engineering Chemistry Research**, 53 (37): 14493-14507.



Liang, X., Yan, W., Thomsen, K., et al. (2014b) On petroleum fluid characterization with the PC-SAFT equation of state. **Fluid Phase Equilibria**, 375: 254-268.

Linek, J. and Wichterle, I. (1974) Liquid–vapor-equilibrium. 67. Liquid–vapor-equilibrium in ternary isopropyl acetate–water–acetic acid and isopropyl acetate–water–acrylic acid systems at 200 torr. **Collection of Czechoslovak Chemical Communications**, 39 (12): 3395-3402.

Lumbroso-Bader, N., Coupry, C., Baron, D., et al. (1975) Dimerization of carboxylic acids: A vapor phase NMR study. **Journal of Magnetic Resonance**, 17 (3): 386-392.

Mackie, J.C. and Doolan, K.R. (1984) High temperature kinetics of thermal decomposition of acetic acid and its products. **International Journal of Chemical Kinetics**, 16 (5): 525-541.

Maity, S.K. (2012) Correlation of solubility of single gases/hydrocarbons in polyethylene using PC-SAFT. **Asia-Pacific Journal of Chemical Engineering**, 7 (3): 406-417.

Marcilla, A., Olaya, M.D., Serrano, M.D., et al. (2013) Pitfalls in the evaluation of the thermodynamic consistency of experimental VLE data sets. **Industrial and Engineering Chemistry Research**, 52 (36): 13198-13208.

Marek, J. (1956) Vapor–liquid equilibria in mixtures containing an associating substance. 3. Binary and ternary systems of water, acetic acid and acetic anhydride at 400 mmHg. **Collection of Czechoslovak Chemical Communications**, 21 (2): 269-280.

Markets and Markets (2013). **Propionic acid and derivatives market by applications (animal feed & grain preservatives, food preservatives, herbicides, cellulose acetate propionate) & geography – global trends & forecasts to 2018** [online]. Available from: <http://www.marketsandmarkets.com/Market-Reports/propionic-acid-derivatives-market-1079.html> July 2013 [Accessed 09 August 2014].

McCabe, C. and Galindo, A. (2010) "SAFT associating fluids and fluid mixtures". In Goodwin, A.R.H.; Sengers, J.V. & Peters, C.J. (Eds.) **Applied thermodynamics of fluids**. Royal Society of Chemistry.

Michelsen, M.L. (1982a) The isothermal flash problem. II. Phase-split calculation. **Fluid Phase Equilibria**, 9 (1): 21-40.



Michelsen, M.L. (1982b) The isothermal flash problem. Part I. Stability. **Fluid Phase Equilibria**, 9 (1): 1-19.

Michelsen, M.L. and Mollerup, J. (2007) **Thermodynamic models: Fundamentals and computational aspects**. 2nd ed. Denmark: Tie-Line Publications.

Miyamoto, S., Nakamura, S., Iwai, Y., et al. (2001) Measurement of isothermal vapor–liquid equilibria for binary and ternary systems containing monocarboxylic acid. **Journal of Chemical and Engineering Data**, 46 (5): 1225-1230.

Moniz, P., Pereira, H., Quilhó, T., et al. (2013) Characterisation and hydrothermal processing of corn straw towards the selective fractionation of hemicelluloses. **Industrial Crops and Products**, 50: 145-153.

Muro-Suné, N., Kontogeorgis, G.M., von Solms, N., et al. (2008) Phase equilibrium modelling for mixtures with acetic acid using an association equation of state. **Industrial and Engineering Chemistry Research**, 47 (15): 5660-5668.

Naeem, S. and Sadowski, G. (2010) pePC-SAFT: Modeling of polyelectrolyte systems 1. Vapor–liquid equilibria. **Fluid Phase Equilibria**, 299 (1): 84-93.

Naeem, S. and Sadowski, G. (2011) pePC-SAFT: Modeling of polyelectrolyte systems 2. Aqueous two-phase systems. **Fluid Phase Equilibria**, 306 (1): 67-75.

Narayana, A.S., Nalk, S.C. and Rath, P. (1985) Salt effect in isobaric vapor–liquid equilibria of acetic acid–water system. **Journal of Chemical and Engineering Data**, 30 (4): 483-485.

National Renewable Energy Action Plan (2010) "National renewable energy action plan for the United Kingdom". United Kingdom.

Navarro-Espinosa, I.R., Cardona, C.A. and López, J.A. (2010) Experimental measurements of vapor–liquid equilibria at low pressure: Systems containing alcohols, esters and organic acids. **Fluid Phase Equilibria**, 287 (2): 141-145.

Nelson, L. and Engelder, J. (1926) The thermal decomposition of formic acid. **Journal of Physical Chemistry**, 30 (4): 470-475.



Nguyen-Huynh, D., de Hemptinne, J.C., Lugo, R., et al. (2011) Modeling liquid–liquid and liquid–vapor equilibria of binary systems containing water with an alkane, an aromatic hydrocarbon, an alcohol or a gas (methane, ethane, CO₂ or H₂S), using group contribution polar perturbed-chain statistical associating fluid theory. **Industrial and Engineering Chemistry Research**, 50 (12): 7467-7483.

Nguyen-Huynh, D., Passarello, J.P., Tobaly, P., et al. (2008) Application of GC-SAFT EOS to polar systems using a segment approach. **Fluid Phase Equilibria**, 264 (1-2): 62-75.

Nickol, G.B. (1979) "Vinegar". In Peppler, H.J. & Perlman, D. (Eds.) **Microbial technology. Fermentation technology**. 2nd ed. London, UK: Academic Press, Inc. pp. 155-172.

Nigam, P.S. and Singh, A. (2011) Production of liquid biofuels from renewable resources. **Progress in Energy and Combustion Science**, 37 (1): 52-68.

Niño-Amézquita, G., van Putten, D. and Enders, S. (2012) Phase equilibrium and interfacial properties of water + CO₂ mixtures. **Fluid Phase Equilibria**, 332: 40-47.

NIST (2011) "Chemistry webbook. NIST standard reference database 69". U.S. <http://webbook.nist.gov/chemistry/>.

Ocon, J., Lamela, M. and Espantoso, J. (1960) Vapor–liquid equilibrium VII: The system water + acetic acid. **Anales de la Sociedad Española de Física y Química**, B, 56: 841-846.

OECD/IEA (2012) **World energy outlook**. [online]. France: International Energy Agency. <http://www.worldenergyoutlook.org/publications/weo-2012/>. [Accessed 12 August 2014].

Olson, J.D., Morrison, R.E. and Wilson, L.C. (2008) Thermodynamics of hydrogen-bonding mixtures. 5. G^E, H^E, and TS^E and zeotropy of water + acrylic acid. **Industrial and Engineering Chemistry Research**, 47 (15): 5127-5131.

Othmer, D.F. (1943) Composition of vapors from boiling binary solutions. **Industrial and Engineering Chemistry**, 35: 614-620.



Othmer, D.F., Silvis, S.J. and Spiel, A. (1952) Composition of vapors from boiling binary solutions. Pressure equilibrium still for studying water–acetic acid system. **Industrial and Engineering Chemistry**, 44 (8): 1864-1872.

Parker, D.J., Hawkesworth, M.R., Broadbent, C.J., et al. (1994) Industrial positron-based imaging: Principles and applications. **Nuclear Instruments and Methods in Physics Research Section A: Accelerators, Spectrometers, Detectors and Associated Equipment**, 348 (2-3): 583-592.

Parker, D.J., Leadbeater, T.W., Fan, X., et al. (2009) Positron emission particle tracking using a modular positron camera. **Nuclear Instruments and Methods in Physics Research Section A: Accelerators, Spectrometers, Detectors and Associated Equipment**, 604 (1–2): 339-342.

Parr Instrument Company (2014). **Stirred reactor series** [online]. Available from: <http://www.parrinst.com/products/stirred-reactors/> [Accessed October 2014].

Partin, L.R. and Heise, W.H. (1993) "Bioderived acetic acid". In Agreda, V.H. & Zoeller, J.R. (Eds.) **Acic acid and its derivatives**. New York, USA: Marcel Dekker Inc. pp. 3-13.

Pascal, P., Dupuy, E. and Garnier, M. (1921) Study of binary and ternary mixtures found in the manufacture of synthetic acetic acid. **Bulletin de la Societe Chimique de France**, 29: 9-21.

Patience, G.S. (2013) "Measurement and analysis". In Patience, G.S. (Ed.) **Experimental methods and instrumentation for chemical engineers**. Amsterdam: Elsevier. pp. 15-66.

Peng, D.-Y. and Robinson, D.B. (1976) A new two-constant equation of state. **Industrial and Engineering Chemistry Fundamentals**, 15 (1): 59-64.

Peng, Y., Goff, K.D., dos Ramos, M.C., et al. (2009) Developing a predictive group-contribution-based SAFT-VR equation of state. **Fluid Phase Equilibria**, 277 (2): 131-144.

Peper, S. and Dohrn, R. (2012) Sampling from fluid mixtures under high pressure: Review, case study and evaluation. **The Journal of Supercritical Fluids**, 66: 2-15.

Perakis, C.A., Voutsas, E.C., Magoulas, K.G., et al. (2007) Thermodynamic modeling of the water + acetic acid + CO₂ system: The



importance of the number of association sites of water and of the nonassociation contribution for the CPA and SAFT-type models. **Industrial and Engineering Chemistry Research**, 46 (3): 932-938.

Pérez-Mohedano, R., Letzelter, N., Amador, C., et al. (2015) Positron emission particle tracking (PEPT) for the analysis of water motion in a domestic dishwasher. **Chemical Engineering Journal**, 259: 724-736.

Pfohl, O., Pagel, A. and Brunner, G. (1999) Phase equilibria in systems containing *o*-cresol, *p*-cresol, carbon dioxide, and ethanol at 323.15–473.15 K and 10–35 MPa. **Fluid Phase Equilibria**, 157 (1): 53-79.

Poling, B.E., Prausnitz, J.M. and O'Connell, J.P. (2001) **The properties of gases and liquids**. 5th ed. McGraw-Hill.

Polishuk, I. (2011a) Hybridizing SAFT and cubic EOS: What can be achieved? **Industrial and Engineering Chemistry Research**, 50 (7): 4183-4198.

Polishuk, I. (2011b) Implementation of SAFT + cubic, PC-SAFT, and Soave-Benedict-Webb-Rubin equations of state for comprehensive description of thermodynamic properties in binary and ternary mixtures of CH₄, CO₂, and *n*-C₁₆H₃₄. **Industrial and Engineering Chemistry Research**, 50 (24): 14175-14185.

Polishuk, I. (2011c) Semi-theoretical versus entirely empirical: Comparing SAFT + cubic and Soave-Benedict-Webb-Rubin (SBWR) equations of state. **Industrial and Engineering Chemistry Research**, 50 (19): 11422-11431.

PR Newswire (2013). **Propionic acid and derivatives market worth \$1,622.2 million by 2018** [online]. Available from: <http://www.prnewswire.com/news-releases/propionic-acid--derivatives-market-worth-16222-million-by-2018-217569611.html> 30 July 2013 [Accessed 09 August 2014].

Prausnitz, J.M., Lichtenthaler, R.N. and de Azevedo, E.G. (1999) "Molecular thermodynamics of fluid-phase equilibria". 3rd ed. London: Prentice-Hall International.

Privat, R., Gani, R. and Jaubert, J.-N. (2010) Are safe results obtained when the PC-SAFT equation of state is applied to ordinary pure chemicals? **Fluid Phase Equilibria**, 295 (1): 76-92.



Qiao, Y., Di, Z., Ma, Y., et al. (2010) Viscosities of pure water, acetic acid + water, and *p*-xylene + acetic acid + water at different temperature and pressure. **Chinese Journal of Chemical Engineering**, 18 (3): 446-454.

Raal, J.D. and Mühlbauer, A.L. (1998) "Phase equilibria: Measurement and computation". In Hewitt, G.F. & Tien, C.L. (Eds.) **Series in chemical and mechanical engineering**. USA: Taylor & Francis.

Rafflenbeul, L. and Hartmann, H. (1978) Eine dynamische apparatur zur bestimmung von dampf-flüssigkeits-phasengleichgewichten. **Chemie Ingenieur Technik**, 7: 145-148.

Ramalho, R.S., James, W. and Carnaham, J.F. (1964) Effect of alkaline-earth chloride on vapor-liquid equilibrium of acetic acid-water system. **Journal of Chemical and Engineering Data**, 9 (2): 215-217.

Rasmussen, H., Sorensen, H.R. and Meyer, A.S. (2014) Formation of degradation compounds from lignocellulosic biomass in the biorefinery: Sugar reaction mechanisms. **Carbohydrate Research**, 385: 45-57.

Richardson, M.J. (2003) **The development of a novel wet oxidation process for the treatment of organic industrial waste**. PhD Thesis, Victoria University of Wellington, New Zealand

Richardson, M.J., Johnston, J.H. and Northcote, P.T. (2006) NMR determination of high temperature acetic acid/water vapor phase equilibria. **AIChE Journal**, 52 (1): 422-424.

Richon, D. (2009) Experimental techniques for the determination of thermophysical properties to enhance chemical processes. **Pure and Applied Chemistry**, 81 (10): 1769-1782.

Rivenc, G. (1953) Thermodynamic study of temperature-vapor composition and of temperature-liquid composition curves for acetic acid-water at 760 mmHg. **Ind. Chim. (Paris)**, 38: 311-321.

Rivenq, F. (1961) Vapor-liquid data for the system water-propionic acid. **Bulletin de la Societe Chimique de France**, 7: 1392-1395.

Rodríguez, V., Pardo, J., López, M.C., et al. (1993) Vapor pressures of binary mixtures of hexane + 1-butanol + 2-butanol + 2-methyl-1-propanol, or + 2-methyl-2-propanol at 298.15 K. **Journal of Chemical and Engineering Data**, 38 (3): 350-352.



Román-Ramírez, L.A., García-Sánchez, F., Ortiz-Estrada, C.H., et al. (2010) Modeling of vapor–liquid equilibria for CO₂ + 1-alkanol binary systems with the PC-SAFT equation of state using polar contributions. **Industrial and Engineering Chemistry Research**, 49 (23): 12276-12283.

Rozmus, J., de Hemptinne, J.C. and Mougin, P. (2011) Application of GC-ppc-SAFT EoS to amine mixtures with a predictive approach. **Fluid Phase Equilibria**, 303 (1): 15-30.

Sadowski, G. (2011) Modeling of polymer phase equilibria using equations of state. **Polymer Thermodynamics: Liquid Polymer-Containing Mixtures**, 238: 389-418.

Sako, T., Hakuta, T. and Yoshitome, H. (1985) Vapor–liquid equilibria for single weak electrolyte aqueous solutions in dilute regions. **Journal of Chemical Engineering of Japan**, 18 (5): 420-426.

Samel, U.-R., Kohler, W., Gamer, A.O., et al. (2011) "Propionic acid and derivatives". **Ullmann's Encyclopedia of Industrial Chemistry**. [online]. Wiley-VCH. pp. 295-311. http://dx.doi.org/10.1002/14356007.a22_223.pub2. [Accessed 07 August 2014].

Sandler, S.I. (1998) **Chemical and engineering thermodynamics**. 3rd ed. USA: John Wiley & Sons.

Schäfer, E. and Sadowski, G. (2012) Liquid–liquid equilibria of systems with linear aldehydes. Experimental data and modeling with PCP-SAFT. **Industrial and Engineering Chemistry Research**, 51 (44): 14525-14534.

Schäfer, E., Sadowski, G. and Enders, S. (2014) Calculation of complex phase equilibria of DMF/alkane systems using the PCP-SAFT equation of state. **Chemical Engineering Science**, 115: 49-57.

Schaschke, C. (2014) **Dictionary of chemical engineering**. [online]. Oxford University Press. Available from: Knovel. <http://app.knovel.com/hotlink/toc/id:kpDCE00021/dictionary-chemical-engineering/dictionary-chemical-engineering>. [Accessed 15 August 2014].

Sear, R.P. and Jackson, G. (1994a) Thermodynamic perturbation-theory for association into doubly bonded dimers. **Molecular Physics**, 82 (5): 1033-1048.



Sear, R.P. and Jackson, G. (1994b) Thermodynamic perturbation theory for association into chains and rings. **Physical Review E**, 50 (1): 386-394.

Sebastiani, E. and Lacquaniti, L. (1967) Acetic acid–water system thermodynamical correlation of vapor–liquid equilibrium data. **Chemical Engineering Science**, 22 (9): 1155-1162.

Secretaría de Energía (2012) **Estrategía nacional de energía 2012-2026**. México.

Sedghi, M. and Goual, L. (2014) PC-SAFT modeling of asphaltene phase behavior in the presence of nonionic dispersants. **Fluid Phase Equilibria**, 369: 86-94.

Shiflett, M.B. and Yokozeki, A. (2006) Vapor–liquid–liquid equilibria of pentafluoroethane and ionic liquid [bmim] [PF₆] mixtures studied with the volumetric method. **Journal of Physical Chemistry B**, 110 (29): 14436-14443.

Sinag, A., Gulbay, S., Uskan, B., et al. (2010) Biomass decomposition in near critical water. **Energy Conversion and Management**, 51 (3): 612-620.

Sinag, A., Gulbay, S., Uskan, B., et al. (2009) Comparative studies of intermediates produced from hydrothermal treatments of sawdust and cellulose. **Journal of Supercritical Fluids**, 50 (2): 121-127.

Sinag, A., Kruse, A. and Rathert, J. (2004) Influence of the heating rate and the type of catalyst on the formation of key intermediates and on the generation of gases during hydrolysis of glucose in supercritical water in a batch reactor. **Industrial and Engineering Chemistry Research**, 43 (2): 502-508.

Smith, J.W. (1955) **Electric dipole moments**. London: Butterworths Scientific Publications.

Soave, G. (1972) Equilibrium constants from a modified Redlich-Kwong equation of state. **Chemical Engineering Science**, 27 (6): 1197-1203.

Soo, C.B. (2011) **Experimental thermodynamic measurements of biofuel-related associating compounds and modeling using the PC-SAFT equation of state**. Doctoral Thesis, École Nationale Supérieure des Mines de Paris, Paris, France



Specovius, J., Leiva, M.A., Scott, R.L., et al. (1981) Tricritical phenomena in "quasi-binary" mixtures of hydrocarbons. 2. Binary ethane systems. **Journal of Physical Chemistry**, 85 (16): 2313-2316.

Srokol, Z., Bouche, A.G., van Estrik, A., et al. (2004) Hydrothermal upgrading of biomass to biofuel; studies on some monosaccharide model compounds. **Carbohydrate Research**, 339 (10): 1717-1726.

Stratford, M. (2000) "Traditional preservatives - organic acids". In Robinson, R.K. (Ed.) **Encyclopedia of Food Microbiology**. [online]. Elsevier. pp. 1729-1737. Available from: Knovel. <http://app.knovel.com/hotlink/toc/id:kpEFMV0004/encyclopedia-food-microbiology/encyclopedia-food-microbiology>. [Accessed 01 August 2014].

Suresh, S.J. and Elliott, J.R. (1992) Multiphase equilibrium analysis via a generalized equation of state for associating mixtures. **Industrial and Engineering Chemistry Research**, 31 (12): 2783-2794.

Tamouza, S., Passarello, J.P., Tobaly, P., et al. (2004) Group contribution method with SAFT EOS applied to vapor-liquid equilibria of various hydrocarbon series. **Fluid Phase Equilibria**, 222-223: 67-76.

Tang, X. and Gross, J. (2010) Modeling the phase equilibria of hydrogen sulfide and carbon dioxide in mixture with hydrocarbons and water using the PCP-SAFT equation of state. **Fluid Phase Equilibria**, 293 (1): 11-21.

Tanksale, A., Beltramini, J.N. and Lu, G.M. (2010) A review of catalytic hydrogen production processes from biomass. **Renewable and Sustainable Energy Reviews**, 14 (1): 166-182.

Taylor, B.N. and Kuyatt, C.E. (1994) **Guidelines for evaluating and expressing the uncertainty of NIST measurement results, NIST technical note 1297**. Gaithersburg: National Institute of Standards and Technology.

Matlab (2013). version 2013a. The MathWorks Inc.

Tihic, A., Kontogeorgis, G.M., Von Solms, N., et al. (2008) A predictive group-contribution simplified PC-SAFT equation of state: Application to polymer systems. **Industrial and Engineering Chemistry Research**, 47 (15): 5092-5101.

Tirpanalan, Ö., Reisinger, M., Huber, F., et al. (2014) Wheat bran biorefinery: An investigation on the starch derived glucose extraction



References

accompanied by pre- and post-treatment steps. **Bioresource Technology**, 163: 295-299.

Tochigi, K. and Kojima, K. (1977) Activity coefficients at infinite dilution for binary systems containing an associating substance. For systems with one associating component in vapor phase. **Journal of Chemical Engineering of Japan**, 10 (5): 343-348.

Tsiparis, I.N. and Smorigai, N. (1964) Liquid-vapor equilibrium in the systems acetic acid-water and acetic acid-water-salt under isothermal (40 and 60 °C) and isobaric (760 mmHg) conditions. **Journal of General Chemistry USSR**, 34 (12): 3927.

Tsivintzelis, I., Bøgh, D., Karakatsani, E., et al. (2014) The role of monomer fraction data in association theories – can we improve the performance for phase equilibrium calculations? **Fluid Phase Equilibria**, 365: 112-122.

Tumakaka, F., Gross, J. and Sadowski, G. (2005) Thermodynamic modeling of complex systems using PC-SAFT. **Fluid Phase Equilibria**, 228: 89-98.

Tumakaka, F. and Sadowski, G. (2004) Application of the perturbed-chain SAFT equation of state to polar systems. **Fluid Phase Equilibria**, 217 (2): 233-239.

Tybjerg, P.C.V., Kontogeorgis, G.M., Michelsen, M.L., et al. (2010) Phase equilibria modeling of methanol-containing systems with the CPA and sPC-SAFT equations of state. **Fluid Phase Equilibria**, 288 (1-2): 128-138.

Umer, M., Albers, K., Sadowski, G., et al. (2014) PC-SAFT parameters from ab initio calculations. **Fluid Phase Equilibria**, 362: 41-50.

Valderrama, J.O. (2003) The state of the cubic equations of state. **Industrial and Engineering Chemistry Research**, 42 (8): 1603-1618.

Vankonynenburg, P.H. and Scott, R.L. (1980) Critical lines and phase equilibria in binary van der Waals mixtures. **Philosophical Transactions of the Royal Society of London. Series A. Mathematical and Physical Sciences**, 298 (1442): 495-540.

Vardon, D.R., Sharma, B.K., Scott, J., et al. (2011) Chemical properties of biocrude oil from the hydrothermal liquefaction of spirulina algae, swine manure, and digested anaerobic sludge. **Bioresource Technology**, 102 (17): 8295-8303.



Vercher, E., Vázquez, M.I. and Martínez-Andreu, A. (2001) Isobaric vapor–liquid equilibria for water + acetic acid + lithium acetate. **Journal of Chemical and Engineering Data**, 46 (6): 1584-1588.

Vimalchand, P. and Donohue, M.D. (1985) Thermodynamics of quadrupolar molecules: The perturbed-anisotropic-chain theory. **Industrial and Engineering Chemistry Fundamentals**, 24 (2): 246-257.

von Solms, N., Michelsen, M.L. and Kontogeorgis, G.M. (2003) Computational and physical performance of a modified PC-SAFT equation of state for highly asymmetric and associating mixtures. **Industrial and Engineering Chemistry Research**, 42 (5): 1098-1105.

von Solms, N., Michelsen, M.L. and Kontogeorgis, G.M. (2005) Prediction and correlation of high-pressure gas solubility in polymers with simplified PC-SAFT. **Industrial and Engineering Chemistry Research**, 44 (9): 3330-3335.

von Solms, N., Michelsen, M.L., Passos, C.P., et al. (2006) Investigating models for associating fluids using spectroscopy. **Industrial and Engineering Chemistry Research**, 45 (15): 5368-5374.

Voutsas, E.C., Pappa, G.D., Magoulas, K., et al. (2006) Vapor–liquid equilibrium modeling of alkane systems with equations of state: "Simplicity versus complexity". **Fluid Phase Equilibria**, 240 (2): 127-139.

Vrabec, J. and Gross, J. (2008) Vapor–liquid equilibria simulation and an equation of state contribution for dipole–quadrupole interactions. **Journal of Physical Chemistry B**, 112 (1): 51-60.

Wagner, F.S. (2014) "Acetic acid". **Kirk-Othmer Encyclopedia of Chemical Technology**. [online]. John Wiley & Sons, Inc. <http://dx.doi.org/10.1002/0471238961.0103052023010714.a01.pub3>. [Accessed 01 August 2014].

Wakeham, W.A. and Stateva, R.P. (2004) Numerical solution of the isothermal, isobaric phase equilibrium problem. **Reviews in Chemical Engineering**, 20 (1-2): 1-56.

Wei, Y.S. and Sadus, R.J. (2000) Equations of state for the calculation of fluid-phase equilibria. **AIChE Journal**, 46 (1): 169-196.

Wertheim, M.S. (1984a) Fluids with highly directional attractive forces. 1. Statistical thermodynamics. **Journal of Statistical Physics**, 35 (1-2): 19-34.



References

Wertheim, M.S. (1984b) Fluids with highly directional attractive forces. 2. Thermodynamic perturbation-theory and integral-equations. **Journal of Statistical Physics**, 35 (1-2): 35-47.

Wertheim, M.S. (1986a) Fluids with highly directional attractive forces. 3. Multiple attraction sites. **Journal of Statistical Physics**, 42 (3-4): 459-476.

Wertheim, M.S. (1986b) Fluids with highly directional attractive forces. 4. Equilibrium polymerization. **Journal of Statistical Physics**, 42 (3-4): 477-492.

Wichterle, I., Linek, J. and Hála, E. (1973) **Vapor–liquid equilibrium data bibliography**. Amsterdam: Elsevier.

Wichterle, I., Linek, J. and Hála, E. (1976) **Vapor–liquid equilibrium data bibliography: Supplement**. Amsterdam: Elsevier.

Wilsak, R.A., Campbell, S.W. and Thodos, G. (1987) Vapor–liquid–equilibrium measurements for the *n*-pentane–methanol system at 372.7, 397.7 and 422.6 K. **Fluid Phase Equilibria**, 33 (1-2): 157-171.

Xie, Q., Wan, H., Han, M.J., et al. (2009) Investigation on isobaric vapor–liquid equilibrium for acetic acid + water + methyl ethyl ketone + isopropyl acetate. **Fluid Phase Equilibria**, 280 (1-2): 120-128.

Xin, H., Wang, X. and Li, J.Q. (2012) Isobaric vapor–liquid equilibria for the system containing acetic acid at 101.3 kPa. **Advanced Materials Research**, 560-561: 79-85.

Xu, W.H. and Yang, J.C. (2010) Computer simulations on aggregation of acetic acid in the gas phase, liquid phase, and supercritical carbon dioxide. **Journal of Physical Chemistry A**, 114 (16): 5377-5388.

Xu, X., Cristancho, D.E., Costeux, S., et al. (2012) Density-functional theory for polymer–carbon dioxide mixtures: A perturbed-chain SAFT approach. **Journal of Chemical Physics**, 137 (5): 1-8.

Yasaka, Y., Yoshida, K., Wakai, C., et al. (2006) Kinetic and equilibrium study on formic acid decomposition in relation to the water-gas-shift reaction. **The Journal of Physical Chemistry A**, 110 (38): 11082-11090.

Yaws, C.L. (2006) **Yaws' handbook of physical properties for hydrocarbons and chemicals**. [online]. Knovel.



<http://app.knovel.com/hotlink/toc/id:kpYHPPHC0B/yaws-handbook-physical/yaws-handbook-physical>. [Accessed August 2014].

Yelash, L., Muller, M., Paul, W., et al. (2005) A global investigation of phase equilibria using the perturbed-chain statistical-associating-fluid-theory approach. **Journal of Chemical Physics**, 123 (1).

York, R. and Holmes, R.C. (1942) Vapor–liquid equilibria of the system acetane–acetic acid–water. **Industrial and Engineering Chemistry**, 34: 345-350.

Yu, J. and Savage, P.E. (1998) Decomposition of formic acid under hydrothermal conditions. **Industrial and Engineering Chemistry Research**, 37 (1): 2-10.

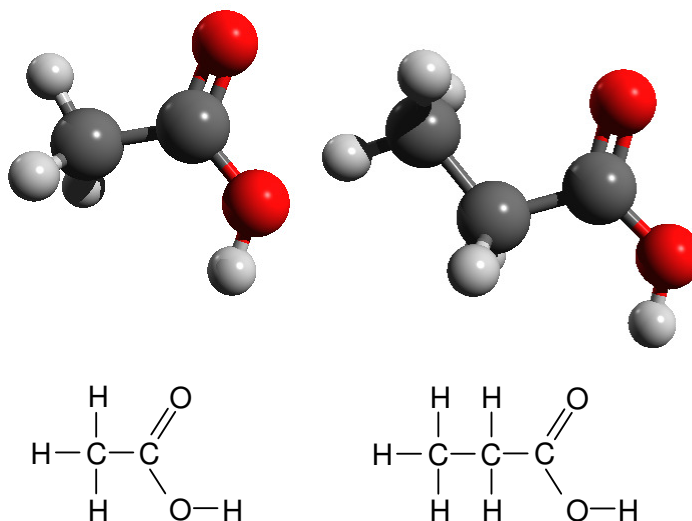
Yue, D., You, F. and Snyder, S.W. (2014) Biomass-to-bioenergy and biofuel supply chain optimization: Overview, key issues and challenges. **Computers and Chemical Engineering**, 66: 36-56.

Zheleznyak, A.S. (1962) Study of the azeotropism in binary systems which forming with low molecular organic acid with water. **Zhurnal Fizicheskoi Khimii**, 36 (2): 322-326.

Zhou, D., Zhang, L., Zhang, S., et al. (2010) Hydrothermal liquefaction of macroalgae *Enteromorpha prolifera* to bio-oil. **Energy & Fuels**, 24 (7): 4054-4061.

Zuñiga-Hinojosa, M.A., Justo-García, D.N., Aquino-Olivos, M.A., et al. (2014) Modeling of asphaltene precipitation from *n*-alkane diluted heavy oils and bitumens using the PC-SAFT equation of state. **Fluid Phase Equilibria**, 376: 210-224.

Appendix A. Brief databank of the compounds



Common name:	Acetic acid	Propionic acid
IUPAC name:	Acetic acid	Propanoic acid
CAS number:	64-19-7	79-09-4
Molecular formula:	C ₂ H ₄ O ₂	C ₃ H ₆ O ₂
Molar mass [g mol⁻¹]:	60.052	74.08
Odour:	Pungent	Pungent/Rancid
Solubility in water:	Miscible	Miscible
Normal boiling point [K]:	391.05	414.32
Freezing point [K]:	289.81	252.45
Flash point [K]:	316.15 (close cup) 330.15 (open cup)	323.15
Autoignition point [K]:	738.15	758.15

The data have been taken from Yaws (2006); Cheung et al. (2011) and Samel et al. (2011).

Appendix C. Gas-Chromatograph methods

C.1 Acetic acid + water

AA_ACID_WATER Method

Method Information

Method: C:\CHEM32\1\METHODS\AA_ACID_WATER.M
Modified: 29/07/2013 at 16:06:13

Injection Source and Location

Injection Source: GC Injector

Injection Location: Front

=====

6850 GC METHOD

=====

OVEN

Initial temp: 150 °C (On) Maximum temp: 190 °C
Initial time: 7.00 min Equilibration time: 2.00 min
Ramps:
Rate Final temp Final time
1 0.0(Off)
Post temp: 50 °C
Post time: 0.00 min
Run time: 7.00 min

INLET (PURGED PACKED)

Initial temp: 230 °C (On)
Flow: 41.1 mL/min (On)
Gas type: Helium

DETECTOR (TCD)

Temperature: 200 °C (On)
Reference flow: 45.0 mL/min (On)
Mode: Constant makeup flow
Makeup flow: 5.0 mL/min (On)
Makeup Gas Type: Helium
Filament: On
Negative polarity: Off

COLUMN

Packed Column
Model Number: ??? Packed 236
3ft x 1/8" SS Porapak N 80/100 for Al
Max temperature: 190 °C
Mode: ramped flow
Initial flow: 40.0 mL/min
Initial time: 1.00 min
Rate Final flow Final time
1 10.00 60.0 4.00
2 0.0(Off)
Post flow: 0.0 mL/min
Source: Inlet
Outlet: Detector
Outlet pressure: ambient

SIGNAL

Data rate: 20 Hz
Type: detector
Save Data: On
Zero: 0.0 (Off)
Range: 0
Fast Peaks: Off
Attenuation: 0

♀

COLUMN COMP

Derive from detector

THERMAL AUX

Use: Valve Box Heater
Description: GSV
Initial temp: 100 °C (On)
Initial time: 0.00 min
Rate Final temp Final time

Page 1



1 0.0(Off) AA_ACID_WATER Method

VALVES POST RUN
Post Time: 0.00 min

TIME TABLE Specifier Parameter & Setpoint

GC Injector

Front Injector:

Sample Washes	0
Sample Pumps	2
Injection Volume	0.20 microliters
Syringe Size	0.5 microliters
PreInj Solvent A Washes	2
PreInj Solvent B Washes	0
PostInj Solvent A Washes	4
PostInj Solvent B Washes	0
Viscosity Delay	0 seconds
Plunger Speed	Fast
PreInjection Dwell	0.00 minutes
PostInjection Dwell	0.00 minutes

Back Injector:
No parameters specified



C.2 Propanoic acid + water.

PROP_ACID_WATER GC Method

Method Information

Method: C:\CHEM32\1\METHODS\PROP_ACID_WATER.M
Modified: 30/08/2013 at 16:40:46

Run Time Checklist

Pre-Run Cmd/Macro: off
Data Acquisition: on
Standard Data Analysis: on
Customized Data Analysis: off
Save GLP Data: off
Post-Run Cmd/Macro: off
Save Method with Data: off

Injection Source and Location

Injection Source: GC Injector
Injection Location: Front

6850 GC METHOD

OVEN

Initial temp: 180 'C (On) Maximum temp: 190 'C
Initial time: 6.00 min Equilibration time: 3.00 min
Ramps:
Rate Final temp Final time
1 0.0(off)
Post temp: 50 'C
Post time: 0.00 min
Run time: 6.00 min

INLET (PURGED PACKED)

Initial temp: 230 'C (On)
Flow: 46.1 mL/min (On)
Gas type: Helium

DETECTOR (TCD)

Temperature: 200 'C (On)
Reference flow: 50.0 mL/min (On)
Mode: Constant makeup flow
Makeup flow: 5.0 mL/min (On)
Makeup Gas Type: Helium
Filament: On
Negative polarity: off

COLUMN

Packed Column
Model Number: ??? Packed 236
3ft x 1/8" SS Porapak N 80/100 for A1
Max temperature: 190 'C
Mode: constant flow

SIGNAL

Data rate: 20 Hz
Type: detector
Save Data: On
Zero: 0.0 (Off)
Range: 0



```
PROP_ACID_WATER GC Method
Nominal initial flow: 45.0 mL/min Fast Peaks: Off
Source: Inlet Attenuation: 0
Outlet: Detector
Outlet pressure: ambient

COLUMN COMP
Derive from detector

THERMAL AUX
Use: Valve Box Heater
Description: GSV
Initial temp: 100 'C (On)
Initial time: 0.00 min
# Rate Final temp Final time
1 0.0(off)

VALVES POST RUN
Post Time: 0.00 min

TIME TABLE
Time Specifier Parameter & Setpoint

GC Injector

Front Injector:
Sample Washes 0
Sample Pumps 2
Injection Volume 0.20 microliters
Syringe Size 0.5 microliters
PreInj Solvent A Washes 0
PreInj Solvent B Washes 0
PostInj Solvent A Washes 7
PostInj Solvent B Washes 0
Viscosity Delay 0 seconds
Plunger Speed Fast
PreInjection Dwell 0.00 minutes
PostInjection Dwell 0.00 minutes

Back Injector:
No parameters specified
```

Appendix D. Table of results of the static – analytical measurements

D.1 Acetic acid + water

Table D.1. Experimental vapour – liquid equilibrium data for acetic acid (1) + water (2) system at pressure P , liquid mole fraction x , vapour mole fraction y and temperatures $T = 413.2, 443.2$ and 483.2 K.^a

$T = 412.6$ K					$T = 443.2$ K					$T = 483.2$ K				
P [bar]	x_1	y_1	$u_c(x_1)$	$u_c(y_1)$	P [bar]	x_1	y_1	$u_c(x_1)$	$u_c(y_1)$	P [bar]	x_1	y_1	$u_c(x_1)$	$u_c(y_1)$
1.96	0.976	0.928	0.005	0.005	4.26	0.983	0.878	0.005	0.005	10.12	0.977	0.840	0.005	0.005
2.10	0.951	0.673	0.005	0.007	4.37	0.975	0.807	0.005	0.005	10.52	0.955	0.672	0.005	0.005
2.30	0.889	0.522	0.005	0.005	4.61	0.955	0.693	0.005	0.005	11.50	0.895	0.481	0.005	0.005
2.66	0.721	0.303	0.005	0.005	5.04	0.903	0.566	0.005	0.005	12.72	0.822	0.348	0.005	0.005
2.90	0.579	0.205	0.005	0.005	5.51	0.823	0.445	0.008	0.007	14.01	0.689	0.227	0.005	0.005
3.11	0.433	0.129	0.005	0.005	6.05	0.697	0.344	0.005	0.005	15.15	0.580	0.162	0.005	0.005
3.26	0.347	0.094	0.005	0.005	6.54	0.568	0.239	0.001	0.009	16.52	0.444	0.107	0.005	0.005
3.33	0.282	0.080	0.005	0.005	7.04	0.409	0.165	0.003	0.005	16.90	0.407	0.092	0.005	0.005
3.41	0.186	0.056	0.005	0.005	7.31	0.315	0.131	0.001	0.005	17.50	0.335	0.074	0.005	0.005
3.48	0.102	0.042	0.010	0.005	7.60	0.195	0.103	0.005	0.007	17.96	0.275	0.063	0.005	0.005
3.49	0.085	0.038	0.005	0.005	7.68	0.178	0.092	0.005	0.005	18.21	0.234	0.058	0.005	0.005
3.53	0.014	0.010	0.005	0.005	7.74	0.148	0.075	0.005	0.005	18.55	0.178	0.052	0.005	0.005
3.56	0.000	0.000			7.80	0.133	0.067	0.005	0.005	18.70	0.153	0.050	0.005	0.005
					7.86	0.105	0.049	0.005	0.005	18.81	0.100	0.044	0.005	0.005
					7.89	0.055	0.031	0.005	0.005	18.90	0.078	0.031	0.005	0.005
					7.92	0.000	0.000			18.96	0.048	0.018	0.005	0.005
										19.00	0.034	0.015	0.005	0.005
										19.02	0.000	0.000		

^a Combined standard uncertainties, u_c , are $u_c(T) = 0.1$ K, $u_c(P) = 0.01$ bar. $u_c(x)$ and $u_c(y)$ are displayed in each temperature column.

D.2 Propanoic acid + water

Table D.2. Experimental vapour – liquid equilibrium data for propanoic acid (1) + water (2) system at pressure P , liquid mole fraction x , vapour mole fraction y and temperatures $T = 423.2, 453.2$ and 483.2 K.^a

$T = 423.2$ K					$T = 453.2$ K					$T = 483.2$ K				
P [bar]	x_1	y_1	$u_c(x_1)$	$u_c(y_1)$	P [bar]	x_1	y_1	$u_c(x_1)$	$u_c(y_1)$	P [bar]	x_1	y_1	$u_c(x_1)$	$u_c(y_1)$
1.87	0.973	0.705	0.005	0.005	4.15	0.960	0.701	0.005	0.005	7.94	0.946	0.647	0.003	0.023
2.34	0.932	0.498	0.005	0.005	5.04	0.918	0.512	0.003	0.005	10.00	0.880	0.393	0.006	0.022
2.74	0.881	0.406	0.005	0.005	6.02	0.850	0.340	0.007	0.013	11.64	0.817	0.271	0.005	0.033
3.26	0.809	0.285	0.004	0.003	6.83	0.774	0.252	0.005	0.005	13.06	0.760	0.204	0.003	0.013
3.77	0.675	0.231	0.008	0.018	7.36	0.724	0.204	0.003	0.004	14.16	0.708	0.152	0.011	0.018
4.11	0.550	0.200	0.005	0.021	8.23	0.600	0.155	0.005	0.005	15.23	0.643	0.119	0.016	0.012
4.31	0.477	0.159	0.004	0.012	8.92	0.482	0.128	0.015	0.005	16.48	0.534	0.105	0.005	0.005
4.56	0.366	0.137	0.005	0.005	9.36	0.398	0.116	0.005	0.005	17.04	0.479	0.098	0.005	0.005
4.60	0.344	0.123	0.003	0.003	9.84	0.292	0.108	0.005	0.005	17.65	0.413	0.094	0.005	0.005
4.70	0.281	0.104	0.005	0.005	10.00	0.226	0.102	0.005	0.005	18.25	0.339	0.090	0.005	0.005
4.75	0.225	0.100	0.005	0.005	10.07	0.169	0.092	0.005	0.005	18.91	0.233	0.086	0.005	0.005
4.78	0.145	0.096	0.005	0.005	10.08	0.160	0.090	0.005	0.005	19.10	0.184	0.081	0.005	0.005
4.80	0.130	0.086	0.005	0.005	10.10	0.133	0.079	0.005	0.005	19.35	0.128	0.072	0.005	0.005
4.82	0.111	0.084	0.005	0.005	10.05	0.017	0.027	0.005	0.005	19.38	0.105	0.069	0.005	0.005
4.81	0.074	0.071	0.005	0.005	10.03	0.000	0.000			19.35	0.017	0.024	0.005	0.005
4.80	0.017	0.026	0.005	0.005						19.02	0.000	0.000		
4.76	0.000	0.000												

^a Combined standard uncertainties, u_c , are $u_c(T) = 0.1$ K, $u_c(P) = 0.01$ bar. $u_c(x)$ and $u_c(y)$ are displayed in each temperature column.

Appendix E. Spectrophotometric method of iron determination

The following method was used to determine the amount of iron in an aqueous mixture of organic acid.

Equipment

Spectrophotometer

Reagents

Iron (III) perchlorate hydrate
Glacial, acetic acid
Perchloric acid, 70%
Hydrogen peroxide solution, 30% w/w in water
Distilled water

Procedure

A calibration plot was done by measuring the absorbance of solutions of iron (III) at the following concentrations: 10, 20, 30, 40 and 50 ppm. The solutions were prepared by taking V_1 volumes of a 100 ppm iron (III) stock solution into 100 mL flasks according to: $V_1 = C_2V_2/C_1$. Where $C_1 = 100$ ppm and $V_2 = 100$ mL. A volume of 50 mL of acetic acid was then added to the flasks and filled up to the mark with water. The absorbance of the solutions were determined with a wave length of 338 nm based on the papers of Ishibashi et al. (1956; 1957). The following linear relationship was found to represent the data (Figure E.1):

$$\text{Absorbance} = 0.0234 (\text{Concentration}) + 0.0056.$$



Spectrophotometric method of iron determination

The samples were evaporated in a vacuum oven. A few drops of 4 M perchloric acid were added to the solid residue until no reaction was observed. Hydrogen peroxide was added to the sample and it was evaporated almost to dryness. The samples were then diluted with water and transferred to 100 mL volumetric flasks. 50 mL of acetic acid was added and the flask filled up to the mark with water. The absorbance of the samples were measured and the concentrations computed from the calibration plot. The results for the concentrated solutions at the maximum temperature studied (483.2 K), and consequently the maximum iron content expected, are shown in [Table E.1](#).

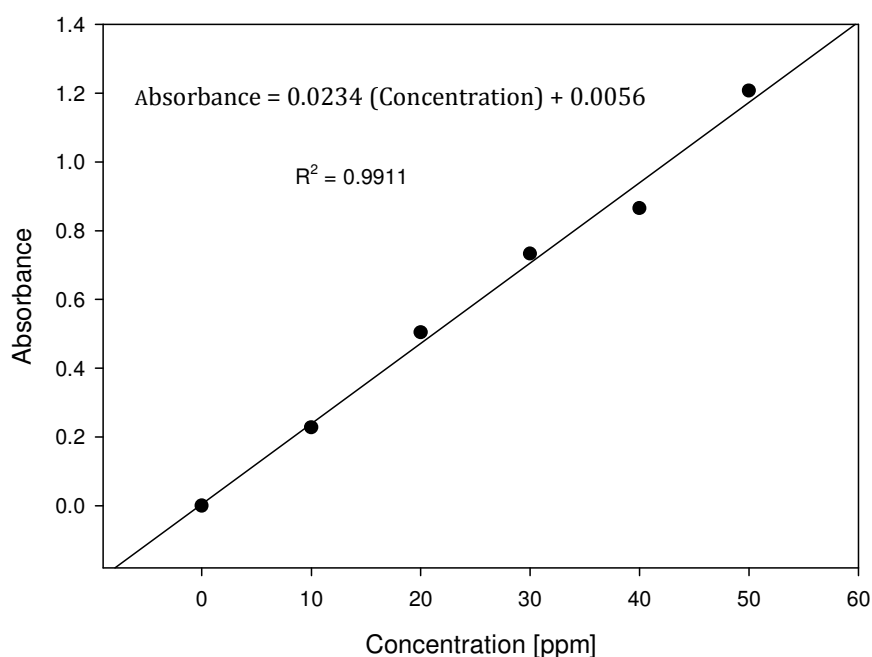


Figure E.1. Spectrophotometer calibration plot. Absorbance vs. concentration of iron (III) solutions.

Table E.1. Maximum iron content on the organic acid mixtures + water systems.

System	Absorbance	Concentration [ppm]	Iron content [%]
acetic acid	0.755	32.03 ^a	0.01
propanoic acid	0.999	42.45	0.004

^a Diluted 50%.

Appendix F. Polypropylene technical data sheet

Technical Information



DOW C711-70RNA Polypropylene Resin Natural Polypropylene Impact Copolymer

DOW C711-70RNA Polypropylene Resin is a high performance impact copolymer developed especially for high speed thin wall injection moulding. DOW C711-70RNA Polypropylene Resin is a very high melt flow rate impact copolymer featuring excellent impact strength, even at low temperatures. DOW C711-70RNA Polypropylene Resin is designed and formulated to allow for simple processing, short cycle times, low shrinkage, minimal warpage and good part dimensional stability. DOW C711-70RNA Polypropylene Resin contains a very efficient antistatic package.

Applications for DOW C711-70RNA Polypropylene Resin:

- Thin wall containers
- Thin wall packaging (margarine tubs, dairy product pots, ice cream containers)
- Caps & closures
- Video cassette cases
- Lids
- Housewares
- Flower pots
- Cool boxes

Properties	Units	Test Method	Value
Physical ⁽¹⁾			
Melt Flow Rate (230 °C, 2.16 kg)	g/10min	ISO 1133	70
Density	g/cm ³	ISO 1183	0.9
Mechanical ^(1,2)			
Flexural Modulus	MPa	ISO 178	1250
Tensile Strength at Yield	MPa	ISO 527-2	24
Tensile Elongation at Yield	%	ISO 527-2	7
Thermal ^(1,2)			
HDT B (0.45 MPa)	°C	ISO 75/B	95
Vicat Softening Point A (10 N)	°C	ISO 306/A	150
Impact ^(1,2)			
CHARPY (notched) Impact Strength (23 °C)	kJ/m ²	ISO 179-1/1eA	8.0
CHARPY (notched) Impact Strength (0 °C)	kJ/m ²	ISO 179-1/1eA	5.5
CHARPY (notched) Impact Strength (-20 °C)	kJ/m ²	ISO 179-1/1eA	4.0

⁽¹⁾Typical values; not to be construed as specification limits.

⁽²⁾Injection moulded specimens.

Regulatory Information

DOW C711-70RNA Polypropylene Resin should comply with U.S. FDA 21 CFR 177.1520(c)3.1a and Europe EU-Directive 2002/72/EC food regulations. It is the responsibility of the manufacturers of food contact articles and industrial food packers to make sure the articles in their actual use are in compliance with the imposed migration requirements. The appropriate regulations should be consulted for more detailed information. Compliance letters can be obtained through the Dow sales representative.

Appendix G. Data sets used in the synthetic measurements

Table G.1. Mass of acetic acid (m_{acetic}), mass of water (m_{water}) and total volume of the liquid phase (V_L) data used in the regression analysis.

P [bar]	m_{acetic} [g]	m_{water} [g]	V_L [mL]
2.389	65.4999	5.1179	75.6893
	74.4769	5.6072	87.7685
	63.4860	4.8961	72.0686
	74.2237	5.6676	83.1383
2.661	65.4999	8.9861	81.4561
	74.4769	9.9956	90.4030
	63.4860	8.0746	76.4266
	74.2237	9.0739	92.6082
3.136	65.4999	29.4260	105.6009
	74.4769	32.6337	120.5420
	63.4860	27.9163	101.5781
	74.2237	32.1079	120.8166

Appendix H. Validation plots

H.1 CPA

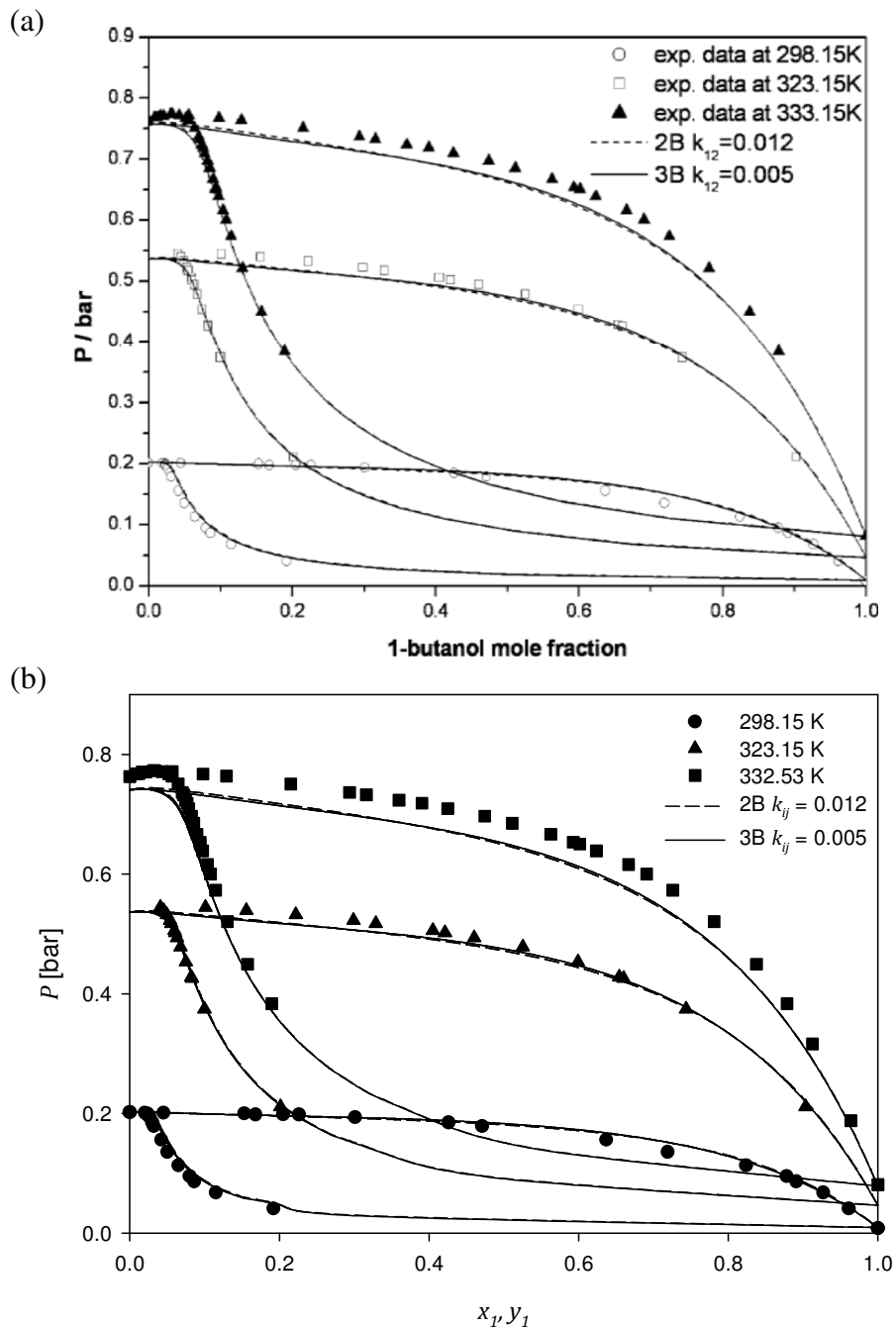


Figure H.1. Phase diagram for the 1-butanol (1) + *n*-hexane (2) system. (a) Original figure in Kontogeorgis et al. (2006a). (b) This work: symbols: experimental data from Berro et al. (1982) and Rodríguez et al. (1993); dash line: 1-butanol as 2B association type; solid line: 1-butanol as 3B.

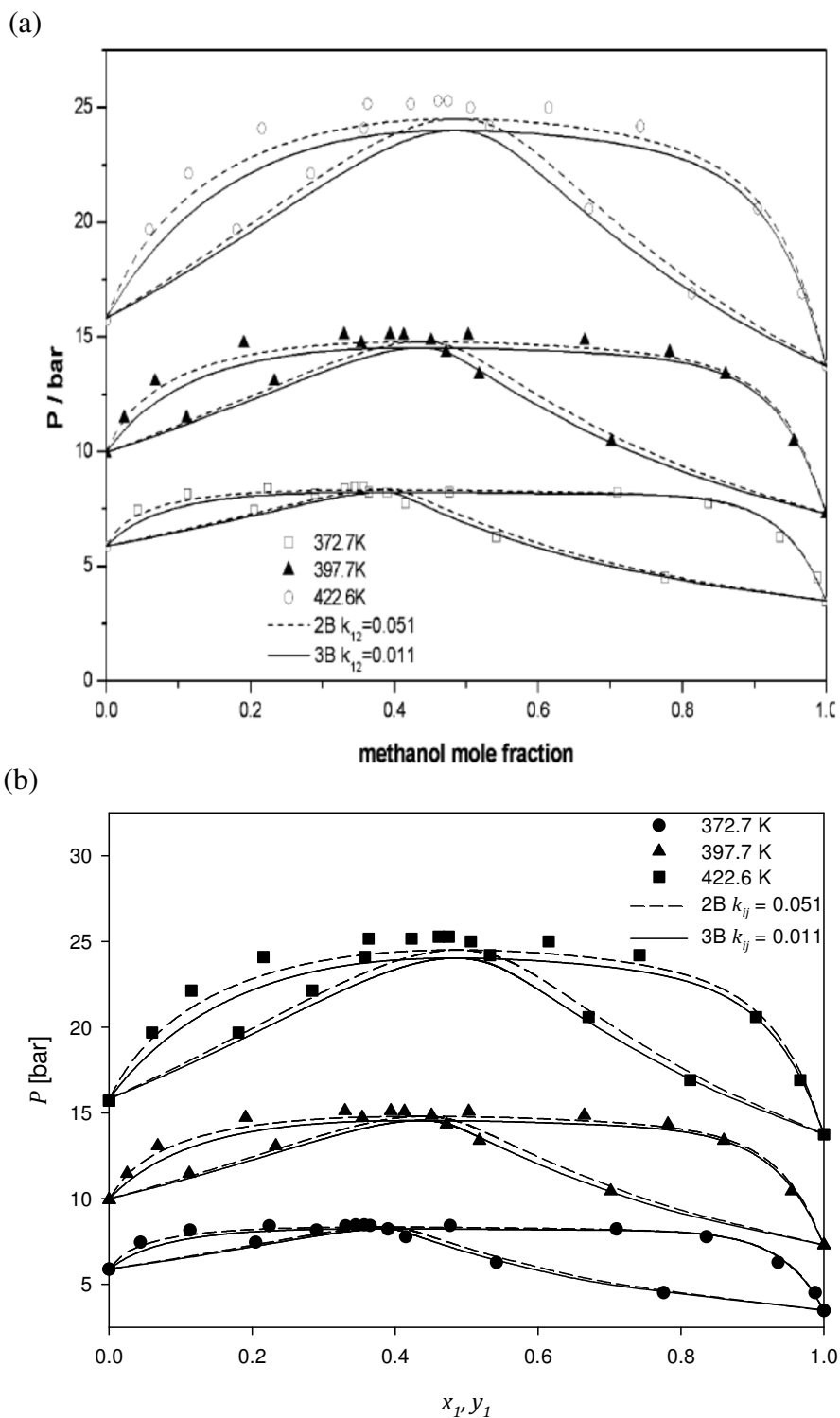


Figure H.2. Phase diagram for the methanol (1) + *n*-pentane (2) system. (a) Original figure in Kontogeorgis et al. (2006a). (b) This work: symbols: experimental data from Wilsak et al. (1987); dash line: methanol as 2B association type; solid line: methanol as 3B.

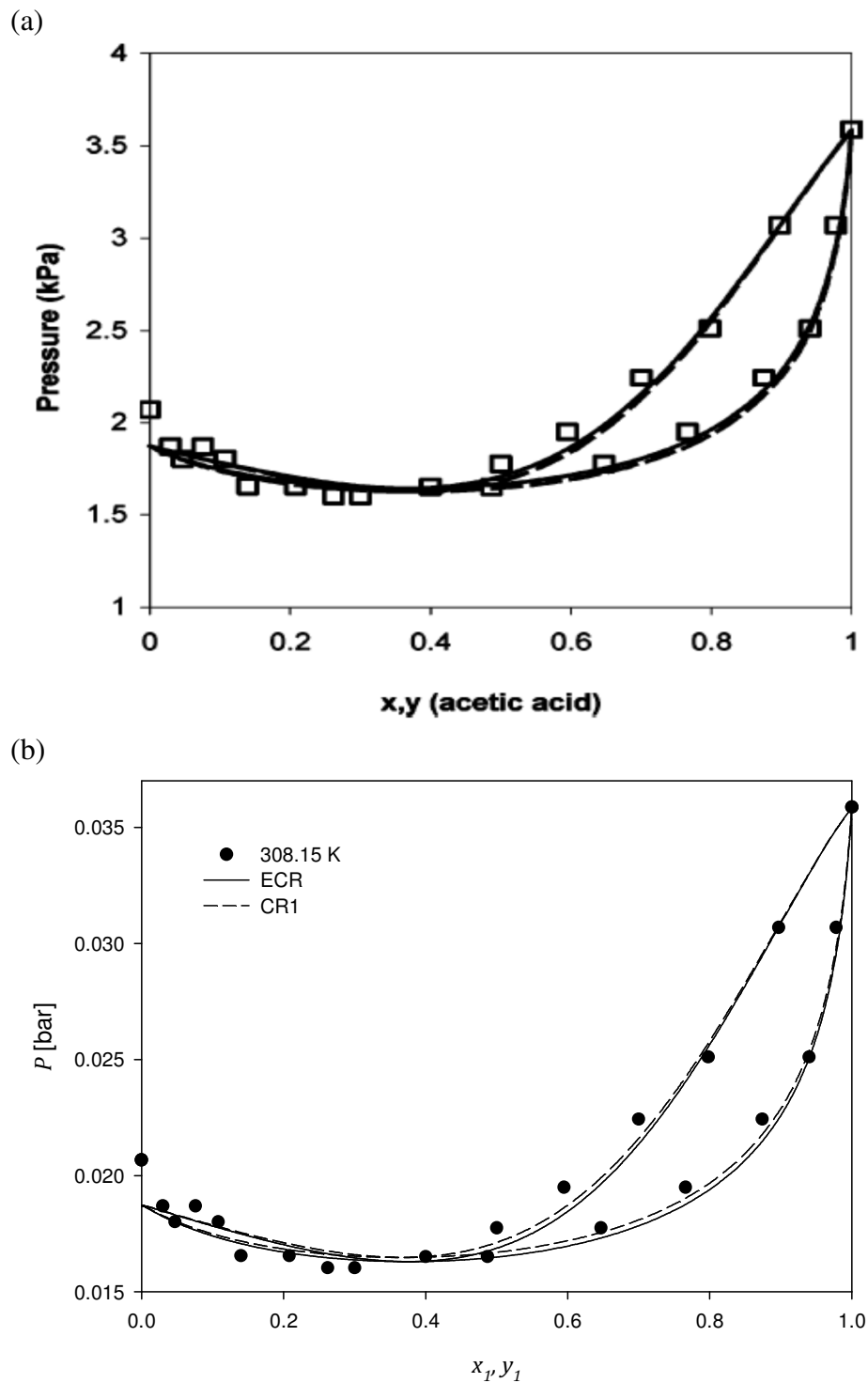


Figure H.3. Phase diagram for the acetic acid (1) + 1-butanol (2) system at 308.15 K. (a) Original figure in Kontogeorgis et al. (2006b). (b) This work: symbols: experimental data from Apelblat et al. (1983); lines: correlations with ECR and CR1 combining rule. Acetic acid modelled as 1A and 1-butanol as 2B.

H.2 PC-SAFT / PCP-SAFT

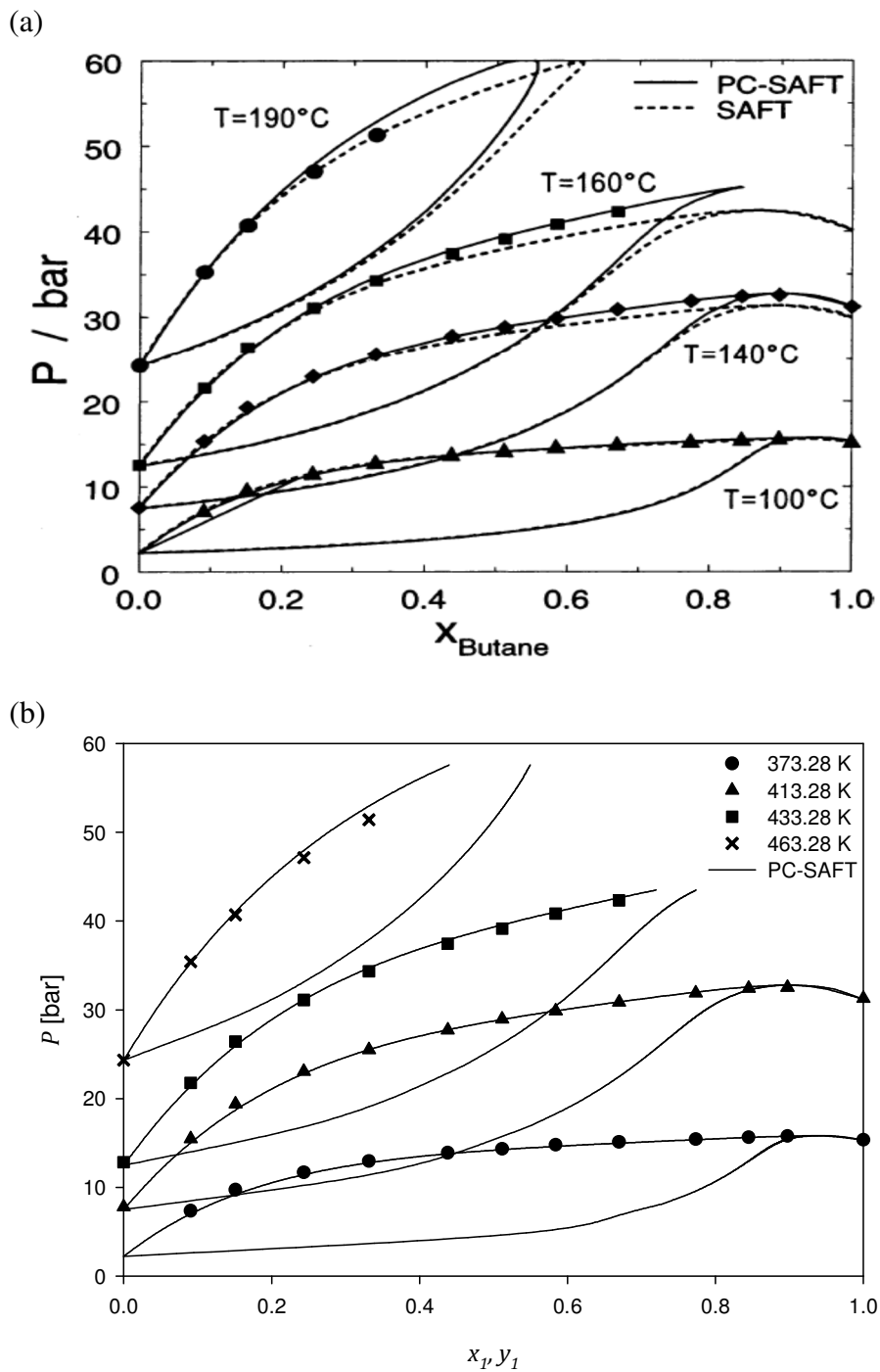


Figure H.4. Phase diagram of the *n*-butane (1) + ethanol (2) system. (a) Original figure in Gross and Sadowski (2002). (b) This work: symbols: experimental data from Deak et al. (1995); lines: correlations with $k_{ij} = 0.028$. Ethanol modelled as 2B.

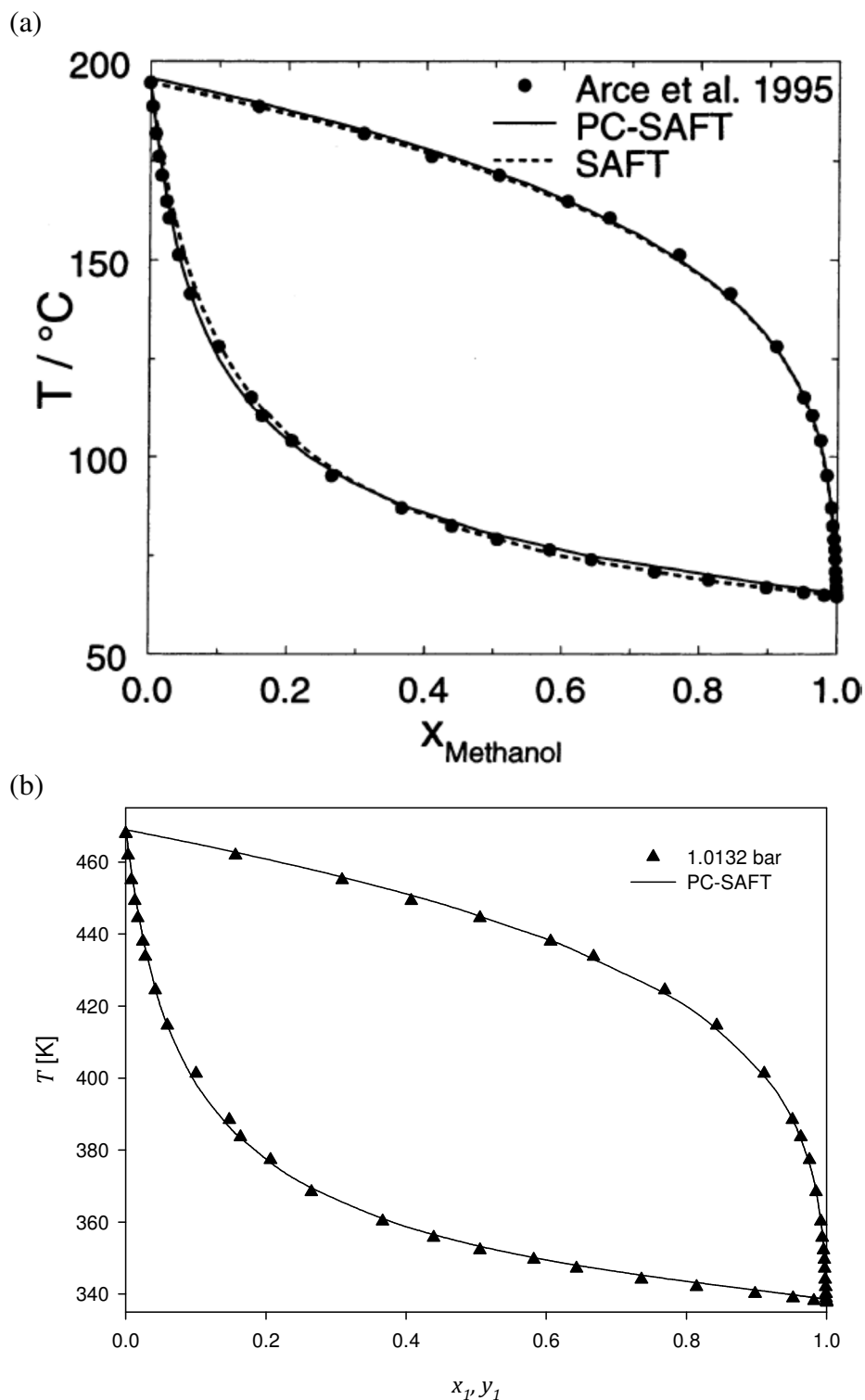


Figure H.5. Phase diagram of methanol (1) + 1-octanol (2) at 1.013 bar. (a) Original figure in Gross and Sadowski (2002). (b) This work: symbols: experimental data from Arce et al. (1995); line: correlations with $k_{ij} = 0.020$. Both compounds modelled as 2B.

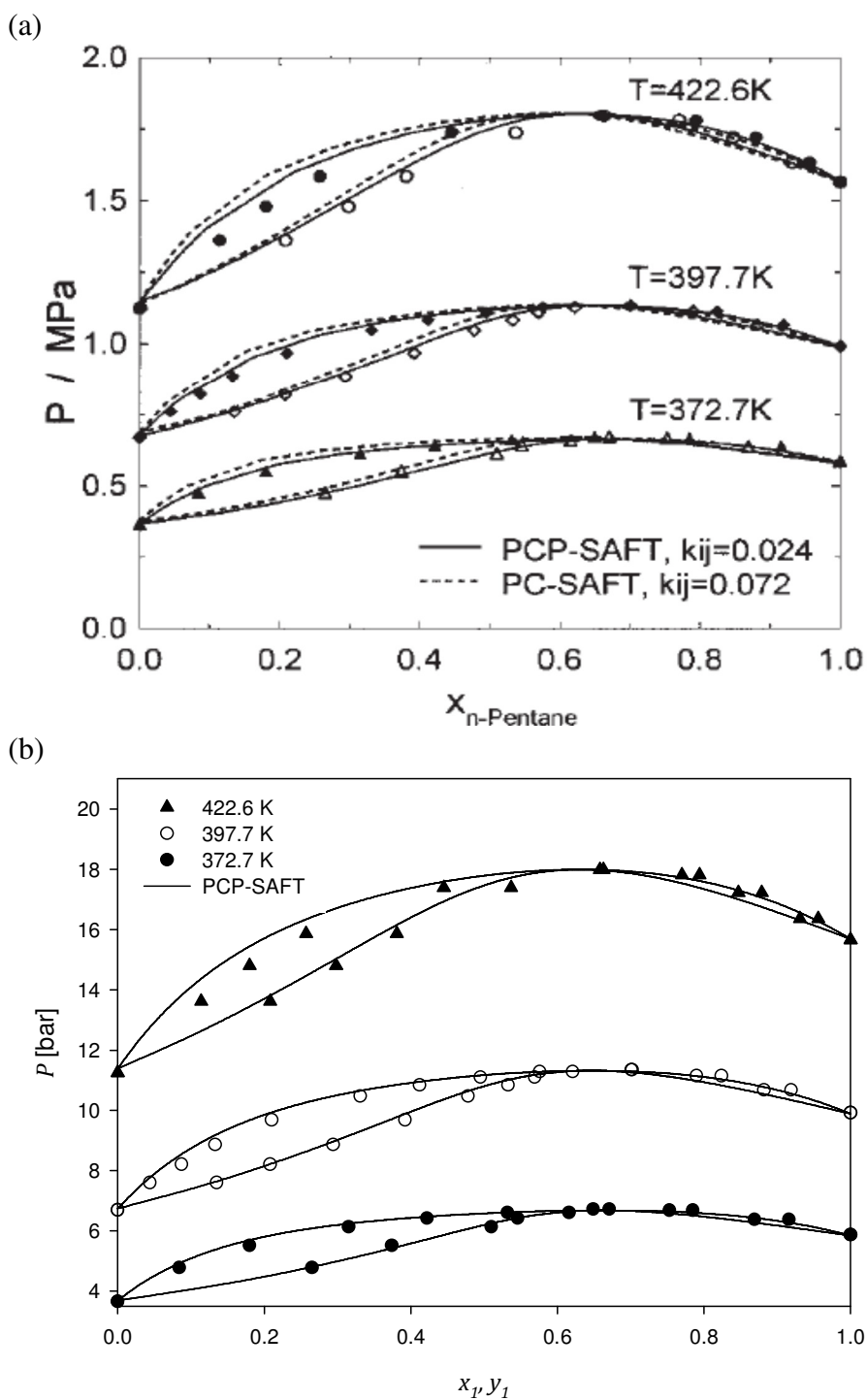


Figure H.6. Phase diagram for the *n*-pentane (1) + acetone (2) system. (a) Original figure in Gross and Vrabec (2006). (b) This work: symbols: experimental data from Campbell et al. (1986); lines: correlations with $k_{ij} = 0.024$. Acetone modelled with dipolar contributions.

Appendix I. Average deviations

I.1 Predictive mode

I.1.1 Acetic acid + water

Table I.1. Average deviations in pressure (ΔP) and acetic acid vapour composition (Δy_1) of the equations of state with different association schemes and $k_{ij} = 0$.

Association scheme								
1A-2B								
	CPA ECR		CPA CR1		PC-SAFT		PCP-SAFT	
T [K]	ΔP [%]	Δy_1	ΔP [%]	Δy_1	ΔP [%]	Δy_1	ΔP [%]	Δy_1
293.15	88.99	0.23	74.00	0.21	12.83	0.04	21.26	0.09
313.15	60.83	0.19	49.93	0.17	15.15	0.04	13.37	0.06
343.2	41.26	0.18	34.26	0.16	8.81	0.03	4.99	0.03
363.02	35.55	0.13	29.31	0.11	13.89	0.04	3.17	0.02
373.12	35.42	0.07	28.75	0.06	16.78	0.05	3.82	0.03
412.6	17.44	0.15	15.22	0.15	12.60	0.14	3.03	0.14
443.2	12.00	0.13	10.91	0.13	13.06	0.12	5.64	0.12
483.2	9.37	0.17	8.22	0.17	12.31	0.16	6.16	0.16
Average	37.61	0.16	31.32	0.14	13.18	0.08	7.68	0.08
1A-3B								
	CPA ECR		CPA CR1		PC-SAFT		PCP-SAFT	
T [K]	ΔP [%]	Δy_1	ΔP [%]	Δy_1	ΔP [%]	Δy_1	ΔP [%]	Δy_1
293.15	31.53	0.11	24.34	0.10	34.69	0.14	5.65	0.02
313.15	22.61	0.10	17.38	0.09	34.53	0.12	8.65	0.03
343.2	15.96	0.07	13.98	0.07	19.63	0.08	6.45	0.02
363.02	15.26	0.06	12.56	0.06	29.00	0.10	11.54	0.03
373.12	15.54	0.04	9.88	0.05	35.96	0.12	13.53	0.05
412.6	9.17	0.14	8.45	0.14	23.41	0.16	12.21	0.14
443.2	7.30	0.12	7.54	0.12	22.11	0.15	13.12	0.13
483.2	5.57	0.16	5.63	0.16	21.09	0.17	12.95	0.16
Average	15.36	0.10	12.47	0.10	27.55	0.13	10.51	0.07



Average deviations

Table I.1. (Continuation)

1A-4C								
CPA ECR			CPA CR1		PC-SAFT		PCP-SAFT	
T [K]	ΔP [%]	Δy_1	ΔP [%]	Δy_1	ΔP [%]	Δy_1	ΔP [%]	Δy_1
293.15	55.55	0.18	42.35	0.15	12.68	0.04	30.56	0.13
313.15	47.03	0.16	35.41	0.14	12.77	0.04	22.77	0.10
343.2	31.35	0.13	24.99	0.11	7.23	0.03	10.06	0.05
363.02	36.60	0.12	28.96	0.10	10.86	0.03	10.31	0.05
373.12	42.33	0.09	33.47	0.07	11.21	0.05	13.83	0.05
412.6	24.21	0.16	20.51	0.16	9.48	0.15	3.19	0.14
443.2	19.61	0.15	17.11	0.15	9.74	0.12	2.16	0.12
483.2	19.66	0.19	16.73	0.19	8.05	0.16	1.44	0.16
Average	34.54	0.15	27.44	0.13	10.25	0.08	11.79	0.10

2B-2B								
CPA ECR			CPA CR1		PC-SAFT		PCP-SAFT	
T [K]	ΔP [%]	Δy_1	ΔP [%]	Δy_1	ΔP [%]	Δy_1	ΔP [%]	Δy_1
293.15	93.57	0.26	75.52	0.23	20.66	0.09	71.47	0.23
313.15	71.70	0.25	56.51	0.21	13.34	0.09	55.23	0.21
343.2	51.11	0.22	39.36	0.18	7.42	0.05	30.72	0.15
363.02	45.67	0.17	35.20	0.14	6.10	0.04	31.47	0.13
373.12	46.05	0.11	35.42	0.09	6.71	0.04	35.17	0.10
412.6	23.90	0.13	17.58	0.13	2.17	0.13	15.09	0.13
443.2	16.59	0.12	11.53	0.11	2.16	0.11	9.56	0.11
483.2	13.43	0.16	9.08	0.16	2.45	0.15	7.10	0.16
Average	45.25	0.18	35.02	0.16	7.63	0.09	31.98	0.15

2B-3B								
CPA ECR			CPA CR1		PC-SAFT		PCP-SAFT	
T [K]	ΔP [%]	Δy_1	ΔP [%]	Δy_1	ΔP [%]	Δy_1	ΔP [%]	Δy_1
293.15	82.81	0.26	67.42	0.22	41.27	0.16	58.92	0.21
313.15	62.41	0.24	48.11	0.20	11.27	0.05	41.70	0.18
343.2	42.20	0.21	35.00	0.16	4.50	0.02	23.15	0.12
363.02	38.59	0.15	28.95	0.12	2.79	0.02	23.16	0.11
373.12	39.20	0.10	28.92	0.09	2.61	0.03	26.02	0.09
412.6	19.46	0.13	14.21	0.13	4.92	0.13	9.24	0.13
443.2	12.99	0.12	9.94	0.11	6.90	0.11	5.34	0.11
483.2	10.48	0.16	7.57	0.16	6.97	0.15	3.24	0.15
Average	38.52	0.17	30.01	0.15	10.15	0.09	23.85	0.14



Table I.1. (Continuation)

2B-4C								
CPA ECR			CPA CR1		PC-SAFT		PCP-SAFT	
T [K]	ΔP [%]	Δy_1	ΔP [%]	Δy_1	ΔP [%]	Δy_1	ΔP [%]	Δy_1
293.15	47.87	0.18	31.74	0.13	15.64	0.08	69.07	0.23
313.15	40.56	0.17	25.25	0.13	11.42	0.08	55.29	0.21
343.2	26.82	0.13	17.09	0.09	6.55	0.05	30.28	0.14
363.02	29.79	0.12	18.49	0.09	6.36	0.05	32.49	0.13
373.12	34.33	0.10	21.17	0.07	8.69	0.05	37.45	0.11
412.6	18.31	0.13	10.74	0.13	1.07	0.13	16.42	0.13
443.2	13.72	0.12	8.14	0.12	1.51	0.11	10.72	0.12
483.2	13.25	0.16	7.41	0.16	0.80	0.16	8.94	0.16
Average	28.08	0.14	17.50	0.11	6.50	0.09	32.58	0.16

Non-associating						
T [K]	PR		PC-SAFT		PCP-SAFT	
	ΔP [%]	Δy_1	ΔP [%]	Δy_1	ΔP [%]	Δy_1
293.15	120.05	0.36	23.45	0.13	37.03	0.17
313.15	94.25	0.34	18.18	0.12	30.30	0.16
343.2	106.71	0.34	13.11	0.06	19.01	0.09
363.02	70.82	0.25	12.41	0.06	19.75	0.08
373.12	62.83	0.16	12.81	0.04	22.47	0.07
412.6	38.32	0.15	5.03	0.12	8.90	0.13
443.2	27.72	0.12	3.15	0.10	4.13	0.10
483.2	23.22	0.17	3.05	0.14	1.72	0.15
Average	67.99	0.24	11.40	0.10	17.91	0.12

**I.1.2 Propanoic acid + water****Table I.2.** Average deviations in pressure (ΔP) and propanoic acid vapour composition (Δy_1) of the equations of state with different association schemes and $k_{ij} = 0$.

Association scheme								
1A-2B								
	CPA ECR		CPA CR1		PC-SAFT		PCP-SAFT	
T [K]	ΔP [%]	Δy_1	ΔP [%]	Δy_1	ΔP [%]	Δy_1	ΔP [%]	Δy_1
313.1	90.00	0.13	90.00	0.13	14.65	0.04	14.14	0.06
343.2	95.45	0.25	87.17	0.27	22.33	0.08	9.19	0.04
373.1	56.15	0.10	59.81	0.13	19.87	0.04	5.47	0.04
423.2	19.75	0.09	19.08	0.09	21.31	0.11	7.02	0.07
453.2	14.31	0.11	15.15	0.12	21.90	0.14	8.91	0.11
483.2	10.24	0.16	11.71	0.17	21.75	0.18	10.04	0.15
Average	47.65	0.14	47.15	0.15	20.30	0.10	9.13	0.08
1A-3B								
	CPA ECR		CPA CR1		PC-SAFT		PCP-SAFT	
T [K]	ΔP [%]	Δy_1	ΔP [%]	Δy_1	ΔP [%]	Δy_1	ΔP [%]	Δy_1
313.1	100.00	0.13	100.00	0.13	4.91	0.02	4.91	0.02
343.2	96.23	0.43	86.85	0.45	14.11	0.04	14.11	0.04
373.1	70.63	0.44	100.00	0.28	10.06	0.02	10.06	0.02
423.2	14.68	0.08	15.38	0.09	30.56	0.14	15.41	0.08
453.2	12.23	0.11	14.31	0.12	30.46	0.17	16.51	0.12
483.2	9.54	0.16	12.53	0.17	29.65	0.20	16.90	0.16
Average	50.55	0.23	54.84	0.21	19.96	0.10	12.98	0.08
1A-4C								
	CPA ECR		CPA CR1		PC-SAFT		PCP-SAFT	
T [K]	ΔP [%]	Δy_1	ΔP [%]	Δy_1	ΔP [%]	Δy_1	ΔP [%]	Δy_1
313.1	46.67	0.18	33.69	0.14	10.95	0.02	31.29	0.10
343.2	26.85	0.11	26.23	0.11	17.87	0.05	15.47	0.08
373.1	33.16	0.10	24.10	0.08	12.10	0.02	20.47	0.08
423.2	21.96	0.10	21.44	0.11	15.02	0.09	11.75	0.08
453.2	18.47	0.12	18.05	0.13	14.58	0.12	9.30	0.11
483.2	14.93	0.16	14.67	0.17	13.60	0.16	7.01	0.15
Average	27.01	0.13	23.03	0.12	14.02	0.08	15.88	0.10



Table I.2. (Continuation)

2B-2B								
	CPA ECR		CPA CR1		PC-SAFT		PCP-SAFT	
T [K]	ΔP [%]	Δy_1	ΔP [%]	Δy_1	ΔP [%]	Δy_1	ΔP [%]	Δy_1
313.1	100.00	0.13	100.00	0.13	7.48	0.02	26.77	0.11
343.2	58.20	0.22	39.43	0.16	15.93	0.04	14.71	0.09
373.1	43.01	0.15	26.05	0.11	12.74	0.02	17.52	0.08
423.2	20.69	0.07	16.39	0.07	16.59	0.08	7.88	0.05
453.2	14.21	0.09	12.35	0.10	17.21	0.12	5.75	0.08
483.2	9.41	0.14	9.13	0.15	17.10	0.16	3.84	0.13
Average	40.92	0.13	33.89	0.12	14.51	0.08	12.75	0.09

2B-3B								
	CPA ECR		CPA CR1		PC-SAFT		PCP-SAFT	
T [K]	ΔP [%]	Δy_1	ΔP [%]	Δy_1	ΔP [%]	Δy_1	ΔP [%]	Δy_1
313.1	62.72	0.42	53.64	0.67	39.98	0.20	23.98	0.09
343.2	81.49	0.38	49.53	0.44	25.43	0.07	14.02	0.06
373.1	43.22	0.14	34.35	0.13	19.06	0.03	10.07	0.06
423.2	19.17	0.07	16.25	0.07	21.48	0.10	6.51	0.05
453.2	13.29	0.09	13.11	0.10	21.98	0.13	6.71	0.09
483.2	9.04	0.14	10.27	0.15	21.62	0.17	7.71	0.14
Average	38.16	0.21	29.52	0.26	24.93	0.12	11.50	0.08

2B-4C								
	CPA ECR		CPA CR1		PC-SAFT		PCP-SAFT	
T [K]	ΔP [%]	Δy_1	ΔP [%]	Δy_1	ΔP [%]	Δy_1	ΔP [%]	Δy_1
313.1	30.71	0.11	16.05	0.07	6.75	0.02	40.20	0.12
343.2	15.77	0.09	13.23	0.06	14.08	0.03	19.77	0.11
373.1	21.91	0.09	9.09	0.05	9.16	0.02	24.74	0.10
423.2	12.74	0.06	10.91	0.07	13.43	0.07	9.94	0.05
453.2	10.50	0.09	10.18	0.10	12.99	0.10	7.48	0.08
483.2	7.62	0.14	8.29	0.15	12.17	0.15	4.38	0.13
Average	16.54	0.10	11.29	0.08	11.43	0.07	17.75	0.10



Average deviations

Table I.2. (Continuation)

T [K]	Non-associating					
	PR		PC-SAFT		PCP-SAFT	
	ΔP [%]	Δy_1	ΔP [%]	Δy_1	ΔP [%]	Δy_1
313.1	100.00	0.13	18.95	0.09	32.98	0.12
343.2	100.34	0.23	11.87	0.06	13.56	0.07
373.1	100.00	0.28	6.85	0.04	15.52	0.07
423.2	35.09	0.09	9.77	0.06	7.71	0.05
453.2	23.35	0.08	11.28	0.10	6.21	0.08
483.2	15.72	0.13	13.37	0.14	6.33	0.12
Average	62.42	0.16	12.01	0.08	13.72	0.09

I.2 Correlative mode

I.2.1 Acetic acid + water

Table I.3. Average deviations in pressure (ΔP) and acetic acid vapour composition (Δy_1) of the equations of state with different association schemes and $k_{ij} = k_{ij}^0 + k_{ij}^1 T$.

T [K]	Association scheme							
	1A-2B							
	CPA ECR		CPA CR1		PC-SAFT		PCP-SAFT	
ΔP [%]	Δy_1	ΔP [%]	Δy_1	ΔP [%]	Δy_1	ΔP [%]	Δy_1	
293.15	5.97	0.04	7.73	0.05	2.96	0.02	2.03	0.02
313.15	6.34	0.04	8.15	0.05	3.41	0.02	1.74	0.01
343.2	4.28	0.03	5.34	0.04	2.06	0.01	1.39	0.01
363.02	4.12	0.03	5.63	0.04	1.88	0.01	1.33	0.01
373.12	2.71	0.03	4.52	0.03	1.46	0.02	2.11	0.02
412.6	3.69	0.14	4.68	0.14	2.08	0.14	1.41	0.14
443.2	4.43	0.12	5.50	0.12	2.81	0.12	1.96	0.12
483.2	3.09	0.16	4.02	0.16	1.78	0.17	1.25	0.16
Average	4.33	0.07	5.69	0.08	2.30	0.06	1.65	0.06

Table I.3. (Continuation)

1A-3B								
	CPA ECR		CPA CR1		PC-SAFT		PCP-SAFT	
T [K]	ΔP [%]	Δy_1	ΔP [%]	Δy_1	ΔP [%]	Δy_1	ΔP [%]	Δy_1
293.15	7.29	0.05	9.82	0.06	1.16	0.01	2.71	0.02
313.15	7.06	0.04	13.89	0.06	1.76	0.01	1.48	0.02
343.2	5.33	0.03	6.78	0.04	1.29	0.00	1.40	0.01
363.02	4.88	0.03	9.40	0.05	0.40	0.00	1.44	0.01
373.12	3.10	0.03	5.41	0.04	1.68	0.02	2.59	0.02
412.6	4.26	0.13	5.51	0.13	1.17	0.14	1.40	0.14
443.2	4.96	0.12	6.29	0.12	1.93	0.12	1.90	0.12
483.2	3.61	0.16	4.76	0.16	1.18	0.17	1.21	0.16
Average	5.06	0.07	7.73	0.08	1.32	0.06	1.77	0.06

1A-4C								
	CPA ECR		CPA CR1		PC-SAFT		PCP-SAFT	
T [K]	ΔP [%]	Δy_1	ΔP [%]	Δy_1	ΔP [%]	Δy_1	ΔP [%]	Δy_1
293.15	3.18	0.02	5.53	0.04	2.81	0.03	4.13	0.04
313.15	4.13	0.03	6.69	0.05	2.19	0.02	2.71	0.03
343.2	2.60	0.02	4.33	0.03	2.12	0.02	2.54	0.02
363.02	2.53	0.02	4.19	0.03	2.27	0.02	2.78	0.02
373.12	0.92	0.04	3.17	0.04	3.07	0.03	3.35	0.03
412.6	2.36	0.14	3.78	0.14	1.93	0.15	2.20	0.14
443.2	3.46	0.13	4.90	0.13	2.41	0.12	2.51	0.12
483.2	2.13	0.17	3.38	0.17	1.54	0.17	1.64	0.17
Average	2.66	0.07	4.50	0.08	2.29	0.07	2.73	0.07

2B-2B								
	CPA ECR		CPA CR1		PC-SAFT		PCP-SAFT	
T [K]	ΔP [%]	Δy_1	ΔP [%]	Δy_1	ΔP [%]	Δy_1	ΔP [%]	Δy_1
293.15	3.74	0.02	4.89	0.03	2.64	0.02	1.98	0.03
313.15	4.54	0.03	5.79	0.03	3.41	0.03	2.30	0.03
343.2	2.37	0.02	3.09	0.02	1.90	0.01	1.37	0.02
363.02	2.06	0.02	3.15	0.02	1.66	0.02	1.40	0.03
373.12	1.13	0.02	2.13	0.02	1.62	0.02	2.63	0.03
412.6	2.08	0.13	2.81	0.13	1.68	0.13	1.13	0.13
443.2	2.69	0.11	3.54	0.11	2.14	0.11	1.42	0.11
483.2	1.70	0.15	2.46	0.15	1.40	0.15	0.97	0.15
Average	2.54	0.06	3.48	0.07	2.06	0.06	1.65	0.07



Average deviations

Table I.3. (Continuation)

2B-3B								
T [K]	CPA ECR		CPA CR1		PC-SAFT		PCP-SAFT	
	ΔP [%]	Δy_1	ΔP [%]	Δy_1	ΔP [%]	Δy_1	ΔP [%]	Δy_1
293.15	6.39	0.04	7.74	0.05	3.75	0.03	3.20	0.03
313.15	7.80	0.04	8.16	0.05	8.92	0.04	2.11	0.03
343.2	16.53	0.03	17.18	0.05	3.53	0.02	0.82	0.02
363.02	3.43	0.03	4.82	0.04	3.22	0.02	1.12	0.03
373.12	1.57	0.03	2.88	0.04	2.42	0.03	1.88	0.03
412.6	2.98	0.13	5.04	0.13	2.22	0.13	1.52	0.13
443.2	3.55	0.11	6.09	0.11	2.63	0.11	2.09	0.11
483.2	2.40	0.15	3.73	0.15	1.96	0.15	1.25	0.15
Average	5.58	0.07	6.95	0.08	3.58	0.07	1.75	0.07

2B-4C								
T [K]	CPA ECR		CPA CR1		PC-SAFT		PCP-SAFT	
	ΔP [%]	Δy_1	ΔP [%]	Δy_1	ΔP [%]	Δy_1	ΔP [%]	Δy_1
293.15	2.74	0.02	3.48	0.02	1.65	0.02	3.47	0.04
313.15	2.78	0.02	4.30	0.03	2.09	0.03	2.78	0.04
343.2	1.16	0.02	2.44	0.02	1.25	0.02	2.07	0.03
363.02	0.91	0.02	1.95	0.02	1.34	0.02	2.32	0.03
373.12	2.27	0.03	1.20	0.03	2.64	0.03	3.64	0.04
412.6	0.95	0.13	2.12	0.13	1.18	0.13	1.67	0.13
443.2	1.60	0.11	2.81	0.11	1.50	0.11	1.54	0.11
483.2	0.82	0.16	1.96	0.16	0.97	0.16	1.22	0.16
Average	1.65	0.06	2.53	0.06	1.58	0.07	2.34	0.07

Non-associating							
T [K]	PR		PC-SAFT		PCP-SAFT		
	ΔP [%]	Δy_1	ΔP [%]	Δy_1	ΔP [%]	Δy_1	
293.15	12.38	0.10	7.45	0.03	5.84	0.03	
313.15	10.79	0.09	6.03	0.03	3.87	0.03	
343.2	6.48	0.04	3.03	0.02	1.32	0.02	
363.02	4.00	0.04	2.38	0.02	1.10	0.02	
373.12	1.79	0.03	1.24	0.02	3.00	0.03	
412.6	2.62	0.12	2.81	0.12	0.83	0.13	
443.2	2.73	0.11	2.90	0.10	1.30	0.11	
483.2	1.92	0.15	2.13	0.14	1.08	0.15	
Average	5.34	0.09	3.50	0.06	2.29	0.06	

I.2.2 Propanoic acid + water

Table I.4. Average deviations in pressure (ΔP) and propanoic acid vapour composition (Δy_1) of the equations of state with different association schemes and $k_{ij} = k_{ij}^0 + k_{ij}^1 T$.

Association scheme								
1A-2B								
	CPA ECR		CPA CR1		PC-SAFT		PCP-SAFT	
T [K]	ΔP [%]	Δy_1	ΔP [%]	Δy_1	ΔP [%]	Δy_1	ΔP [%]	Δy_1
313.1	48.49	0.18	59.00	0.23	9.00	0.03	4.13	0.02
343.2	58.24	0.14	59.41	0.18	12.28	0.05	8.74	0.03
373.1	51.00	0.47	54.88	0.11	6.89	0.03	3.34	0.03
423.2	10.93	0.08	13.17	0.09	9.63	0.08	7.04	0.07
453.2	10.81	0.12	13.32	0.12	9.68	0.11	7.21	0.10
483.2	9.00	0.16	11.52	0.17	8.22	0.16	6.13	0.15
Average	31.41	0.19	35.22	0.15	9.28	0.08	6.10	0.07
1A-3B								
	CPA ECR		CPA CR1		PC-SAFT		PCP-SAFT	
T [K]	ΔP [%]	Δy_1	ΔP [%]	Δy_1	ΔP [%]	Δy_1	ΔP [%]	Δy_1
313.1	13.18	0.25	16.32	0.25	9.53	0.03	4.68	0.02
343.2	14.05	0.07	17.33	0.09	11.92	0.05	9.29	0.04
373.1	9.10	0.03	13.31	0.05	6.49	0.03	3.83	0.03
423.2	11.37	0.08	13.41	0.09	9.22	0.07	7.66	0.07
453.2	11.20	0.11	14.06	0.12	9.30	0.11	7.99	0.10
483.2	9.56	0.16	13.03	0.17	7.71	0.15	6.99	0.15
Average	11.41	0.12	14.58	0.13	9.03	0.08	6.74	0.07
1A-4C								
	CPA ECR		CPA CR1		PC-SAFT		PCP-SAFT	
T [K]	ΔP [%]	Δy_1	ΔP [%]	Δy_1	ΔP [%]	Δy_1	ΔP [%]	Δy_1
313.1	4.75	0.02	5.12	0.02	3.92	0.02	4.39	0.02
343.2	10.40	0.04	9.45	0.05	9.67	0.04	9.85	0.04
373.1	4.00	0.03	5.62	0.03	3.94	0.03	4.73	0.04
423.2	7.52	0.09	10.54	0.09	6.78	0.08	6.64	0.07
453.2	7.86	0.12	11.43	0.13	7.21	0.11	6.73	0.11
483.2	6.75	0.17	10.33	0.17	6.30	0.16	5.92	0.15
Average	6.88	0.08	8.75	0.08	6.30	0.07	6.38	0.07



Average deviations

Table I.4. (Continuation)

2B-2B								
<i>T</i> [K]	CPA ECR		CPA CR1		PC-SAFT		PCP-SAFT	
	ΔP [%]	Δy_1	ΔP [%]	Δy_1	ΔP [%]	Δy_1	ΔP [%]	Δy_1
313.1	8.33	0.03	10.71	0.03	7.80	0.03	2.27	0.02
343.2	11.15	0.05	14.01	0.06	10.29	0.04	7.62	0.02
373.1	6.09	0.04	9.35	0.04	4.89	0.03	2.77	0.04
423.2	9.18	0.06	11.28	0.07	8.20	0.06	5.20	0.05
453.2	8.67	0.09	10.93	0.10	7.90	0.09	5.11	0.09
483.2	6.95	0.14	9.03	0.15	6.29	0.14	3.84	0.13
Average	8.40	0.07	10.89	0.07	7.56	0.06	4.47	0.06

2B-3B								
<i>T</i> [K]	CPA ECR		CPA CR1		PC-SAFT		PCP-SAFT	
	ΔP [%]	Δy_1	ΔP [%]	Δy_1	ΔP [%]	Δy_1	ΔP [%]	Δy_1
313.1	8.34	0.17	11.78	0.18	9.16	0.03	2.56	0.02
343.2	34.35	0.16	35.61	0.17	10.80	0.05	7.93	0.03
373.1	20.88	0.12	22.19	0.12	5.45	0.04	2.67	0.04
423.2	9.97	0.06	12.65	0.07	8.54	0.06	6.33	0.05
453.2	9.50	0.09	12.19	0.10	8.33	0.09	6.20	0.09
483.2	7.63	0.14	10.45	0.15	6.46	0.14	4.84	0.13
Average	15.11	0.13	17.48	0.13	8.12	0.07	5.09	0.06

2B-4C								
<i>T</i> [K]	CPA ECR		CPA CR1		PC-SAFT		PCP-SAFT	
	ΔP [%]	Δy_1	ΔP [%]	Δy_1	ΔP [%]	Δy_1	ΔP [%]	Δy_1
313.1	6.47	0.04	8.29	0.03	2.73	0.02	3.01	0.03
343.2	7.39	0.04	12.47	0.05	5.99	0.03	8.22	0.02
373.1	10.23	0.06	6.74	0.03	2.02	0.03	4.31	0.04
423.2	5.83	0.06	9.71	0.07	5.35	0.06	5.12	0.06
453.2	5.67	0.10	9.76	0.10	5.30	0.09	4.09	0.09
483.2	4.29	0.14	8.32	0.15	4.06	0.14	3.24	0.13
Average	6.65	0.07	9.22	0.07	4.24	0.06	4.66	0.06



Table I.4. (Continuation)

T [K]	Non-associating					
	PR		PC-SAFT		PCP-SAFT	
	ΔP [%]	Δy_1	ΔP [%]	Δy_1	ΔP [%]	Δy_1
313.1	9.35	0.06	8.67	0.03	3.71	0.01
343.2	12.41	0.06	10.55	0.05	6.84	0.03
373.1	6.48	0.05	6.36	0.04	2.76	0.03
423.2	9.84	0.06	10.12	0.05	6.39	0.05
453.2	9.48	0.09	9.53	0.08	6.28	0.08
483.2	7.98	0.13	7.53	0.12	5.05	0.12
Average	9.26	0.07	8.79	0.06	5.17	0.05

Appendix J. Binary interaction parameters

J.1 k_{ij}

J.1.1 Acetic acid + water

Table J.1. Temperature dependent binary interaction parameters (k_{ij}) for each equation of state and association scheme.

k_{ij}				
Association scheme				
1A-2B				
T [K]	CPA ECR	CPA CR1	PC-SAFT	PCP-SAFT
293.15	-0.171	-0.157	0.028	-0.043
313.15	-0.159	-0.145	0.035	-0.031
343.2	-0.162	-0.159	0.035	-0.020
363.02	-0.145	-0.128	0.045	-0.011
373.12	-0.132	-0.112	0.049	-0.009
412.6	-0.129	-0.117	0.056	0.011
443.2	-0.119	-0.107	0.061	0.024
483.2	-0.098	-0.083	0.066	0.032
1A-3B				
T [K]	CPA ECR	CPA CR1	PC-SAFT	PCP-SAFT
293.15	-0.090	-0.075	0.108	0.012
313.15	-0.083	-0.064	0.112	0.018
343.2	-0.092	-0.089	0.110	0.026
363.02	-0.078	-0.061	0.116	0.037
373.12	-0.067	-0.045	0.117	0.039
412.6	-0.073	-0.060	0.123	0.058
443.2	-0.068	-0.055	0.128	0.069
483.2	-0.053	-0.038	0.128	0.075



Table J.1. (Continuation)

1A-4C				
T [K]	CPA ECR	CPA CR1	PC-SAFT	PCP-SAFT
293.15	-0.204	-0.178	0.031	-0.064
313.15	-0.202	-0.182	0.033	-0.059
343.2	-0.228	-0.211	0.039	-0.046
363.02	-0.226	-0.204	0.035	-0.040
373.12	-0.229	-0.197	0.033	-0.041
412.6	-0.238	-0.220	0.046	-0.016
443.2	-0.234	-0.226	0.052	-0.001
483.2	-0.261	-0.240	0.046	-0.002

2B-2B				
T [K]	CPA ECR	CPA CR1	PC-SAFT	PCP-SAFT
293.15	-0.227	-0.207	-0.050	-0.119
313.15	-0.215	-0.189	-0.041	-0.108
343.2	-0.214	-0.193	-0.037	-0.101
363.02	-0.201	-0.173	-0.024	-0.090
373.12	-0.190	-0.153	-0.018	-0.089
412.6	-0.176	-0.145	-0.007	-0.064
443.2	-0.160	-0.133	0.001	-0.049
483.2	-0.146	-0.108	0.010	-0.041

2B-3B				
T [K]	CPA ECR	CPA CR1	PC-SAFT	PCP-SAFT
293.15	-0.208	-0.183	-0.031	-0.097
313.15	-0.198	-0.170	-0.022	-0.088
343.2	-0.212	-0.151	-0.012	-0.079
363.02	-0.188	-0.162	-0.001	-0.067
373.12	-0.170	-0.134	0.006	-0.066
412.6	-0.161	-0.125	0.016	-0.042
443.2	-0.143	-0.118	0.028	-0.029
483.2	-0.127	-0.088	0.034	-0.019



Table J.1. (Continuation)

2B-4C				
T [K]	CPA ECR	CPA CR1	PC-SAFT	PCP-SAFT
293.15	-0.220	-0.173	-0.044	-0.140
313.15	-0.217	-0.168	-0.036	-0.128
343.2	-0.238	-0.182	-0.035	-0.123
363.02	-0.221	-0.165	-0.028	-0.108
373.12	-0.228	-0.150	-0.029	-0.110
412.6	-0.210	-0.148	-0.010	-0.078
443.2	-0.200	-0.140	-0.001	-0.064
483.2	-0.211	-0.140	-0.002	-0.056

Non-associating				
T [K]	PR	PC-SAFT	PCP-SAFT	
293.15	-0.137	-0.034	-0.045	
313.15	-0.136	-0.030	-0.044	
343.2	-0.144	-0.030	-0.044	
363.02	-0.140	-0.024	-0.038	
373.12	-0.138	-0.020	-0.036	
412.6	-0.138	-0.012	-0.024	
443.2	-0.136	-0.003	-0.014	
483.2	-0.127	0.008	-0.005	

J.1.2 Propanoic acid + water

Table J.2. Temperature dependent binary interaction parameters (k_{ij}) for each equation of state and association scheme.

k_{ij}				
Association scheme				
1A-2B				
T [K]	CPA ECR	CPA CR1	PC-SAFT	PCP-SAFT
313.1	-0.186	-0.182	0.028	-0.031
343.2	-0.150	-0.141	0.049	-0.009
373.1	-0.097	-0.099	0.050	-0.013
423.2	-0.113	-0.096	0.060	0.002
453.2	-0.071	-0.042	0.075	0.014
483.2	-0.042	-0.008	0.087	0.029
1A-3B				
T [K]	CPA ECR	CPA CR1	PC-SAFT	PCP-SAFT
313.1	-0.094	-0.111	0.086	0.006
343.2	-0.090	-0.073	0.102	0.028
373.1	-0.074	-0.051	0.098	0.020
423.2	-0.070	-0.053	0.105	0.033
453.2	-0.031	-0.029	0.115	0.044
483.2	-0.004	-0.030	0.123	0.057
1A-4C				
T [K]	CPA ECR	CPA CR1	PC-SAFT	PCP-SAFT
313.1	-0.178	-0.165	0.032	-0.073
343.2	-0.155	-0.138	0.042	-0.044
373.1	-0.193	-0.162	0.032	-0.061
423.2	-0.200	-0.177	0.038	-0.036
453.2	-0.205	-0.172	0.037	-0.033
483.2	-0.194	-0.144	0.044	-0.018
2B-2B				
T [K]	CPA ECR	CPA CR1	PC-SAFT	PCP-SAFT
313.1	-0.203	-0.182	0.005	-0.062
343.2	-0.165	-0.147	0.028	-0.045
373.1	-0.158	-0.134	0.035	-0.046
423.2	-0.142	-0.096	0.045	-0.022
453.2	-0.106	-0.045	0.060	-0.014
483.2	-0.077	-0.010	0.072	0.005



Table J.2. (Continuation)

2B-3B				
T [K]	CPA ECR	CPA CR1	PC-SAFT	PCP-SAFT
313.1	-0.237	-0.038	0.021	-0.043
343.2	-0.092	-0.147	0.049	-0.027
373.1	-0.169	-0.137	0.051	-0.027
423.2	-0.129	-0.075	0.061	-0.004
453.2	-0.091	-0.029	0.077	0.006
483.2	-0.059	0.011	0.089	0.025

2B-4C				
T [K]	CPA ECR	CPA CR1	PC-SAFT	PCP-SAFT
313.1	-0.165	-0.111	0.016	-0.088
343.2	-0.124	-0.067	0.034	-0.071
373.1	-0.151	-0.080	0.025	-0.075
423.2	-0.140	-0.064	0.040	-0.038
453.2	-0.136	-0.023	0.043	-0.033
483.2	-0.105	0.007	0.056	-0.023

Non-associating				
T [K]	PR	PC-SAFT	PCP-SAFT	
313.1	-0.140	-0.025	-0.039	
343.2	-0.129	-0.011	-0.024	
373.1	-0.136	-0.004	-0.026	
423.2	-0.118	0.009	-0.010	
453.2	-0.098	0.018	-0.002	
483.2	-0.079	0.036	0.014	

J.2 $k_{ij} = k_{ij}^0 + k_{ij}^1 T$

J.2.1 Acetic acid + water

Table J.3. Parameters k_{ij}^0 and k_{ij}^1 in $k_{ij} = k_{ij}^0 + k_{ij}^1 T^a$ for the acetic acid (i) + water (j) system.

Association scheme	PR		CPA ECR		CPA CR1		PC-SAFT		PCP-SAFT	
	k_{ij}^0	$k_{ij}^1 \times 10^4$	k_{ij}^0	$k_{ij}^1 \times 10^4$	k_{ij}^0	$k_{ij}^1 \times 10^4$	k_{ij}^0	$k_{ij}^1 \times 10^4$	k_{ij}^0	$k_{ij}^1 \times 10^4$
1A-2B			-0.28	3.70	-0.27	3.76	-0.03	2.08	-0.16	4.08
1A-3B			-0.14	1.80	-0.13	1.75	0.07	1.18	-0.09	3.61
1A-4C			-0.12	-2.72	-0.09	-3.13	0.00	1.03	-0.17	3.69
2B-2B			-0.36	4.35	-0.35	5.09	-0.14	3.25	-0.25	4.34
2B-3B			-0.35	4.57	-0.32	4.68	-0.13	3.51	-0.22	4.33
2B-4C			-0.26	1.05	-0.24	2.14	-0.12	2.49	-0.28	4.73
Non-associating	-0.15	0.45					-0.10	2.24	-0.12	2.25

^a Temperature, T , in K.



J.2.2 Propanoic acid + water

Table J.4. Parameters k_{ij}^0 and k_{ij}^1 in $k_{ij} = k_{ij}^0 + k_{ij}^1 T^a$ for the propanoic acid (i) + water (j) system.

Association scheme	PR		CPA ECR		CPA CR1		PC-SAFT		PCP-SAFT	
	k_{ij}^0	$k_{ij}^1 \times 10^4$	k_{ij}^0	$k_{ij}^1 \times 10^4$	k_{ij}^0	$k_{ij}^1 \times 10^4$	k_{ij}^0	$k_{ij}^1 \times 10^4$	k_{ij}^0	$k_{ij}^1 \times 10^4$
1A-2B			-0.41	7.46	-0.46	9.30	-0.06	3.08	-0.12	3.10
1A-3B			-0.26	5.04	-0.23	4.25	0.03	1.88	-0.07	2.57
1A-4C			-0.11	-1.94	-0.15	-0.19	0.02	0.41	-0.15	2.73
2B-2B			-0.41	6.61	-0.49	9.72	-0.10	3.54	-0.18	3.68
2B-3B			-0.43	7.44	-0.29	5.59	-0.08	3.46	-0.16	3.75
2B-4C			-0.22	2.18	-0.29	5.93	-0.04	1.97	-0.21	3.94
Non-associating	-0.25	3.36					-0.13	3.24	-0.13	2.84

^a Temperature, T , in K.

Appendix K. Communications

K.1 Publications

- Román-Ramírez L.A., García-Sánchez, F., Santos R.C.D., Leeke, G.A. (2015) Vapour–liquid equilibrium of propanoic acid + water at 423.2, 453.2 and 483.2 K from 1.87 to 19.38 bar. Experimental and modelling with PR, CPA, PC-SAFT and PCP-SAFT. **Fluid Phase Equilibria**, 388: 151-159.

K.2 Conferences

- Román-Ramírez L.A., García-Sánchez, F., Santos R.C.D., Leeke, G.A. High pressure VLE of the propionic acid + water system. Experimental and modelling. 27th European Symposium on Applied Thermodynamics. 6 – 9th July 2014. Oral presentation.
- Román-Ramírez L.A., Leeke, G.A. Experimental study and thermodynamic modelling of systems comprising organic acids and water. III Symposium CONACyT in Europe. Strasbourg, France, 6 – 9th November, 2013. Oral presentation.
- Román-Ramírez L.A., García-Sánchez, F., Santos R.C.D., Leeke, G.A. Comparison of performance of the PC-SAFT, Soave-Redlich-Kwong and Peng-Robinson equations of state in modelling vapour–liquid equilibria of binary CO₂ – 1-alkanol mixtures. Industrial Molecular Thermodynamics (InMother) Conference. Lyon, France, 19 – 20th March, 2012. Oral presentation.

